Università degli Studi di Milano-Bicocca

Dipartimento di Biotecnologie e Bioscienze

Dottorato di Ricerca in Biotecnologie Industriali - XXVIII Ciclo

A screen for synthetic phenotypes reveals new Sae2 functions and interactions in the repair of DNA double-strand breaks

Coordinatore: Prof. Marco Ercole Vanoni

Tutor: Prof.ssa Maria Pia Longhese

Elisa Gobbini

Matr. 701839

Anno Accademico 2014-2015

Università degli Studi di Milano-Bicocca

Dipartimento di Biotecnologie e Bioscienze

Dottorato di Ricerca in Biotecnologie Industriali - XXVIII Ciclo

A screen for synthetic phenotypes reveals new Sae2 functions and interactions in the repair of DNA double-strand breaks

Coordinatore: Prof. Marco Ercole Vanoni

Tutor: Prof.ssa Maria Pia Longhese

Elisa Gobbini

Matr. 701839

Anno Accademico 2014-2015

INDEX

Index

Index

ABSTRACT

Abstract

Genome instability is one of the most pervasive characteristics of cancer cells and can be due to DNA repair defects and failure to arrest the cell cycle. Among the many types of DNA damage, the DNA Double Strand Break (DSB) is one of the most severe, because it can cause mutations and chromosomal rearrangements. Generation of DSBs triggers a highly conserved mechanism, known as DNA damage checkpoint, which arrests the cell cycle until DSBs are repaired. DSBs can be repaired by Homologous Recombination (HR), which requires the DSB ends to be nucleolytically processed (resected) to generate single-strand DNA. In *Saccharomyces cerevisiae*, initiation of DSB resection requires the conserved MRX/MRN complex (Mre11-Rad50-Xrs2 in yeast; MRE11-RAD50-NBS1 in mammals) that, together with Sae2 (CtIP in mammals), catalyzes an endonucleolytic cleavage of the 5' strands. More extensive resection depends on two pathways: one catalyzed by the exonuclease Exo1, and a second requiring the nuclease Dna2 with the helicase Sgs1. The absence of Sae2 not only impairs DSB resection, but also causes prolonged MRX binding at the DSBs that leads to persistent Tel1 (ATM in humans)- and Rad53-dependent DNA damage checkpoint activation and cell cycle arrest. Whether this enhanced checkpoint signaling contributes to the DNA damage sensitivity and/or the resection defect of *sae2*Δ cells is not known. *sae2*Δ cells are sensitive to DNA damaging agents, such as camptothecin (CPT), which traps covalent topoisomerase I (Top1)-DNA cleavable complexes and induces DNA replication-dependent

cell death. Since this sensitivity has been shown to be due to resection defect, we searched for extragenic suppressors of the *sae2*Δ sensitivity to CPT. By performing a genetic screen, we identify three mutant alleles (*SGS1-ss*, *rad53-ss* and *tel1-ss*) that suppress both the DNA damage hypersensitivity and the resection defect of *sae2*Δ cells.

We show that Sgs1-ss mediated suppression depends on the Dna2 nuclease but not on Exo1. Furthermore, not only Sgs1-ss suppresses the resection defect of *sae2*Δ cells but it also increases resection efficiency compared to wild type cells. The checkpoint protein Rad9 limits the action of Sgs1/Dna2 in DSB resection by inhibiting Sgs1 binding/persistence at the DSB ends. When inhibition by Rad9 is abolished by the Sgs1-ss mutant variant or by deletion of *RAD9*, the requirement for Sae2 and functional MRX in DSB resection is reduced.

rad53-ss and *tel1-ss* mutant alleles, but also the kinase defective alleles (*rad53-kd* and *tel1-kd*), suppress both the DNA damage hypersensitivity and the resection defect of *sae2*Δ cells through an Sgs1-Dna2-dependent mechanism. These suppression events do not involve escaping the checkpoint-mediated cell cycle arrest. Rather, defective Rad53 or Tel1 signaling bypasses Sae2 function at DSBs by decreasing the amount of Rad9 bound at DSBs. As a consequence, reduced Rad9 association to DNA ends relieves inhibition of Sgs1-Dna2 activity, which can then compensate for the lack of Sae2 in DSB resection and DNA damage resistance. We propose that persistent

Abstract

Tel1 and Rad53 checkpoint signaling in cells lacking Sae2 cause DNA damage hypersensitivity and defective DSB resection by increasing the amount of Rad9 bound at the DSBs, which in turn inhibits the Sgs1-Dna2 resection machinery.

RIASSUNTO

Riassunto

L'instabilità genomica è una delle caratteristiche principali delle cellule tumorali e può essere causata da difetti nella riparazione del DNA e mancato arresto del ciclo cellulare. Tra i vari tipi di danno al DNA, le rotture della doppia elica del DNA (*Double-Strand Break* o DSB) rappresentano una delle lesioni più pericolose, poiché possono causare mutazioni o riarrangiamenti cromosomici. La presenza di un DSB induce una complessa e conservata risposta cellulare, detta checkpoint da danno al DNA, che causa l'arresto del ciclo cellulare finché il danno non è stato riparato. Tali rotture possono essere riparate mediante ricombinazione omologa (*Homologous Recombination* o HR), che richiede il processamento delle estremità del DNA (*resection*), in modo da generare DNA a singolo filamento. In *Saccharomyces cerevisiae*, l'inizio della *resection* prevede l'azione del complesso MRX/MRN (Mre11, Rad50 e Xrs2 in lievito o NBS1 in mammifero) che, insieme alla proteina Sae2 (CtIP nell'uomo), catalizza un taglio endonucleolitico del filamento 5'. La *resection* più estesa dipende dall'azione dalle nucleasi Exo1 e Dna2, coadiuvata dall'elicasi Sgs1. L'assenza di Sae2 causa un difetto di *resection* e un prolungato legame del complesso MRX al DSB che porta ad una persistente attivazione del checkpoint da danno al DNA, mediato dalle chinasi Tel1 (ATM nell'uomo) e Rad53, ed all'arresto del ciclo cellulare. Non è noto se la persistente attivazione del checkpoint contribuisce alla sensibilità ai danni al DNA e/o al difetto di *resection* di cellule *sae2*Δ. La delezione di *SAE2* causa sensibilità agli agenti

genotossici, ad esempio alla camptotecina (CPT), che stabilizza l'intermedio covalente DNA-Topoisomerasi I normalmente transiente, con conseguente morte cellulare in seguito alla replicazione del DNA. Poiché è stato dimostrato che tale sensibilità è causata da difetti di *resection*, abbiamo effettuato uno screening genetico per trovare soppressori extragenici della sensibilità alla CPT di un ceppo *sae2*Δ, identificando tre mutanti (*SGS1-ss*, *rad53-ss* e *tel1-ss*) in grado di sopprimere l'ipersensibilità agli agenti genotossici e il difetto di *resection* di cellule *sae2*Δ.

La soppressione mediata da Sgs1-ss dipende dall'azione della nucleasi Dna2 e non da Exo1. Sgs1-ss oltre a sopprimere il difetto di *resection* di cellule *sae2*Δ, aumenta l'efficienza di *resection* rispetto ad un ceppo selvatico. La proteina di checkpoint Rad9 limita l'azione di Sgs1-Dna2 inibendo il legame e la persistenza di Sgs1 all'estremità del DNA durante il processamento di un DSB. Quando l'inibizione ad opera di Rad9 viene abolita, come nella variante Sgs1-ss o in cellule *rad9*Δ, si riduce la richiesta di Sae2 e di un complesso MRX funzionante per la *resection* di un DSB.

Gli alleli *rad53-ss* e *tel1-ss*, così come i mutanti privi di attività chinasica (*rad53-kd* e *tel1-kd*), sopprimono la sensibilità e il difetto di *resection* di cellule *sae2*Δ, in maniera dipendente da Sgs1-Dna2. Tale soppressione non dipende dal superamento dell'arresto del ciclo cellulare indotto dall'attivazione del checkpoint. Abbiamo dimostrato che un difetto nell'attivazione di Rad53 e Tel1 è in grado di bypassare

la funzione di Sae2 a livello del DSB riducendo la quantità di Rad9 legato al DNA. Una ridotta associazione di Rad9 ne diminuisce l'attività inibitoria su Sgs1-Dna2, compensando la mancanza di Sae2 nella *resection* e nella resistenza ai danni al DNA. Proponiamo pertanto un modello in cui, in cellule prive di Sae2, una persistente segnalazione da parte delle chinasi Tel1 e Rad53, causa l'ipersensibilità agli agenti genotossici e il difetto di *resection* aumentando la quantità di Rad9 legato al DSB, che a sua volta inibisce la *resection* limitando l'attività di Sgs1-Dna2.

INTRODUCTION

Maintaining genome integrity: The DNA damage response

Maintaining the integrity of the genome is crucial for all organisms. In fact, preservation of genomic integrity is a pre-requisite for proper cell function and faithful transmission of the genome to progeny. However, environmental factors and the chemical properties of DNA do not guarantee lifelong stability and proper functioning of the genome. It is estimated that each cell has approximately 10^4-10^5 lesions per day, which must be repaired to ensure genomic integrity. In eukaryotes, the mechanisms involved in maintaining genome integrity and in preventing the generation of potentially deleterious mutations are extremely sophisticated and they include a complex cellular response, called DNA Damage Response (DDR), highly conserved during evolution. The DDR is a network of cellular pathways that sense, signal and repair DNA lesions: they are able to detect the presence of DNA lesions and activate a specialized surveillance mechanism, known as DNA damage checkpoint, that coordinates the repair of the damage with cell cycle progression (Fig. 1) (Giglia-Mari *et al.*, 2011).

There are several endogenous and exogenous agents that can damage DNA. Spontaneous DNA alterations can be due to side effects of normal cellular metabolism, such as replication errors, uncontrolled recombination, off-target mutation induction by somatic hypermutation during antigen production, inaccurate VDJ

recombination. Furthermore, reactive oxygen species produced by normal cellular metabolism can oxidize DNA bases and generate DNA breaks. DNA damage can be also produced by viral infections, environmental agents such as ultraviolet light (UV), ionizing radiation (IR), and numerous genotoxic chemicals, like substances that modify the DNA bases or intercalating agents (Fig. 1) (Giglia-Mari *et al.*, 2011). The cell has a network of complex signaling pathways that arrest the cell cycle and may ultimately lead to programmed cell death. The DDR includes direct damage repair, recombinational repair, transcriptional program activation, damage tolerance, damage-induced growth arrest and apoptosis (Fig. 1).

Since there are different types of DNA damage, cells have evolved several mechanisms to protect the genetic heritage of the cell. DNA repair involves the excision of bases and DNA synthesis, which requires double-stranded DNA (dsDNA): mispaired bases, usually generated by mistakes during DNA replication, are excised as single nucleotides during the MisMatch Repair (MMR); a damaged base is excised as a single free base in Base Excision Repair (BER), or as an oligonucleotide fragment in Nucleotide Excision Repair (NER). Repair of DNA Double-Strand Breaks (DSBs) can be achieved by either the Non Homologous End Joining (NHEJ) or the Homologous Recombination (HR) pathway. In particular conditions acts a damage-tolerance mechanism called translesion DNA synthesis, where damaged sites are recognized by the replication machinery before they

can be repaired, resulting in an arrest that can be relieved by replicative bypass (Friedberg, 2003).

The biological significance of a functional DDR for human health is clearly illustrated by the severe consequences of inherited defects in DDR factors resulting in various diseases, including immune deficiency, neurological degeneration, premature aging, and severe cancer susceptibility (Hoeijmakers, 2009). Taken advantage of the extreme conservation of DDR among eukaryotes, we can use model organisms, like the yeast *Saccharomyces cerevisiae*, to better characterize the molecular mechanisms of these pathways. Given the importance of DDR in maintaining genome stability and the correlation of loss of this function with human pathology and cancer, is important to improve our knowledge in response to DNA damage.

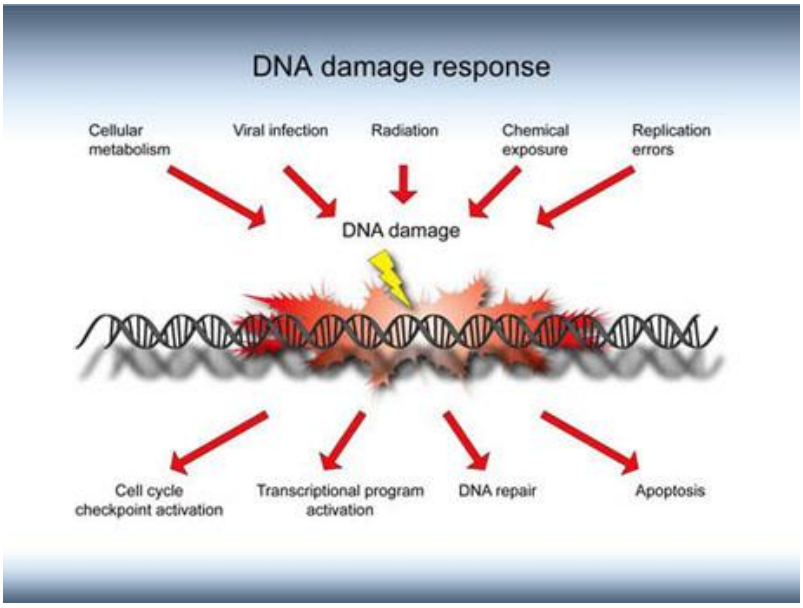

Figure 1. Cell response to DNA damage: causes and consequences. DNA damage caused by cellular metabolism, viral infection, radiation, chemical agents and errors during DNA replication induce the DNA damage response. The presence of DNA damage leads to: checkpoint activation, transcriptional program activation, DNA repair and apoptosis.

Sensing and processing of a Double-Strand Break (DSB)

DNA DSBs are among the most cytotoxic forms of DNA damage because failure to repair them can lead to loss of genetic information and chromosome rearrangements. DSBs are generated when the phospho-sugar backbones of both DNA strands are broken at the same position or in sufficient proximity to allow physical dissociation of the double helix into two separate molecules (Aparicio *et al.*, 2014).

DSBs can occur either accidentally during normal cell metabolism or can be caused by exposure to exogenous agents, such as certain types

of chemotherapeutic drugs or IR. In fact, drugs that generate DSBs are widely used in cancer chemotherapy since tumor cells are often more sensitive to DSBs than normal cells. These include: base alkylating agents such as methylmethane sulfonate (MMS); crosslinking agents that introduce covalent crosslinks between bases, like psoralen and platinum derivatives; ribonucleotide reductase inhibitors, such as hydroxyurea (HU); DNA topoisomerase inhibitors, which induce the formation of DSBs by trapping topoisomerase-DNA intermediates (cleavable complexes), like camptothecins (CPT) and their derivatives (irinotecan and topotecan) that inhibit type IB topoisomerases (Deng *et al.*, 2005). DSBs are also generated during normal cell metabolism, for example by Reactive Oxygen Species (ROS) that can oxidize bases and trigger both single and double strand breaks. Nevertheless, they are also obligate intermediates during physiological cellular processes, such as meiotic recombination and programmed rearrangements of the immunoglobulin and T cell receptor loci during lymphoid cell development. Finally, DNA replication is thought to be the major source of DSBs in proliferating cells since the DNA intermediates at replication forks are fragile and susceptible to breakage (Aparicio *et al.*, 2014).

Inherited defects in DSB repair are implicated in a variety of human pathologies, including increased cancer susceptibility, neurological defects and/or immunodeficiencies, in disease syndromes such as

Ataxia telangiectasia, Nijmegen Breakage syndrome or the Severe Combined ImmunoDeficiency (SCID) (McKinnon, 2012).

DSBs can be repaired through two different pathways: NHEJ and HR. Whereas NHEJ directly joins the DNA ends, HR uses the sister chromatid or the homologous chromosome to repair DSBs. HR and NHEJ mechanisms are evolutionarily conserved, but the preferential use of either varies from species to species and depends on the cell cycle phase in which the damage occurs. In fact, NHEJ can occur in all phases of the cycle, but in G1 is the main mechanism of repair of a DSB because HR is inhibited. On the contrary, during S/G2 phase cells basically repair the DSB by HR (Fig. 2). Making the right choice between NHEJ and HR is important to ensure genome stability (Longhese *et al.*, 2010; Symington and Gautier, 2011).

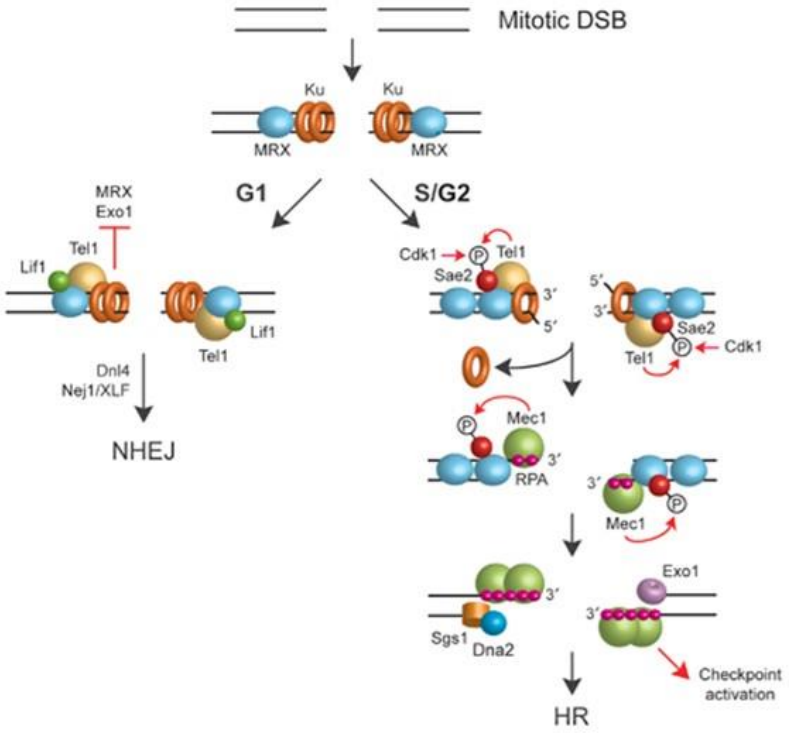

Figure 2. DNA-end resection at DSBs. The MRX complex and Ku almost simultaneously bind the DSB ends. In G1, Ku and MRX mediate recruitment of the NHEJ proteins (Lif1, Dnl4 and Nej1), which allow religation of the DSB ends. Recognition of the DSB by MRX also leads to Tel1 recruitment. Both Ku and the NHEJ proteins prevent initiation of resection. In the absence of Ku or NHEJ, the DSB undergoes MRX-dependent resection even in the absence of Cdk1. When the DSB ends are not bound by MRX, Ku also prevents Exo1-mediated resection. In S/G2, Sae2 is activated by Cdk1- and Tel1-dependent phosphorylation events. MRX and Sae2 then catalyse the initial processing of the 5′ strand possibly by endonucleolytic cleavage, which reduces the ability of Ku to bind the ends and promotes extensive 5′ strand resection by Sgs1, Exo1 and Dna2. The 3′-ended ssDNA tails coated by RPA allow recruitment of Mec1, which in turn phosphorylates Sae2, thus contributing to potentiate resection. Mec1 association to DSB ends also leads to DNA damage checkpoint activation. (Longhese *et al.*, 2010)

DSB repair pathways: Non-Homologous End-Joining (NHEJ)

The NHEJ is a repair process that directly ligates two broken ends with little or no processing. If the ends are compatible, the enzyme DNA ligase directly reconstitutes the phosphodiester bond; but if, as is often the case, are not perfectly compatible, they are first processed by different protein and then religate. This makes the process prone to the loss of small stretches of DNA and therefore the NHEJ repair process is called error prone. It is highly efficient, but it can lead to mutations at the joining sites, as well as inversions and translocations (Lieber, 2010).

NHEJ is the main repair pathways in mammals and is conserved from yeast to humans. The initial step in NHEJ is the recognition and binding of the Ku heterodimer to the DSB. The Ku heterodimer is composed of the Ku70 and Ku80 subunits. Once a DSB occurs, the highly conserved MRX/MRN complex (Mre11, Rad50 and Xrs2 in budding yeast and MRE11, RAD50 and NBS1 in mammals) is recruited to DNA ends with the Ku heterodimer.

NHEJ is active only on blunt or minimally processed DNA ends, and therefore is inhibited by the nucleolytic degradation of the 5' strands (resection) that leads to HR (Fig. 2). If cells are in the G1 cell cycle phase, the presence of Ku prevents resection and, together with MRX, mediates recruitment of downstream NHEJ factors (Lee *et al.*, 1998; Chen *et al.*, 2001; Clerici *et al.*, 2008; Palmbos *et al.*, 2008).

Once Ku is bound to the DSB ends, it then serves as a scaffold to recruit the other NHEJ factors to the damage site. The Ku heterodimer has been shown to recruit either directly or indirectly the main NHEJ factors, including DNA Ligase IV (Dnl4 in yeast and DNL4 in mammals) with its cofactor (Lif1 in yeast and XRCC4 in human) and XRCC4-like factor (XLF in human and Nej1 in yeast) (Fig. 2) (Longhese *et al.*, 2010). Given that most of the DNA damage generate ends not compatible, before the action of the DNA ligase, if necessary, there is processing of the DNA ends to create ligatable ends. Depending on the nature of the break, different DNA end processing enzymes may be required, including those that resect DNA ends, fill in gaps, remove blocking end groups, and make the ends ligatable. In mammals, Ku also recruits the DNA-PKcs, a member of the phosphoinositide 3-kinase related protein kinase (PIKK) family, which phosphorylates different substrates involved in NHEJ.

Mutations in components of NHEJ caused different diseases including hypersensitivity to IR and the Lig4 syndrome, a rare disorder caused by mutations in the gene encoding for the Ligase 4 and characterized by immune deficiency, microcephaly, and developmental delay (Davis and Chen, 2013).

DSB repair pathways: Homologous Recombination (HR)

Homologous recombination is a highly conserved pathway to repair DSBs. It is a more accurate process, because uses the undamaged homologous DNA sequences (sister chromatids or homologous chromosomes) as a template for repair in an error-free manner (San Filippo *et al.*, 2008). HR is defined as the exchange of genetic information between donor and recipient DNA molecules with similar or identical sequence. Availability of a homologous sequence for recombinational repair is mainly defined by ploidy and cell cycle phase. However, additional factors such as proximity of the donor and recipient sequences, chromatin structure, and nuclear compartmentalization also contribute to the availability of a sequence for HR (Mathiasen and Lisby, 2014).

HR is the main repair pathways in yeast and is conserved from yeast to humans. It is a process finely regulated during the cell cycle and the DSB is processed (resected) only after the DNA has been replicated and thus limiting the recombination in the phases S and G2. Thus, if NHEJ is the preferred pathway for DSBs with compatible ends in G1, HR is the predominant pathway in S/G2 phase. If cells are in the S or G2 cell cycle phase when a DSB is detected, processing of the 5' DSB ends generates 3'-ended ssDNA tails that inhibit NHEJ and target DSB repair to HR (Fig. 2). HR requires that the 5' ends of a DSB are nucleolytically processed (resected) to generate 3'-ended ssDNA that

can invade an undamaged homologous DNA template (Symington and Gautier, 2011; Mehta and Haber, 2014).

The enzymes that mediate the pairing and shuffling of DNA sequences during HR are called recombinases, and the reaction mediated by these enzymes is termed homologous DNA pairing and strand exchange. Two recombinases, Rad51 and Dmc1, exist in eukaryotes. Rad51 is needed for mitotic HR events such as DSB repair and also for meiotic HR, whereas Dmc1 is only expressed in meiosis so its function is restricted therein. Once the ssDNA is generated, it is coated by Replication Protein A (RPA). Then, RPA is replaced by Rad51, which is a recombinase that shows a high degree of conservation between all eukaryotes and also presents a strong conservation with the bacterial RecA recombinase (San Filippo *et al.*, 2008). The Rad51 recombinase functions in all three phases of HR: presynapsis, synapsis and post-synapsis (Fig. 3A) (Sung *et al.*, 2003). In the presynaptic phase, Rad51 is loaded onto single-strand DNA (ssDNA) that either is generated by degrading 5'-strands at DSBs or arises from replication perturbation. The resulting Rad51-ssDNA filament (presynaptic filament) is right-handed and comprises six Rad51 molecules and 18 nucleotides per helical turn. The stretching of the filament is essential for fast and efficient homology search. During synapsis, Rad51 facilitates the formation of a physical connection between the invading DNA substrate and homologous duplex DNA template, leading to the generation of heteroduplex DNA (D-loop)

(Fig. 3A). Here, Rad51-dsDNA filaments are formed by accommodating both the invading and donor ssDNA strands within the filament. Finally, during post-synapsis when DNA is synthesized using the invading 3'-end as a primer, Rad51 dissociates from dsDNA to expose the 3'-OH required for DNA synthesis (Krejci *et al.,* 2012). Mph1 (FANCM in humans) is a translocases involved in the dissociation of the D-loops formed by Rad51.

RPA is replaced by Rad51 with the help of other proteins known as recombination mediators. In yeast, these include at least two types of proteins: Rad52 and the Rad51 paralogues, Rad55 and Rad57 that share the RecA core sequences with Rad51. Mediators can facilitate Rad51 loading on ssDNA, increase intrinsic stability of Rad51 presynaptic filament and protect Rad51 from removal by factors such as helicases. Rad52 interacts with Rad51 and can also bind RPA once the latter coats ssDNA (Seong *et al.,* 2008). The Rad51-Rad52 interaction is required to recruit and nucleate Rad51 onto RPA-coated DNA. Only catalytic amounts of Rad52 are needed for presynaptic filament formation (Sung *et al.,* 2003), suggesting that RPA is not displaced from DNA directly by Rad52, but rather as a consequence of filament extension by the polymerization of nucleated Rad51 molecules. The mediator function of Rad52 is largely attributable to its C-terminus where the Rad51 and DNA interacting domains are located (San Filippo *et al.,* 2008). Despite the presence of human RAD52 protein, the central RAD51 mediator function in humans is

carried out by another protein, BRCA2. Although BRCA2 has no homology with yeast Rad52, BRCA2 is its functional equivalent since it controls the assembly of human RAD51 into nucleoprotein filaments. BRCA2 is a tumor suppressor and several mutations predispose to the development of breast and ovarian cancer (Roy *et al.*, 2012).

Like Rad51, the Rad55 and Rad57 heterodimer exhibits ATPase activity and binds ssDNA; but unlike Rad51, it cannot catalyze the strand-exchange reaction. The Rad55-Rad57 heterodimer directly interacts with Rad51 and can load Rad51 onto RPA-coated ssDNA. It can also form co-filaments with Rad51 and the resulting nucleofilament is more resistant to Srs2 anti-recombinase activity (Krejci *et al.*, 2012). Srs2 is a helicase involved in the disruption of Rad51 presynaptic filament. Srs2 is capable of dismantling Rad51 filaments in an ATP-dependent manner, leading to the displacement of Rad51 by RPA. This prevents untimely or unwanted recombination. However, Rad52 and Rad55/Rad57 can antagonize Srs2 activity. Although Srs2 is often referred to as an anti-recombinase due to its ability to disassemble presynaptic filaments it also plays a pro-recombination role to promote SDSA. Although no mammalian homologue of Srs2 has been identified, several helicases (for example RecQ5 and BLM) appear to have acquired a similar function (Krejci *et al.*, 2012).

In *S. cerevisiae*, Rad54 is a chromatin remodeler member of the Swi/Snf2 protein family and shows dsDNA-dependent ATPase, DNA supercoiling and chromatin remodeling activities. Rad54 interacts physically with Rad51 and is required at multiple stages in HR, in the early stages to promote a search for DNA homology, chromatin remodeling, and D-loop formation, and in the postsynaptic stage to catalyze the removal of Rad51 protein from dsDNA. The ability of Rad54 to remove Rad51 from dsDNA is believed to prevent the nonspecific association of Rad51 with bulk chromatin and to provide DNA polymerases access to the 3'-OH primer terminus in the nascent D-loop to initiate the repair DNA synthesis reaction (Sung *et al.*, 2003). Next, the invading strand primes DNA synthesis in a process that requires DNA polymerase and DNA replication proteins, such as PCNA, RFC and Dpb11.

There are several pathways of DNA repair by homologous recombination, which involve three main steps: a nucleolytic degradation of 5'-3' DSB ends, a process called resection; the strand invasion and the subsequent DNA synthesis; the resolution of the Holliday Junctions (HJs) (Fig. 3B-3D).

The first HR model for repair of a DSB is called the Double-Strand Break-Repair (DSBR) model, where the second end of DSB can be engaged to stabilize the D-loop structure (second-end capture), leading to the generation of a double-Holliday Junction (dHJ) (Fig. 3B) (Krejci *et al.*, 2012). The most important key features are:

initiation of HR by a DSB, processing of the DSB by nucleolytic resection to give single-strand tails with 3'-OH ends, formation of a recombinase filament on the ssDNA ends, strand invasion into a homologous sequence to form a D-loop intermediate, DNA polymerase extension, from the 3' end of the invading strand, capture of the second DSB end by annealing to the extended D-loop, formation of two crossed strand or HJs (San Filippo *et al.*, 2008). A dHJ is then resolved to produce Crossover (CO) or Non-Crossover (NCO) products (Fig. 3B) or dissolved, by the action of Sgs1-Top1-Rmi1, complex to exclusively generate NCO products. The orientation of resolvases at the DNA level, determines the formation of CO and NCO products: NCO are obtained if the enzymes cut horizontally at the level of HJs, CO products are obtained if there is a vertically and a horizontally cut.

Second, the invading strand can be displaced from the D-loop and anneals either with its complementary strand as in gap repair or with the complementary strand associating with the other end of the DSB (Nassif *et al.*, 1994). Since the model involves DNA synthesis followed by strand annealing, it is called Synthesis-Dependent Strand Annealing (SDSA) (Fig. 3C). SDSA mechanism is preferred over DSBR during mitosis. *In S. cerevisiae*, the Mph1 helicase is a major negative regulator of CO, and it acts by resolving D-loop intermediates via the NCO pathway of SDSA (Daley *et al.*, 2013). During meiosis, COs are formed by resolution of dHJs via the DSBR

mechanism, while NCOs are primarily produced via SDSA mechanism. This repair mechanism is conservative, since ensures the production of only NCO product because no HJs are formed. Here there is a migrating D-loop that never leads to capture of the second DSB end. Instead, after the initial steps of DSB resection, DNA strand invasion, and repair DNA synthesis, the invading strand is displaced and anneals with the second resected DSB end.

In the third mode, the D-loop structure can assemble into a replication fork and copy the entire chromosome arm in single-ended invasion process called Break-Induced Replication (BIR) (Fig. 3D). This mechanism is evoked more often when there is only one DNA end, either due to the loss of the other end or in the process of lengthening telomeres in telomerase-deficient cells. In BIR, the DSB end is nucleolytically processed similar to the resection that occurs in other DSB HR repair events. The single-strand tail then invades a homologous DNA sequence, often the sister chromatid or homolog chromosome, but sometimes a repeated sequence on a different chromosome. The invading end is used to copy information from the invaded donor chromosome by DNA synthesis (San Filippo *et al.*, 2008).

All the above pathways require Rad51, with the exception of some forms of BIR. However, DSBs can also be repaired by pathways independent of Rad51. One of these pathways is the Single-Strand Annealing pathway (SSA) (Fig. 3E) and the other is the already talked

NHEJ pathway (Fig. 3F). SSA does not require Rad51 but requires other HR proteins that mediate annealing. For example, Rad59 protein, which is involved in ssDNA annealing and Rad51 filament stability, has a minor role in Rad51-dependent recombination but a critical role in SSA. RPA-ssDNA complex can also lead to Rad51-independent repair wherein Rad52 and Rad59 replace RPA from DNA and anneal complementary strands. In SSA, ssDNA sequences generated during DSB processing contain regions of homology at both sides of DSB, therefore a DSB is closely flanked by two direct repeats. This DNA organization provides the opportunity to repair the DSB by a deletion process using the repeated DNA sequences. In this process, the DSB ends are resected, but then instead of engaging a homologous DNA sequence for strand invasion, the resected ends anneal to each other. The process is finished by nucleolytic removal of the protruding single-strand tails, and results in deletion of the sequences between the direct repeats and also one of the repeats. In this case the repair is highly efficient, and caused the deletion of one of the repeats (Krejci *et al.*, 2012).

Stability and resolution of HJs is essential for the conclusion of the recombination. HJs can be resolved in two different ways: by nucleases and by helicases and topoisomerases complexes. In the first case, both in yeast and humans, have been identified the endonuclease Yen1/GEN1 (Ip *et al.*, 2008), or the complex Mms4-Mus81 in yeast and SLX-MUS in humans (Ciccia and Elledge, 2010; Sarbajna *et al.*,

2014). These enzymes, called resolvases, are able to recognize particular DNA structures and resolve them, generating CO or NCO products depending on the manner in which the DNA strands are bound to each other (Ip *et al.*, 2008). Especially in human cells, the CO products can be dangerous for genomic stability. In fact, if recombination occurs between homologous chromosomes, can lead to the loss of genetic information, defined as Loss Of Heterozygosity (LOH), given that the sequence of a portion of chromosome is duplicated on the other (Moynahan and Jasin, 2010). In addition, COs may be responsible for deletions leading to the loss or acquisition of DNA fragments. In conclusion, both in human and yeast cells there is a propensity for repair through SDSA, which is achieved through specific complexes involved in the destabilization of the D-loop or the dissolution of HJs. Among these, there are the mammalian helicases RECQ5, FANCJ and BLM and yeast helicases Srs2 and Sgs1. Srs2 and Sgs1 eliminate Rad51 from ssDNA and then break the D-loop promoting the repair of DSBs by SDSA (Branzei and Foiani, 2007; Krejci *et al.*, 2012).

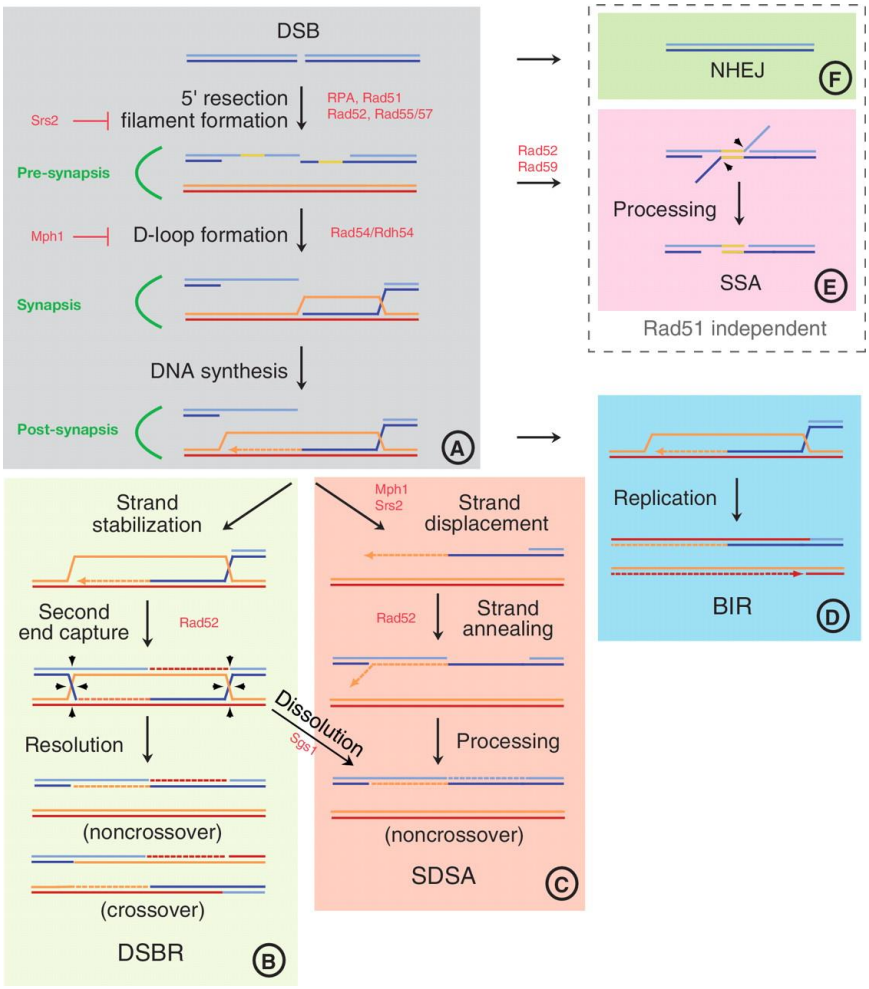

Figure 3. Figure 1. Models for the repair of DNA double-strand breaks. DNA DSBs are resected to generate 3'-protruding ends followed by formation of Rad51 filaments that invade into homologous template to form D-loop structures. A) After priming DNA synthesis, three pathways can be invoked. In the DSBR pathway, the second end is captured and a dHJ intermediate is formed. B) Resolution of dHJs can occur in either plane to generate crossover or non-crossover products. Alternatively, dHJs can be dissolved by the action of Sgs1-Top1-Rmi1 complex to generate only non-crossovers. C) In the SDSA pathway, the extended nascent strand is displaced, followed by pairing with the other 3'-single-stranded tail, and DNA synthesis completes repair. Nucleolytic trimming might be also required. D) In the third

pathway of BIR, which can act when the second end is absent, the D-loop intermediate turns into a replication fork capable of both lagging and leading strand synthesis. Two other Rad51-independent recombinational repair pathways are also depicted. E) In SSA, extensive resection can reveal complementary sequences at two repeats, allowing annealing. The 3'-tails are removed nucleolytically and the nicks are ligated. SSA leads to the deletion of one of the repeats and the intervening DNA. F) Finally, the ends of DSB can be directly ligated resulting in NHEJ. Newly synthesized DNA is represented by dashed lines. (Krejci *et al.*, 2012).

Resection: a crucial step in DSB repair

The repair of DNA double-strand breaks by homologous recombination initiates by nucleolytic degradation of the 5'-terminated strand of the DNA break. This leads to the formation of 3'-tailed DNA, which serves as a substrate for the strand exchange protein Rad51. The nucleoprotein filament then invades homologous DNA to drive template-directed repair. Long tracts of ssDNA are also required for activation of the DNA damage checkpoint response. Thus, identifying the proteins required and the underlying mechanism for DNA end resection has been an intense area of investigation. The initiation of resection is a critical determinant for repair pathway choice. Once resection has initiated, the DNA ends become poor substrates for binding by Ku complex and cells are committed to HR (Fig. 2). Not surprisingly, resection is regulated during the cell cycle to ensure commitment to HR is coordinated with DNA replication, and occurs primarily in S and G2 phases of the cell cycle when a sister chromatid is available as a repair template (Symington and Gautier, 2011).

Genetic studies in *S. cerevisiae* show that end resection takes place in two steps. Initially, a short oligonucleotide tract is removed from the 5' strand to create an early intermediate with a short 3' overhang. Then in a second step the early intermediate is rapidly processed generating an extensive tract of ssDNA. The first step is dependent on the highly conserved MRX complex and Sae2, while the second step employs the exonuclease Exo1 and the helicase Sgs1 with the endonuclease Dna2. Resection mechanisms are highly conserved between yeast and humans, and analogous machineries are found in prokaryotes as well (Cejka, 2015).

Positive regulators of DSB resection

DSB repair by HR initiates by the 5'-3' resection of the DNA ends to create ssDNA, the substrate for Rad51 binding. The mechanisms of DNA end resection in *S. cerevisiae* includes short-range resection by the MRX complex and Sae2 protein, and a processive long-range resection by Sgs1-Dna2 or Exo1 pathways.

The MRX (Mre11, Rad50, Xrs2) complex in yeast or MRN complex (MRE11, RAD50, NBS1) in mammal initiates DSB resection together with the Sae2 protein (CtIP in human) (Clerici *et al.*, 2005). MRX has an affinity for DNA ends, and was shown to be one of the first proteins recruited to DSBs (Lisby *et al.*, 2004). It has both catalytic and structural roles in DNA end processing. The intrinsic nuclease activity of Mre11 is capable of degrading 5'-terminated DNA in the

vicinity of the DNA end. Mre11 exhibits 3'-5' dsDNA DNA exonuclease activity and ssDNA endonuclease activity (Paull and Gellert, 1998; Trujillo *et al.*, 1998). The structural role of MRX involves recruitment of components belonging to the second long-range processing step (Zhu *et al.*, 2008; Mimitou and Symington, 2008; Niu *et al.*, 2010; Cejka *et al.*, 2010). The MRX complex likely functions as a dimer (Hopfner *et al.*, 2002; Hohl *et al.*, 2011). It has DNA binding activity with a preference toward DNA ends (Trujillo *et al.*, 2003). The Rad50 subunit is an ATPase that controls conformation changes within the complex upon DNA binding, which regulates its functions in DNA end tethering, resection, and DNA damage signaling (Deshpande *et al.*, 2014). *In vitro*, Mre11 is a manganese-dependent exonuclease that is moderately stimulated by Xrs2 (Trujillo *et al.*, 2003). Mre11 also has a much weaker endonuclease activity on diverse secondary structures that is moderately promoted by Rad50 in the presence of ATP. It has been demonstrated that Sae2 strongly promotes the endonuclease of Mre11 within the MRX complex (Cannavo and Cejka, 2014). The preferential cleavage of the 5'-terminated DNA suggests that the Mre11 nuclease initiates DNA resection via its Sae2-promoted endonuclease, rather than exonuclease activity (Cannavo and Cejka, 2014). It has been proposed that MRX together with Sae2 can remove oligonucleotides from the 5' ends of the break, giving rise to short 3'-

ended ssDNA tails of 50-200 nucleotides that are then subjected to extensive resection (Mimitou *et al.*, 2008; Zhu *et al.*, 2008) (Fig. 4).

Sae2 involvement in DSB processing is conserved among eukaryotes, as also its putative ortholog in humans CtIP have critical functions in DSB resection (Sartori *et al.*, 2007). The regulation of resection mainly involves the kinase activity of cyclin-CDK complexes. In *S. cerevisiae* it was demonstrated that the kinase Cdk1 is essential for allowing the resection in cells arrested in G2 and to induce the repair by HR (Ira *et al.*, 2004). The function of Sae2 in end resection requires its phosphorylation on Ser267 by Cyclin-Dependent Kinases (CDK) (Huertas *et al.*, 2008). In fact, a *sae2-S267A* mutant exhibits defective generation of 3'-ended ssDNA and reduced HR-mediated DSB repair. Therefore, the CDK dependent regulation of Sae2 activity represents one of the key control mechanisms ensuring that resection only takes place in the S/G2 phase of the cell cycle when a homologous template is available for repair. In addition to CDK, Sae2 is also regulated by the Mec1 and Tel1 kinases in response to DNA damage (Cejka, 2015).

The requirement for MRX and Sae2 in end resection depends upon the nature of DNA ends. The initial endonucleolytic cleavage of the 5' strands catalyzed by MRX and Sae2 is crucial for the processing of "dirty" DNA ends such as those created after exposure to IR, CPT, bleomycin and methylating agents, where protein-DNA adducts or altered DSB ends structures must be removed to allow further

processing. Conversely, resection of "clean" DSB ends, such as those generated by endonucleases, can occur also in the absence of MRX and Sae2 (Gobbini *et al.*, 2013). In fact, initiation of resection at an endonuclease-induced DSB is impaired in cells lacking MRX or Sae2, but once resection is initiated its rate is similar to that of wild type cells (Clerici *et al.*, 2005). It is worth noting that the defect in initiating resection is more severe in *mre11*Δ cells than in *sae2*Δ cells or *mre11* nuclease defective mutants, and this difference is likely due to reduced recruitment at DSBs of other proteins involved in resection (Sgs1, Dna2 and Exo1) rather than to a specific requirement for MRX to initiate resection (Gobbini *et al.*, 2013).

More extensive DSB resection is catalyzed by the 5'-3' exonuclease Exo1 and the 3'-5' RecQ helicase Sgs1, which control two partially redundant pathways (Mimitou *et al.*, 2008; Zhu *et al.*, 2008) (Fig. 4). Inactivation of a single pathway results in only a minor resection defect, because the other pathway can effectively compensate. Major resection defects were only revealed when both pathways were inactivated simultaneously, for example in *sgs1*Δ *exo1*Δ double mutants (Zhu *et al.*, 2008; Mimitou and Symington, 2008). The extension of resection generates a longer ssDNA fragment 3' protruding necessary to activate the subsequent step of HR.

Sgs1 is a DNA helicase belonging to the RecQ family (Cejka and Kowalczykowski, 2010). Sgs1 translocates with a 3'-5' polarity on one DNA strand and unwinds DNA. Unwound ssDNA is coated by

RPA, which directs the nucleolytic activity of Dna2 toward the 5'-terminated DNA strand. Then the ssDNA formed by Sgs1-mediated DNA unwinding is degraded by the endonuclease Dna2, which is a CDK target in DSB resection (Chen *et al.*, 2011). Sgs1 interacts with the type I topoisomerase Top3 and the oligonucleotide/ oligosaccharide-binding (OB)-fold containing protein Rmi1 to form the STR complex (Cejka *et al.*, 2010; Niu *et al.*, 2010). In *S. cerevisiae*, Sgs1 has been implicated in the resection since *sgs1*Δ mutant show defects in extensive resection (Zhu *et al.*, 2008). The double mutants *sgs1*Δ *top3*Δ or *sgs1*Δ *rmi1*Δ show resection defects comparable to those of single *sgs1*Δ mutant, demonstrating that the topoisomerase activity of the complex is not required and that Top3-Rmi1 play a structural and not catalytic role (Zhu *et al.*, 2008).

Dna2 is a bifunctional helicase-nuclease, which possess both 3'-5' and 5'-3' nuclease activities and a DNA helicase activity with a 5'-3' polarity. Dna2 must load on a free ssDNA end but then degrades DNA endonucleolytically, resulting in degradation products of 5-10 nucleotides in length (Zhu *et al.*, 2008; Niu *et al.*, 2010; Cejka *et al.*, 2010).

Both Sgs1 and Dna2 have separate functions unrelated to DNA end resection. Sgs1 functions together with Top3 and Rmi1 to dissolve dHJs into NCO products, thereby preventing sister chromatid exchanges and chromosome instability. Dna2 is responsible for removing DNA flaps arising by strand displacement synthesis by

DNA polymerase δ during lagging strand DNA synthesis. The Okazaki fragment processing function of Dna2 is essential, although the viability of *dna2*Δ mutants can be rescued by multiple mechanisms (Cejka, 2015).

Exo1 is an exonuclease with 5'-3' nuclease activity. Unlike the Dna2 nuclease that is specific for ssDNA, the nuclease activity of Exo1 degrades the 5'-terminated strand within dsDNA (Tran *et al.*, 2002). Therefore, Exo1 does not require a helicase partner to unwind DNA, and directly produces the required 3'-tailed DNA (Tran *et al.*, 2002). The MRX complex provides a structural role to stimulate Exo1 (Shim *et al.*, 2010), which is further enhanced by Sae2. However, efficient Exo1-dependent resection occurred even in the absence of the MRX complex *in vivo*, suggesting that other factors may promote the Exo1 nuclease (Zhu *et al.*, 2008; Mimitou and Symington, 2008)

Recruitment of Sgs1, Dna2 and Exo1 to DSBs requires the MRX complex (Shim *et al.*, 2010), and this can explain why *mre11*Δ cells have more severe resection defects than *sae2*Δ and *mre11* nuclease defective mutants. By contrast, Sgs1 and Dna2 are still recruited in *sae2*Δ and *mre11* nuclease defective mutants, indicating that these proteins can compensate for MRX-Sae2 nuclease function in initiation of resection (Gobbini *et al.*, 2013).

Resection in humans occurs via two pathways, which are similar to those described for *S. cerevisiae*. In one of them, BLM, the human counterpart of Sgs1, and DNA2 physically interact and collaborate in

5'-3' resection of DNA ends, while MRN promotes resection by recruiting BLM to DNA ends (Nimonkar *et al.*, 2008). In addition, DNA2 also interacts with another RecQ family helicase, Werner (WRN). In the second pathway, MRN, RPA and BLM stimulate resection by promoting the action of human EXO1 to DNA ends, with BLM enhancing EXO1 affinity for DSB ends and MRN increasing EXO1 processivity (Nimonkar *et al.*, 2011).

DSB resection is also influenced by histone modifications and ATP-dependent chromatin remodeling reactions (Seeber *et al.*, 2013). For example, the chromatin remodeler Fun30 promotes DSB resection by removing Rad9 from the DSB ends. Interestingly, recent data indicate that Exo1- and Sgs1/Dna2-mediated DSB processing require distinct chromatin remodeling events. In fact, either removal of H2A-H2B dimers or incorporation of the histone variant H2A.Z markedly enhances Exo1 activity, suggesting that ATP-dependent chromatin-remodeling enzymes regulate Exo1-mediated resection. By contrast, resection by the Sgs1-Dna2 machinery remains efficient when chromatin fibers are subsaturated with nucleosomes, suggesting that initiation of resection by this pathway might simply require a nucleosome-free gap next to the DSB. Consistent with this hypothesis, the helicase activity of yeast Sgs1 is reduced on nucleosomal substrates, and efficient resection by the Sgs1-Dna2-dependent machinery requires a nucleosome-free gap adjacent to the DSB (Gobbini *et al.*, 2013).

Negative regulators of DSB resection

DNA end resection is also negatively regulated to prevent that nucleolytic degradation takes place in a different phase of cell cycle and to avoid the generation of excessive ssDNA. In particular, deletion of *YKU70* or *YKU80* allows DSB resection in *S. cerevisiae* G1 cells. Ku and the MRX complex have been shown to bind independently and simultaneously the DSB ends. Moreover, G1 cells lacking Ku show an increased recruitment of Mre11 at the DSB ends, whereas loss of MRX increases Ku binding (Gobbini *et al.*, 2013). These results suggest that Ku and MRX compete for binding to DSBs and that DSB-bound Ku limits the formation of ssDNA by impairing the loading and/or the activity of resection factors. Notably, resection of a single DSB in Ku-deficient G1 cells occurs independently of CDK activity, although it is limited to DNA regions close to the break site (Clerici *et al.*, 2008). This finding indicates that Ku is the principal rate-limiting factor for initiation of resection in G1, and its action is prevented in G2 by CDK-dependent phosphorylation events. Interestingly, the lack of Ku suppresses the DNA damage sensitivity of Sae2-deficient cells, and this suppression requires both Exo1 and Sgs1 (Mimitou and Symington, 2010). These results suggest that CDK-mediated Sae2 activation promotes Exo1 and Dna2 action by removing Ku from DNA ends (Fig. 4).

The negative regulation of Ku complex in DSB resection is conserved also in mammalian cells. Human Ku (KU70 and KU80) blocks

EXO1-mediated DNA end resection. Unlike in yeast, the displacement of Ku from DNA ends is not mediated by the MRN complex (Sun *et al.*, 2012).

Extensive DSB resection is inhibited by the checkpoint adaptor protein Rad9, which acts as a barrier toward nucleases and end processing enzymes (Lazzaro *et al.*, 2008). The role of Rad9 as negative regulator derives from its ability to bind ssDNA determining the formation of a barrier that prevents the resection of DNA ends (Fig. 4) (Lee *et al.*, 1998). In fact, *rad9*Δ is characterized by a more rapid and efficient resection if compared to wild type cells. The inhibition of DSB resection caused by Rad9 is dependent on its ability to DNA binding via the Tudor domain, which recognizes the methylated histone H3 at Lys79. Moreover, deletion of *RAD9* or *DOT1* partially bypasses the requirement for CDK in DSB resection (Lazzaro *et al.*, 2008).

It has been recently shown that the ATP-dependent chromatin remodeler Fun30 is capable to overcome the Rad9 barrier to resection by promoting both Exo1 and Sgs1/Dna2-dependent pathways (Chen *et al.*, 2012; Eapen *et al.*, 2012) (Fig. 4). This finding suggests that the role for Fun30 during DSB resection is not to disrupt nucleosomes *per se*, but rather to antagonize the resection inhibitor Rad9.

Extension of DSB resection is inhibited by histone H2A modifications. In fact, Rad9 is known to be recruited at the sites of damage by interaction with histone H2A that has been phosphorylated

on Ser129 (γH2A) by Mec1 and Tel1 (Fig. 4) (Shroff *et al.*, 2004; Javaheri *et al.*, 2006; Toh *et al.*, 2006; Hammet at al., 2007).

The human structural and functional ortholog of Rad9 is 53BP1, a protein that interacts with histones and histone-binding proteins. Similarly to *S. cerevisiae* Rad9, mammalian 53BP1 inhibits DSB resection promoted by CtIP in G1. DSB resection is allowed by the removal of 53BP1 from DSB ends, which is promoted by the BRCA1 protein. Moreover, loss of 53BP1 partially rescues the HR defects of BRCA1 mutant cells, confirming that BRCA1 overcomes 53BP1 function at DSBs (Gobbini *et al.*, 2013).

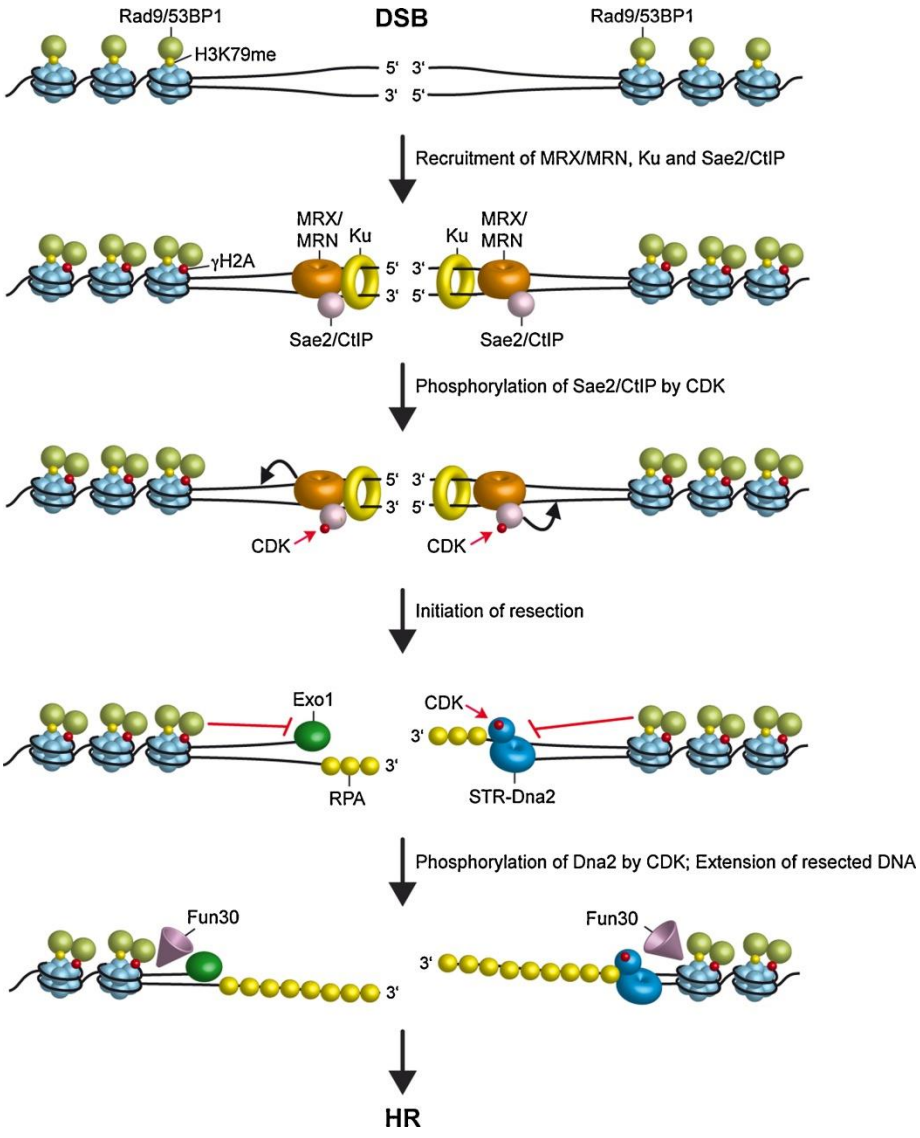

Figure 4. Model for DNA-end resection. MRX/MRN, Ku and Sae2/CtIP rapidly bind DNA ends. Upon phosphorylation of Sae2/CtIP by CDK, MRX/MRN and Sae2/CtIP catalyze the initial processing of the 5' strand. This clipping removes Ku or creates substrates that are no longer bound by Ku. The 5' strand is then extensively processed through two parallel pathways governed by Exo1 and the STR complex in concert with Dna2. MRX facilitates the extensive resection by

promoting the recruitment of Exo1 and STR-Dna2. Extensive DSB resection is inhibited by the checkpoint adaptor protein Rad9/53BP1, which is bound to methylated histone H3 at Lysine 79 (H3K79me) and histone H2A that has been phosphorylated at Serine 129 (γH2A). The chromatin remodeler Fun30 promotes DSB resection by removing Rad9 from the DSB ends. The phosphorylation events are indicated as red dots. (Gobbini *et al.*, 2013)

The DNA damage checkpoint

The DDR ensures the rapid detection and repair of DSBs in order to maintain genome integrity. Central to the DDR is the DNA damage checkpoint response. When activated by DNA damage, these sophisticated surveillance mechanisms induce transient cell cycle arrests, allowing sufficient time for DNA repair. Activation of the DNA damage checkpoint results in cell cycle arrest, activation of transcriptional programs, initiation of DNA repair or, if the damage is too severe, cellular senescence or programmed cell death (Fig. 5) (Ciccia and Elledge, 2010). Once repair is completed, the DNA damage checkpoint response is downregulated and cells reenter the cell cycle in a process known as recovery. Alternatively, if the lesion is irreparable, cells may undergo adaptation and eventually reenter the cell cycle in the presence of DNA damage (Finn *et al.*, 2012).

In *S. cerevisiae*, DNA damage checkpoints operate at three distinct stages in the cell cycle. The G1 checkpoint arrests cells at the G1/S transition prior to START (Fitz Gerald *et al.*, 2002) before cells irreversibly commit to the next cell cycle. This transient arrest delays bud emergence, spindle pole body duplication and S phase entry, allowing time for DNA lesions to be repaired before the onset of DNA

replication (Fitz Gerald *et al.*, 2002). However, certain DNA aberrations such as alkylated DNA do not activate the G1 checkpoint and instead cells pass through START. Essentially, these lesions elicit a checkpoint response during S phase since they need to be converted to secondary lesions during DNA replication before being recognized by the checkpoint machinery (Longhese *et al.*, 2003). The intra-S phase checkpoint slows the rate of replication in response to DNA damage, coordinating fork repair mechanisms and cell cycle progression to ensure the fidelity and completion of replication before cells enter mitosis. The G2/M checkpoint arrests cells at the metaphase to anaphase transition, preventing cells from progressing through mitosis in the presence of DNA damage. The different DNA damage checkpoints share many components and are now known to target many aspects of cellular metabolism besides cell cycle transitions (Finn *et al.*, 2012).

These pathways are highly conserved from yeast to humans. Thus, significant findings in yeast, providing a comprehensive overview of how these signaling pathways function to orchestrate the cellular response to DNA damage and preserve genome stability in eukaryotic cells. Studies of cancer-predisposition syndromes and sporadic tumors in humans have identified mutations in many DNA damage checkpoint genes, underscoring the importance of the checkpoint response. Recent work has also shown that the checkpoint is activated

in early cancerous lesions and may function more generally to prevent human tumorigenesis (Harrison and Haber, 2006).

The checkpoint pathways involve three major groups of proteins that act in concert to transduce the signal of damage in order to promote cell cycle arrest and DNA repair. These groups include: (a) sensor proteins that recognize damaged DNA directly or indirectly and signal the presence of alterations in DNA structure, initiating the transduction cascade; (b) transducer proteins, typically protein kinases, that relay and amplify the damage signal from the sensors by phosphorylating other kinases or downstream target proteins; and (c) effector proteins, which include the most downstream targets of the transducer protein kinases, and are regulated, usually by phosphorylation, to prevent cell cycle progression and initiate DNA repair (Fig. 5) (Nyberg *et al.*, 2002).

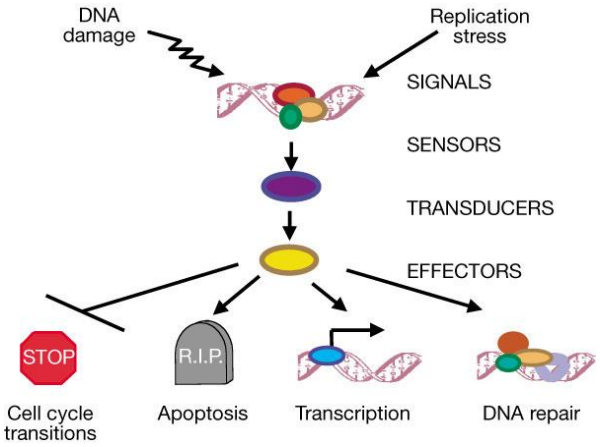

Figure 5. A contemporary view of the general outline of the DNA damage response signal-transduction pathway. Arrowheads represent activating events and perpendicular ends represent inhibitory events. Cell-cycle arrest is depicted with a stop sign, apoptosis with a tombstone. The DNA helix with an arrow represents damage-induced transcription, while the DNA helix with several oval-shaped subunits represents damage-induced repair. For the purpose of simplicity, the network of interacting pathways is depicted as a linear pathway consisting of signals, sensors, transducers and effectors. (Zhou and Elledge, 2000)

The Tel1/ATM and Mec1/ATR checkpoint kinases

Key players in the checkpoint response are mammalian ATM (Ataxia-Telangiectasia-Mutated) and ATR (ATM and Rad3-related) and orthologs *S. cerevisiae* Tel1 and Mec1 (Fig. 6). In collaboration with accessory proteins, these kinases respond to DNA damage by phosphorylating downstream effectors that coordinate cell cycle progression with DNA repair (Ciccia and Elledge, 2010).

In humans, ATM congenital deficiency results in ataxia-telangiectasia (Savitsky *et al.*, 1995), which is a rare, autosomal recessive disorder characterized by progressive cerebellar ataxia, neuro-degeneration, radiosensitivity, checkpoint defects, genome instability and

predisposition to cancer. Similarly, mutations in ATR are associated with Seckel syndrome, a clinically distinct disorder characterized by proportionate growth retardation and severe microcephaly (O'Driscoll *et al.*, 2003).

Mec1/ATR and Tel1/ATM are members of the PIKK family. The consensus motif for phosphorylation is hydrophobic-X-hydrophobic-[S/T]-Q. Other members of the PIKK family include the DNA-dependent protein kinase (DNA-PK), the mammalian target of rapamycin (mTOR). The PIKK enzymes are large proteins (270-450 kDa) that have analogous structures, characterized by N-terminal HEAT repeat domains followed by relatively small kinase domains (Lempiäinen and Halazonetis, 2009). The kinase domain is located near the C-terminus and is flanked by two regions of sequence similarity called FAT (FRAP, ATM, TRRAP) and FATC (FAT C-terminus) domains, which might interact and participate in the regulation of the kinase activity (Bosotti *et al.*, 2000). The remaining part of each protein consists of multiple α-helical HEAT repeats (Perry and Kleckner, 2003), which mediate protein and DNA interactions.

Both Tel1/ATM and Mec1/ATR are activated by DNA damage, but their DNA damage specificities are distinct. Tel1/ATM is activated by DSBs, whereas Mec1/ATR responds to a broad spectrum of DNA lesions that induces the generation of ssDNA (Ciccia and Elledge, 2010).

Tel1/ATM activation requires the MRX/MRN complex. Mre11 contains a C-terminal DNA binding domain as well as a phosphoesterase domain that provides ssDNA endonuclease and 3'-5' dsDNA exonuclease activities (Paull and Gellert, 1998; Trujillo *et al.*, 1998). Cells defective in any component of the MRX/MRN complex are defective in Tel1/ATM activation, indicating that this complex is crucial for Tel1/ATM function. Tel1/ATM is recruited to sites of DNA DSBs through its interaction with the C-terminal domain of Xrs2/NBS1 (Nakada *et al.*, 2003; Lee *et al.*, 2005). Furthermore, Tel1 kinase activity is stimulated by MRX binding to DNA-protein complexes at DSBs (Fukunaga *et al.*, 2011), suggesting that the MRX complex might control Tel1 catalytic activity by monitoring protein binding at DNA ends.

While in human the checkpoint activated by ATM has a strong role, the checkpoint activated by Tel1 is much less significant. In fact, *tel1*Δ cells do not show obvious hypersensitivity to DNA damaging agents and are not defective in checkpoint activation in response to a single DSB (Mantiero *et al.*, 2007). This might be due to differences between ATM and Tel1 in their intrinsic kinase activity and/or in their ability to interact with specific targets and/or DNA-protein complexes at DNA ends. The apparent minor role of Tel1 in DSB signaling may be explained by the ability of yeast cells to rapidly convert the DSB ends into ssDNA substrates that preferentially stimulate Mec1 kinase activity. Thus, although Tel1 contribution to the checkpoint can be

masked by the prevailing activity of Mec1, the mechanism governing ATM- and ATR-dependent checkpoint activation in humans operates also in *S. cerevisiae* (Gobbini *et al.*, 2013).

Full activation of human ATM is dependent on autophosphorylation on Ser1981 and interaction with the MRN complex at the DSB sites. ATM exists as an inactive dimer in unperturbed cells, but it undergoes intermolecular autophosphorylation on Ser1981 after DSB formation or treatment with agents that alter chromatin structure, resulting in dissociation of the dimer into active monomers (Bakkenist *et al.*, 2003). Besides Ser1981, other autophosphorylation sites (Ser367, Ser1893 and Ser2996) play a role in the ATM activation process.

Although ATR is primarily activated by replication stresses, its activation can be promoted also by DNA DSBs. However, in mammals ATR activation is slower than ATM activation and occurs predominantly in the S/G2 phase of the cell cycle. In both yeast and mammals, recruitment of Mec1/ATR at the DSB sites requires the presence of RPA-coated ssDNA 3' overhangs, which are generated by nuclease-mediated DSB resection (Fig. 6). Recognition of RPA-coated ssDNA by Mec1/ATR depends on an Mec1/ATR interacting protein, called Ddc2 in *S. cerevisiae* and ATRIP in mammals. Loss of Ddc2/ATRIP causes the same phenotypes as loss of Mec1/ATR, indicating that Ddc2/ATRIP is required for all known Mec1/ATR functions (Gobbini *et al.*, 2013).

In response to DNA damage, the heterotrimeric ring-shaped complex 9-1-1 (Ddc1-Rad17-Mec3 in *S. cerevisiae*; RAD9-RAD1-HUS1 in humans) is loaded at the junctions between ssDNA and dsDNA by the RFC-like clamp loader, Rad24-Rfc2-5 in S. *cerevisiae* and RAD17-RFC2-5 in mammals.

In budding yeast, co-localization of Mec1-Ddc2 and 9-1-1 at damage sites directly stimulates Mec1 kinase activity (Navadgi-Patil and Burgers, 2009). The Ddc1 subunit of the 9-1-1 complex recruits Dpb11 (ortholog of TopBP1) to DNA damage sites and the interaction between Mec1 and Ddc1, both *in vivo* and *in vitro*, stimulates enzyme activity of Mec1 (Finn *et al.*, 2012). Phosphorylation of Ddc1 by Mec1 is critical for Dpb11 function in checkpoint signaling, suggesting that RPA-recruited Mec1-Ddc2 may have sufficient activity to phosphorylate Ddc1 before Ddc1-Dbp11 interaction takes place. Interestingly, some data in both yeast and mammals suggest that the MRX/MRN complex is involved in Mec1/ATR activation (Gobbini *et al.*, 2013).

In mammals, the 9-1-1 complex has been proposed to stimulate ATR kinase activity by recruiting TopBP1 via an interaction between phosphorylated RAD9 and TopBP1. This interaction facilitates the association of TopBP1 with ATRIP, which in turn stimulates ATR kinase activity (Gobbini *et al.*, 2013).

A challenging question is how Tel1/ATM and Mec1/ATR are coordinated at DSBs. Interestingly, while activation of both ATM and

ATR depends on the ss/dsDNA junctions, they are oppositely regulated by the lengthening of ssDNA (Shiotani and Zou, 2009). Blunt double-strand ends, as well as ends with short single-stranded tails, are the preferred substrates for ATM activation. As the single-stranded tail increases in length, it simultaneously potentiates ATR activation and attenuates ATM activation (Shiotani and Zou, 2009). A similar mechanism has been proposed for budding yeast Tel1, whose signaling activity is disrupted when the DSB ends are subjected to resection (Mantiero *et al.*, 2007). Resection would have two consequences: generation of ssDNA that activates Mec1, and displacement of MRX from the DSB site to limit Tel1/ATM signaling activity. In both yeast and human, Tel1/ATM activation promotes the accumulation of ssDNA at DSB ends and therefore is important for the subsequent activation of Mec1/ATR, ensuring an efficient switch from Tel1/ATM to Mec1/ATR response (Mantiero *et al.*, 2007; Shiotani and Zou, 2009).

Altogether, these data are consistent with a working model where, after DSB formation, binding of MRX/MRN to DNA ends promotes the recruitment of Tel1/ATM to the DSB and subsequent Tel1/ATM-dependent checkpoint activation (Fig. 6). Then, Tel1/ATM promotes the generation of ssDNA, which in turn activates Mec1/ATR and concomitantly inhibits Tel1/ATM signaling. Interestingly, Mec1/ATR itself might regulate the generation of ssDNA at DNA ends, as Mec1-dependent phosphorylation of Sae2 is important for Sae2 function in

DSB resection (Clerici *et al.*, 2006). Furthermore, Mec1 phosphorylates histone H2A on Ser129, and this phosphorylation event seems to regulate the resection rate at DSBs (Eapen *et al.*, 2012). Finally, Mec1 activates the Rad53 checkpoint kinase that phosphorylates Exo1, and this phosphorylation appears to negatively regulate Exo1 activity in resection (Morin *et al.*, 2008). Thus, it is possible that Mec1/ATR might regulate its own activation by acting on the resection machinery, and this can be part of a negative feedback loop to prevent excessive resection (Gobbini *et al.*, 2013).

The Rad53/CHK2 and Chk1/CHK1 effector kinases and their mediators

DNA damage-activated Mec1/ATR and/or Tel1/ATM promote the activation of the downstream yeast effector kinases Rad53 and Chk1 (vertebrate CHK2 and CHK1). In *S. cerevisiae*, Mec1 activates both Rad53 and Chk1, while human ATM and ATR primarily activate CHK2 and CHK1, respectively. Rad53, the principal effector kinase, is essential for the proper response to DNA damage in all cell cycle phases and to replication blocks, while Chk1 is required only for the DNA damage G2/M checkpoint. Once activated, Rad53 and Chk1 phosphorylate several downstream targets that are involved in cell cycle control and transcriptional regulation. On the contrary, CHK1 is the primary effector of both the DNA damage and replication

checkpoints in vertebrates, with CHK2 playing a subsidiary role (Finn *et al.*, 2012).

Activation of the effector kinases requires mediator proteins, among which are the BRCT-domain-containing protein Rad9 (53BP1 in mammals) (Fig. 6) and Mrc1 (Claspin in humans). Rad9 is the mediator required for DNA damage signal transduction and DSB repair. It is required for Rad53 and Chk1 activation. Conversely, Mrc1 is the molecular adaptor required for S phase checkpoint activation and is required for Rad53 activation in response to replication stress. CHK1 activation is mediated by ATR and the adaptor protein Claspin and occurs primarily in response to replication stress and UV-induced DNA damage (Finn *et al.*, 2012).

Recruitment of the Rad9/53BP1 mediator to chromatin involves multiple pathways (Fig. 6). In unperturbed conditions, Rad9 is already bound to chromatin via interaction between its Tudor domain and methylated histone H3 at Lys79 by Dot1 (Giannattasio *et al.*, 2005; Javaheri *et al.*, 2006; Hammet *et al.*, 2007; Granata *et al.*, 2010). This constitutive Rad9 recruitment to chromatin is thought to facilitate the efficiency of the Rad9-dependent response to DNA damage, which requires additional histone modifications. In fact, Rad9 binding to the sites of damage is further strengthened by the interaction between its BRCT domain with histone H2A that has been phosphorylated at Ser129 (γH2A) by Mec1 (Javaheri *et al.*, 2006; Toh *et al.*, 2006; Hammet *et al.*, 2007). Finally, Rad9 is recruited to chromatin through

the interaction with Dpb11 (Granata *et al.*, 2010; Pfander and Diffley, 2011). In particular, phospho-H2A mediated Rad9 recruitment spreads many kilobases around a DNA lesion (Shroff *et al.*, 2004); whereas Dpb11 appears to be more specific at the site of lesion, by binding to a damage-induced phosphorylation in the Ddc1 subunit of the 9-1-1 complex (Pfander and Diffley, 2011). All of these three pathways cooperate for efficient checkpoint arrest and cell survival after genotoxic treatments throughout the cell cycle.

Mrc1 is a component of the replication machinery and a checkpoint mediator that transduces the signal from Mec1 to the effector kinase Rad53 (Alcasabas *et al.*, 2001), which becomes phosphorylated and activated. Mrc1 is only involved in the S phase checkpoint. In fact, *mrc1*Δ cells treated with MMS crossing the shows an S phase faster if compared to wild type cells. Mrc1 is required for the complete activation of Rad53 in response to treatments with HU which inhibits DNA replication (Alcasabas *et al.*, 2001).

Rad9 is phosphorylated in a Mec1- and/or Tel1-dependent manner upon DNA damage, and these phosphorylation events create a binding site for Rad53, which then undergoes in-trans autophosphorylation events required for its full activation as a kinase (Sun *et al.*, 1998; Sweeney *et al.*, 2005). Mec1-dependent phosphorylation of Rad53 allows further autoactivation. Moreover, Rad9 oligomerization is required to maintain checkpoint signaling through a feedback loop involving Rad53-dependent phosphorylation of the Rad9 BRCT

domain (Usui *et al.*, 2009). Fully activated Rad53 is then released from the hyper-phosphorylated Rad9 complex in an ATP-dependent manner (Gilbert *et al.*, 2001). Rad9 also contribute to Chk1 activation with a mechanism involving its N-terminal portion, which is not required for Rad53 activation (Harrison and Haber, 2006).

Rad53 belongs to a subfamily of protein kinases characterized by the presence of one or more phospho-Threonine recognition modules known as ForkHead Associated (FHA) domains (Durocher *et al.*, 1999). Rad53 contains two FHA domains, FHA1 and FHA2, which flank a central Serine/Threonine protein kinase domain (Durocher *et al.*, 1999). Rad9 recruits Rad53 through interaction of phosphorylated Rad9 domains and Rad53' FHA domains, increasing Rad53 concentration at the lesion and facilitating in trans phosphorylation, which induces Rad53 activation (Gilbert *et al.*, 2001). Rad53 contains also two Serine-Glutamine/ Threonine-Glutamine cluster domains (SCD) located N-terminal to FHA1 and immediately C-terminal to the kinase. Mammalian CHK2 is similarly organized but notably with only one SCD and one FHA domain N-terminal to the kinase domain. Within the SCD are clusters of Serine-Glutamine and Threonine-Glutamine (SQ/TQ) motifs, potential target of Mec1 and Tel1.

The two FHA domains of Rad53 are only partially redundant for its activation. Mutation of the FHA2 domain, which strongly interacts with Rad9, reduces Rad53 phosphorylation and the Rad53-Rad9 interaction in MMS-treated cells but not in HU-treated cells (Sun *et*

al., 1998; Schwartz *et al.*, 2003). Mutation of FHA1, which binds more strongly to Rad53 itself, slightly sensitizes cells to HU and impairs the S-phase checkpoint (Sun *et al.*, 1998; Schwartz *et al.*, 2003). Rad53's FHA domains are likely to interact with a cluster of 7 SQ/TQ motifs in Rad9's central region, and mutation of the first 6 of these is sufficient to prevent Rad9 phosphorylation, Rad9-Rad53 binding, Rad53 activation, and checkpoint arrest in damaged cells (Harrison and Haber, 2006).

Activation of Rad53 in vivo requires its phospho-dependent interaction with the signaling adaptors Rad9 and Mrc1 (Sun *et al.*, 1998; Vialard *et al.*, 1998; Durocher *et al.*, 1999). The Rad53-Rad9 interaction is FHA-dependent and occurs following Mec1-dependent phosphorylation of Rad9 at multiple Threonine residues (Emili, 1998; Vialard *et al.*, 1998). Rad9 bound Rad53 proteins are phosphorylated at multiple sites (within the SCD1 by Mec1), which primes Rad53 for activation. Rad53 subsequently undergoes extensive autophosphorylation that is likely facilitated by the clustering of multiple Rad53 molecules on hyperphosphorylated Rad9 (Chen *et al.*, 2014). In particular, autophosphorylation of a key regulatory site in the activation segment, Thr354, is required for the catalytic activation of Rad53.

Loss-of-function mutations of *RAD53* result in loss of viability due to an essential function in maintaining dNTP levels during DNA replication, but hypomorphic *RAD53* mutations result in DNA damage

sensitivity and deficits in nearly all checkpoint responses in yeast (Fay *et al.*, 1997).

In vertebrates, ATR-dependent phosphorylation of Ser317 and Ser345 on CHK1 promotes CHK1 activation by inducing a conformational change that relieves the inhibition of the N-terminal kinase domain by the C-terminal regulatory domain and stimulates the release of CHK1 from chromatin. CHK1 phosphorylates several downstream targets, for example key regulators of the cell cycle. Vertebrate CHK2 is also known to dimerize and trans-autophosphorylate in an ATM-dependent manner (Finn *et al.*, 2012).

Once activated, the checkpoint effector kinases phosphorylate several downstream targets, thus regulating a variety of cellular processes. One of the primary events governed by the checkpoint response is the cell cycle arrest, which is induced by the phosphorylation of different substrates depending on the cell cycle phase in which the DNA damage is detected. The arrest of the cell cycle is likely required to allow DNA repair to occur. Numerous proteins directly involved in this repair have been identified as targets of the checkpoint kinases (Putnam *et al.*, 2009).

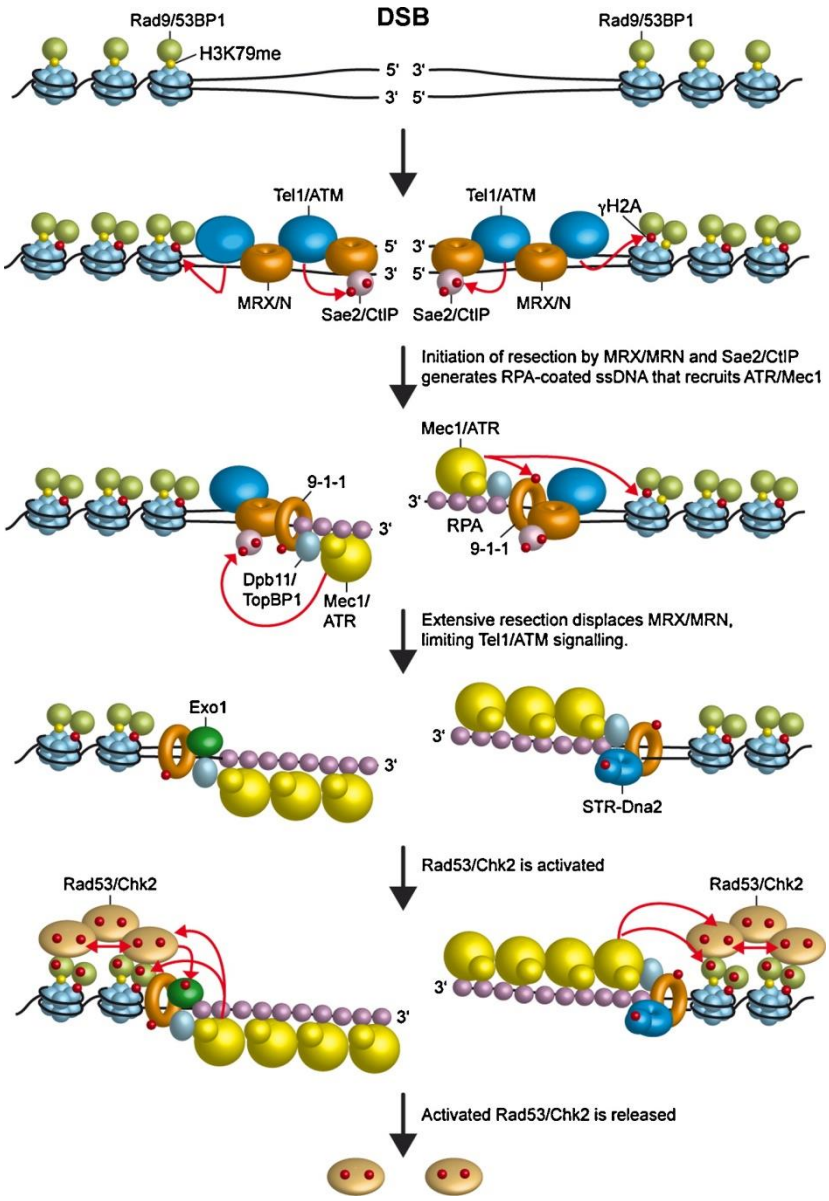

Figure 6. Tel1/ATM and Mec1/ATR activation by DSBs. Recognition of the DSB by MRX/MRN (MRX/N) leads to recruitment of Tel1/ATM, which phosphorylates Sae2/CtIP and histone H2A (γH2A). MRX/MRN, Sae2/CtIP and other nucleases

resect the DSB ends to generate 3'-ended ssDNA tails that, once coated by RPA, allow the loading of the Mec1-Ddc2/ATR-ATRIP complex. Tel1/ATM, possibly by acting on the MRX/MRN complex, promotes DSB resection, which activates Mec1/ATR and concomitantly inhibits Tel1/ATM signaling. Mec1/ATR activation requires Dpb11/TopBP1, the 9-1-1 complex and possibly the MRX/MRN complex itself. Once recruited to the DSB, Mec1/ATR regulates the generation of 3'-ended ssDNA by phosphorylating Sae2/CtIP and histone H2A. Mec1 activates the downstream checkpoint kinase Rad53/Chk2 by phosphorylating Rad9 and Rad53/Chk2 itself. Moreover, phosphorylated Rad9/53BP1 promotes activation of Rad53/Chk2 by allowing its in-trans autophosphorylation. Activated Rad53 is then released from DNA and can regulate both DSB processing by phosphorylating and inhibiting Exo1 and its specific targets in the checkpoint cascade. (Gobbini *et al.*, 2013)

RESULTS

(Bonetti *et al.*, 2015)

EMBO REPORTS

March 2015, Vol. 16, N° 3: 351-361

doi: 10.15252/embr.201439764.

Escape of Sgs1 from Rad9 inhibition reduces the requirement for Sae2 and functional MRX in DNA end resection

Diego Bonetti*, Matteo Villa, Elisa Gobbini,

Corinne Cassani, Giulia Tedeschi, Maria Pia Longhese

Dipartimento di Biotecnologie e Bioscienze, Università di Milano-Bicocca, Milano, Italy.

* Present address: Institute of Molecular Biology (IMB), Mainz, Germany.

DNA Double-Strand Breaks (DSBs) can be repaired by Homologous Recombination (HR), which uses undamaged homologous DNA sequences as a template for repair in a mostly error-free manner. The first step in HR is the processing of DNA ends by 5' to 3' nucleolytic degradation (resection) to generate 3'-ended single-stranded DNA (ssDNA) that can invade a homologous template (Symington and Gautier, 2011). This ssDNA generation also induces activation of the DNA damage checkpoint, whose key players are the protein kinases ATM and ATR in mammals as well as their functional orthologs Tel1 and Mec1 in *Saccharomyces cerevisiae* (Ciccia and Elledge, 2010).

Initiation of DSB resection requires the conserved MRX/MRN complex (Mre11/Rad50/Xrs2 in yeast; MRE11/RAD50/NBS1 in mammals) that, together with Sae2, catalyzes an endonucleolytic cleavage of the 5' strands (Mimitou and Symington, 2008; Zhu *et al.*, 2008; Cannavo and Cejka, 2014). More extensive resection of the 5' strands depends on two pathways, which require the 5' to 3' double-stranded DNA exonuclease Exo1 and the nuclease Dna2 working in concert with the 3' to 5' helicase Sgs1 (Mimitou and Symington, 2008; Zhu *et al.*, 2008).

DSB resection is controlled by the activity of cyclin-dependent kinases (Cdk1 in yeast) (Ira *et al.*, 2004), which promotes DSB resection by phosphorylating Sae2 (Huertas *et al.*, 2008) and Dna2 (Chen *et al.*, 2011), as well as by ATP-dependent nucleosome remodelling complexes (Seeber *et al.*, 2013). Recently, the chromatin

remodeler Fun30 has been shown to be required for extensive resection (Chen *et al.*, 2012; Costelloe et al, 2012; Eapen *et al.*, 2012), possibly because it overcomes the resection barrier exerted by the histone-bound checkpoint protein Rad9 (Lydall and Weinert, 1995; Lazzaro *et al.*, 2008; Chen *et al.*, 2012).

The MRX/Sae2-mediated initial endonucleolytic cleavage becomes essential to initiate DSB resection when covalent modifications or bulky adducts are present at the DSB ends and prevent the access of the long-range Exo1 and Dna2/Sgs1 resection machinery. For example, Sae2 and the MRX nuclease activity are essential during meiosis to remove Spo11 from the 5'-ended strand of the DSBs (Keeney and Kleckner, 1995; Usui at al., 1998). Furthermore, both *sae2*Δ and *mre11* nuclease-defective (*mre11-nd*) mutants exhibit a marked sensitivity to methyl methanesulfonate (MMS) and ionizing radiation (IR), which can generate chemically complex DNA termini, and to camptothecin (CPT), which extends the half-life of topoisomerase I (Top1)-DNA cleavable complexes (Deng *et al.*, 2005). CPT-induced DNA lesions need to be processed by Sae2 and MRX unless the Ku heterodimer is absent. In fact, elimination of Ku restores partial resistance to CPT in both *sae2*Δ and *mre11-nd* cells (Mimitou and Symington, 2010; Foster *et al.*, 2011). This suppression requires Exo1, indicating that Ku increases the requirement for MRX/Sae2 activities in DSB resection by inhibiting Exo1.

To identify other possible mechanisms regulating MRX/Sae2 requirement in DSB resection, we searched for extragenic mutations that suppressed the sensitivity to DNA damaging agents of *sae2*Δ cells. This search allowed the identification of the *SGS1-ss* allele, which suppresses the resection defect of *sae2*Δ cells by escaping Rad9-mediated inhibition of DSB resection. The Sgs1-ss variant is robustly associated with the DSB ends both in the presence and in the absence of Rad9 and resects the DSB more efficiently than wild type Sgs1. Moreover, we found that Rad9 limits the binding at the DSB of Sgs1, which is in turn responsible for rapid resection in *rad9*Δ cells. We propose that Rad9 limits the activity in DSB resection of Sgs1/Dna2 and the escape from this inhibition can reduce the requirement of Sae2 and functional MRX in DSB resection.

Sgs1-ss suppresses the sensitivity to DNA damaging agents of *sae2*Δ and *mre11-nd* mutants

SAE2 deletion causes hypersensitivity to CPT, which creates replication-associated DSBs. The lack of Ku suppresses CPT hypersensitivity of *sae2*Δ mutants, and this rescue requires Exo1 (Mimitou and Symington, 2010; Foster *et al.*, 2011), indicating that Ku prevents Exo1 from initiating DSB resection. To identify other possible pathways bypassing Sae2 function in DSB resection, we searched for extragenic mutations that suppress the CPT sensitivity of *sae2*Δ cells. CPT-resistant *sae2*Δ candidates were crossed to each

other and to the wild type strain to identify, by tetrad analysis, 15 single-gene suppressor mutants that fell into 11 distinct allelism groups. Genome sequencing of the five non-allelic suppressor clones that stood from the others for the best suppression phenotype identified single-base pair substitutions either in the *TOP1* gene, encoding the CPT target topoisomerase I, or in the *PDR3*, *PDR10* and *SAP185* genes, which encode for proteins involved in multi-drug resistance. The mutation responsible for the suppression in the fifth clone was a single-base pair substitution in the *SGS1* gene (*SGS1-ss*), causing the amino acid change Gly1298Arg in the HRDC domain that is conserved in the RecQ helicase family. The identity of the genes that are mutated in the six remaining suppressor clones remained to be determined.

The *SGS1-ss* allele suppressed the sensitivity of the *sae2*Δ mutant not only to CPT, but also to phleomycin (phleo) and MMS, resulting in almost wild type survival of *sae2*Δ *SGS1-ss* cells treated with these drugs (Fig. 7A). The ability of Sgs1-ss to suppress the sensitivity of *sae2*Δ to genotoxic agents was dominant, as *sae2*Δ/*sae2*Δ *SGS1*/*SGS1-ss* diploid cells were less sensitive to CPT, phleomycin and MMS compared to *sae2*Δ/*sae2*Δ *SGS1*/*SGS1* diploid cells (Fig. 7B).

Besides providing the endonuclease activity to initiate DSB resection, MRX also promotes stable association of Exo1, Sgs1 and Dna2 at the DSB ends (Shim *et al.*, 2010), thus explaining the severe resection

defect of cells lacking the MRX complex compared to cells lacking either Sae2 or the Mre11 nuclease activity. Sgs1-ss suppressed the hypersensitivity to genotoxic agents of *mre11-H125N* cells, which were specifically defective in Mre11 nuclease activity (Fig. 7A). By contrast, *mre11*Δ *SGS1-ss* double-mutant cells were as sensitive to genotoxic agents as the *mre11*Δ single mutant (Fig. 7A). Altogether, these findings indicate that Sgs1-ss can bypass the requirement of Sae2 or MRX nuclease activity for survival to genotoxic agents, but it still requires the physical integrity of the MRX complex to exert its function.

Sgs1 promotes DSB resection by acting as a helicase (Mimitou and Symington, 2008; Zhu *et al.*, 2008), prompting us to investigate whether Sgs1-ss requires its helicase activity to exert the suppression effect. Both the lack of Sgs1 and its helicase-dead Sgs1-hd variant, carrying the Lys706Ala amino acid substitution (Mullen *et al.*, 2000), impaired viability of *sae2*Δ cells (Zhu *et al.*, 2008) (Fig. 7C). This synthetic sickness is likely due to poor DSB resection, as it is known to be alleviated by making DNA ends accessible to the Exo1 nuclease (Mimitou and Symington, 2010; Foster *et al.*, 2011). The Lys706Ala substitution was therefore introduced in Sgs1-ss, thus generating the Sgs1-hd-ss variant, and meiotic tetrads from diploid strains double heterozygous for *sae2*Δ and *sgs1-hd-ss* were analyzed for spore viability on YEPD plates. All *sae2*Δ *sgs1-hd-ss* double-mutant spores formed much smaller colonies than each single-mutant spore (Fig.

7D), with a colony size similar to that obtained from *sae2*Δ *sgs1-hd* double-mutant spores (Fig. 7C). Thus, Sgs1-ss appears to require its helicase activity to suppress the lack of Sae2 function.

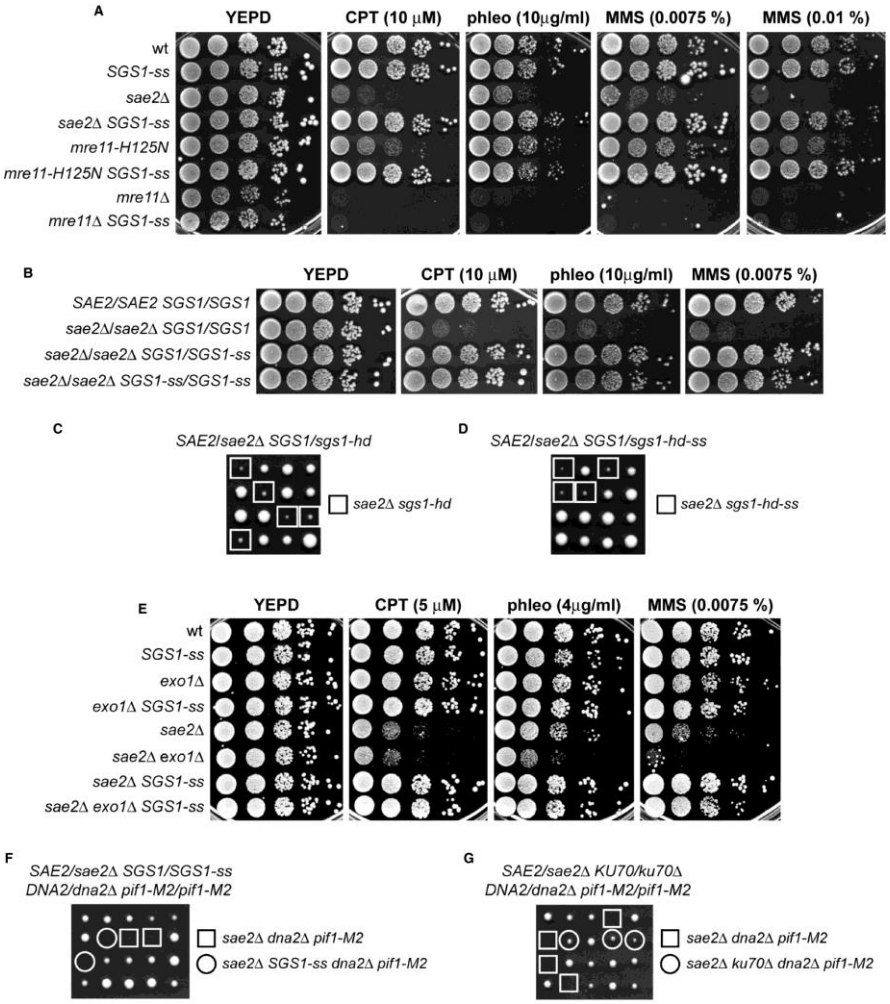

Figure 7. Suppression of the sensitivity to genotoxic agents of *sae2*Δ and *mre11* nuclease-defective mutants by Sgs1-ss. A, B) Exponentially growing cells were serially diluted (1:10), and each dilution was spotted out onto YEPD plates with or without camptothecin (CPT), phleomycin or MMS. C, D) Meiotic tetrads were dissected on YEPD plates that were incubated at 25°C, followed by spore genotyping. E) Exponentially growing cells were serially diluted (1:10), and each dilution was spotted out onto YEPD plates with or without camptothecin (CPT), phleomycin or MMS. F, G) Meiotic tetrads were dissected on YEPD plates that were incubated at 25°C, followed by spore genotyping.

Suppression of *sae2*Δ by Sgs1-ss requires Dna2, but not Exo1

The ssDNA formed by Sgs1 unwinding is degraded by the nuclease Dna2, which acts in DSB resection in a parallel pathway with respect to Exo1 (Zhu *et al.*, 2008). Thus, we asked whether the suppression of *sae2*Δ hypersensitivity to DNA damaging agents by Sgs1-ss requires Exo1 and/or Dna2. Although the lack of Exo1 exacerbated the sensitivity of *sae2*Δ cells to some DNA damaging agents (Fig. 7E), the *SGS1-ss* allele was still capable to suppress the sensitivity to CPT, phleomycin and MMS of *sae2*Δ *exo1*Δ double-mutant cells (Fig. 7E), indicating that the suppression of *sae2*Δ by Sgs1-ss is independent of Exo1.

As *DNA2* is essential for cell viability, *dna2*Δ cells were kept viable by the *pif1-M2* mutation, which impairs the ability of Pif1 to promote formation of long flaps that are substrates for Dna2 (Budd *et al.*, 2006). Diploids homozygous for the *pif1-M2* mutation and heterozygous for *sae2*Δ, *dna2*Δ and *SGS1-ss* were generated, followed by sporulation and tetrads dissection. No viable *sae2*Δ *dna2*Δ *pif1-M2* cells could be recovered, and the presence of the *SGS1-ss* allele did not restore viability of *sae2*Δ *dna2*Δ *pif1-M2* triple-mutant spores (Fig. 7F). By contrast, tetrads from a diploid homozygous for the *pif1-M2* mutation and heterozygous for *sae2*Δ, *dna2*Δ and *ku70*Δ showed that the lack of Ku70, which relieved Exo1 inhibition (Mimitou and Symington, 2010; Foster *et al.*, 2011), restored viability of *dna2*Δ

*sae2*Δ *pif1-M2* spores (Fig. 7G). These findings indicate that Sgs1-ss requires Dna2 to bypass Sae2 requirement.

Sgs1-ss suppresses the adaptation defect of *sae2*Δ cells

A single irreparable DSB triggers a checkpoint-mediated cell cycle arrest. Yeast cells can escape an extended checkpoint arrest and resume cell cycle progression even with an unrepaired DSB (adaptation) (Lee *et al.*, 1998; Pellicioli *et al.*, 2001). Sae2 lacking cells, like other resection deficient mutants, fail to turn off the checkpoint triggered by an unrepaired DSB and remain arrested at G2/M as large budded cells (Usui *et al.*, 2001; Clerici *et al.*, 2006; Eapen *et al.*, 2012; Clerici *et al.*, 2014). To investigate whether Sgs1-ss suppresses the adaptation defect of *sae2*Δ cells, we used JKM139 derivative strains carrying the HO endonuclease gene under the control of a galactose-inducible promoter. Galactose addition leads to generation at the *MAT* locus of a single DSB that cannot be repaired by HR, because the homologous donor loci *HML* or *HMR* are deleted (Lee *et al.*, 1998). When G1-arrested cell cultures were spotted on galactose-containing plates, *sae2*Δ *SGS1-ss* cells formed microcolonies with more than two cells more efficiently than *sae2*Δ cells, which were still arrested at the two-cell dumbbell stage after 24 hours (Fig. 8A). Checkpoint activation was monitored also by following Rad53 phosphorylation, which is required for Rad53 activation and is detectable as a decrease of its electrophoretic

mobility. When galactose was added to exponentially growing cell cultures of the same strains, *sae2*Δ and *sae2*Δ *SGS1-ss* mutant cells showed similar amounts of phosphorylated Rad53 after HO induction (Fig. 8B), indicating that Sgs1-ss did not affect checkpoint activation. However, Rad53 phosphorylation decreased in *sae2*Δ *SGS1-ss* double-mutant cells within 12-14 hours after galactose addition, whereas it persisted longer in *sae2*Δ cells that were defective in re-entering the cell cycle (Fig. 8B). Thus, Sgs1-ss suppresses the inability of *sae2*Δ cells to turn off the checkpoint in the presence of an unrepaired DSB.

The adaptation defect of *sae2*Δ cells has been proposed to be due to an increased persistence at DSBs of the MRX complex, which in turn causes unscheduled Tel1 activation (Clerici *et al.*, 2006; Clerici *et al.*, 2014). We then asked by chromatin immunoprecipitation (ChIP) and quantitative real-time PCR (qPCR) analysis whether Sgs1-ss can reduce the binding of MRX to the DSB ends in *sae2*Δ cells. When HO was induced in exponentially growing cells, the amount of Mre11 bound at the HO-induced DSB end was lower in *sae2*Δ *SGS1-ss* than in *sae2*Δ cells (Fig. 8C). As MRX persistence at the DSB in *sae2*Δ cells has been proposed to be due to defective DSB resection, this finding suggests that Sgs1-ss suppresses the resection defect of *sae2*Δ cells.

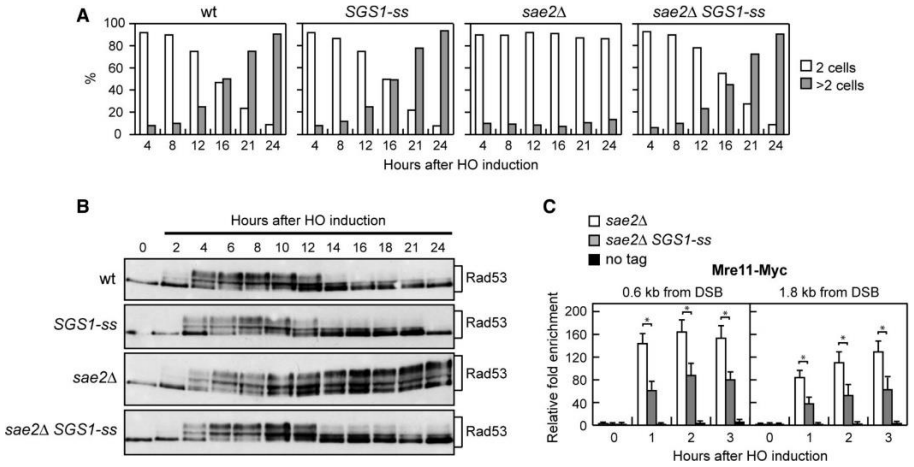

Figure 8. Suppression of the adaptation defect of *sae2*Δ cells by Sgs1-ss. A) YEPR G1-arrested cell cultures of wild type JKM139 derivative strains were plated on galactose-containing plates (time zero). At the indicated time points, 200 cells for each strain were analyzed to determine the frequency of large budded cells and of cells forming microcolonies of more than 2 cells. The mean values from three independent experiments are represented (n=3). B) Exponentially growing YEPR cultures of the strains in (A) were transferred to YEPRG (time zero), followed by Western blot analysis with anti-Rad53 antibodies. C) ChIP analysis. Exponentially growing YEPR cell cultures of JKM139 derivative strains were transferred to YEPRG, followed by ChIP analysis of the recruitment of Mre11-Myc at the indicated distance from the HO-cut compared to untagged Mre11 (no tag). In all diagrams, the ChIP signals were normalized for each time point to the corresponding input signal. The mean values are represented with error bars denoting s.d. (n=3).

Sgs1-ss suppresses the resection defect of *sae2*Δ cells

To investigate whether Sgs1-ss suppresses the sensitivity to genotoxic agents and the adaptation defect of *sae2*Δ cells by restoring DSB resection, we used JKM139 derivative strains to monitor directly generation of ssDNA at the DSB ends (Lee *et al.*, 1998). Because ssDNA is resistant to cleavage by restriction enzymes, we directly monitored ssDNA formation at the irreparable HO-cut by following the loss of SspI restriction fragments after galactose addition by Southern blot analysis under alkaline conditions, using a single-stranded probe that anneals to the 3' end at one side of the break (Fig. 9A). Resection in *sae2*Δ *SGS1-ss* cells was markedly increased compared to *sae2*Δ cells, indicating that Sgs1-ss suppresses the resection defect caused by the lack of Sae2 (Fig. 9B and 9C).

Repair of a DSB flanked by direct repeats occurs primarily by Single-Strand Annealing (SSA), which requires nucleolytic degradation of the 5' DSB ends to reach the complementary DNA sequences that can then anneal (Vaze *et al.*, 2002). To assess whether the Sgs1-ss-mediated suppression of the resection defect caused by the lack of Sae2 was physiologically relevant, we asked whether Sgs1-ss suppresses the SSA defect of *sae2*Δ cells. To this end, we introduced the *SGS1-ss* allele in YMV45 strain, which carries two tandem *leu2* repeats located 4.6 kb apart, with a HO recognition site adjacent to one of the repeats (Vaze *et al.*, 2002). This strain also harbours a *GAL-HO* construct for galactose-inducible *HO* expression. As expected,

accumulation of the repair product was reduced in *sae2*Δ compared to wild type cells, whereas it occurred with almost wild type kinetics in *sae2*Δ *SGS1-ss* double-mutant cells (Fig. 9D and 9E), indicating that Sgs1-ss improves SSA-mediated DSB repair in the absence of Sae2.

Altogether, these findings indicate that Sgs1-ss suppresses both the sensitivity to genotoxic agents of *sae2*Δ cells and the MRX persistence at DSBs by restoring DSB resection. Interestingly, the effects of the *SGS1-ss* mutation are opposite to those of the separation-of-function *sgs1-D664*Δ allele, which specifically impairs viability of *sae2*Δ cells and DSB resection without affecting other Sgs1 functions (Bernstein *et al.*, 2013).

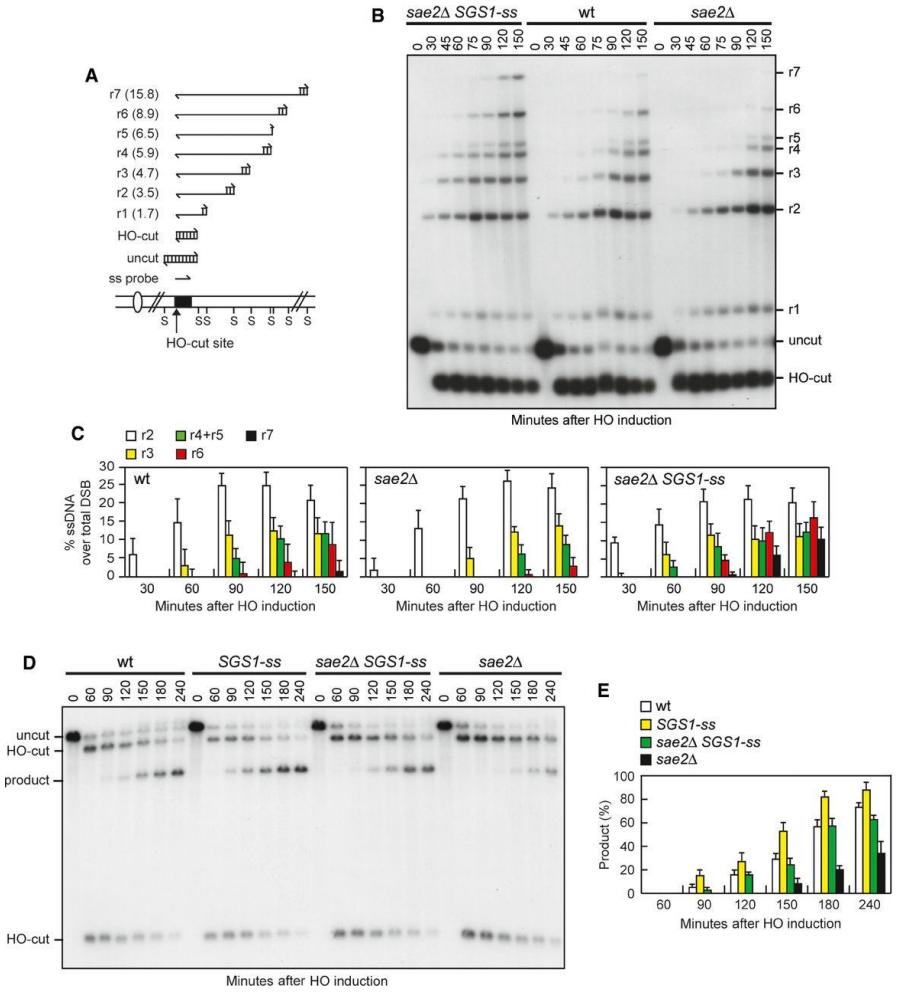

Figure 9. Sgs1-ss suppresses the resection defect of *sae2*Δ cells. A) Method to measure DSB resection. Gel blots of SspI-digested genomic DNA separated on alkaline agarose gel were hybridized with a single-stranded *MAT* probe (ss probe) that anneals to the unresected strand. 5'-3' resection progressively eliminates SspI sites (S), producing larger SspI fragments (r1 through r7) detected by the probe. B) DSB resection. YEPR exponentially growing cell cultures of JKM139 derivative strains were transferred to YEPRG at time zero. Genomic DNA was analyzed for ssDNA formation at the indicated times after HO induction as described in (A). C) Densitometric analyses. The experiment as in (B) has been independently repeated three times, and the mean values are represented with error bars denoting s.d. (n=3).

D) DSB repair by single-strand annealing (SSA). In YMV45 strain, the HO-cut site is flanked by homologous leu2 sequences that are 4.6 kb apart. HO-induced DSB formation results in generation of 12 and 2.5 kb DNA fragments (HO-cut) that can be detected by Southern blot analysis with a *LEU2* probe of KpnI-digested genomic DNA. DSB repair by SSA generates an 8 kb fragment (product). E) Densitometric analysis of the product band signals. The intensity of each band was normalized with respect to a loading control (not shown). The mean values are represented with error bars denoting s.d. (n=3).

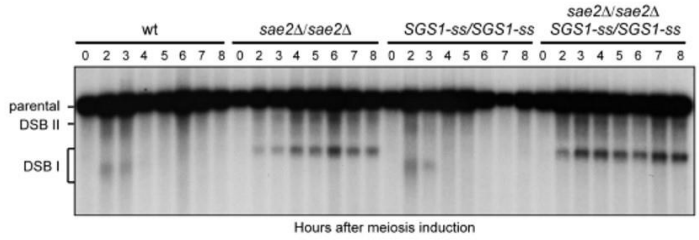

Figure 10. Meiotic DSB formation and processing. Diploid cells were grown to stationary phase in YPA medium and then resuspended in SPM at time zero. Cell samples were collected at the indicated time points after transfer to SPM to analyze meiotic DSB formation by Southern blot analysis. Southern blot was performed on EcoRI-digested genomic DNA run on native agarose gel and the filter was hybridized with a probe complementary to the 5' non-coding region of the *THR4* gene. This probe reveals an intact EcoRI fragment (parental) of 7.9 kb and two bands of 5.7 and 7.1 kb corresponding to the two prominent meiotic DSB sites (DSB I and DSB II).

Sgs1-ss accelerates DSB resection by escaping Rad9 inhibition

The Sgs1-ss mutant variant can bypass Sae2 requirement in initiation of DSB resection either because it allows Dna2 to substitute for Sae2/MRX endonuclease activity or because it increases the resection efficiency. To distinguish between these two possibilities, we asked whether Sgs1-ss could bypass Sae2 requirement in resecting meiotic DSBs, where the Sae2/MRX-mediated endonucleolytic cleavage is absolutely required to initiate DSB resection by allowing the removal of Spo11 from the DSB ends (Keeney and Kleckner, 1995; Usui *et al.*, 1998). A *sae2*Δ/*sae2*Δ *SGS1-ss*/*SGS1-ss* diploid strain was constructed and its kinetics of processing/repair of meiotic DSBs generated at the *THR4* hotspot was compared to those of a *sae2*Δ/*sae2*Δ diploid. DSBs disappeared in both wild type and *SGS1-ss*/*SGS1-ss* cells about 4 hours after transfer to sporulation medium, while they persisted until the end of the experiment in both *sae2*Δ/*sae2*Δ and *sae2*Δ/*sae2*Δ *SGS1-ss*/*SGS1-ss* diploid cells (Fig. 10). Thus, Sgs1-ss cannot substitute the endonucleolytic clipping by Sae2/MRX when this is absolutely required to initiate DSB resection.

Interestingly, the Sgs1-ss mutant variant accelerates both DSB resection and SSA compared to wild type Sgs1 (Fig. 9B-9E), suggesting that Sgs1-ss might increase the resection efficiency by escaping the effect of negative regulators of this process. In particular, Rad9 provides a barrier to resection through an unknown mechanism

(Lydall and Weinert, 1995; Lazzaro *et al.*, 2008). As shown in Fig. 11A and 11B, both *SGS1-ss* and *rad9*Δ mutant cells accumulated the resection products more efficiently than wild type cells, and the presence of Sgs1-ss did not accelerate further the generation of ssDNA in *rad9*Δ cells. Thus, the lack of Rad9 and the presence of Sgs1-ss appear to increase the efficiency of DSB resection through the same mechanism. Furthermore, cells lacking Rad9 displayed sensitivity to CPT and phleomycin (Fig. 11C). Consistent with the finding that the *SGS1-ss* and *rad9*Δ alleles affect the same process, *rad9*Δ was epistatic to *SGS1-ss* with respect to the survival to genotoxic agents, as *sae2*Δ *rad9*Δ *SGS1-ss* cells were as sensitive to CPT and phleomycin as *sae2*Δ *rad9*Δ and *rad9*Δ cells (Fig. 11C).

DSB resection in the G1 phase of the cell cycle is specifically inhibited by the Ku complex, whose lack allows nucleolytic processing in G1 cells independently of Cdk1 activity (Clerici *et al.*, 2008). *RAD9* deletion does not allow DSB resection in G1, but it enhances resection in G1-arrested *ku*Δ cells (Trovesi *et al.*, 2011), indicating that Rad9 inhibits DSB resection in G1, but this function becomes apparent only when Ku is absent. To investigate whether Sgs1-ss was capable to counteract the inhibitory function of Rad9 in G1, we monitored DSB resection in *SGS1-ss* and *ku70*Δ *SGS1-ss* cells that were kept arrested in G1 by α-factor during HO induction. Consistent with the requirement of Cdk1 activity for efficient DSB resection, the 3'-ended resection products were barely detectable in

wild type G1 cells, whereas their amount increased in *ku70*Δ G1 cells that, as previously reported (Clerici *et al.*, 2008), accumulated mostly 1.7, 3.5 and 4.7 kb ssDNA products (r1, r2, r3) (Fig. 12). By contrast, DSB resection in *SGS1-ss* cells was undistinguishable from that observed in wild type cells (Fig. 12), indicating that Sgs1-ss does not allow DSB resection in G1. Furthermore, while *RAD9* deletion enhanced the resection efficiency of *ku70*Δ G1 cells, G1-arrested *ku70*Δ and *ku70*Δ *SGS1-ss* cells accumulated resection products with similar kinetics (Fig. 11D and 11E). Altogether, these findings indicate that Sgs1-ss is not capable to allow DSB resection in G1 either in the presence or in the absence of Ku. As Sgs1-ss function in DSB resection depends on Dna2, whose activity requires Cdk1-mediated phosphorylation (Chen *et al.*, 2011), the inability of Sgs1-ss to overcome both Ku- and Rad9-mediated inhibition in G1 may be due to the requirement of Cdk1 activity to support Dna2 and therefore Sgs1-ss function in DSB resection.

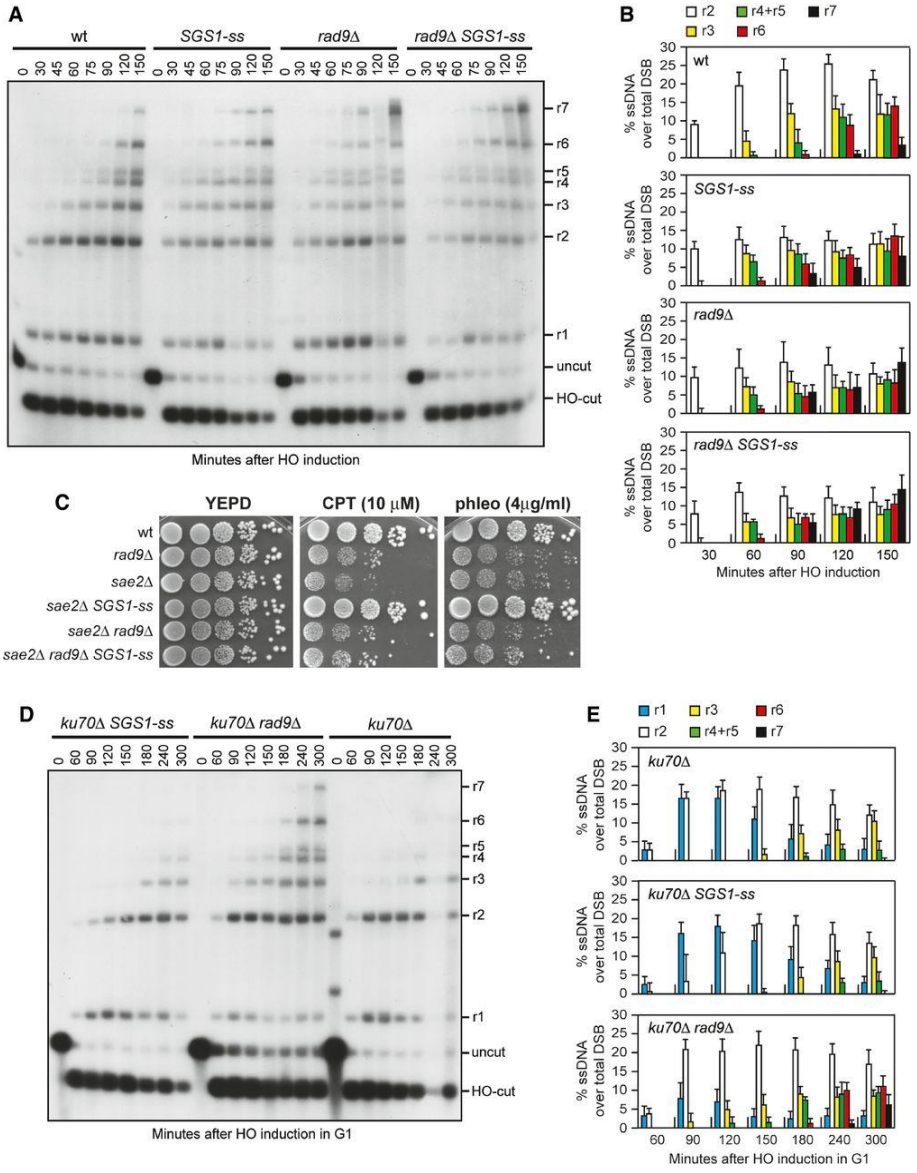

Figure 11. DSB resection is accelerated by the same mechanism in *SGS1-ss* and *rad9*Δ cells. A) DSB resection. YEPR exponentially growing cell cultures of JKM139 derivative strains were transferred to YEPRG at time zero. Genomic DNA was analyzed for ssDNA formation as described in Fig. 9A. B) Densitometric

analyses. The experiment as in (A) has been independently repeated three times, and the mean values are represented with error bars denoting s.d. (n=3). C) Exponentially growing cells were serially diluted (1:10), and each dilution was spotted out onto YEPD plates with or without camptothecin (CPT) or phleomycin. D) DSB resection. HO was induced at time zero in α-factor-arrested JKM139 derivative cells that were kept arrested in G1 with α-factor throughout the experiment. Genomic DNA was analyzed for ssDNA formation as described in Fig. 9A. E) Densitometric analyses. The experiment as in (D) has been independently repeated three times, and the mean values are represented with error bars denoting s.d. (n=3).

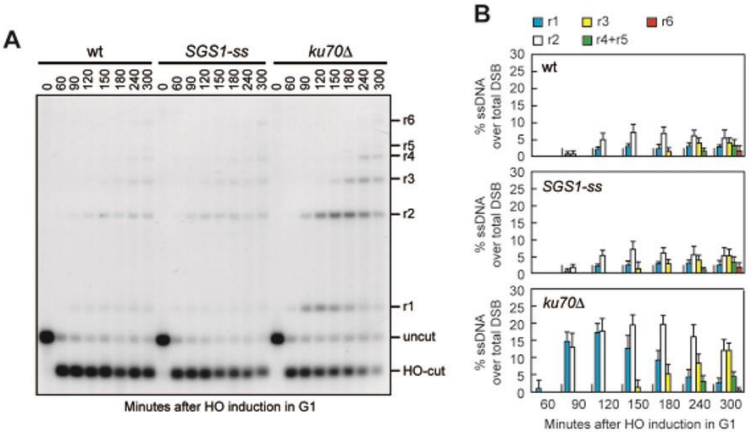

Figure 12. Sgs1-ss does not allow DSB resection in G1. A) DSB resection. HO was induced at time zero in α-factor-arrested JKM139 derivative cells that were kept arrested in G1 with α-factor throughout the experiment. Genomic DNA was analyzed for ssDNA formation at the indicated times after HO induction. B) Densitometric analyses. The experiment as in (A) has been independently repeated three times and the mean values are represented with error bars denoting s.d. (n=3).

Rapid DSB resection in *rad9*Δ cells depends mainly on Sgs1

Generation of ssDNA at uncapped telomeres in *rad9*Δ cells has been shown to be more dependent on Dna2/Sgs1 than on Exo1 (Ngo *et al.*, 2014). This observation, together with the finding that *SGS1-ss* does not accelerate further the generation of ssDNA in *rad9*Δ cells (Fig. 11A and 11B), raises the possibility that Rad9 inhibits DSB resection by limiting Sgs1 activity and that the Sgs1-ss variant can escape this inhibition. We tested this hypothesis by investigating the contribution of Sgs1 and Exo1 to the accelerated DSB resection displayed by *rad9*Δ cells. As shown in Fig. 13A and 13B, *sgs1*Δ was epistatic to *rad9*Δ with respect to DSB resection, as *sgs1*Δ *rad9*Δ double-mutant and *sgs1*Δ single-mutant cells resected the HO-induced DSB with similar kinetics. By contrast, DSB resection in *exo1*Δ *rad9*Δ cells was more efficient than in *exo1*Δ cells, although it was delayed compared to *rad9*Δ cells (Fig. 13C and 13D). Thus, the rapid resection in the absence of Rad9 depends mainly on Sgs1, although also Exo1 contributes to resect the DSB in the absence of Rad9. Consistent with the finding that Sgs1-ss overrides Rad9 inhibition, *SGS1-ss exo1*Δ cells resected the DSB with kinetics similar to that of *rad9*Δ *exo1*Δ cells (Fig. 14).

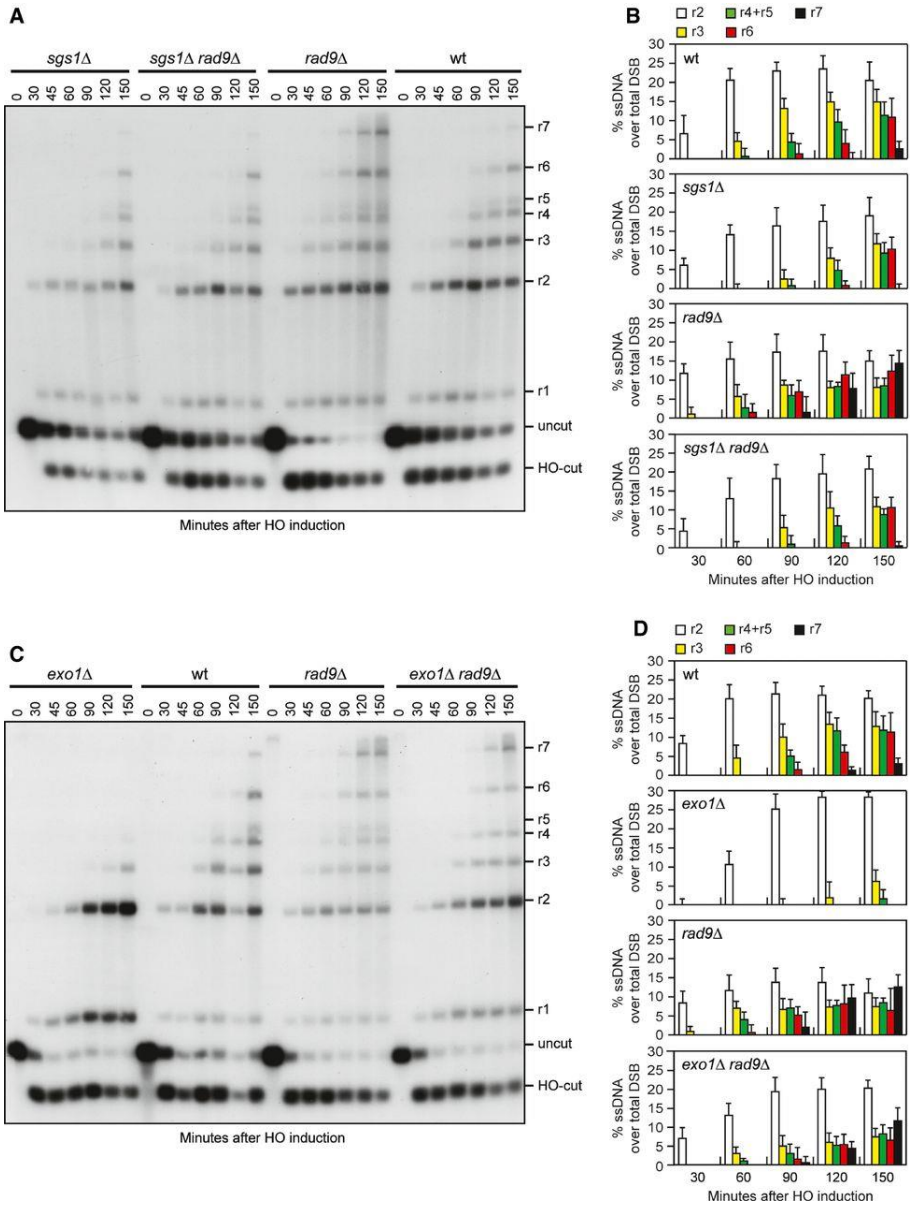

Figure 13. Rapid resection in *rad9*Δ cells depends mainly on Sgs1. A) DSB resection. YEPR exponentially growing cell cultures of JKM139 derivative strains were transferred to YEPRG at time zero. Genomic DNA was analyzed for ssDNA

formation as described in Fig. 9A. B) Densitometric analyses. The experiment as in (A) has been independently repeated three times, and the mean values are represented with error bars denoting s.d. (n=3). C) DSB resection. The experiment was performed as in (A). D) Densitometric analyses. The experiment as in (C) has been independently repeated three times, and the mean values are represented with error bars denoting s.d. (n=3).

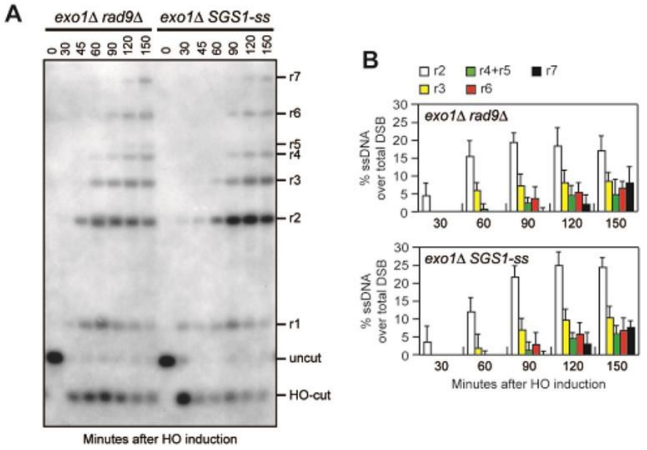

Figure 14. *exo1*Δ *rad9*Δ and *exo1*Δ *SGS1-ss* cells resect the DSB with similar kinetics. A) DSB resection. YEPR exponentially growing cell cultures of JKM139 derivative strains were transferred to YEPRG at time zero. Genomic DNA was analyzed for ssDNA formation at the indicated times after HO induction. B) Densitometric analyses. The experiment as in (A) has been independently repeated three times and the mean values are represented with error bars denoting s.d. (n=3).

Rad9 inhibits DSB resection by limiting Sgs1 association at DNA breaks

If loss of end protection by Rad9 allowed Sgs1 to initiate DSB resection, which normally requires Sae2, then *RAD9* deletion, like Sgs1-ss, should suppress the resection defect of *sae2*Δ cells. Indeed, DSB resection in *sae2*Δ *rad9*Δ cells was as fast as in *rad9*Δ cells, which resected the DSB more efficiently than wild type and *sae2*Δ cells (Fig. 15A and 15B), indicating that the lack of Rad9 bypasses Sae2 function in DSB resection.

We then asked by ChIP and qPCR analysis whether Rad9 limits Sgs1 activity by regulating Sgs1 binding/persistence to the DSB ends. When HO was induced in exponentially growing cells, the amount of Sgs1 bound at the HO-induced DSB was higher in *rad9*Δ than in wild type cells (Fig. 15C), indicating that Rad9 counteracts Sgs1 recruitment to the DSB. Interestingly, the Sgs1-ss variant was recruited at the DSB with equivalent efficiencies in both exponentially growing wild type and *rad9*Δ cells (Fig. 15C). These differences were not due to different resection kinetics, as we obtained similar results also when the HO-induced DSB was generated in G1-arrested cells (Fig. 15D), which resected the DSB very poorly due to the low Cdk1 activity (Ira *et al.*, 2004). Interestingly, the amount of Sgs1-ss bound to the DSB was higher than the amount of wild type Sgs1 in *rad9*Δ cells (Fig. 15C and 15D), suggesting that Sgs1-ss has a higher intrinsic ability to bind/persist at the DSB. Altogether, these results

indicate that Rad9 limits the association of Sgs1 to the DSB ends and that the Sgs1-ss variant escapes this inhibition possibly because it binds more tightly the DSB. Interestingly, the robust association of Sgs1-ss to the DSB in G1-arrested cells (low Cdk1 activity) did not result in DSB resection (Fig. 12) possibly because Sgs1 acts in DSB resection together with Dna2, whose activity requires Cdk1-mediated phosphorylation (Chen *et al.*, 2011). Consistent with a contribution of Exo1 in promoting DSB resection in the absence of Rad9, *rad9*Δ cells showed an increased Exo1 recruitment to the DSB compared to wild type cells (Fig. 15E).

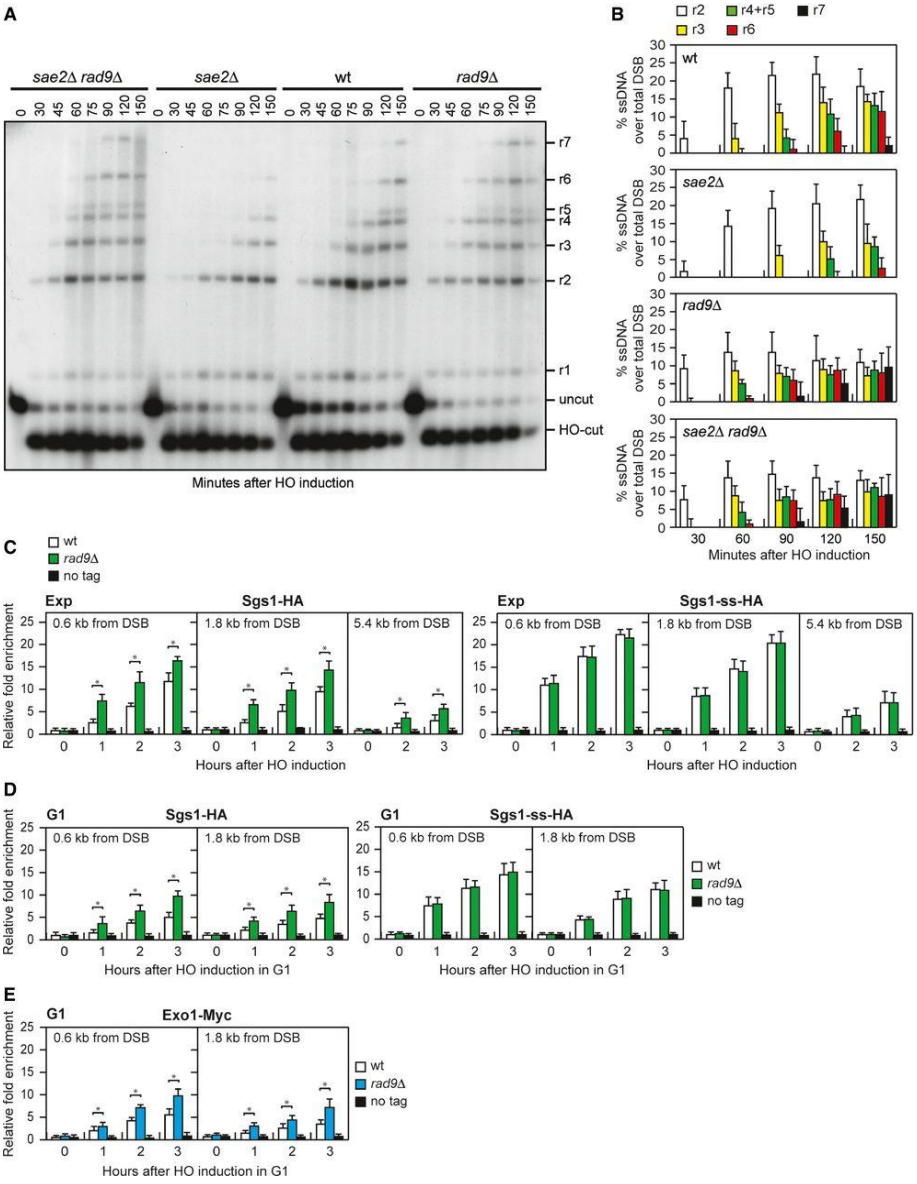

Figure 15. Rad9 inhibits Sgs1 association at the DSBs. A) DSB resection. YEPR exponentially growing cell cultures of JKM139 derivative strains were transferred to YEPRG at time zero. Genomic DNA was analyzed for ssDNA formation as described in Fig. 9A. B) Densitometric analyses. The experiment as in (A) has been

independently repeated three times, and the mean values are represented with error bars denoting s.d. (n=3). C) ChIP analysis. Exponentially growing YEPR cell cultures of JKM139 derivative strains were transferred to YEPRG, followed by ChIP analysis of the recruitment of Sgs1-HA and Sgs1-ss-HA at the indicated distance from the HO-cut compared to untagged Sgs1 (no tag). In all diagrams, the ChIP signals were normalized for each time point to the corresponding input signal. The mean values are represented with error bars denoting s.d. (n=3). D) ChIP analysis in G1-arrested cells. As in (C), but showing ChIP analysis of the recruitment of Sgs1-HA and Sgs1-ss-HA in cells that were kept arrested in G1 by α-factor. The mean values are represented with error bars denoting s.d. (n=3). E) ChIP analysis in G1-arrested cells. As in (C), but showing ChIP analysis of the recruitment of Exo1–Myc in cells that were kept arrested in G1 by α-factor. The mean values are represented with error bars denoting s.d. (n=3).

(Gobbini *et al.*, 2015)

PLOS GENETICS

November 2015, Vol. 11, N° 11: e1005685

doi: 10.1371/journal.pgen.1005685.

Sae2 function at DNA double-strand breaks is bypassed by dampening Tel1 or Rad53 activity

Elisa Gobbini, Matteo Villa, Marco Gnugnoli, Luca Menin, Michela Clerici, Maria Pia Longhese

Dipartimento di Biotecnologie e Bioscienze, Università di Milano-Bicocca, Milano, Italy.

Programmed DNA DSBs are formed during meiotic recombination and rearrangement of the immunoglobulin genes in lymphocytes. Furthermore, potentially harmful DSBs can arise by exposure to environmental factors, such as ionizing radiations and radiomimetic chemicals, or by failures in DNA replication. DSB generation elicits a checkpoint response that depends on the mammalian protein kinases ATM and ATR, whose functional orthologs in *S. cerevisiae* are Tel1 and Mec1, respectively (Gobbini *et al.*, 2013). Tel1/ATM is recruited to DSBs by the MRX (Mre11-Rad50-Xrs2)/MRN (MRE11-RAD50-NBS1) complex, whereas Mec1/ATR recognizes ssDNA covered by Replication Protein A (RPA) (Ciccia and Elledge, 2010). Once activated, Tel1/ATM and Mec1/ATR propagate their checkpoint signals by phosphorylating the downstream checkpoint kinases Rad53 (Chk2 in mammals) and Chk1, to couple cell cycle progression with DNA repair (Ciccia and Elledge, 2010).

Repair of DSBs can occur by either non-homologous end joining (NHEJ) or HR. Whereas NHEJ directly joins the DNA ends, HR uses the sister chromatid or the homologous chromosome to repair DSBs. HR requires that the 5' ends of a DSB are nucleolytically processed (resected) to generate 3'-ended ssDNA that can invade an undamaged homologous DNA template (Mehta and Haber, 2014; Symington and Gautier, 2011). In *S. cerevisiae*, recent characterization of core resection proteins has revealed that DSB resection is initiated by the MRX complex, which catalyzes an endonucleolytic cleavage near a

DSB (Symington and Gautier, 2011), with the Sae2 protein (CtIP in mammals) promoting MRX endonucleolytic activity (Cannavo and Cejka, 2014). This MRX-Sae2-mediated DNA clipping generates 5' DNA ends that are optimal substrates for the nucleases Exo1 and Dna2, the latter working in concert with the helicase Sgs1 (Mimitou and Symington, 2008; Zhu *et al.*, 2008; Cejka *et al.*, 2010; Niu *et al.*, 2010). In addition, the MRX complex recruits Exo1, Sgs1 and Dna2 to DSBs independently of the Mre11 nuclease activity (Shim *et al.*, 2010). DSB resection is also negatively regulated by Ku and Rad9, which inhibit the access to DSBs of Exo1 and Sgs1-Dna2, respectively (Mimitou and Symington, 2010; Foster *et al.*, 2011; Bonetti *et al.*, 2015; Ferrari *et al.*, 2015).

The MRX-Sae2-mediated endonucleolytic cleavage is particularly important to initiate resection at DNA ends that are not easily accessible to Exo1 and Dna2-Sgs1. For instance, both *sae2*Δ and *mre11* nuclease defective mutants are completely unable to resect meiotic DSBs, where the Spo11 topoisomerase-like protein remains covalently attached to the 5'-terminated strands (Keeney and Kleckner, 1995; Usui *et al.*, 1998). Furthermore, the same mutants exhibit a marked sensitivity to CPT, which extends the half-life of DNA-topoisomerase I cleavable complexes (Liu *et al.*, 2002; Deng *et al.*, 2005), and to MMS, which can generate chemically complex DNA termini. The lack of Rad9 or Ku suppresses both the hypersensitivity to DSB-inducing agents and the resection defect of

*sae2*Δ cells (Shim *et al.*, 2010; Mimitou and Symington, 2010; Foster *et al.*, 2011; Bonetti *et al.*, 2015; Ferrari *et al.*, 2015). These suppression events require Dna2-Sgs1 and Exo1, respectively, indicating that Rad9 increases the requirement for MRX-Sae2 activity in DSB resection by inhibiting Sgs1-Dna2 (Bonetti *et al.*, 2015; Ferrari *et al.* 2015), while Ku mainly limits the action of Exo1 (Shim *et al.*, 2010; Mimitou and Symington, 2010; Foster *et al.*, 2011). By contrast, elimination of either Rad9 or Ku does not bypass Sae2/MRX function in resecting meiotic DSBs (Mimitou and Symington, 2010; Bonetti *et al.*, 2015), likely because Sgs1-Dna2 and Exo1 cannot substitute for the Sae2/MRX mediated endonucleolytic cleavage when this event is absolutely required to generate accessible 5'-terminated DNA strands.

Sae2 plays an important role also in modulating the checkpoint response. Checkpoint activation in response to DSBs depends primarily on Mec1, with Tel1 playing a minor role (Mantiero *et al.*, 2007). On the other hand, impaired Mre11 endonuclease activity caused by the lack of Sae2 leads to increased MRX persistence at the DSB ends. The enhanced MRX signaling in turn causes unscheduled Tel1-dependent checkpoint activation that is associated to prolonged Rad53 phosphorylation (Usui *et al.*, 2001; Lisby *et al.*, 2004; Clerici *et al.*, 2006). Mutant *mre11* alleles that reduce MRX binding to DSBs restore DNA damage resistance in *sae2*Δ cells and reduce their persistent checkpoint activation without restoring efficient DSB

resection (Chen *et al.*, 2015; Puddu *et al.*, 2015), suggesting that enhanced MRX association to DSBs contributes to the DNA damage hypersensitivity caused by the lack of Sae2. Persistently bound MRX might increase the sensitivity to DNA damaging agents of *sae2*Δ cells by hyperactivating the DNA damage checkpoint. If this were the case, then the DNA damage hypersensitivity of *sae2*Δ cells should be restored by the lack of Tel1 or of its downstream effector Rad53, as they are responsible for the *sae2*Δ enhanced checkpoint signaling (Usui *et al.*, 2001; Clerici *et al.*, 2006). However, while Rad53 inactivation has never been tested, *TEL1* deletion not only fails to restore DNA damage resistance in *sae2*Δ cells, but also it exacerbates their sensitivity to DNA damaging agents (Chen *et al.*, 2015; Puddu *et al.*, 2015). Therefore, other studies are required to understand whether the Tel1- and Rad53-mediated checkpoint signaling has any role in determining the DNA damage sensitivity of *sae2*Δ cells.

By performing a genetic screen, we identified *rad53* and *tel1* mutant alleles that suppress both the hypersensitivity to DNA damaging agents and the resection defect of *sae2*Δ cells by reducing the amount of Rad9 at DSBs. Decreased Rad9 binding at DNA ends bypasses Sae2 function in DNA damage resistance and resection by relieving the inhibition of the Sgs1-Dna2 resection machinery. Altogether our data suggest that the primary cause of the resection defect of *sae2*Δ cells is Rad9 association to DSBs, which is promoted by persistent Tel1 and Rad53 signaling activities in these cells.

The Rad53-H88Y and Tel1-N2021D variants suppress the DNA damage hypersensitivity of *sae2*Δ cells

We have previously described our search for extragenic mutations that suppress the CPT hypersensitivity of *sae2*Δ cells (Bonetti *et al.*, 2015). This genetic screen identified 15 single-gene suppressor mutants belonging to 11 distinct allelism groups. Analysis of genomic DNA by next-generation Illumina sequencing of 5 non allelic suppressor mutants revealed that the DNA damage resistance was due to single base pair substitutions in the genes encoding Sgs1, Top1, or the multidrug resistance proteins Pdr3, Pdr10 and Sap185 (Bonetti *et al.*, 2015). Subsequent genome sequencing and genetic analysis of 2 more non allelic suppressor mutants allowed to link suppression to either the *rad53-H88Y* mutant allele, causing the replacement of Rad53 amino acid residue His88 by Tyr, or the *tel1-N2021D* allele, resulting in the replacement of Tel1 amino acid residue Asn2021 by Asp. Both *rad53-H88Y* and *tel1-N2021D* alleles restored resistance of *sae2*Δ cells not only to CPT, but also to phleomycin (phleo) and MMS (Fig. 16A). While both *rad53-H88Y* and *tel1-N2021D* fully rescued the hypersensitivity of *sae2*Δ cells to phleomycin and MMS, the CPT hypersensitivity of *sae2*Δ cells was only partially suppressed by the same alleles (Fig. 16A), suggesting that they did not bypass all Sae2 functions.

Both *rad53-H88Y* and *tel1-N2021D* suppressor alleles were recessive, as the sensitivity to genotoxic agents of *sae2*Δ/*sae2*Δ *RAD53*/*rad53*-

H88Y and *sae2*Δ/*sae2*Δ *TEL1*/*tel1-N2021D* diploid cells was similar to that of *sae2*Δ/*sae2*Δ *RAD53*/*RAD53 TEL1*/*TEL1* diploid cells (Fig. 17), suggesting that *rad53-H88Y* and *tel1-N2021D* alleles encode hypomorphic variants. Furthermore, both variants suppressed the hypersensitivity to DNA damaging agents of *sae2*Δ cells by altering the same mechanism, as *sae2*Δ *rad53-H88Y tel1-N2021D* triple mutant cells survived in the presence of DNA damaging agents to the same extent as *sae2*Δ *rad53-H88Y* and *sae2*Δ *tel1-N2021D* double mutant cells (Fig. 16B).

The MRX complex not only provides the nuclease activity for initiation of DSB resection, but also it promotes the binding of Exo1, Sgs1 and Dna2 at the DSB ends (Shim *et al.*, 2010). These MRX multiple roles explain the severe DNA damage hypersensitivity and resection defect of cells lacking any of the MRX subunits compared to cells lacking either Sae2 or the Mre11 nuclease activity. As Sae2 has been proposed to activate Mre11 nuclease activity (Cannavo and Cejka, 2014), we asked whether the suppression of *sae2*Δ DNA damage hypersensitivity by Rad53-H88Y and Tel1-N2021D requires Mre11 nuclease activity. Both *rad53-H88Y* and *tel1-N2021D* alleles suppressed the hypersensitivity to DNA damaging agents of *sae2*Δ cells carrying the nuclease defective *mre11-H125N* allele (Fig. 16C). By contrast, *sae2*Δ *mre11*Δ *rad53-H88Y* and *sae2*Δ *mre11*Δ *tel1-N2021D* triple mutant cells were as sensitive to genotoxic agents as *sae2*Δ *mre11*Δ double mutant cells (Fig. 16D), indicating that neither

the *rad53-H88Y* nor the *tel1-N2021D* allele can suppress the hypersensitivity to DNA damaging agents of *sae2*Δ *mre11*Δ cells. Altogether, these findings indicate that both Rad53-H88Y and Tel1-N2021D require the physical presence of the MRX complex, but not its nuclease activity, to bypass Sae2 function in cell survival to genotoxic agents.

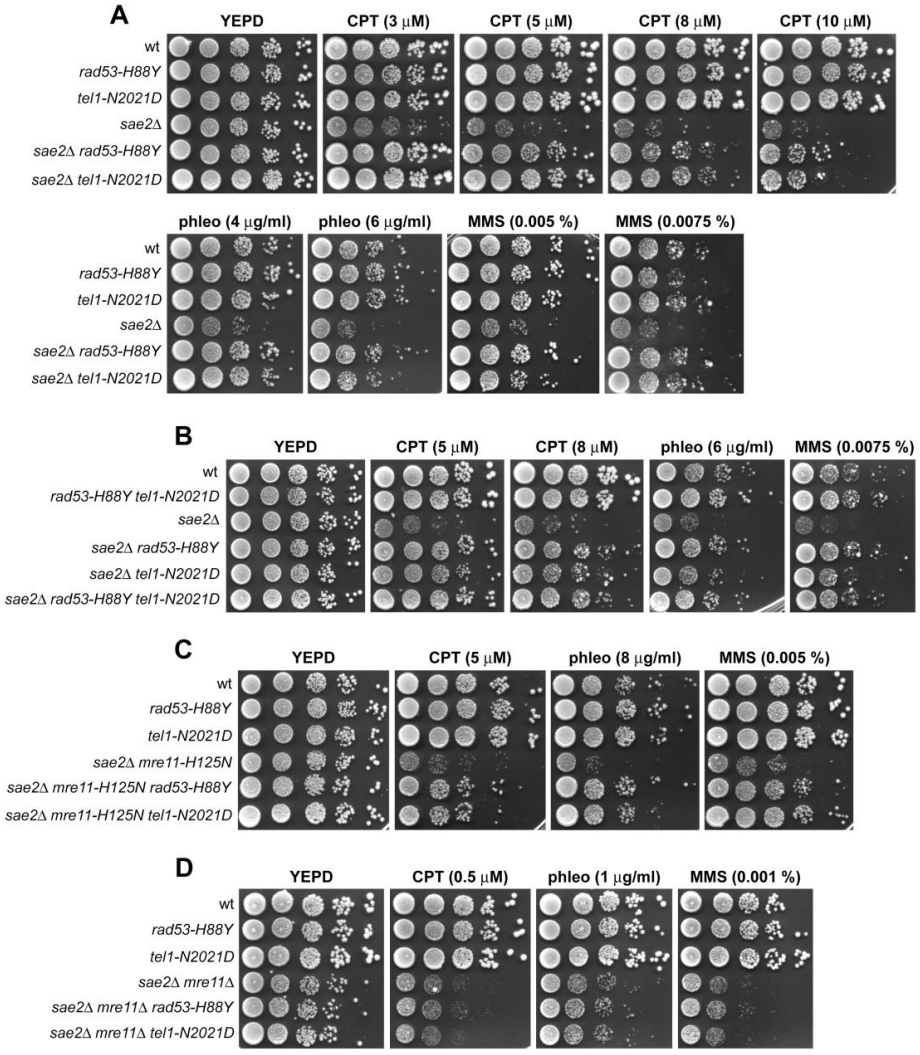

Figure 16. Rad53-H88Y and Tel1-N2021D suppress the hypersensitivity to genotoxic agents of *sae2*Δ cells. A-D) Exponentially growing cells were serially diluted (1:10) and each dilution was spotted out onto YEPD plates with or without camptothecin (CPT), phleomycin or MMS.

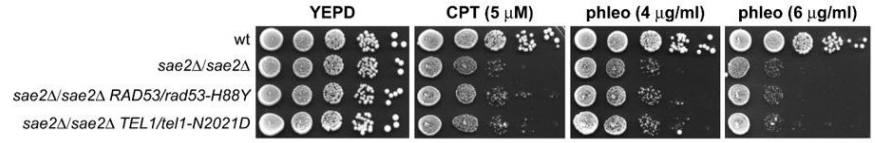

Figure 17. *rad53-H88Y* and *tel11-N2021D* suppressor alleles are recessive. Exponentially growing cells were serially diluted (1:10) and each dilution was spotted out onto YEPD plates with or without camptothecin (CPT) or phleomycin.

The Rad53-H88Y variant is defective in the interaction with Rad9 and bypasses the adaptation defect of *sae2*Δ cells by impairing checkpoint activation

A single unrepairable DSB induces a DNA damage checkpoint that depends primarily on Mec1, with Tel1 playing a minor role (Mantiero *et al.*, 2007). This checkpoint response can be eventually turned off, allowing cells to resume cell cycle progression through a process that is called adaptation (Sandell and Zakian, 1993; Toczyski *et al.*, 1997; Lee *et al.*, 1998). In the absence of Sae2, cells display heightened checkpoint activation that prevents cells from adapting to an unrepaired DSB (Usui *et al.*, 2001; Clerici *et al.*, 2006). This persistent checkpoint activation is due to increased MRX amount/persistence at the DSB that in turn causes enhanced and prolonged Tel1 activation that is associated with persistent Rad53 phosphorylation (Usui *et al.*, 2001; Lisby *et al.*, 2004; Clerici *et al.*, 2006; Fukunaga *et al.*, 2011).

If the *rad53-H88Y* mutation impaired Rad53 activity, then it is expected to suppress the adaptation defect of *sae2*Δ cells by lowering checkpoint activation. We addressed this point by using JKM139 derivative strains, where a single DSB at the *MAT* locus can be generated by expression of the HO endonuclease gene under the control of a galactose-dependent promoter. This DSB cannot be repaired by HR because of the deletion of the homologous donor loci *HML* and *HMR* (Lee *et al.*, 1998). We measured checkpoint activation by monitoring the ability of cells to arrest the cell cycle and to phosphorylate Rad53 after HO induction. Both *rad53-H88Y* and *sae2*Δ *rad53-H88Y* cells formed microcolonies of more than 2 cells with higher efficiency than either wild type or *sae2*Δ cells (Fig. 18A). Furthermore, the Rad53-H88Y variant was poorly phosphorylated after HO induction both in the presence and in the absence of Sae2 (Fig. 18B). Thus, the *rad53-H88Y* mutation suppresses the adaptation defect of *sae2*Δ cells by impairing Rad53 activation.

DNA damage-dependent activation of Rad53 requires its phospho-dependent interaction with Rad9, which acts as a scaffold to allow Rad53 intermolecular authophosphorylation and activation (Sun *et al.*, 1998; Gilbert *et al.*, 2001; Sweeney *et al.*, 2005). Interestingly, the His88 residue, which is replaced by Tyr in the Rad53-H88Y variant, is localized in the forkhead-associated domain 1 of the protein and has been implicated in mediating Rad9-Rad53 interaction (Durocher *et al.*, 1999). Thus, we asked whether the Rad53-H88Y variant was

defective in the interaction with Rad9. When HA-tagged Rad9 was immunoprecipitated with anti-HA antibodies from wild type and *rad53-H88Y* cells grown for 4 hours in the presence of galactose to induce HO, wild type Rad53 could be detected in Rad9-HA immunoprecipitates, whereas Rad53-H88Y did not (Fig. 18C). This defective interaction of Rad53-H88Y with Rad9 could explain the impaired checkpoint activation in *sae2*Δ *rad53-H88Y* double mutant cells.

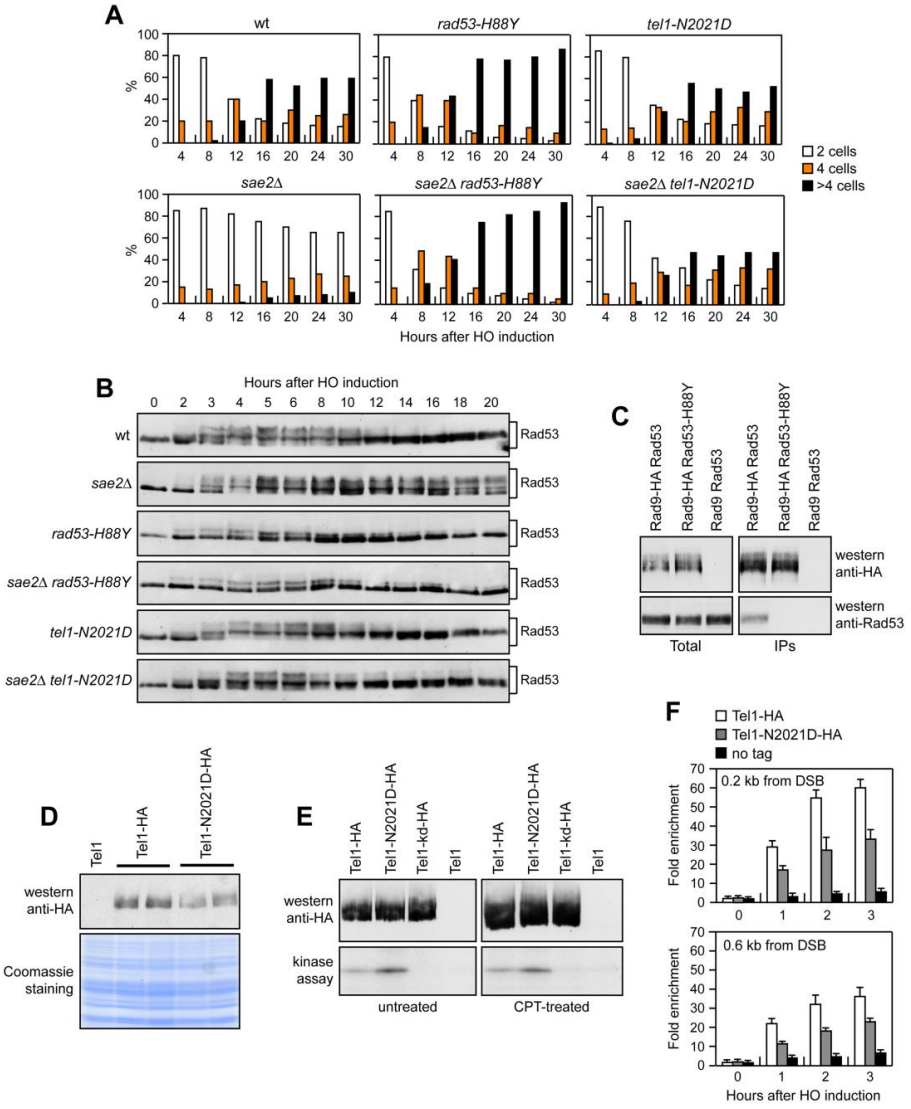

Figure 18. Rad53-H88Y and Tel1-N2021D suppress the checkpoint shut off defect of *sae2*Δ cells. A) YEPR G1-arrested cell cultures of JKM139 derivative strains were plated on galactose-containing plates (time zero). At the indicated time points, 200 cells for each strain were analyzed to determine the frequency of large budded cells (2 cells) and of cells forming microcolonies of 4 or more than 4 cells. B) Exponentially growing YEPR cultures of the strains in (A) were transferred to

YEPRG (time zero), followed by western blot analysis with anti-Rad53 antibodies. C) Protein extracts were analyzed by western blot with anti-HA or anti-Rad53 antibodies either directly (Total) or after Rad9-HA immunoprecipitation (IPs) with anti-HA antibodies. D) Protein extracts from exponentially growing cells were analyzed by western blotting with anti-HA antibodies. The same amounts of protein extracts were separated by SDS-PAGE and stained with Coomassie as loading control. E) Kinase assay was performed on equal amounts of anti-HA immunoprecipitates of protein extracts from cells either exponentially growing in YEPD or after treatment with 50 μM CPT for 1 hour. All the immunoprecipitates were also subjected to western blot analysis using anti-HA antibodies. F) Relative fold enrichment of Tel1-HA and Tel1-N2021D-HA compared to untagged Tel1 (no tag) at the indicated distance from the HO cleavage site was evaluated after ChIP with anti-HA antibodies and qPCR analysis. In all diagrams, the ChIP signals were normalized for each time point to the amount of the corresponding immunoprecipitated protein and input signal. The mean values are represented with error bars denoting s.d. (n=3).

The Tel1-N2021D variant binds poorly to DSBs and bypasses the adaptation defect of *sae2*Δ cells by reducing persistent Rad53 activation

Tel1 signaling activity is responsible for the prolonged Rad53 activation that prevents *sae2*Δ cells to adapt to the checkpoint triggered by an unrepairable DSB (Usui *et al.*, 2001; Clerici *et al.*, 2006). Although telomere length in *tel1-N2021D* mutant cells was unaffected both in the presence and in the absence of Sae2 (Fig. 19), the recessivity of *tel1-N2021D* suppressor effect on *sae2*Δ DNA damage hypersensitivity suggests that the Asn2021Asp substitution impairs Tel1 function. If this were the case, Tel1-N2021D might suppress the adaptation defect of *sae2*Δ cells by reducing the DSB-induced persistent Rad53 phosphorylation. When G1-arrested cell cultures were spotted on galactose containing plates to induce HO,

wild type, *sae2*Δ, *tel1-N2021D* and *sae2*Δ *tel1-N2021D* cells accumulated large budded cells within 4 hours (Fig. 18A). This cell cycle arrest is due to checkpoint activation. In fact, when the same cells exponentially growing in raffinose were transferred to galactose, Rad53 phosphorylation was detectable about 2-3 hours after galactose addition (Fig. 18B). However, while *sae2*Δ cells remained arrested as large budded cells for at least 30 hours (Fig. 18A) and showed persistent Rad53 phosphorylation (Fig. 18B), wild type, *tel1-N2021D* and *sae2*Δ *tel1-N2021D* cells formed microcolonies with more than 2 cells (Fig. 18A) and decreased the amounts of phosphorylated Rad53 (Fig. 18B) with similar kinetics 10-12 hours after HO induction. Therefore, the Tel1-N2021D variant impairs Tel1 signaling activity, as it rescues the *sae2*Δ adaptation defect by reducing the persistent Rad53 phosphorylation.

The Asn2021Asp substitution resides in the Tel1 FAT domain, a helical solenoid that encircles the kinase domain of all the phosphoinositide 3-kinase (PI3K)-related kinases (PIKKs) (Bosotti *et al.*, 2000; Baretić and Williams 2014), suggesting that this amino acid change might reduce Tel1 kinase activity. Western blot analysis revealed that the amount of Tel1-N2021D was slightly lower than that of wild type Tel1 (Fig. 18D). We then immunoprecipitated equivalent amounts of Tel1-HA and Tel1-N2021D-HA variants from both untreated and CPT-treated cells (Fig. 18E, top), and we measured their kinase activity *in vitro* using the known artificial substrate of the

PIKKs family PHAS-I (Phosphorylated Heat and Acid Stable protein) (Mallory and Petes, 2000). Both Tel1-HA and Tel1-N2021D-HA were capable to phosphorylate PHAS-I, with the amount of phosphorylated substrate being slightly higher in Tel1-N2021D-HA than in Tel1-HA immunoprecipitates (Fig. 18E, bottom). This PHAS-I phosphorylation was dependent on Tel1 kinase activity, as it was not detectable when the immunoprecipitates were prepared from strains expressing either kinase dead Tel1-kd-HA or untagged Tel1 (Fig. 18E, bottom). Thus, the *tel1-N2021D* mutation does not affect Tel1 kinase activity.

Interestingly, the FAT domain is in close proximity to the FATC domain, which was shown to be important for Tel1 recruitment to DNA ends (Ogi *et al.*, 2015), suggesting that the Tel1-N2021D variant might be defective in recruitment/association to DSBs. Strikingly, when we analyzed Tel1 and Tel1-N2021D binding at the HO-induced DSB by chromatin immunoprecipitation (ChIP) and quantitative real time PCR (qPCR), the amount of Tel1-N2021D bound at the DSB turned out to be lower than that of wild type Tel1 (Fig. 18F). This decreased Tel1-N2021D association was not due to lower Tel1-N2021D levels, as the ChIP signals were normalized for each time point to the amount of immunoprecipitated protein. Thus, the inability of *sae2*Δ *tel1-N2021D* cells to sustain persistent Rad53 phosphorylation after DSB generation can be explained by a decreased association of Tel1-N2021D to DSBs.

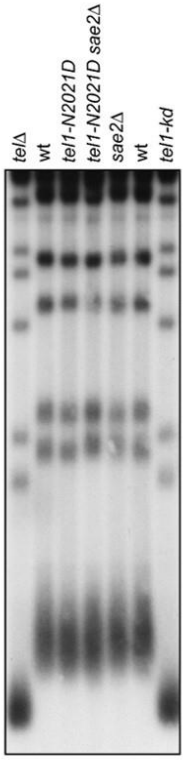

Figure 19. The Tel1-N2021D variant does not affect telomere length. Genomic DNA prepared from exponentially growing cells was digested with XhoI and hybridized with a poly(GT) telomere-specific probe.

Checkpoint-mediated cell cycle arrest is not responsible for the DNA damage hypersensitivity of *sae2*Δ cells

As both Rad53-H88Y and Tel1-N2021D reduce checkpoint signaling in *sae2*Δ cells, we asked whether the increased DNA damage resistance of *sae2*Δ *rad53-H88Y* and *sae2*Δ *tel1-N2021D* cells was due to the elimination of the checkpoint-mediated cell cycle arrest. This hypothesis could not be tested by deleting the *MEC1*, *DDC1*, *RAD24*, *MEC3* or *RAD9* checkpoint genes, because they also regulate DSB resection (Lydall and Weinert, 1995; Jia *et al.*, 2004; Ngo and Lydall, 2015). On the other hand, an HO-induced DSB activates also the Chk1 checkpoint kinase (Pellicioli *et al.*, 2001), which contributes to arrest the cell cycle in response to DSBs by controlling a pathway that is independent of Rad53 (Sanchez *et al.*, 1999). Importantly, *chk1*Δ cells do not display DNA damage hypersensitivity and are not defective in resection of uncapped telomeres (Sanchez *et al.*, 1999; Jia *et al.*, 2004). We therefore asked whether *CHK1* deletion restores DNA damage resistance in *sae2*Δ cells. Consistent with the finding that Chk1 contributes to arrest the cell cycle after DNA damage independently of Rad53 (Sanchez *et al.*, 1999), Rad53 was phosphorylated with wild type kinetics after HO induction in both *chk1*Δ and *sae2*Δ *chk1*Δ cells (Fig. 20A). Furthermore, *CHK1* deletion suppresses the adaptation defect of *sae2*Δ cells. In fact, both *chk1*Δ and *sae2*Δ *chk1*Δ cells spotted on galactose-containing plates formed microcolonies of more than 2 cells with higher efficiency than wild

type and *sae2*Δ cells (Fig. 20B), although they did it less efficiently than *mec1*Δ cells, where both Rad53 and Chk1 signaling were abrogated (Sanchez *et al.*, 1999). Strikingly, the lack of Chk1 did not suppress the hypersensitivity to DNA damaging agents of *sae2*Δ cells (Fig. 20C), although it overrides the checkpoint-mediated cell cycle arrest.

To rule out the possibility that *CHK1* deletion failed to restore DNA damage resistance in *sae2*Δ cells because it impairs DSB resection, we used JKM139 derivative strains to monitor directly generation of ssDNA at the DSB ends in the absence of Chk1. As ssDNA is resistant to cleavage by restriction enzymes, we followed loss of SspI restriction sites as a measure of resection by Southern blot analysis under alkaline conditions, using a single-stranded probe that anneals to the 3' end at one side of the break. Consistent with previous indications that Chk1 is not involved in DNA-end resection (Jia *et al.*, 2004), *chk1*Δ single mutant cells resected the DSB with wild type kinetics (Fig. 20D). Furthermore, *CHK1* deletion did not exacerbate the resection defect of *sae2*Δ cells (Fig. 20E). Altogether, these data indicate that the prolonged checkpoint-mediated cell cycle arrest of *sae2*Δ cells is not responsible for their hypersensitivity to DNA damaging agents.

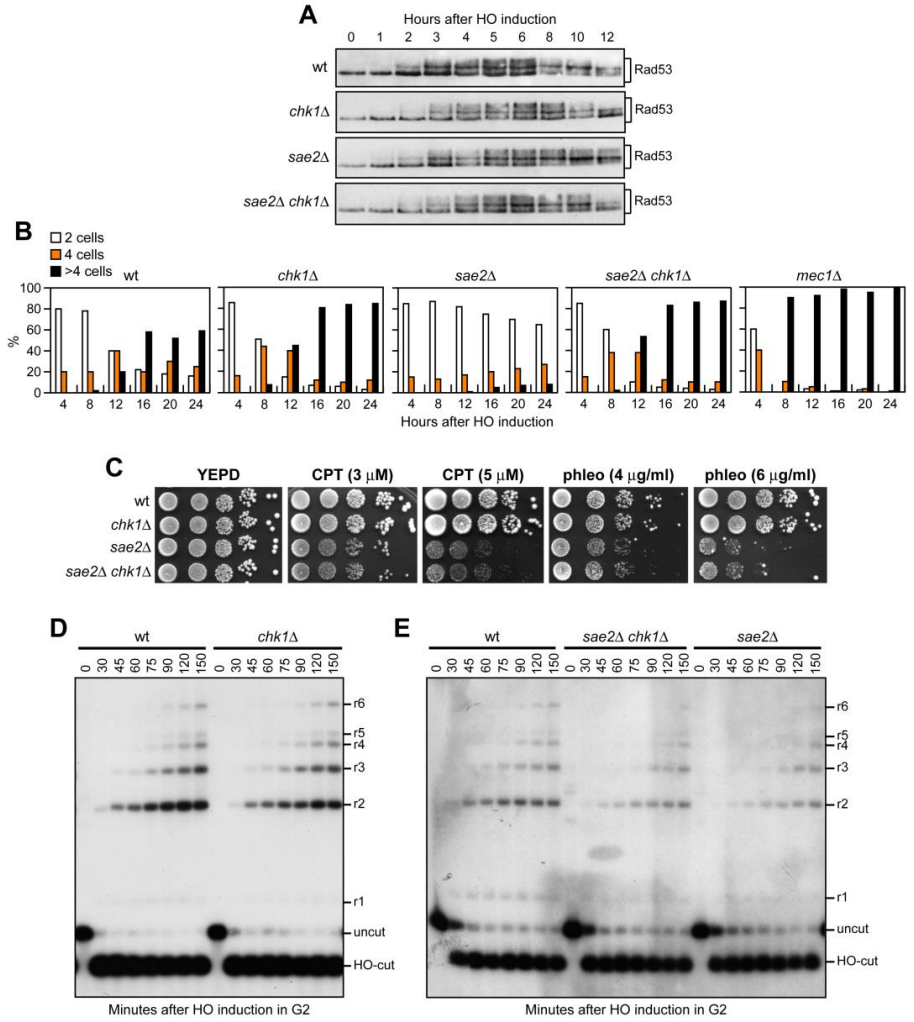

Figure 20. The lack of Chk1 does not suppress the hypersensitivity to DNA damaging agents of *sae2*Δ cells. A) Exponentially growing YEPR cultures of JKM139 derivative strains were transferred to YEPRG (time zero), followed by western blot analysis with anti-Rad53 antibodies. B) YEPR G1-arrested cell cultures of JKM139 derivative strains were plated on galactose-containing plates (time zero). At the indicated time points, 200 cells for each strain were analyzed to determine the frequency of large budded cells (2 cells) and of cells forming microcolonies of 4 or more than 4 cells. C) Exponentially growing cells were serially diluted (1:10) and each dilution was spotted out onto YEPD plates with or without camptothecin (CPT)

and phleomycin. D, E) DSB resection. YEPR exponentially growing cultures of JKM139 derivative cells were arrested in G2 with nocodazole and transferred to YEPRG in the presence of nocodazole at time zero. Gel blots of SspI-digested genomic DNA separated on alkaline agarose gel were hybridized with a single-stranded *MAT* probe that anneals to the unresected strand on one side of the break. 5'-3' resection progressively eliminates SspI sites, producing larger SspI fragments (r1 through r6) detected by the probe.

The Rad53-H88Y and Tel1-N2021D variants restore resection and SSA in *sae2*Δ cells

As the checkpoint-mediated cell cycle arrest was not responsible for the DNA damage hypersensitivity of *sae2*Δ cells, we asked whether Rad53-H88Y and/or Tel1-N2021D suppressed the *sae2*Δ resection defect. We first measured the efficiency of SSA, a mechanism that repairs a DSB flanked by direct DNA repeats when sufficient resection exposes the complementary DNA sequences, which can then anneal to each other (Mehta and Haber, 2014). The *rad53-H88Y* and *tel1-N2021D* alleles were introduced in the YMV45 strain, which carries two tandem *leu2* gene repeats located 4.6 kb apart on chromosome III, with a HO recognition site adjacent to one of the repeats (Vaze *et al.*, 2002). This strain also harbors a GAL-HO construct for galactose-inducible HO expression. Both Rad53-H88Y and Tel1-N2021D bypass Sae2 function in SSA-mediated DSB repair. In fact, accumulation of the SSA repair product after HO induction occurred more efficiently in both *sae2*Δ *rad53-H88Y* (Fig. 21A and 21B) and *sae2*Δ *tel1-N2021D* (Fig. 21C and 21D) than in *sae2*Δ cells, where it was delayed compared to wild type.

To confirm that Rad53-H88Y and Tel1-N2021D suppress the SSA defect of *sae2*Δ cells by restoring DSB resection, we used JKM139 derivative strains to monitor directly generation of ssDNA at the DSB ends. Indeed, *sae2*Δ *rad53-H88Y* (Fig. 22A) and *sae2*Δ *tel1-N2021D* (Fig. 22B) cells resected the HO-induced DSB more efficiently than *sae2*Δ cells, indicating that both Rad53-H88Y and Tel1-N2021D suppress the resection defect of *sae2*Δ cells.

The DSB resection defect of sae2Δ cells is thought to be responsible for the increased persistence of MRX at the DSB (Clerici *et al.*, 2014). Because Rad53-H88Y and Tel1-N2021D restore DSB resection in *sae2*Δ cells, we expected that the same variants also reduce the amount of MRX bound at the DSB. The amount of Mre11 bound at the HO-induced DSB end turned out to be lower in both *sae2*Δ *rad53-H88Y* and *sae2*Δ *tel1-N2021D* than in *sae2*Δ cells (Fig. 22C). Therefore, the Rad53-H88Y and Tel1-N2021D variants restore DSB resection in *sae2*Δ cells and reduce MRX association/persistence at the DSB.

Consistent with the finding that Rad53-H88Y and Tel1-N2021D do not fully restore CPT resistance in *sae2*Δ cells (Fig. 16A), and therefore do not bypass completely all Sae2 functions, the *rad53-H88Y* and *tel1-N2021D* mutations were unable to suppress the sporulation defects of *sae2*Δ/*sae2*Δ diploid cells (Fig. 22D), suggesting that they cannot bypass the requirement for Sae2/MRX endonucleolytic cleavage to remove Spo11 from meiotic DSBs.

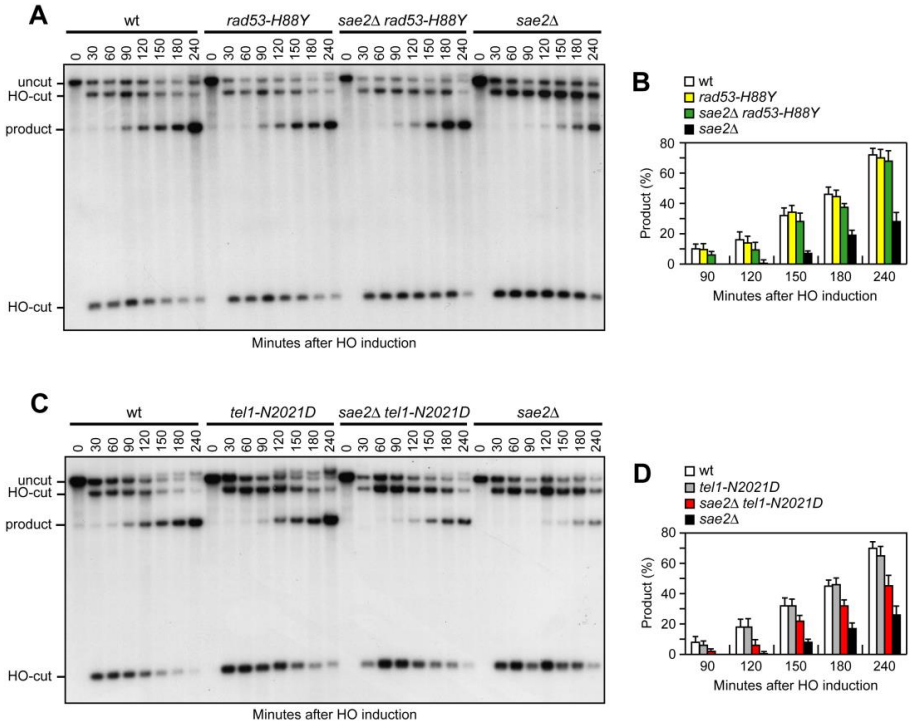

Figure 21. Rad53-H88Y and Tel1-N2021D suppress the SSA defect of *sae2*Δ cells. A) DSB repair by SSA. YEPR exponentially growing cell cultures of YMV45 derivative strains, carrying the HO-cut site flanked by homologous *leu2* sequences that are 4.6 kb apart, were transferred to YEPRG at time zero. HO-induced DSB formation results in generation of 12 kb and 2.5 kb DNA fragments (HO-cut) that can be detected by Southern blot analysis with a *LEU2* probe of KpnI-digested genomic DNA. DSB repair by SSA generates an 8 kb fragment (product). B) Densitometric analysis of the product band signals. The experiment as in (A) has been independently repeated three times and the mean values are represented with error bars denoting s.d. (n=3). C) DSB repair by SSA was analyzed as in (A). D) Densitometric analysis of the product band signals. The experiment as in (C) has been independently repeated three times and the mean values are represented with error bars denoting s.d. (n=3).

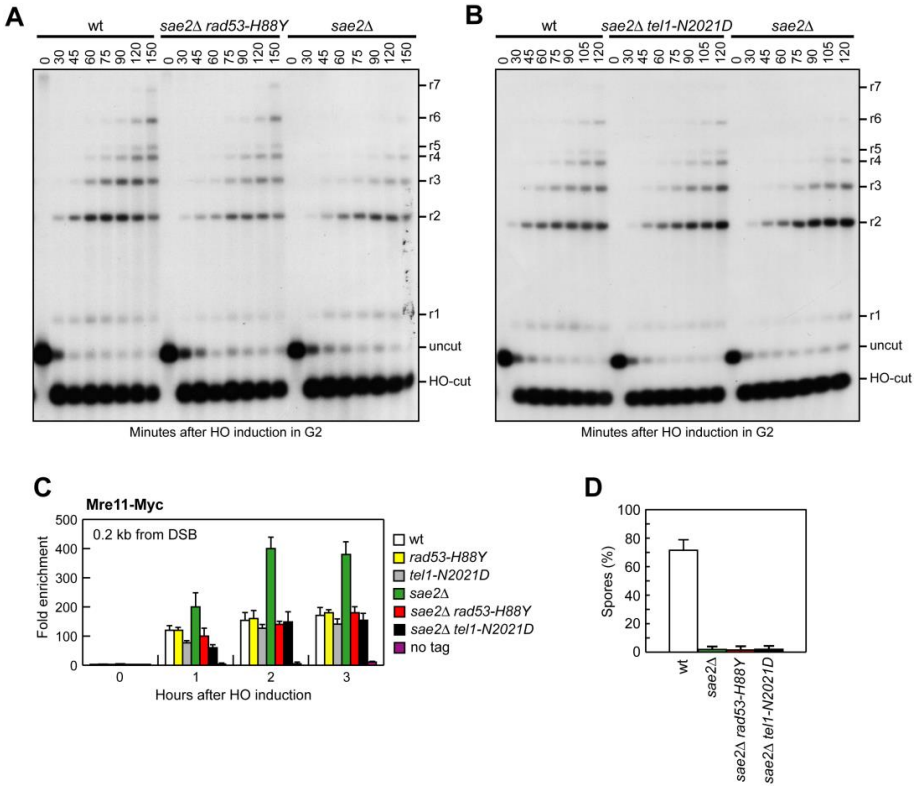

Figure 22. Rad53-H88Y and Tel1-N2021D suppress the resection defect of *sae2*Δ cells. A, B) DSB resection. YEPR exponentially growing cultures of JKM139 derivative strains were arrested in G2 with nocodazole and transferred to YEPRG in the presence of nocodazole at time zero. Detection of ssDNA was carried out as described in Fig. 20D. 5'-3' resection produces SspI fragments indicated as r1 to r7. C) ChIP analysis. Exponentially growing YEPR cell cultures of JKM139 derivative strains were transferred to YEPRG. Relative fold enrichment of Mre11-Myc at 0.2 kb from the HO cleavage site was evaluated after ChIP with anti-Myc antibodies and qPCR analysis compared to untagged Mre11 (no tag). In all diagrams, the ChIP signals were normalized for each time point to the amount of the corresponding input signal. The mean values are represented with error bars denoting s.d. (n=3). D) Sporulation efficiency. Spores after 24 hours in sporulation medium of diploid cells homozygous for the indicated mutations.

Suppression of the DNA damage hypersensitivity of *sae2*Δ cells by Rad53-H88Y and Tel1-N2021D variants requires Sgs1-Dna2

The MRX complex not only provides the nuclease activity for initiation of DSB resection, but also allows extensive resection by promoting the binding at the DSB ends of the resection proteins Exo1 and Sgs1-Dna2 (Mimitou and Symington, 2008; Zhu *et al.*, 2008; Shim *et al.*, 2010). Suppression of the DNA damage hypersensitivity of *sae2*Δ cells by Rad53-H88Y and Tel1-N2021D requires the physical presence of the MRX complex but not its nuclease activity (Fig. 16C and 16D). As the loading of Exo1, Sgs1-Dna2 at DSBs depends on the MRX complex independently of its nuclease activity (Shim *et al.*, 2010), we asked whether the investigated suppression events require Exo1, Sgs1 and/or Dna2. This question was particularly interesting, as Rad53 was shown to inhibit resection at uncapped telomeres through phosphorylation and inhibition of Exo1 (Jia *et al.*, 2004; Morin *et al.*, 2008). As shown in Fig. 23A, *sae2*Δ suppression by Rad53-H88Y and Tel1-N2021D was Exo1-independent. In fact, although the lack of Exo1 exacerbated the sensitivity to DNA damaging agents of *sae2*Δ cells, both *sae2*Δ *exo1*Δ *rad53-H88Y* and *sae2*Δ *exo1*Δ *tel1-N2021D* triple mutants were more resistant to genotoxic agents than *sae2*Δ *exo1*Δ double mutant cells (Fig. 23A).

By contrast, neither Rad53-H88Y nor Tel1-N2021D were able to suppress the sensitivity to DNA damaging agents of *sae2*Δ cells carrying the temperature sensitive *dna2-1* allele (Fig. 23B), suggesting that Dna2 activity is required for their suppressor effect. Dna2, in concert with the helicase Sgs1, functions as a nuclease in DSB resection (Zhu *et al.*, 2008). The *dna2-E675A* allele abolishes Dna2 nuclease activity, which is essential for cell viability and whose requirement is bypassed by the *pif1-M2* mutation that impairs the nuclear activity of the Pif1 helicase (Budd *et al.*, 2000). The lack of Sgs1 or expression of the Dna2-E675A variant in the presence of the *pif1-M2* allele impaired viability of *sae2*Δ cells even in the absence of genotoxic agents. The synthetic lethality of *sae2*Δ *sgs1*Δ cells, and possibly of *sae2*Δ *dna2-E675A pif1-M2*, is likely due to defects in DSB resection, as it is known to be suppressed by either *EXO1* overexpression or *KU* deletion (Mimitou and Symington, 2010). Thus, we asked whether Rad53-H88Y and/or Tel1-N2021D could restore viability of *sae2*Δ *sgs1*Δ and/or *sae2*Δ *dna2-E675A pif1-M2* cells. Tetrad dissection of diploid cells did not allow to find viable spores with the *sae2*Δ *dna2-E675A pif1-M2 rad53-H88Y* (Fig. 23C) or *sae2*Δ *dna2-E675A pif1-M2 tel1-N2021D* genotypes (Fig. 23D), indicating that neither Rad53-H88Y nor Tel1-N2021D can restore the viability of *sae2*Δ *dna2-E675A pif1-M2* cells. Similarly, no viable *sae2*Δ *sgs1*Δ spores could be recovered, while *sae2*Δ *sgs1*Δ *rad53-H88Y* and *sae2*Δ *sgs1*Δ *tel1-N2021D* triple mutant spores formed very small colonies

that could not be further propagated (Fig. 23E and 23F). Finally, neither Rad53-H88Y nor Tel1-N2021D, which allowed DNA damage resistance in *sae2*Δ *exo1*Δ cells (Fig. 23A), were able to suppress the growth defect of *sgs1*Δ *exo1*Δ double mutant cells even in the absence of genotoxic agents (Fig. 23G). Altogether, these findings indicate that suppression by Rad53-H88Y and Tel1-N2021D of the DNA damage hypersensitivity caused by the absence of Sae2 is dependent on Sgs1-Dna2.

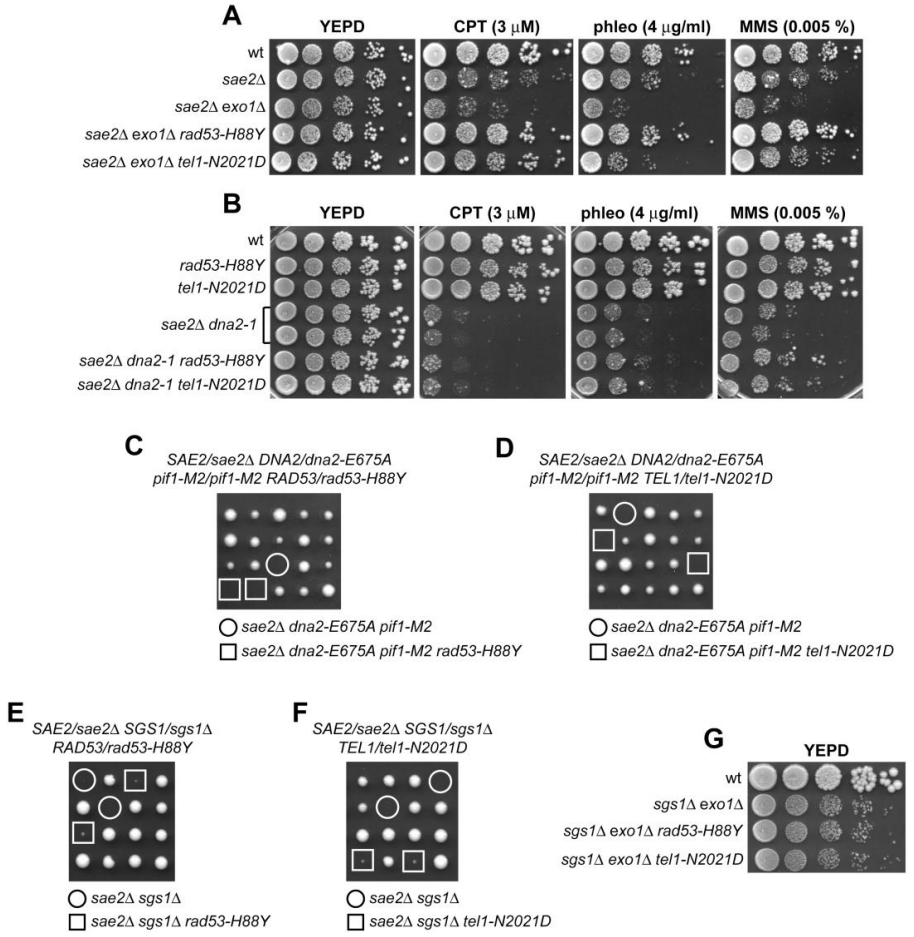

Figure 23. The Rad53-H88Y and Tel1-N2021D bypass of Sae2 function is Sgs1-Dna2-dependent. A, B) Exponentially growing cells were serially diluted (1:10) and each dilution was spotted out onto YEPD plates with or without camptothecin (CPT), phleomycin or MMS. C-F) Meiotic tetrads were dissected on YEPD plates that were incubated at 25°C, followed by spore genotyping. G) Exponentially growing cells were serially diluted (1:10) and each dilution was spotted out onto YEPD plates.

The lack of Rad53 kinase activity suppresses the DNA damage hypersensitivity and the resection defect of *sae2*Δ cells

The Rad53-H88Y protein is defective in interaction with Rad9 (Fig. 18C) and therefore fails to undergo autophosphorylation and activation, prompting us to test whether other mutations affecting Rad53 activity can bypass Sae2 functions. To this end, we could not use *rad53*Δ cells because they show growth defects even when the lethal effect of *RAD53* deletion is suppressed by the lack of Sml1 (Zhao *et al.*, 1998). We then substituted the chromosomal wild type *RAD53* allele with the kinase-defective *rad53-K227A* allele (*rad53-kd*), which does not impair cell viability in the absence of genotoxic agents but affects checkpoint activation (Fay *et al.*, 1997). The *rad53-kd* allele rescued the sensitivity of *sae2*Δ cells to CPT and MMS to an extent similar to Rad53-H88Y (Fig. 24A). Furthermore, accumulation of the SSA repair products occurred more efficiently in *sae2*Δ *rad53-kd* cells than in *sae2*Δ (Fig. 24B and 24C), indicating that the lack of Rad53 kinase activity bypasses Sae2 function in SSA-mediated DSB repair.

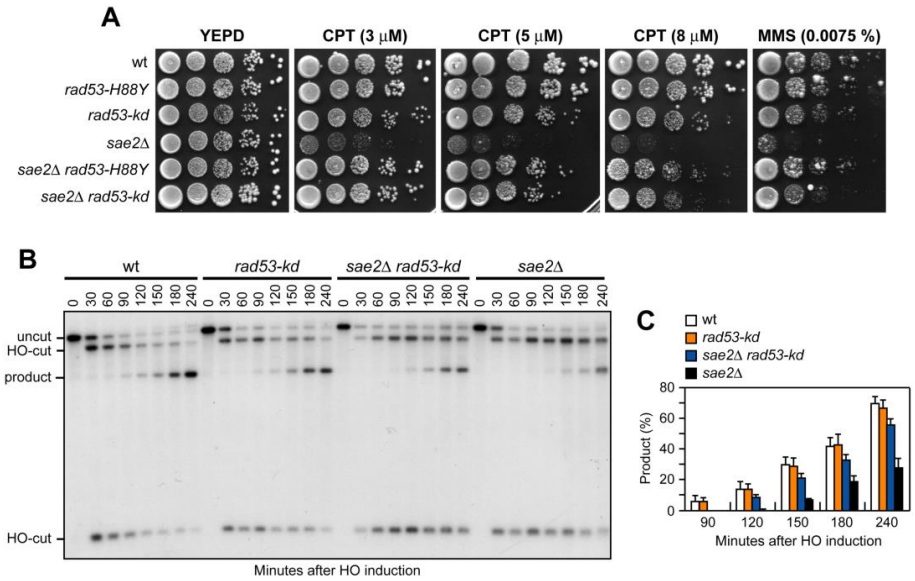

Figure 24. The Rad53-kd variant restores DNA damage resistance and SSA in *sae2*Δ cells. A) Exponentially growing cells were serially diluted (1:10) and each dilution was spotted out onto YEPD plates with or without camptothecin (CPT) or MMS. B) DSB repair by SSA. The analysis was performed as described in Fig. 21A. C) Densitometric analysis of the product band signals. The experiment as in (B) has been independently repeated three times and the mean values are represented with error bars denoting s.d. (n=3).

The lack of Tel1 kinase activity bypasses Sae2 function at DSBs, whereas Tel1 hyperactivation increases Sae2 requirement

Suppression of *sae2*Δ may be peculiar to Tel1-N2021D, which is poorly recruited to DSBs (Fig. 18F), or it might be performed also by *TEL1* deletion (*tel1*Δ) or by expression of a Tel1 kinase defective variant (Tel1-kd). Indeed, the Tel1-kd variant, carrying the Gly2611Asp, Asp2612Ala, Asn2616Lys, and Asp2631Glu amino acid substitutions that abolish Tel1 kinase activity *in vitro* (Fig. 18E) (Mallory and Petes, 2000), rescued the hypersensitivity of *sae2*Δ cells to genotoxic agents to an extent similar to Tel1-N2021D (Fig. 25A). The lack of Tel1 kinase activity bypassed also Sae2 function in DSB resection, because *sae2*Δ *tel1-kd* cells repaired a DSB by SSA more efficiently than *sae2*Δ cells (Fig. 25B and 25C). By contrast, and consistent with previous studies (Chen *et al.*, 2015; Puddu *et al.*, 2015), *TEL1* deletion was not capable to suppress the hypersensitivity to DNA damaging agents of *sae2*Δ cells (Fig. 8A). Rather, *tel1*Δ *sae2*Δ double mutant cells displayed higher sensitivity to CPT than *sae2*Δ cells

(Fig. 25A). Altogether, these data indicate that the lack of Tel1 kinase activity can bypass Sae2 function both in DNA damage resistance and DSB resection, but these suppression events require the physical presence of the Tel1 protein.

As impairment of Tel1 function rescued the *sae2*Δ defects, we asked whether Tel1 hyperactivation exacerbates the DNA damage hypersensitivity of *sae2*Δ cells. We previously isolated the *TEL1-hy909* allele, which encodes a Tel1 mutant variant with enhanced kinase activity that causes an impressive telomere overelongation (Baldo *et al.*, 2008). As shown in Fig. 25D, *sae2*Δ *TEL1-hy909* double mutant cells were more sensitive to DNA damaging agents than *sae2*Δ single mutant cells. This enhanced DNA damage sensitivity was likely due to Tel1 kinase activity, as *sae2*Δ cells expressing a kinase defective Tel1-hy909-kd variant were as sensitive to DNA damaging agents as *sae2*Δ cells (Fig. 25D). Thus, impairment of Tel1 activity bypasses Sae2 function at DSBs, whereas Tel1 hyperactivation increases the requirement for Sae2 in survival to genotoxic stress.

The absence of Tel1 failed not only to restore DNA damage resistance in *sae2*Δ cells (Fig. 25A), but also to suppress their SSA defect (Fig. 26A and 26B). The difference in the effects of *tel1*Δ and *tel1-kd* was not due to checkpoint signaling, as Rad53 phosphorylation decreased with similar kinetics in both *sae2*Δ *tel1-kd* and *sae2*Δ *tel1*Δ double mutant cells 10-12 hours after HO induction (Fig. 26C). Interestingly, SSA-mediated DSB repair occurred with wild type kinetics in *tel1-kd* mutant cells (Fig. 25B and 25C), while *tel1*Δ cells repaired a DSB by SSA less efficiently than wild type cells (Fig. 26A and 26B), suggesting that Tel1 might have a function at DSBs that does not require its kinase activity. Indeed, *TEL1* deletion was shown to slight

impair DSB resection (Mantiero *et al.*, 2007). Furthermore, it did not exacerbate the resection defect (Mantiero *et al.*, 2007) and the hypersensitivity to DNA damaging agents of *mre11*Δ cells (Fig. 26D), suggesting that the absence of Tel1 can impair MRX function. Tel1 was also shown to promote MRX association at DNA ends flanked by telomeric DNA repeats independently of its kinase activity (Hirano *et al.*, 2009), and we are showing that suppression of *sae2*Δ by Tel1-N2021D requires the physical presence of the MRX complex (Fig. 16D). Thus, it is possible that the lack of Tel1 fails to bypass Sae2 function at DSBs because it reduces MRX association at DSBs to a level that is not sufficient to restore DNA damage resistance and DSB resection in *sae2*Δ cells. Indeed, the amount of Mre11 bound at the HO-induced DSB was decreased in *tel1*Δ, but not in *tel1-kd* cells, compared to wild type (Fig. 26E). In agreement with a partial loss of Tel1 function, the Tel1-N2021D variant, whose association to DSBs is diminished compared to wild type Tel1 but not abolished (Fig. 18F), only slightly decreased Mre11 association to the DSB (Fig. 26E). As the rescue of *sae2*Δ by Tel1-N2021D requires the physical presence of the MRX complex, this Tel1 function in promoting MRX association to DSBs can explain the inability of *tel1*Δ to bypass Sae2 function in DNA damage resistance and resection.

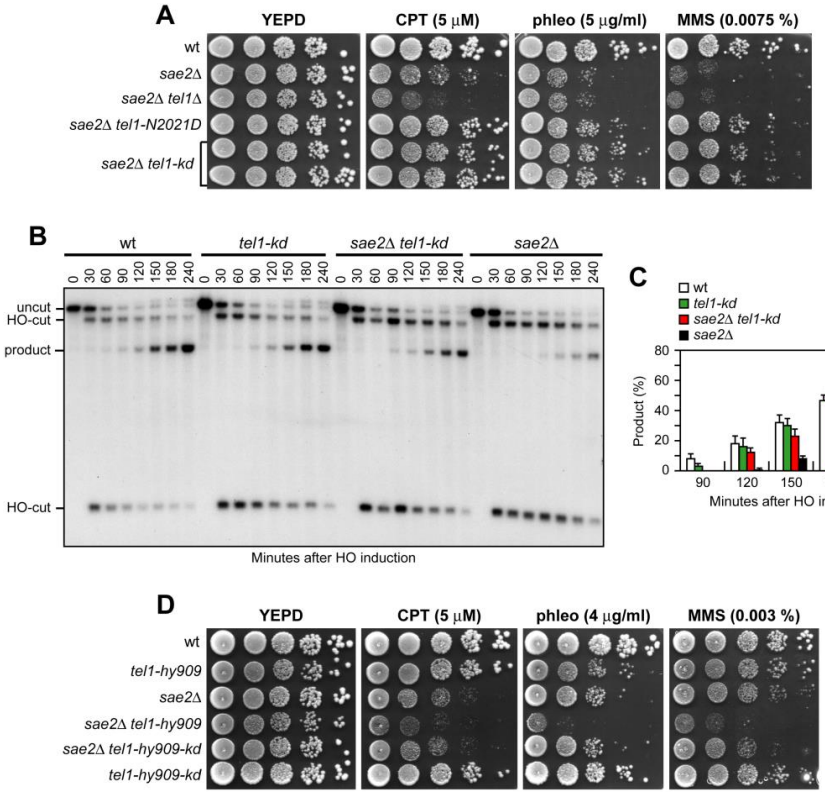

Figure 25. The Tel1-kd variant restores DNA damage resistance and SSA in *sae2*Δ cells. A) Exponentially growing cells were serially diluted (1:10) and each dilution was spotted out onto YEPD plates with or without camptothecin (CPT), phleomycin or MMS. B) DSB repair by SSA. The analysis was performed as described in Fig. 21A. C) Densitometric analysis of the product band signals. The experiment as in (B) has been independently repeated three times and the mean values are represented with error bars denoting s.d. (n=3). D) Exponentially growing cells were serially diluted (1:10) and each dilution was spotted out onto YEPD plates with or without camptothecin (CPT), phleomycin or MMS.

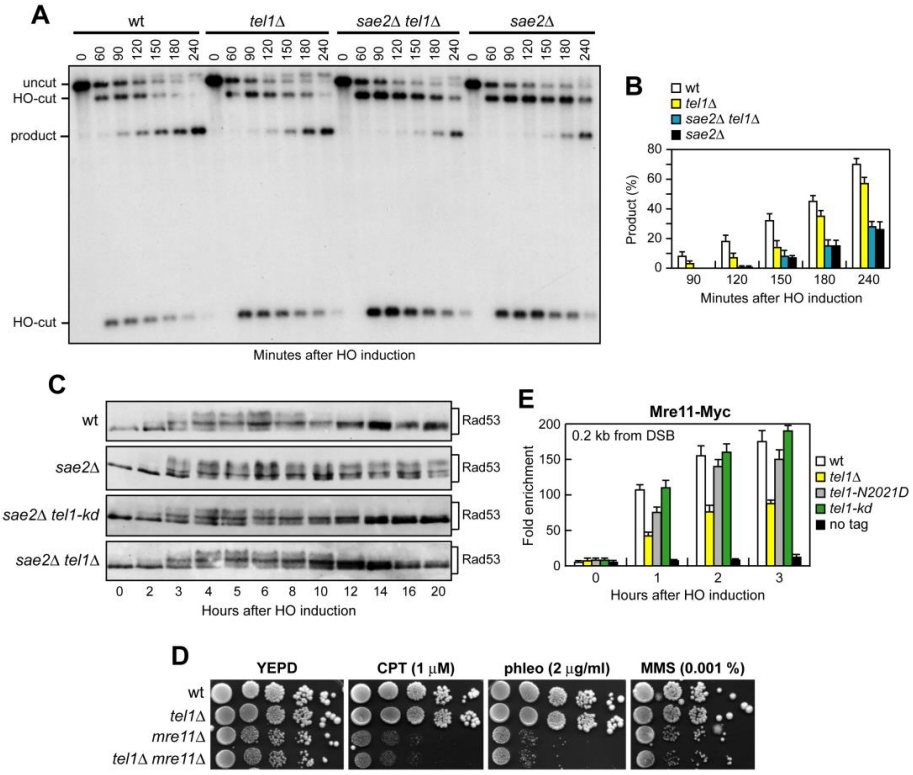

Figure 26. The lack of Tel1 does not restore DNA damage resistance and SSA in *sae2*Δ cells. A) DSB repair by SSA. The analysis was performed as described in Fig. 21A. B) Densitometric analysis of the product band signals. The experiment as in (A) has been independently repeated three times and the mean values are represented with error bars denoting s.d. (n=3). C) Exponentially growing YEPR cell cultures of JKM139 derivative strains were transferred to YEPRG (time zero), followed by western blot analysis with anti-Rad53 antibodies of protein extracts prepared at the indicated time points. D) Exponentially growing cells were serially diluted (1:10) and each dilution was spotted out onto YEPD plates with or without camptothecin (CPT), phleomycin or MMS. E) ChIP analysis. Exponentially growing YEPR cell cultures of JKM139 derivative strains were transferred to YEPRG. Recruitment of Mre11-Myc compared to untagged Mre11 (no tag) at 0.2 kb from the HO-cut was determined by ChIP analysis and qPCR. In all diagrams, the ChIP signals were normalized for each time point to the amount of the corresponding input signal. The mean values are represented with error bars denoting s.d. (n=3).

Tel1 and Rad53 kinase activities promote Rad9 binding to the DSB ends

The suppression of the DNA damage hypersensitivity of *sae2*Δ cells by Rad53-H88Y and Tel1-N2021D requires Dna2-Sgs1 (Fig. 23B-23G). Because Sgs1-Dna2 activity is counteracted by Rad9, whose lack restores DSB resection in *sae2*Δ cells (Bonetti *et al.*, 2015; Ferrari *et al.*, 2015), we asked whether suppression of the DSB resection defect of *sae2*Δ cells by Rad53 or Tel1 dysfunction might be due to decreased Rad9 association to the DSB ends. We have previously shown that wild type and *sae2*Δ cells have similar amounts of Rad9 bound at 1.8 kb from the DSB (Fig. 27A) (Clerici *et al.*, 2014). However, a robust increase in the amount of Rad9 bound at 0.2 kb and 0.6 kb from the DSB was detected in *sae2*Δ cells compared to wild type (Fig. 27A) (Ferrari *et al.*, 2015). Strikingly, this enhanced Rad9 accumulation in *sae2*Δ cells was reduced in the presence of the Rad53-kd or Tel1-kd variant, which both decreased the amount of Rad9 bound at the DSB also in otherwise wild type cells (Fig. 27A). Thus, Rad9 association close to the DSB depends on Rad53 and Tel1 kinase activity.

Rad9 inhibits DSB resection by counteracting Sgs1 recruitment to DSBs (Bonetti *et al.*, 2015) and, as expected, Sgs1 binding to DSBs was lower in *sae2*Δ cells than in wild type (Fig. 27B). By contrast, the presence of Rad53-kd or Tel1-kd variants increased the amount of Sgs1 at the DSB in both wild type and *sae2*Δ cells (Fig. 27B).

Together with the observation that the suppression of *sae2*Δ hypersensitivity to genotoxic agents by Rad53 and Tel1 dysfunctions requires Sgs1-Dna2, these findings indicate that the lack of Rad53 or Tel1 kinase activity restores DSB resection in *sae2*Δ cells by decreasing Rad9 association close to the DSB and therefore by relieving Sgs1-Dna2 inhibition. Although both *rad53-kd* and *tel1-kd* cells showed some lowering of Rad9 binding at DSBs compared to wild type cells (Fig. 27A), they did not appear to accelerate SSA, suggesting that this extent of Rad9 binding is anyhow sufficient to limit resection in a wild type context.

Rad9 is known to be enriched at the sites of damage by interaction with histone H2A that has been phosphorylated on Serine 129 (γH2A) by Mec1 and Tel1 (Shroff *et al.*, 2004; Javaheri *et al.*, 2006; Toh *et al.*, 2006; Hammet at al., 2007). As the lack of γH2A suppresses the SSA defect of *sae2*Δ cells (Ferrari *et al.*, 2015), Tel1 activity might increase the amount of Rad9 bound at the DSB in *sae2*Δ cells by promoting generation of γH2A. Indeed, the *hta1-S129A* allele, which encodes a H2A variant where Ser129 is replaced by a non-phosphorylatable Alanine residue, thus causing the lack of γH2A, suppressed the resection defect of *sae2*Δ cells (Fig. 28). Furthermore, γH2A formation turned out to be responsible for the enhanced Rad9 binding close to the break site, as *sae2*Δ *hta1-S129A* cells showed wild type levels of Rad9 bound at the DSB (Fig. 27C). Finally, γH2A formation close to the DSB depends on Tel1 kinase activity, as γH2A

at the DSB was not detectable in *sae2*Δ *tel1-kd* cells (Fig. 27D). Altogether, these data indicate that Tel1 promotes Rad9 association to DSB in *sae2*Δ cells through γH2A generation.

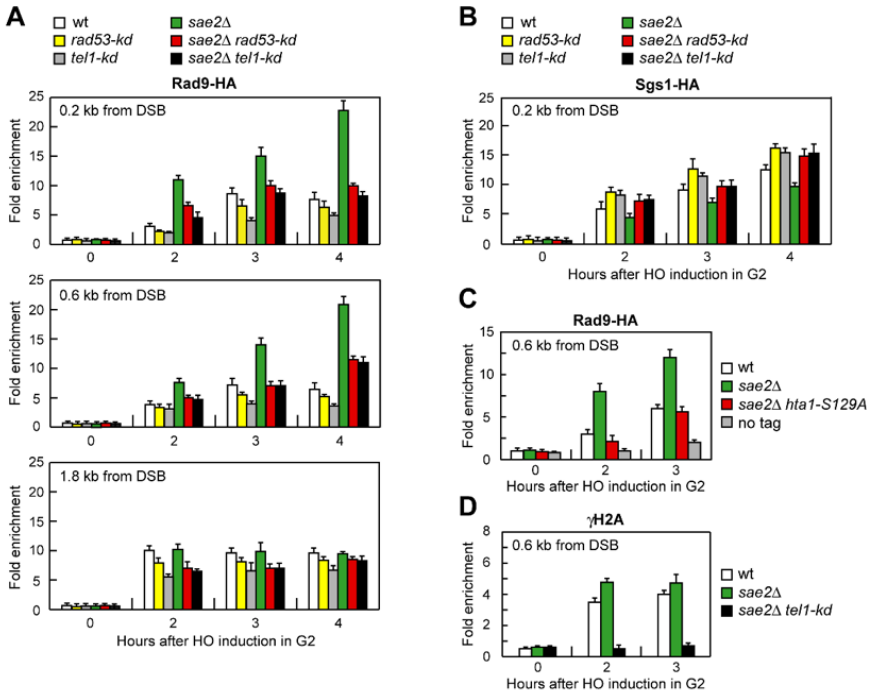

Figure 27. Rad53-kd and Tel1-kd prevent Rad9 association at DSBs. A) ChIP analysis. Exponentially growing YEPR cell cultures of JKM139 derivative strains were arrested in G2 with nocodazole and transferred to YEPRG in the presence of nocodazole. Recruitment of Rad9-HA at the indicated distance from the HO-cut was determined by ChIP and qPCR. In all diagrams, the ChIP signals were normalized for each time point to the amount of the corresponding input signal. The mean values are represented with error bars denoting s.d. (n=3). B) As in (A), but showing Sgs1-HA binding. C) As in (A). All strains carried also the deletion of *HTA2* gene. D) As in (A), but showing γH2A binding.

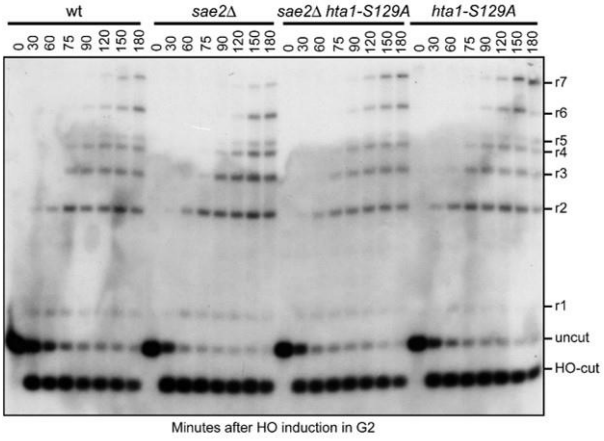

Figure 28. The lack of γH2A suppresses the resection defect of *sae2*Δ cells. DSB resection. YEPR exponentially growing cultures of JKM139 derivative cells with the indicated genotypes were arrested in G2 with nocodazole and transferred to YEPRG in the presence of nocodazole at time zero. All strains carried also the deletion of *HTA2* gene. Gel blots of SspI-digested genomic DNA separated on alkaline agarose gel were hybridized with a single-stranded *MAT* probe that anneals to the unresected strand on one side of the break. 5'-3' resection progressively eliminates SspI sites, producing larger SspI fragments (r1 through r7) detected by the probe.

DISCUSSION

Homologous Recombination (HR) requires nucleolytic degradation (resection) of DNA Double-Strand Break (DSB) ends. In *Saccharomyces cerevisiae*, the MRX complex and Sae2 are involved in the onset of DSB resection, whereas extensive resection requires Exo1 and the concerted action of Dna2 and Sgs1 (Mimitou and Symington, 2008; Zhu *et al.*, 2008; Cannavo and Cejka, 2014). The absence of Sae2 not only impairs DSB resection, but also causes prolonged MRX binding at the DSBs that leads to persistent Tel1- and Rad53-dependent DNA damage checkpoint activation and cell cycle arrest. *SAE2* deletion causes hypersensitivity to camptothecin (CPT), which traps covalent topoisomerase I (Top1)-DNA cleavable complexes and creates replication-associated DSBs. CPT-induced DNA lesions need to be processed by Sae2 and MRX unless the Ku heterodimer is absent. The lack of Ku suppresses CPT hypersensitivity of *sae2*Δ mutants, and this rescue requires Exo1 (Mimitou and Symington, 2010; Foster *et al.*, 2011), indicating that Ku prevents Exo1 from initiating DSB resection.

To identify other possible pathways bypassing Sae2 function in DSB resection, we searched for extragenic mutations that suppress the DNA damage sensitivity of *sae2*Δ cells. By performing a genetic screen, we identify *SGS1-ss*, *rad53-ss* and *tel1-ss* mutant alleles that suppress both the DNA damage hypersensitivity and the resection defect of *sae2*Δ cells.

In the first part of the thesis, I have contributed to the characterization of the Sgs1-ss mutant variant (Bonetti D, Villa M, Gobbini E, Cassani C, Tedeschi G, Longhese MP. Escape of Sgs1 from Rad9 inhibition reduces the requirement for Sae2 and functional MRX in DNA end resection. EMBO Rep, 2015). We show that Sgs1-ss can bypass the requirement of Sae2 or MRX nuclease activity for survival to genotoxic agents, but it still requires the physical integrity of the MRX complex to exert its function. In fact, Sgs1-ss is not able to suppress the hypersensitivity to genotoxic agents of *mre11*Δ cells, but suppresses the sensitivity of *mre11-H125N* cells, which were specifically defective in Mre11 nuclease activity. These data are in agreement with the fact that the MRX complex is required for the recruitment of Sgs1 to the lesion (Mimitou and Symington, 2008), and indicate that the Sgs1-ss variant could be able to promote initiation of DSB resection even without Sae2 and Mre11 nuclease activity. Furthermore, Sgs1-ss mediated suppression depends on the Dna2 nuclease but not on Exo1. In fact, Sgs1-ss supports survival of *sae2*Δ mutants in the presence of genotoxic agents even in the absence of Exo1. By contrast, *sae2*Δ *dna2*Δ synthetic lethality is note rescued by the presence of Sgs1-ss.

A further characterization of the mutant showed that Sgs1-ss suppress the sensitivity to genotoxic agents and the adaptation defect of *sae2*Δ cells. Resection in *sae2*Δ *SGS1-ss* cells was markedly increased compared to *sae2*Δ cells, indicating that Sgs1-ss suppresses the

resection defect caused by the lack of Sae2. Sgs1-ss is also able to suppress the Single-Strand-Annealing (SSA) defect of *sae2*Δ cells. Altogether, these findings indicate that Sgs1-ss suppresses both the sensitivity to genotoxic agents of *sae2*Δ cells and the MRX persistence at DSBs by restoring DSB resection.

The Sgs1-ss mutant variant accelerates both DSB resection and SSA compared to wild-type Sgs1, suggesting that Sgs1-ss might increase the resection efficiency by escaping the effect of negative regulators of this process. In particular, it is known that Rad9 provides a barrier to resection through an unknown mechanism (Lydall and Weinert, 1995; Lazzaro *et al.*, 2008). We show that the checkpoint protein Rad9 increases the requirement for the MRX/Sae2 activities in DSB resection by inhibiting the action of the Sgs1/Dna2 long-range resection machinery. Extensive resection in Rad9-deficient cells is mainly dependent on Sgs1, whose recruitment at DSBs is inhibited by Rad9. By contrast, Sgs1-ss, which suppresses the resection defect of *sae2*Δ cells, is robustly associated with the DSB ends both in the presence and in the absence of Rad9 and resects the DSB more efficiently than wild type Sgs1. These findings indicate that Rad9 inhibits the activity of Sgs1/Dna2 by limiting Sgs1 binding/persistence at DSB ends and that the Sgs1-ss mutant variant escapes this inhibition possibly because it is more tightly bound to DNA. When inhibition by Rad9 is abolished by the Sgs1-ss mutant variant or by

deletion of *RAD9*, the requirement for Sae2 and functional MRX in DSB resection is reduced.

This increase in resection efficiency depends on the ability of Sgs1-ss of escaping Rad9 inhibition. In fact, genetic analysis that Sgs1-ss and *RAD9* deletion promotes resection by acting in the same pathway. In addition, ChIP analysis show that Rad9 limits the recruitment of Sgs1 at an HO-DSB and Sgs1-ss is able to bypass this negative effect. Thus, while Ku increases the requirement for the MRX/Sae2 activities in DSB resection by inhibiting preferentially Exo1 (Shim *et al.*, 2010), Rad9 mainly restricts the action of Sgs1/Dna2. As MRX and Sae2 are especially important for initial processing of DNA ends that contain adducts, the Rad9- and Ku-mediated inhibitions of Sgs1/Dna2 and Exo1 activities in initiating DSB resection ensure that all DSBs are processed in a similar manner independently of their nature. To summarize, Rad9 specifically inhibits Sgs1-Dna2 activity and the escape of Sgs1 from this inhibition reduces the requirement for Sae2 in DNA end resection. These results provide new insights into how early and long-range resection is coordinated.

In the second part of the thesis, I have characterized the *rad53-ss* and *tel1-ss* mutant alleles (Gobbini E, Villa M, Gnugnoli M, Menin L, Clerici M, Longhese MP. Sae2 function at DNA double-strand breaks is bypassed by dampening Tel1 or Rad53 activity. PLoS Genet, 2015). We show that impairment of Rad53 activity either by affecting its interaction with Rad9 (Rad53-H88Y) or by abolishing its kinase

activity (Rad53-kd) suppresses the sensitivity to DNA damaging agents of *sae2*Δ cells. A similar effect can be detected also when Tel1 function is compromised either by reducing its recruitment to DSBs (Tel1-N2021D) or by abrogating its kinase activity (Tel1-kd). These suppression effects are not due to the escape of the checkpoint-mediated cell cycle arrest, as *CHK1* deletion, which overrides the persistent cell cycle arrest of *sae2*Δ cells, does not suppress the hypersensitivity of the same cells to DNA damaging agents. Rather, we found that impairment of Rad53 or Tel1 signaling suppresses the resection defect of *sae2*Δ by decreasing the amount of Rad9 bound very close to the break site. As it is known that Rad9 inhibits Sgs1-Dna2 (Bonetti *et al.*, 2015; Ferrari *et al.*, 2015), this reduced Rad9 association at DSBs relieves inhibition of Sgs1-Dna2 activity that can then compensate for the lack of Sae2 function in DSB resection. In this view, active Rad53 and Tel1 increase the requirement for Sae2 in DSB resection by promoting Rad9 binding to DSBs and therefore by inhibiting Sgs1-Dna2. Consistent with a role of Sgs1 in removing MRX from the DSBs (Bernstein *et al.*, 2013), the relieve of Sgs1-Dna2 inhibition by Rad53 or Tel1 dysfunction leads to a reduction of MRX association to DSBs in *sae2*Δ cells.

Our finding that Tel1 or Rad53 inactivation can restore both DNA damage resistance and DSB resection in *sae2*Δ cells is apparently at odds with previous findings that attenuation of the Rad53-dependent checkpoint signaling by decreasing MRX association to DSBs

suppresses the DNA damage hypersensitivity of *sae2*Δ cells but not their resection defect (Chen *et al.*, 2015; Puddu *et al.*, 2015). Noteworthy, the bypass of Sae2 function by Rad53 or Tel1 dysfunction requires the physical presence of MRX bound at DSBs, which is known to promote stable association of Exo1, Sgs1 and Dna2 to DSBs (Shim *et al.*, 2010). Thus, we speculate that a reduced MRX association at DSBs allows *sae2*Δ cells to initiate DSB resection by relieving Rad9-mediated inhibition of Sgs1-Dna2 activity. As DSB repair by HR has been shown to require limited amount of ssDNA at DSB ends (Jinks-Robertson *et al.*, 1993; Ira and Haber, 2002), the ssDNA generated by this initial DSB processing might be sufficient to restore DNA damage resistance in *sae2*Δ cells even when wild type levels of resection are not restored because DSB bound MRX is not enough to ensure stable Sgs1 and Dna2 association.

Surprisingly, *TEL1* deletion, which relieves the persistent Tel1-dependent checkpoint activation caused by the lack of Sae2, did not restore DNA damage resistance and DSB resection in *sae2*Δ cells. We found that the lack of Tel1 protein affects the association of MRX to the DSB ends independently of its kinase activity. As the rescue of *sae2*Δ by Tel1-N2021D requires the physical presence of the MRX complex, this reduced MRX-DNA association can explain the inability of *TEL1* deletion to restore DNA damage resistance and resection in *sae2*Δ cells. Therefore, while an enhanced Tel1 signaling activity in the absence of Sae2 leads to DNA damage hypersensitivity

and resection defects, a sufficient amount of Tel1 needs to be present at DSBs to support MRX function at DSBs.

How do Rad53 and Tel1 control Rad9 association to DSB? Rad53-mediated phosphorylation of Rad9 does not appear to promote Rad9 binding to the DSB (Naiki *et al.*, 2004; Usui *et al.*, 2009). Because Rad53 and RPA compete for binding to Sgs1 (Hegnauer *et al.*, 2012), it is tempting to propose that impaired Rad53 signaling activity might shift Sgs1 binding preference from Rad53 to RPA, leading to increased Sgs1 association to RPA-coated DNA that can counteract Rad9 binding and inhibition of resection. In turn, Tel1 and Mec1 can phosphorylate Rad9 (Emili, 1998; Vialard *et al.*, 1998), and abrogation of these phosphorylation events rescues the sensitivity to DNA damaging agents of *sae2*Δ cells (Ferrari *et al.*, 2015), suggesting that Tel1 might control Rad9 association to DSBs directly through phosphorylation. On the other hand, Tel1 promotes generation of γH2A (Shroff *et al.*, 2004; Javaheri *et al.*, 2006; Toh *et al.*, 2006; Hammet *et al.*, 2007), which counteracts DSB resection by favoring Rad9 association at the DSB (Clerici *et al.*, 2014). We show that expression of a non-phosphorylatable H2A variant in *sae2*Δ cells suppresses their resection defect and prevents the accumulation of Rad9 at the DSB. Furthermore, γH2A generation close to the break site depends on Tel1 kinase activity. Thus, although we cannot exclude a direct control of Tel1 on Rad9 association to DNA ends, our

findings indicate that Tel1 acts in this process mostly through γH2A generation.

Altogether, our results support a model whereby Tel1 and Rad53, once activated, limit DSB resection by promoting Rad9 binding to DSBs and therefore by inhibiting Sgs1-Dna2. Sae2 activates Mre11 endonucleolytic activity that clips the 5'-terminated DNA strand, thus generating 5' and 3' tailed substrates that can be processed by Exo1/Sgs1-Dna2 and Mre11 activity, respectively (Fig. 29, left). When Sae2 function fails, defective Mre11 nuclease activity causes increased MRX persistence at the DSB that leads to enhanced and prolonged Tel1-dependent Rad53 activation. As a consequence, Tel1- and Rad53-mediated phosphorylation events increase the amount of Rad9 bound at the DSB, which inhibits DSB resection by counteracting Sgs1-Dna2 activity (Fig. 29, middle). Dysfunction of Rad53 or Tel1 reduces Rad9 recruitment at the DSB ends and therefore relieves inhibition of Sgs1-Dna2, which can compensate for the lack of Sae2 in DNA damage resistance and resection (Fig. 29, right). In conclusion, we demonstrate that Rad9 increases the requirement for MRX/Sae2 activities in DSB resection by inhibiting the action of Sgs1/Dna2 and that dampening Tel1 or Rad53 signaling bypass Sae2 function in DSB resection. Altogether, these finding indicate that the primary cause of the resection defect of *sae2*Δ cells is an enhanced Rad9 binding to DSBs that is promoted by the persistent MRX-dependent Tel1 and Rad53 signaling activities. This work

reveals new details of the molecular mechanisms of DSB resection and the role of Sae2 at DSBs in the model organism *S. cerevisiae*.

ATM inhibition has been proposed as a strategy for cancer treatment (Cremona and Behrens, 2014). Therefore, the observation that dampening Tel1/ATM signaling activity restores DNA damage resistance in *sae2*Δ cells might have implications in cancer therapies that use ATM inhibitors for synthetic lethal approaches to threat tumors with deficiencies in the DNA damage response.

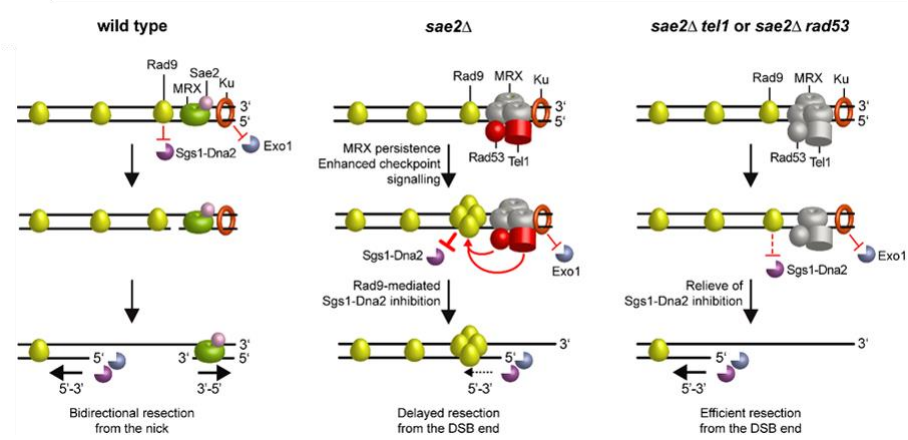

Figure 29. Model for the role of Sae2 at DSBs. Wild type, left) Sae2 activates the Mre11 endonuclease activity to incise the 5' strand. Generation of the nick allows bidirectional processing by Exo1/Sgs1-Dna2 in the 5'-3' direction from the nick and MRX in the 3' to 5' direction toward the DSB ends. Ku and Rad9 inhibit DSB resection by limiting Exo1 and Sgs1-Dna2, respectively. *sae2*Δ, middle) The absence of Sae2 impairs the MRX nuclease activity (nonfunctional MRX nuclease is in grey). As a consequence, the endonucleolytic cleavage of the 5' strand does not occur and resection is carried out by Exo1 and Dna2-Sgs1 that degrade the 5' strands from the DSB ends. Impairment of Mre11 nuclease activity also causes increased MRX association at the DSB, which leads to enhanced Tel1-dependent Rad53 activation. Tel1 and Rad53 activities limit DSB resection from the DSB end (dashed arrow) by increasing the amount of DSB-bound Rad9, which inhibits Sgs1-Dna2 recruitment at DSBs. *sae2*Δ *tel1* or *sae2*Δ *rad53*, right) Impairments of Tel1 or Rad53 activity (nonfunctional Tel1 and Rad53 are in grey) restore efficient resection in *sae2*Δ cells by relieving Rad9-mediated inhibition of Sgs1-Dna2. Restored DSB resection by Sgs1-Dna2 also reduces MRX persistence at the DSB.

MATERIALS AND METHODS

Yeast and bacterial strains

Yeast strains

The yeast strains used in this study are derivatives of W303, JKM139, YMV45 and SK1 strains and are listed in Table 1. Strains JKM139 and YMV45 were kindly provided by J. Haber (Brandeis University, Waltham, USA). Strains YMV45 are isogenic to YFP17 (*mat*Δ*::hisG hml*Δ*::ADE1 hmr*Δ*::ADE1 ade1 lys5 ura3-52 trp1 ho ade3::GAL-HO leu2::cs*) except for the presence of a *LEU2* fragment inserted 4.6 kb centromere-distal to *leu2::cs* (Vaze *et al.*, 2002). To induce a persistent G1 arrest with α-factor, some strains carried the deletion of the *BAR1* gene, which encodes a protease that degrades the α-factor. Deletions were generated by one-step PCR disruption method. PCR one-step tagging methods was used to obtain strains carrying fully functional MYC-tagged or HA-tagged alleles. The accuracy of all gene replacement and integrations was verified by PCR. Cells were grown in YEP medium (1% yeast extract, 2% peptone) supplemented with 2% glucose (YEPD), 2% raffinose (YEPR) or 2% raffinose and 3% galactose (YEPRG).

Strain	Relevant genotype	Source
W303	*MAT*a/α *ade2-1 can1-100 his3-11,15 leu2-3,112 trp1-1 ura3-1 rad5-535*	Bonetti *et al.*, 2009
YLL 1069.3	W303 *sae2*Δ*::KANMX*	Bonetti *et al.*, 2009
YLL 936.1	W303 *mre11*Δ*::HIS3*	Bonetti *et al.*, 2009
YLL 2402.1	W303 *exo1*Δ*::LEU2*	Bonetti *et al.*, 2009
YLL 2403.7	W303 *exo1*Δ*::LEU2 sae2*Δ*::KANMX*	Bonetti *et al.*, 2009
YLL 2511.4	W303 *dna2*Δ*::NATMX pif1-M2::URA3*	This study
YLL 3497.9	W303 *sae2*Δ*::KANMX SGS1-ss-3HA::URA3*	This study
YLL 3503.2	W303 *sae2*Δ*::KANMX SGS1-ss::TRP1*	This study
YLL 3557.1	W303 *sgs1-hd::LEU2*	This study
YLL 3558.7	W303 *sgs1-ss-hd::TRP1*	This study
DMP 2949/1C	W303 *rad9*Δ*::URA3*	This study
DMP 5694/1A	W303 *mre11-H125N*	This study
DMP 5936/4A	W303 *SGS1-ss::TRP1*	This study
DMP 5952/5D	W303 *pif1-M2::URA3 yku70*Δ*::HIS3 sae2*Δ*::KANMX*	This study
DMP 5956/6D	W303 *mre11-H125N SGS1-ss::TRP1*	This study
DMP 5964/7A	W303 *exo1*Δ*::LEU2 sae2*Δ*::KANMX SGS1-ss::TRP1*	This study
DMP 5964/1B	W303 *exo1*Δ*::LEU2 SGS1-ss::TRP1*	This study
DMP 6008/3D	W303 *pif1-M2::URA3 sae2*Δ*::KANMX SGS1-ss::TRP1*	This study
DMP 6011/4C	W303 *mre11*Δ*::KANMX SGS1-ss::TRP1*	This study
DMP 6068/2B	W303 *sae2*Δ*::KANMX rad9*Δ*::URA3*	This study
DMP 6068/4C	W303 *sae2*Δ*::KANMX rad9*Δ*::URA3*	This study
DMP 6068/2D	W303 *sae2*Δ*::KANMX rad9*Δ*::URA3 SGS1-ss::TRP1*	This study
DMP 6068/6B	W303 *sae2*Δ*::KANMX rad9*Δ*::URA3 SGS1-ss::TRP1*	This study
JKM139	*MAT*a *hml*Δ*::ADE1, hmr*Δ*::ADE1, ade1-100, lys5, leu2-3,112, trp1::hisG ura3-52, ho, ade3::GAL-HO site*	Lee *et al.*, 1998
YLL 1523.3	JKM139 *sae2*Δ*::KANMX*	This study
YLL 1540.4	JKM139 *exo1*Δ*::LEU2*	This study
YLL 1643.1	JKM139 *bar1*Δ*::HPHMX*	This study
YLL 2482.2	JKM139 *sgs1*Δ*::NATMX*	This study

YLL 3397.6	JKM139 *SGS1-3HA::URA3 bar1Δ::HPHMX*	This study
YLL 3507.3	JKM139 *sae2Δ::KANMX SGS1-ss::TRP1*	This study
YLL 3564.1	JKM139 *SGS1-3HA::URA3 rad9Δ::KANMX bar1Δ::HPHMX*	This study
DMP 5685/2A	JKM139 *ku70Δ::URA3 bar1Δ::HPHMX*	This study
DMP 5793/4D	JKM139 *rad9Δ::KANMX*	This study
DMP 5984/10D	JKM139 *SGS1-ss::TRP1*	This study
DMP 5985/15B	JKM139 *SGS1-ss::TRP1 bar1Δ::HPHMX*	This study
DMP 6005/2C	JKM139 *rad9Δ::KANMX SGS1-ss::TRP1*	This study
DMP 6012/9D	JKM139 *rad9Δ::KANMX sgs1Δ::NATMX*	This study
DMP 6034/4B	JKM139 *rad9Δ::KANMX sae2Δ::KANMX*	This study
DMP 6080/2B	JKM139 *exo1Δ::LEU2 rad9Δ::KANMX*	This study
DMP 6084/2B	JKM139 *SGS1-ss-3HA::URA3 bar1Δ::HPHMX*	This study
DMP 6084/5D	JKM139 *SGS1-ss-3HA::URA3 rad9Δ::KANMX bar1Δ::HPHMX*	This study
DMP 6125/8A	JKM139 *EXO1-18MYC::TRP1 bar1Δ::HPHMX*	This study
DMP 6125/5A	JKM139 *EXO1-18MYC::TRP1 rad9Δ::KANMX bar1Δ::HPHMX*	This study
DMP 6127/3D	JKM139 *exo1Δ::LEU2 SGS1-ss::TRP1*	This study
DMP 6129/8A	JKM139 *ku70Δ::URA3 SGS1-ss::TRP1 bar1Δ::HPHMX*	This study
DMP 6129/15B	JKM139 *ku70Δ::URA3 rad9Δ::KANMX bar1Δ::HPHMX*	This study
DMP 6145/10B	JKM139 *MRE11-18MYC::TRP1 sae2Δ::KANMX SGS1-ss::TRP1*	This study
YLL 3638.1	JKM139 *rad53-kd::KANMX*	This study
DMP 6225/1B	JKM139 *rad53-kd::KANMX sae2Δ::KANMX*	This study
DMP 6187/3B	JKM139 *tel1-kd::LEU2*	This study
DMP 6187/5C	JKM139 *sae2Δ::KANMX tel1-kd::LEU2*	This study
YLL 2766.7	JKM139 *sae2Δ::HPHMX tel1Δ::NATMX*	This study
YLL 1794.3	JKM139 *tel1Δ::NATMX*	This study
YLL 3222.6	JKM139 *TEL1-3HA::NATMX*	This study

YLL 3540.1	JKM139 *tel1-N2021D-3HA::NATMX*	This study
YLL 3670.14	JKM139 *tel1-kd-3HA::NATMX*	This study
DMP 5719/2A	JKM139 *RAD9-3HA::HIS3*	This study
DMP 6163/1D	JKM139 *RAD9-3HA::HIS3 rad53-H88Y::URA3*	This study
DMP 5816/1A	JKM139 *sae2Δ::KANMX RAD9-3HA::HIS3*	This study
DMP 6226/5A	JKM139 *rad53-kd::KANMX RAD9-3HA::TRP1*	This study
DMP 6208/14A	JKM139 *tel1-kd::LEU2 RAD9-3HA::TRP1*	This study
DMP 6226/3C	JKM139 *sae2Δ::KANMX rad53-kd::KANMX RAD9-3HA::TRP1*	This study
DMP 6208/5D	JKM139 *sae2Δ::KANMX tel1-kd::LEU2 RAD9-3HA::TRP1*	This study
DMP 6023/5A	JKM139 *SGS1-3HA::URA3*	This study
DMP 6239/8C	JKM139 *sae2Δ::KANMX SGS1-3HA::URA3*	This study
DMP 6186/5D	JKM139 *rad53-kd::KANMX SGS1-3HA::URA3*	This study
DMP 6240/7A	JKM139 *tel1-kd::LEU2 SGS1-3HA::URA3*	This study
DMP 6227/5D	JKM139 *sae2Δ::HPHMX rad53-kd::KANMX SGS1-3HA::URA3*	This study
DMP 6240/2D	JKM139 *sae2Δ::KANMX tel1-kd::LEU2 SGS1-3HA::URA3*	This study
YLL 1769.3	JKM139 *mre11Δ::NATMX*	This study
YLL 2839. 1	JKM139 *mre11Δ::HPHMX tel1Δ::NATMX*	This study
DMP 6243/9A	JKM139 *RAD9-3HA::TRP1 hta2Δ::NATMX*	This study
DMP 6243/18A	JKM139 *RAD9-3HA::TRP1 hta2Δ::NATMX sae2Δ::KANMX*	This study
DMP 6243/5C	JKM139 *RAD9-3HA::TRP1 hta1-S129A::URA3 hta2Δ::NATMX sae2Δ::KANMX*	This study
DMP 5396/4C	JKM139 *hta2Δ::NATMX*	This study
DMP 5129/19B	JKM139 *hta2Δ::NATMX hta1-S129A::URA3*	This study
DMP 5129/34A	JKM139 *hta2Δ::NATMX hta1-S129A::URA3 sae2Δ::KANMX*	This study
DMP 5129/10B	JKM139 *hta2Δ::NATMX sae2Δ::KANMX*	This study

YMV45	*ho hml::ADE1 mata::hisG hmr::ADE1 leu2::leu2(Asp718-SalI)-URA3*-pBR332-*MATa ade3::GAL::HO ade1 lys5 ura3-52 trp1::hisG*	Vaze *et al.*, 2002
YLL 3583.6	YMV45 *sae2Δ::KANMX SGS1-ss::TRP1*	This study
YLL 3584.4	YMV45 *SGS1-ss::TRP1*	This study
YLL 1621.9	YMV45 *sae2Δ::KANMX*	This study
YLL 3635.2	YMV45 *sae2Δ::HPHMX rad53-H88Y::TRP1*	This study
YLL 3533.3	YMV45 *sae2Δ::KANMX tel1-N2021D::HPHMX*	This study
YLL 3636.1	YMV45 *rad53-kd::KANMX*	This study
YLL 3628.1	YMV45 *tel1-kd::HPHMX*	This study
YLL 3637.2	YMV45 *sae2Δ:HPHMX rad53-kd::KANMX*	This study
YLL 3610.1	YMV45 *sae2Δ::KANMX tel1-kd::HPHMX*	This study
YLL 3529.1	YMV45 *tel1Δ::KANMX*	This study
YLL 3563.2	YMV45 *sae2Δ::NATMX tel1Δ::KANMX*	This study
SK1	*MATa/MATα HO/HO lys2/lys2 ura3::hisG/ura3::hisG leu2::hisG/leu2::hisG*	Manfrini *et al.*, 2010
YLL 2679.27/ 9C	SK1 *sae2Δ::NATMX/sae2Δ::NATMX*	Manfrini *et al.*, 2010
DMP 6071/2B	SK1 *SGS1-ss::TRP1/SGS1-ss::TRP1*	This study
DMP 6071/2A	SK1 *sae2Δ::NATMX/sae2Δ::NATMX SGS1-ss::TRP1/SGS1-ss::TRP1*	This study

Table 1. *Saccharomyces cerevisiae* strains used in this study.

E. coli STRAIN

E. coli DH5α™ strain (*F-, φ80 dlacZM15, D(lacZTA-argF) U169, deoR, recA1, endA1, hsdR17, (rK-,mK+) phoA supE44, λ−, thi-1, gyrA96, relA1*) is used as bacterial host for plasmid manipulation and amplification. *E. coli* DH5α™ competent cells to transformation are purchased from Invitrogen.

Growth media

S. cerevisiae media

YEP (Yeast-Extract Peptone) is the standard rich media for *S. cerevisiae* and contains 10 g/L yeast extract, 20 g/L peptone and 50 mg/L adenine. YEP must be supplemented with 2% glucose (YEPD), 2% raffinose (YEP+raf) or 2% raffinose and 2% galactose (YEP+raf+gal) as carbon source. YEP-based selective media are obtained including 400 μg/mL G418, 300 μg/mL hygromicin-B or 100 μg/mL nourseotricin. Solid media are obtained including 2% agar. Stock solutions are 50% glucose, 30% raffinose, 30% galactose, 80 mg/mL G418, 50 mg/mL hygromicin-B and 50 mg/mL nourseotricin. YEP and glucose stock solution are autoclave-sterilized and stored at RT. Sugars and antibiotics stock solutions are sterilized by micro-filtration and stored at RT and 4°C respectively.

S.C. (Synthetic Complete) is the minimal growth media for *S. cerevisiae* and contains 1.7 g/L YNB (Yeast Nitrogen Base) without amino acids, 5 g/L ammonium sulphate, 200μM inositol, 25 mg/L uracil, 25 mg/L adenine, 25 mg/L hystidine, 25 mg/L leucine, 25 mg/L tryptophan. S.C. can be supplemented with drop-out solution (20 mg/L arginine, 60 mg/L isoleucine, 40 mg/L lysine, 10 mg/L methionine, 60 mg/L phenylalanine, 50 mg/L tyrosine) based on yeast strains requirements. Different carbon sources can be used in rich media (2% glucose, 2% raffinose or 2% raffinose and 3% galactose). One or more amino acid/base can be omitted to have S.C.-based

selective media (e.g. S.C.-ura is S.C. lacking uracil). To obtain G418 or NAT S.C. selective medium the 5 g/L ammonium sulphate are replaced with 1 g/L monosodic glutamic acid. Solid media are obtained by including 2% agar. Stock solutions are 17 g/L YNB + 50 g/L ammonium sulphate (or 10g/L monosodic glutamic acid), 5 g/L uracil, 5 g/L adenine, 5 g/L hystidine, 5 g/L leucine, 5 g/L tryptophan, 100X drop out solution (2 g/L arginine, 6 g/L isoleucine, 4 g/L lysine, 1 g/L methionine, 6 g/L phenylalanine, 5 g/L tyrosine), 20mM inositol. All of these solutions are sterilized by micro-filtration and stored at 4°C.

VB sporulation medium contains 13.6 g/L sodium acetate, 1.9 g/L KCl, 0.35 g/L MgSO4, 1.2 g/L NaCl. pH is adjusted to 7.0. To obtain solid medium include 2% agar. pH is adjusted to 7.0. Sterilization by autoclavation.

***E. coli* media**

LD is the standard growth medium for *E. coli*. LD medium contains 10 g/L tryptone, 5 g/L yeast extract and 5 g/L NaCl. Solid medium is obtained by including 1% agar. LD+Amp selective medium is obtained including 50 μg/mL Ampicillin. LD is autoclave-sterilized and stored at RT. Ampicillin stock solution (2.5 g/L) is sterilized by micro-filtration and stored at 4°C.

Conservation and storage of *S. cerevisiae* and *E. coli* strains

Yeast cells are grown 2-3 days at 30°C on YEPD plates, resuspended in 15% glycerol and stored at -80°C. Bacteria are grown o/n at 37°C on LD+Amp plates, resuspended in 50% glycerol and stored at -80°C. Yeast and bacteria cells can be stored for years in these conditions.

Molecular biology techniques

Agarose gel electrophoresis

Agarose gel elctrophoresis is the easiest and common way of separating and analyzing DNA molecules. This technique allows the separation of DNA fragments based on their different molecular weight (or length in kb). The purpose of this technique might be to visualize the DNA, to quantify it or to isolate a particular DNA fragment. The DNA is visualized by the addition in the gel of ethidium bromide, which is a fluorescent dye that intercalates between bases of nucleic acids. Ethidium bromide absorbs UV light and transmits the energy as visible orange light, revealing the DNA molecules to which is bound.

To pour a gel, agarose powder is mixed with TAE (0.04M Tris-Acetate 0.001M EDTA) to the desired concentration, and the solution is microwaved until completely melted. Most gels are made between 0.8% and 2% agarose. A 0.8% gel will show good resolution of large DNA fragments (5-10 Kb) and a 2% gel will show good resolution for small fragments (0.2-1 Kb). Ethidium bromide is added to the gel at a

final concentration of 1 μg/mL to facilitate visualization of DNA after electrophoresis. After cooling the solution to about 60°C, it is poured into a casting tray containing a sample comb and allowed to solidify at RT or at 4°C. The comb is then removed and the gel is placed into an electrophoresis chamber and just covered with the buffer (TAE). Sample containing DNA mixed with loading buffer are then pipetted into the sample wells. The loading buffer contains 0.05% bromophenol blue and 5% glycerol, which give color and density to the sample. A marker containing DNA fragments of known length and concentration is loaded in parallel to determine size and quantity of DNA fragments in the samples. Then current is applied and DNA will migrate toward the positive electrode. When adequate migration has occurred, DNA fragments are visualized by placing the gel on a UV trans illuminator.

DNA extraction from agarose gels (paper strip method)

This method allows to isolate a DNA fragment of interest. Using a scalpel blade cut a slit immediately in front of the band to be extracted. Cut a piece of GF-C filter to size to fit inside the slit. Place the paper strip in the slit and switch on the current for 1-2 minutes at 150 V. The DNA runs onward into the paper and is delayed in the smaller mesh size of the paper. Remove the strip of paper and place it into a 0.5 mL micro centrifuge tube. Make a tiny hole in the bottom of the tube using a syringe needle, place the 0.5 mL tube inside a 1.5 mL

tube and spin for 30 seconds. Buffer and DNA are retained in the 1.5 mL tube. Extract the DNA with 1 volume of phenol/chloroform and precipitate the DNA with 100mM sodium acetate and 3 volumes of 100% ethanol. After micro centrifugation re-dissolve DNA in an appropriate volume of water, TRIS (10mM Tris HCl pH 8.5) or TE (10mM Tris HCl, 1mM EDTA pH7.4) buffer.

Restriction endonucleases

Type II endonucleases (also known as restriction endonucleases or restriction enzymes) cut DNA molecules at defined positions close to their recognitions sequences in a reaction known as enzymatic digestion. They produce discrete DNA fragments that can be separated by agarose gel electrophoresis, generating distinct gel banding patterns. For these reasons they are used for DNA analysis and gene cloning. Restriction enzymes are generally stored at -20°C in a solution containing 50% glycerol, in which they are stable but not active. Glycerol concentration in the reaction mixture must be below 5% in order to allow enzymatic reaction to occur. They generally work at 37°C with some exceptions (e.g. ApaI activity is maximal at 25°C) and they must be supplemented with a reaction buffer provided by the manufacturer, and in some cases with Bovin Serum Albumin. We use restriction endonucleases purchased from NEB and PROMEGA.

Ligation

DNA is previously purified from agarose gel with the paper strip method, phenol/chloroform extracted, ethanol precipitated and resuspended in the appropriate volume of water or TE buffer. The ligation reaction is performed in the following conditions: DNA fragment and vector are incubated overnight at 16°C with 1 μl T4 DNA Ligase (PROMEGA) and T4 DNA Ligase Buffer (PROMEGA). The ligation reaction is then used to transform competent E. coli cells. Plasmids are recovered from Amp+ transformants and subjected to restriction analysis.

Polymerase Chain Reaction (PCR)

PCR allows to obtain high copy number of a specific DNA fragment of interest starting from very low quantity of DNA fragment. The reaction is directed to a specific DNA fragment by using a couple of oligonucleotides flanking the DNA sequence of interest. These oligonucleotides work as primers for the DNA polymerase. The reaction consists of a number of polymerization cycles which are based on 3 main temperature-dependent steps: denaturation of DNA (which occur over 90°C), primer annealing to DNA (typically take place at 45-55°C depending on primer characteristic), synthesis of the DNA sequence of interest by a thermophilic DNA polymerase (which usually works at 68 or 72°C). Different polymerases with different properties (processivity, fidelity, working temperature, etc) are

commercially available and suitable for different purpose. Taq polymerase works at 72°C and is generally used for analytical PCR. Polymerases with higher fidelity like Pfx and VENT polymerases, which work respectively at 68 and 72°C, are generally employed when 100% polymerization accuracy is required.

The typical 50 µL PCR mixture contains 1µL of template DNA, 0.5 µM each primer, 200µM dNTPs, 5 µL of 10X Reaction Buffer, 1mM $MgCl_2$, 1-2 U DNA polymerase and water to 50 µL. The typical cycle-program for a reaction is: 1. 3 minutes' denaturation at 94-95°C; 2. 30 seconds denaturation at 94-95°C; 3. 30 seconds annealing at primers Tm (melting temperature); 4. 1 minute polymerization per kb at 68 or 72°C (depending on polymerase); 5. repeat 30 times from step 2; 6. 5-10 minutes polymerization at 68-72°C. The choice of primer sequences determines the working Tm, which depends on the length (L) and GC% content of the oligonucleotides and can be calculated as follows: $Tm = 59.9 + 0.41(GC\%) – 675/L$.

Preparation of yeast genomic DNA for PCR

Resuspend yeast cells in 200 µL Yeast Lysis Buffer (2% TRITON X100, 1% SDS, 100mM NaCl, 10mM Tris HCl pH 8, 1mM EDTA pH 8), add 200 µL glass beads, 200 µL phenol/chloroform and vortex 3 minutes. Ethanol precipitate the aqueous phase obtained after 5 minutes' centrifugation. Resuspend DNA in the appropriate volume of water and use 1 µL as a template for PCR.

Plasmid DNA extraction from *E. coli* (I): minipreps boiling

E. coli cells (2mL overnight culture) are harvested by centrifugation and resuspended in 500 µL STET buffer (8% sucrose, 5% TRITON X-100, 50mM EDTA, 50mM Tris-HCl, pH 8). Bacterial cell wall is digested boiling the sample for 2 minutes with 1 mg/mL lysozyme. Cellular impurities are removed by centrifugation and DNA is precipitated with isopropanol and resuspended in the appropriate volume of water or TE.

Plasmid DNA extraction from *E. coli* (II): minipreps with QIAGEN columns

This protocol allows the purification of up to 20 µg high copy plasmid DNA from 1-5 mL overnight *E. coli* culture in LD medium. Cells are pelleted by centrifugation and resuspended in 250 µL buffer P1 (100 µg/mL RNase, 50mM Tris HCl pH 8, 10mM EDTA pH 8). After addition of 250 µL buffer P2 (200mM NaOH, 1% SDS) the solution is mixed thoroughly by inverting the tube 4-6 times, and the lysis reaction occur in 5 minutes at RT. 350 µL N3 buffer (QIAGEN) are added to the solution, which is then centrifuged for 10 minutes. The supernatant is applied to a QIAprep spin column which is washed once with PB buffer (QIAGEN) and once with PE buffer (QIAGEN). The DNA is eluted with EB buffer (10mM Tris HCl pH 8.5) or water.

Transformation of *E. coli* DH5α

DH5α competent cells are thawed on ice. Then, 50-100 µL cells are incubated 30 minutes in ice with 1 µL plasmid DNA. Cells are then subjected to heat shock at 37°C for 30 seconds and then incubated on ice for 2 minutes. Finally, 900 µL LD are added to the tube and cells are incubated 30 minutes at 37°C to allow expression of ampicillin resistance. Cells are then plated on LD+Amp and overnight incubated at 37°C.

Transformation of *S. cerevisiae*

YEPD exponentially growing yeast cells are harvested by centrifugation and washed with 1 mL 1M lithium acetate (LiAc) pH 7.5. Cells are then resuspended in 1M LiAc pH 7.5 to obtain a cells/LiAc 1:1 solution. 12 µL cells/LiAc are incubated 30-45 minutes at RT with 45 µL 50% PEG (PolyEthyleneGlycol) 3350, 4 µL carrier DNA (salmon sperm DNA) and 1-4 µL DNA of interest (double each quantity when transform with PCR products). After addition of 6 µL 60% glycerol cells are incubated at RT for 30-45 minutes, heat-shocked at 42°C for 5-10 minutes and plated on appropriate selective medium.

Extraction of yeast genomic DNA (Teeny yeast DNA preps)

Yeast cells are harvested from overnight cultures by centrifugation, washed with 1 mL of 0.9M sorbytol 0.1M EDTA pH 7.5 and resuspended in 0.4 mL of the same solution supplemented with 14mM

β-mercaptoethanol. Yeast cell wall is digested by 45 minutes' incubation at 37°C with 0.4 mg/mL 20T zimoliase. Spheroplasts are harvested by 30 seconds centrifugation and resuspended in 400 µL TE. After addition of 90 µL of a solution containing EDTA pH 8.5, Tris base and SDS, spheroplasts are incubated 30 minutes at 65°C. Samples are kept on ice for 1 hour following addition of 80 µL 5M potassium acetate. Cell residues are eliminated by 15 minutes' centrifugation at 4°C. DNA is precipitated with chilled 100% ethanol, resuspended in 500 µL TE and incubated 30 minutes with 25 µL 1 mg/mL RNase to eliminate RNA. DNA is then precipitated with isopropanol and resuspended in the appropriate volume (typically 50 µL) of TE.

Southern blot analysis

Yeast genomic DNA prepared with standard methods is digested with the appropriate restriction enzyme(s). The resulting DNA fragments are separated by agarose gel electrophoresis in a 0.8% agarose gel. When adequate migration has occurred, gel is washed 40 minutes with a denaturation buffer (0.2N NaOH, 0.6M NaCl), and 40 minutes with a neutralization buffer (1.5M NaCl, 1M Tris HCl, pH 7.4). DNA is blotted onto a positively charged nylon membrane by overnight capillary transfer with 10X SSC buffer (20X SSC: 3M sodium chloride, 0.3M sodium citrate, pH 7.5). Membrane is then washed with 4X SSC and UV-crosslinked. Hybridization is carried out by

incubating membrane for 5 hours at 50°C with pre-hybridization buffer (50% formamide, 5X SSC, 0.1% N-lauroylsarcosine, 0.02% SDS, 2% Blocking reagent) following by o/n incubation at 50°C with pre-hybridization buffer + probe. The probe is obtained by random priming method (DECAprime™ kit by Ambion) on a suitable DNA template and with 32P d-ATP. Filter is then washed (45 minutes + 15 minutes) at 55°C with a washing solution (0.2M sodium phosphate buffer pH 7.2, SDS 1%, water), air dried and then exposed to an autoradiography film.

Denaturing gel electrophoresis and southern blot analysis to visualize single-stranded DNA (ssDNA)

A 0.8% agarose gel (in H_2O) is submerged in a gel box containing a 50mM NaOH, 1mM EDTA solution for 30 minutes to equilibrate. Ethidium bromide is omitted because it does not efficiently bind to DNA under these conditions. After digestion with the appropriate restriction enzyme(s), DNA samples are prepared by adjusting the solution to 0.3M sodium acetate and 5mM EDTA (pH 8.0) following by addition of 2 volumes of ethanol to precipitate DNA. After chilling (o/n) and centrifuging the samples (15 minutes, possibly at 4°C), pellet is resuspended in alkaline gel loading buffer (1X buffer: 50mM NaOH, 1mM EDTA pH 8.5, 2.5% Ficoll (Type 400) and 0.025% bromophenol blue). After loading the DNA in the gel, a glass plate can be placed on the gel to prevent the dye from diffusing from the

agarose during the course of the run. Because of the large currents that can be generated with denaturing gels, gels are usually run slowly at lower voltages (e.g. 30 V over-night). After the DNA has migrated far enough, the gel can be stained with 0.5 μg/mL ethidium bromide in 1X TAE electrophoresis buffer (1 hour). The DNA will be faint because the DNA is single stranded. Gel is then soaked in 0.25N HCl for 7 minutes with gentle agitation, rinsed with water and soaked in 0.5M NaOH, 1.5M NaCl for 30 minutes with gentle agitation. Gel is then rinsed briefly with water and DNA is blotted by capillary transfer onto neutral nylon membrane using 10X SSC. Hybridization is carried out by incubating membrane for 5 hours at 42°C with pre-hybridization buffer (50% formamide, denhardts solution + 4X BSA, 6% destran sulphate, 100 μg/mL salmon sperm DNA, 200 μg/mL tRNA carrier) following by o/n incubation at 42°C with pre-hybridization buffer + single-stranded RNA (ssRNA) probe. The ssRNA probe is obtained by *in vitro* transcription using Promega Riboprobe System-T7 and a pGEM-7Zf-based plasmid as a template. Following hybridization, membrane is washed twice with 5X SSPE (20X SSPE = 3M NaCl, 200μM NaH_2PO_4, 20μM EDTA, pH 7.4) at 42°C for 15 minutes, 30 minutes with 1X SSPE 0.1% SDS at 42°C, 30 minutes with 0.1X SSPE 0.1% SDS at 42°C, 15 minutes with 0.2X SSPE 0.1% SDS at 68°C and 5 minutes with 0.2X SSPE at RT. Finally, membrane is exposed to an X-ray film.

DSB resection and repair by Single-Strand Annealing (SSA)

DSB end resection at the *MAT* locus in JKM139 derivative strains was analyzed on alkaline agarose gels as previously described (Trovesi *et al.*, 2011), by using a single-stranded probe complementary to the unresected DSB strand. This probe was obtained by *in vitro* transcription using Promega Riboprobe System-T7 and plasmid pML514 as a template. Plasmid pML514 was constructed by inserting in the pGEM7Zf EcoRI site a 900-bp fragment containing part of the *MATα* locus (coordinates 200870 to 201587 on chromosome III). Quantitative analysis of DSB resection was performed by calculating the ratio of band intensities for ssDNA and total amount of DSB products.

DSB formation and repair in YMV45 strain were detected by Southern blot analysis using an Asp718-SalI fragment containing part of the *LEU2* gene as a probe as previously described (Trovesi *et al.*, 2011). Quantitative analysis of the repair product was performed by calculating the ratio of band intensities for SSA product with respect to a loading control.

Chromatin ImmunoPrecipitation (ChIP) analysis

Exponentially growing cells (50 mL of $8x10^6$-$1x10^7$) are treated with 1.4 mL of 37% formaldehyde for 5 minutes while shaking, in order to create DNA-protein and protein-protein covalent bounds (cross-link). Then 2.5 mL of 2.5M glycine are added for other 5 minutes while

shaking. Treated cells are kept in ice until centrifugation at 1800 rpm for 5 minutes at 4°C. Cell pellet is then washed first with HBS buffer (50mM HEPES pH 7.5, 140mM NaCl) and then with ChIP buffer (50mM HEPES pH 7.5, 140mM NaCl, 1mM EDTA pH 8, 1% IGEPAL CA-630, 0.1% Sodium deoxycholate, 1mM PMSF). Before each wash cells are pelleted by centrifugation at 1800 rpm for 5 minutes at 4°C. After the wash with ChIP buffer and subsequent centrifugation, the supernatant is carefully and completely removed. Then add 0.4 mL of ChIP buffer + complete anti-proteolitic tablets (Roche) is added and samples are stored at -80°C until the following day. After breaking cells for 30 minutes at 4°C with glass beads, the latter are eliminated. This passage is followed by centrifugation at 4°C for 30 minutes. Pellet is resuspended in 0.5 mL ChIP buffer + anti-proteolitics and then sonicated, in order to share DNA in 500-1000 bp fragments (4 cycles of 25 seconds). At this point 5 μL as "input DNA" for PCR reactions and 20 μL as "input" for western blot analysis are taken. Then 400 μL of the remaining solution is immunoprecipitated with specific Dynabeads-coated antibodies. After proper incubation with desired antibodies, Dynabeads can be washed RT as follow: 2X with SDS buffer (50mM HEPES pH 7.5, 1mM EDTA pH 8, 140mM NaCl, 0.025% SDS), 1X with High-salt buffer (50mM HEPES pH 7.5, 1mM EDTA pH 8, 1M NaCl), 1X with T/L buffer (20mM Tris-Cl, pH 7.5, 250mM LiCl, 1mM EDTA pH 8, 0.05% sodium deoxycholate, 0.5%IGEPAL-CA630), and then 2X with T/E buffer (20mM Tris-Cl

pH 7.5, 0.1mM EDTA pH 8). All washes are done by pulling down Dynabeads 1 minute and then nutating for 4 minutes with the specific buffer. After the last wash Dynabeads are resuspended in 145 µL TE + 1% SDS buffer, shaked on a vortex, put at 65°C for 2 minutes, shaked on vortex again and then pulled down. then 120 µL of the supernatant are put at 65°C over-night for reverse cross-linking, while 20 µL are stored as sample for western blot analysis of the immunoprecipitated protein amount. Previously taken input DNA samples must be put at 65°C over-night with 115 µL of TE + 1% SDS buffer. The next day DNA must be purified for PCR analysis with QIAGEN columns.

ChIP assays were performed as previously described (Viscardi *et al.*, 2007). Quantification of immunoprecipitated DNA was achieved by quantitative real-time (qPCR) on a Bio-Rad MiniOpticon apparatus using primer pairs located at different distances from the HO-induced DSB and at the *ARO1* fragment of chromosome IV. Data are expressed as fold enrichment at the HO-induced DSB over that at the non-cleaved *ARO1* locus, after normalization of each ChIP signals to the corresponding amount of immunoprecipitated protein and input for each time point. Fold enrichment was then normalized to the efficiency of DSB induction.

Synchronization of yeast cells

Synchronization of yeast cells with α-factor

α-factor allows to synchronize a population of yeast cells in G1 phase. This pheromone activates a signal transduction cascade which arrests yeast cells in G1 phase. Only *MATa* cells are responsive to α-factor. To synchronize in G1 a population of exponentially growing yeast cells in YEPD, 2 μg/mL α-factor is added to $6x10^6$ cells/mL culture. As the percentage of budded cells will fall below 5% cells are considered to be G1-arrested. Cells are then washed and resuspended in fresh medium with or without 3 μg/mL α-factor to keep cells G1-arrested or release them into the cell cycle respectively. At this time cell cultures can be either treated with genotoxic agents or left untreated. If cells carry the deletion of *BAR1* gene, that encodes a protease that degrades the α-factor, 0.5 μg/mL α-factor is sufficient to induce a G1-arrest that lasts several hours.

Synchronization of yeast cells with nocodazole

Nocodazole allows to synchronize a population of yeast cells in G2 phase. This drug causes the depolimerization of microtubules, thus activating the mitotic checkpoint which arrests cells at the metaphase to anaphase transition (G2 phase). To synchronize in G2 a population of exponentially growing yeast cells in YEPD, 0.5 μg/mL nocodazole is added to $6x10^6$ cells/mL culture together with DMSO at a final concentration of 1% (use a stock solution of 100X nocodazole in

100% DMSO). As the percentage of dumbbell cells will reach 95% cells are considered to be G2-arrested. Cells are then washed and resuspended in fresh medium with or without 1.5 μg/mL nocodazole to keep cells G2-arrested or release them into the cell cycle respectively. At this time cell cultures can be either treated with genotoxic agents or left untreated.

Other techniques

FACS analysis of DNA contents

FACS (Fluorescence-Activated Cell Sorting) analysis allow to determine the DNA content of every single cell of a given population of yeast cells. $6x10^6$ cells are harvested by centrifugation, resuspended in 70% ethanol and incubated at RT for 1 hour. Cells are then washed with 1 mL 50mM Tris pH 7.5 and incubated overnight at 37°C in the same solution with 1 mg/mL RNase. Samples are centrifuged and cells are incubated at 37°C for 30 minutes with 5 mg/mL pepsin in 55mM HCl, washed with 1 mL FACS Buffer and stained in 0.5 mL FACS buffer with 50 μg/mL propidium iodide. 100 μL of each sample are diluted in 1 mL 50mM Tris pH 7.5 and analyzed with a Becton-Dickinson FACS-Scan. The same samples can also be analyzed by fluorescence microscopy to score nuclear division.

Total protein extracts

Total protein extracts were prepared from 10^8 cells collected from exponentially growing yeast cultures. Cells are harvested by

centrifugation and washed with 20% trichloracetic acid (TCA) in order to prevent proteolysis and resuspended in 50 µL 20% TCA. After addition of 200 µL of glass beads, cells are disrupted by vortexing for 8 minutes. Glass beads are washed with 400 µL 5% TCA, and the resulting extract are centrifuged at 3000 rpm for 10 minutes. The pellet is resuspended in 70 µL Laemmli buffer (0.62M Tris, 2% SDS, 10% glycine, 0.001% Bfb, 100mM DTT), neutralized with 30 µL 1M Tris base, boiled for 3 minutes, and finally clarified by centrifugation.

SDS-PAGE and western blot analysis

Protein extracts for western blot analysis were prepared by TCA precipitation. Protein extracts are loaded in 10% polyacrylamide gels (composition). Proteins are separated based on their molecular weight by polyacrylamide gel electrophoresis in the presence of sodium dodecyl sulphate (SDS-PAGE). When adequate migration has occurred proteins are blotted onto nitrocellulose membrane. Membrane is saturated by 1-hour incubation with 4% milk in TBS containing 0.2% TRITON X-100 and incubated for 2 hours with primary antibodies. Membrane is washed three times with TBS for 10 minutes, incubated for 1 hour with secondary antibodies and again washed with TBS. Detection is performed with ECL (Enhanced ChemiLuminescence - GE Healthcare) and X-ray films according to the manufacturer.

Primary polyclonal rabbit anti-Rad53 antibodies are purchased at Abcam (ab104232). Primary monoclonal 12CA5 anti-HA and 9E10 anti-MYC antibodies are purchased at GE Healthcare, as well as peroxidase conjucated IgG anti-rabbit and anti-mouse secondary antibodies. γH2A was immunoprecipitated by using anti-γH2A antibodies (ab15083) from Abcam.

Drop test

For spot assays, exponentially growing overnight cultures were counted, and 10-fold serial dilutions of equivalent cell numbers were spotted onto plates containing the indicated media.

Synchronous meiotic time course and detection of meiotic DSBs

To obtain synchronous G1/G0 cell population, overnight liquid YEPD cell cultures were diluted to a final concentration of 1×10^7 cells/mL in 200 mL YPA (1% yeast extract, 2% bactopeptone, 1% potassium acetate) and grown for 13 hours at 30°C. Cells were then washed and transferred into the same volume of SPM (0.3% potassium acetate, 0.02% raffinose) to induce meiosis. Genomic DNA was digested with EcoRI and separated on native agarose gels. DSBs at the *THR4* hotspot were detected with a 1.6 kb DNA fragment spanning the 5' region of *THR4*.

Immunoprecipitation and kinase assay

The kinase assay and coimmunoprecipitation were performed as previously described (Baldo *et al.*, 2008). Protein extracts for the immunoprecipitations were prepared in a lysis buffer containing 50mM HEPES (pH 7.4), 100mM KCl, 0.1mM EDTA (pH 7.5), 0.2% Tween-20, 1mM dithiothreitol (DTT), 25mM NaFl, 100μM sodium orthovanadate, 0.5 mM phenylmethylsulfonyl fluoride, 25mM β-glycerophosphate, and a protease inhibitor cocktail (Roche Diagnostics). After the addition of a 1:1 volume of acid-washed glass beads and breakage, equal amounts of protein of the different clarified extracts were incubated for 2 hours at 4°C with 75 μL of a 50% (vol/vol) protein A-Sepharose resin covalently linked to 12CA5 monoclonal antibody. Resins then were washed three times in the lysis buffer and were resuspended in 450 μL of a kinase buffer containing 10mM HEPES (pH 7.4), 50mM NaCl, 10mM $MgCl_2$, 10mM $MnCl_2$, 1mM DTT. Resuspended resins (150 μL) were dried, followed by the addition of 11.5 μL of kinase buffer, 1.5 μL of 20μM unlabeled ATP, 10 μCi of 32P-labeled ATP, and 1 μL of Phosphorylated Heat- and Acid-Stable protein I (PHAS-I; 1 μg/μL; Stratagene). Kinase reactions were incubated at 30°C for 30 minutes. Sodium dodecyl sulfate (SDS) gel-loading buffer (15 μL) was added to the resins, and bound proteins were resolved by SDS-18% polyacrylamide gel electrophoresis and visualized after exposure of the gels to autoradiography films. The residual 300 μL of each resuspended resin was dried, resuspended in

10 µL of loading buffer, and subjected to Western blot analysis with anti-HA antibody.

Search for suppressors of *sae2*Δ sensitivity to CPT

To search for suppressor mutations of the CPT-sensitivity of *sae2*Δ mutant, $5x10^6$ *sae2*Δ cells were plated on YEPD in the presence of 30µM CPT. Survivors were crossed to wild type cells to identify by tetrad analysis the suppression events that were due to single-gene mutations. Subsequent genetic analyses allowed grouping the single-gene suppression events in 11 classes. The seven classes that showed the most efficient suppression were chosen and the suppressor genes were identified by genome sequencing and genetic analyses. Genomic DNA from seven single-gene suppressors was analyzed by next-generation Illumina sequencing (IGA technology services) to identify mutations altering open reading frames within the reference *S. cerevisiae* genome. To confirm that, *SGS1-ss, rad53-H88Y* and *tel1-N2021D* mutations were responsible for the suppression, either *TRP1*, *URA3* or *HIS3* gene was integrated downstream of the *rad53-H88Y* and *tel1-N2021D* stop codon, respectively, and the resulting strain was crossed to wild type cells to verify by tetrad dissection that the suppression of the *sae2*Δ CPT sensitivity co-segregated with the *TRP1*, *URA3* or *HIS3* allele.

REFERENCES

References

Alcasabas AA, Osborn AJ, Bachant J, Hu F, Werler PJ, Bousset K, Furuya K, Diffley JF, Carr AM, Elledge SJ (2001) Mrc1 transduces signals of DNA replication stress to activate Rad53. Nat Cell Biol *3*, 958-965.

Aparicio T, Baer R, Gautier J (2014) DNA double-strand break repair pathway choice and cancer. DNA Repair *19*, 169-175.

Bakkenist CJ, Kastan MB (2003) DNA damage activates ATM through intermolecular autophosphorylation and dimer dissociation. Nature *421*, 499-506.

Baldo V, Testoni V, Lucchini G, Longhese MP (2008) Dominant *TEL1-hy* mutations compensate for Mec1 lack of functions in the DNA damage response. Mol Cell Biol *28*, 358-375.

Baretić D, Williams RL (2014) PIKKs-the solenoid nest where partners and kinases meet. Curr Opin Struct Biol *29*, 134-142.

Bernstein KA, Mimitou EP, Mihalevic MJ, Chen H, Sunjaveric I, Symington LS, Rothstein R (2013) Resection activity of the Sgs1 helicase alters the affinity of DNA ends for homologous recombination proteins in *Saccharomyces cerevisiae*. Genetics *195*, 1241-1251.

Bonetti D, Martina M, Clerici M, Lucchini G, Longhese MP (2009) Multiple pathways regulate 3' overhang generation at *S. cerevisiae* telomeres. Mol Cell *35*, 70-81.

Bonetti D, Villa M, Gobbini E, Cassani C, Tedeschi G, Longhese MP (2015) Escape of Sgs1 from Rad9 inhibition reduces the requirement for Sae2 and functional MRX in DNA end resection. EMBO Rep *16*, 351-361.

Bosotti R, Isacchi A, Sonnhammer EL (2000) FAT, a novel domain in PIK-related kinases. Trends Biochem Sci *25*, 225-227.

References

Branzei D, Foiani M (2007) RecQ helicases queuing with Srs2 to disrupt Rad51 filaments and suppress recombination. Genes Dev *21*, 3019-3026.

Budd ME, Choe Wc, Campbell JL (2000) The nuclease activity of the yeast DNA2 protein, which is related to the RecB-like nucleases, is essential *in vivo*. J Biol Chem *275*, 16518-16529.

Budd ME, Reis CC, Smith S, Myung K, Campbell JL (2006) Evidence suggesting that Pif1 helicase functions in DNA replication with the Dna2 helicase/nuclease and DNA polymerase delta. Mol Cell Biol *26*, 2490-2500.

Cannavo E, Cejka P (2014) Sae2 promotes dsDNA endonuclease activity within Mre11-Rad50-Xrs2 to resect DNA breaks. Nature *514*, 122-125.

Cejka P, Cannavo E, Polaczek P, Masuda-Sasa T, Pokharel S, Campbell JL, Kowalczykowski SC. (2010) DNA end resection by Dna2-Sgs1-RPA and its stimulation by Top3-Rmi1 and Mre11-Rad50-Xrs2. Nature *467*, 112-116.

Cejka P, Kowalczykowski SC (2010) The full-length *Saccharomyces cerevisiae* Sgs1 protein is a vigorous DNA helicase that preferentially unwinds Holliday junctions. J Biol Chem *285*, 8290-8301.

Cejka P (2015) DNA End Resection, Nucleases Team Up with the Right Partners to Initiate Homologous Recombination. J Biol Chem *290*, 22931-22938.

Chen ES, Hoch NC, Wang SC, Pellicioli A, Heierhorst J, Tsai MD (2014) Use of quantitative mass spectrometric analysis to elucidate the mechanisms of phospho-priming and auto-activation of the checkpoint kinase Rad53 *in vivo*. Mol Cell Proteomics *13*, 551-565.

Chen H, Donnianni RA, Handa N, Deng SK, Oh J, Timashev LA, Kowalczykowski SC, Symington LS. (2015) Sae2 promotes DNA damage resistance by removing the Mre11-Rad50-Xrs2 complex from DNA and attenuating Rad53 signaling. Proc Natl Acad Sci USA *112*, 1880-1887.

Chen L, Trujillo K, Ramos W, Sung P, Tomkinson AE (2001) Promotion of Dnl4-catalyzed DNA end-joining by the Rad50/Mre11/Xrs2 and Hdf1/Hdf2 complexes. Mol Cell *8*, 1105-1115.

Chen X, Niu H, Chung WH, Zhu Z, Papusha A, Shim EY, Lee SE, Sung P, Ira G (2011) Cell cycle regulation of DNA double-strand break end resection by Cdk1-dependent Dna2 phosphorylation. Nat Struct Mol Biol *18*, 1015-1019.

Chen X, Cui D, Papusha A, Zhang X, Chu CD, Tang J, Chen K, Pan X, Ira G (2012) The Fun30 nucleosome remodeller promotes resection of DNA double-strand break ends. Nature *489*, 576-580.

Ciccia A, Elledge SJ (2010) The DNA damage response, making it safe to play with knives. Mol Cell *40*, 179-204.

Clerici M, Mantiero D, Lucchini G, Longhese MP (2005) The *Saccharomyces cerevisiae* Sae2 protein promotes resection and bridging of double strand break ends. J Biol Chem *280*, 38631-38638.

Clerici M, Mantiero D, Lucchini G, Longhese MP (2006) The *Saccharomyces cerevisiae* Sae2 protein negatively regulates DNA damage checkpoint signalling. EMBO Rep *7*, 212-218.

Clerici M, Mantiero D, Guerini I, Lucchini G, Longhese MP (2008) The Yku70-Yku80 complex contributes to regulate double-strand break processing and checkpoint activation during the cell cycle. EMBO Rep *9*, 810-818.

Clerici M, Trovesi C, Galbiati A, Lucchini G, Longhese MP (2014) Mec1/ATR regulates the generation of single-stranded DNA that attenuates Tel1/ATM signaling at DNA ends. EMBO J *33*, 198-216.

Costelloe T, Louge R, Tomimatsu N, Mukherjee B, Martini E, Khadaroo B, Dubois K, Wiegant WW, Thierry A, Burma S, van Attikum H, Llorente B. (2012) The yeast Fun30 and human SMARCAD1 chromatin remodellers promote DNA end resection. Nature *489*, 581-584.

Cremona CA, Behrens A (2014) ATM signalling and cancer. Oncogene *33*, 3351-3360.

Daley JM, Kwon Y, Niu H, Sung P (2013) Investigations of Homologous Recombination Pathways and Their Regulation. Yale J Biol Med *86*, 453-461.

Davis AJ, Chen DJ (2013) DNA double strand break repair via non-homologous end-joining. Transl Cancer Res *2*,130-143.

Deng C, Brown JA, You D, Brown JM (2005) Multiple endonucleases function to repair covalent topoisomerase I complexes in *Saccharomyces cerevisiae*. Genetics *170*, 591-600.

Deshpande RA, Williams G.J, Limbo O, Williams RS, Kuhnlein J, Lee JH, Classen S, Guenther G, Russell P, Tainer JA, Paull TT (2014) ATP-driven Rad50 conformations regulate DNA tethering, end resection, and ATM checkpoint signaling. EMBO J *33*, 482-500.

Durocher D, Henckel J, Fersht AR, Jackson SP (1999) The FHA domain is a modular phosphopeptide recognition motif. Mol Cell *4*, 387-394.

Eapen VV, Sugawara N, Tsabar M, Wu WH, Haber JE (2012) The *Saccharomyces cerevisiae* chromatin remodeler Fun30 regulates DNA end resection and checkpoint deactivation. Mol Cell Biol *32*, 4727-4740.

Emili A (1998) MEC1-dependent phosphorylation of Rad9p in response to DNA damage. Mol Cell *2*, 183-189.

Fay DS, Sun Z, Stern DF (1997) Mutations in SPK1/RAD53 that specifically abolish checkpoint but not growth-related functions. Curr Genet *31*, 97-105.

Ferrari M, Dibitetto D, De Gregorio G, Eapen VV, Rawal CC, Lazzaro F, Tsabar M, Marini F, Haber JE, Pellicioli A (2015) Functional interplay between the 53BP1-ortholog Rad9 and the Mre11 complex regulates resection, end-tethering and repair of a double-strand break. PLoS Genet *11*, e1004928.

Finn K, Lowndes NF, Grenon M (2012) Eukaryotic DNA damage checkpoint activation in response to double-strand breaks. Cell Mol Life Sci *69*, 1447-1473.

Fitz Gerald JN, Benjamin JM, Kron SJ (2002) Robust G1 checkpoint arrest in budding yeast, dependence on DNA damage signaling and repair. J Cell Sci *115*, 1749-1757.

Foster SS, Balestrini A, Petrini JH (2011) Functional interplay of the Mre11 nuclease and Ku in the response to replication-associated DNA damage. Mol Cell Biol *31*, 4379-4389.

Friedberg EC (2003) DNA damage and repair. Nature *421*, 436-440.

Fukunaga K, Kwon Y, Sung P, Sugimoto K (2011) Activation of protein kinase Tel1 through recognition of protein-bound DNA ends. Mol Cell Biol *31*, 1959-1971.

Giannattasio M, Lazzaro F, Plevani P, Muzi-Falconi M (2005) The DNA damage checkpoint response requires histone H2B ubiquitination by Rad6-Bre1 and H3 methylation by Dot1. J Biol Chem *280*, 9879-9886.

Giglia-Mari G, Zotter A, Vermeulen W (2011) DNA Damage Response. Cold Spring Harb Perspect Biol *3*, a000745.

Gilbert CS, Green CM, Lowndes NF (2001) Budding yeast Rad9 is an ATP-dependent Rad53 activating machine. Mol Cell *8*, 129-136.

Gobbini E, Cesena D, Galbiati A, Lockhart A, Longhese MP (2013) Interplays between ATM/Tel1 and ATR/Mec1 in sensing and signaling DNA double-strand breaks. DNA Repair *12*, 791-799.

Gobbini E, Villa M, Gnugnoli M, Menin L, Clerici M, Longhese MP (2015) Sae2 function at DNA double-strand breaks is bypassed by dampening Tel1 or Rad53 activity. PLoS Genet *11*, e1005685.

Granata M, Lazzaro F, Novarina D, Panigada D, Puddu F, Abreu CM, Kumar R, Grenon M, Lowndes NF, Plevani P, Muzi-Falconi M (2010) Dynamics of Rad9 chromatin binding and checkpoint function are mediated by its dimerization and are cell cycle-regulated by CDK1 activity. PLoS Genet *6*, e1001047.

Hammet A, Magill C, Heierhorst J, Jackson SP (2007) Rad9 BRCT domain interaction with phosphorylated H2AX regulates the G1 checkpoint in budding yeast. EMBO Rep *8*, 851-857.

Harrison JC, Haber JE (2006) Surviving the breakup, the DNA damage checkpoint. Annu Rev Genet *40*, 209-235.

Hegnauer AM, Hustedt N, Shimada K, Pike BL, Vogel M, Amsler P, Rubin SM, van Leeuwen F, Guénolé A, van Attikum H, Thomä NH, Gasser SM (2012) An N-terminal acidic region of Sgs1 interacts with Rpa70 and recruits Rad53 kinase to stalled forks. EMBO J *31*, 3768-3783.

Hirano Y, Fukunaga K, Sugimoto K (2009) Rif1 and Rif2 inhibit localization of Tel1 to DNA ends. Mol Cell *33*, 312-322.

Hoeijmakers JH (2009) DNA damage, aging, and cancer. N Engl J Med *361*, 1475-1485.

Hohl M, Kwon Y, Galván SM, Xue X, Tous C, Aguilera A, Sung P, Petrini JH (2011) The Rad50 coiled-coil domain is indispensable for Mre11 complex functions. Nat Struct Mol Biol *18*, 1124-1131.

Hopfner KP, Putnam CD, Tainer J A (2002) DNA double-strand break repair from head to tail. Curr Opin Struct Biol *12*, 115-122.

Huertas P, Cortés-Ledesma F, Sartori AA, Aguilera A, Jackson SP (2008) CDK targets Sae2 to control DNA-end resection and homologous recombination. Nature *455*, 689-692.

Ip SCY, Rass U, Blanco MG, Flynn HR, Skehel JM, West SC (2008) Identification of Holliday junction resolvases from humans and yeast. Nature *456*, 357-361.

Ira G, Haber JE (2002) Characterization of RAD51-independent break-induced replication that acts preferentially with short homologous sequences. Mol Cell Biol *22*, 6384-6392.

Ira G, Pellicioli A, Balijja A, Wang X, Fiorani S, Carotenuto W, Liberi G, Bressan D, Wan L, Hollingsworth NM, Haber JE, Foiani M. (2004) DNA end resection, homologous recombination and DNA damage checkpoint activation require CDK1. Nature *431*, 1011-1017.

Javaheri A, Wysocki R, Jobin-Robitaille O, Altaf M, Côté J, Kron SJ (2006) Yeast G1 DNA damage checkpoint regulation by H2A phosphorylation is independent of chromatin remodeling. Proc Natl Acad Sci USA *103*, 13771-13776.

Jia X, Weinert T, Lydall D (2004) Mec1 and Rad53 inhibit formation of single-stranded DNA at telomeres of *Saccharomyces cerevisiae cdc13-1* mutants. Genetics *166*, 753-764.

Jinks-Robertson S, Michelitch M, Ramcharan S (1993) Substrate length requirements for efficient mitotic recombination in *Saccharomyces cerevisiae*. Mol Cell Biol *13*, 3937-3950.

Keeney S, Kleckner N (1995) Covalent protein-DNA complexes at the 5' strand termini of meiosis-specific double-strand breaks in yeast. Proc Natl Acad Sci USA *92*, 11274-11278.

Krejci L, Altmannova V, Spirek M, Zhao X (2012) Homologous recombination and its regulation. Nucleic Acids Res *40*, 5795-5818.

Lazzaro F, Sapountzi V, Granata M, Pellicioli A, Vaze M, Haber JE, Plevani P, Lydall D, Muzi-Falconi M (2008) Histone methyltransferase Dot1 and Rad9 inhibit single-stranded DNA accumulation at DSBs and uncapped telomeres. EMBO J *27*, 1502-1512.

Lee JH, Paull TT (2005) ATM activation by DNA double-strand breaks through the Mre11-Rad50-Nbs1 complex. Science *308*, 551-554.

Lee SE, Moore JK, Holmes A, Umezu K, Kolodner RD, Haber JE (1998) *Saccharomyces* Ku70, Mre11/Rad50 and RPA proteins regulate adaptation to G2/M arrest after DNA damage. Cell *94*, 399-409.

Lempiäinen H, Halazonetis TD (2009) Emerging common themes in regulation of PIKKs and PI3Ks. EMBO J *28*, 3067-3073.

Lieber MR (2010) The mechanism of double-strand DNA break repair by the non-homologous DNA end-joining pathway. Annu Rev Biochem *79*, 181-211.

Lisby M, Barlow JH, Burgess RC, Rothstein R (2004) Choreography of the DNA damage response, spatiotemporal relationships among checkpoint and repair proteins. Cell *118*, 699-713.

Liu C, Pouliot JJ, Nash HA (2002) Repair of topoisomerase I covalent complexes in the absence of the tyrosyl-DNA phosphodiesterase Tdp1. Proc Natl Acad Sci USA *99*, 14970-14975.

Longhese MP, Clerici M, Lucchini G (2003) The S-phase checkpoint and its regulation in *Saccharomyces cerevisiae*. Mutat Res *532*, 41-58.

Longhese MP, Bonetti D, Manfrini N, Clerici M (2010) Mechanisms and regulation of DNA end resection. EMBO J *29*, 2864-74.

Lydall D, Weinert T (1995) Yeast checkpoint genes in DNA damage processing, implications for repair and arrest. Science *270*, 1488-1491.

Mallory JC, Petes TD (2000) Protein kinase activity of Tel1p and Mec1p, two *Saccharomyces cerevisiae* proteins related to the human ATM protein kinase. Proc Natl Acad Sci USA *97*, 13749-13754.

Manfrini N, Guerini I, Citterio A, Lucchini G, Longhese MP (2010) Processing of meiotic DNA double strand breaks requires cyclin-dependent kinase and multiple nucleases. J Biol Chem *285*, 11628-11637.

Mantiero D, Clerici M, Lucchini G, Longhese MP (2007) Dual role for *Saccharomyces cerevisiae* Tel1 in the checkpoint response to double-strand breaks. EMBO Rep *8*, 380-387.

Mathiasen DP, Lisby M. (2014). Cell cycle regulation of homologous recombination in *Saccharomyces cerevisiae*. FEMS Microbiol Rev *38*, 172-184.

McKinnon PJ (2012) ATM and the molecular pathogenesis of ataxia telangiectasia. Annu Rev Pathol *7*, 303-321.

Mehta A, Haber JE (2014) Sources of DNA double-strand breaks and models of recombinational DNA repair. Cold Spring Harb Perspect Biol *6*, a016428.

Mimitou EP, Symington LS (2008) Sae2, Exo1 and Sgs1 collaborate in DNA double-strand break processing. Nature *455*, 770-774.

Mimitou EP, Symington LS (2010) Ku prevents Exo1 and Sgs1-dependent resection of DNA ends in the absence of a functional MRX complex or Sae2. EMBO J *29*, 3358-3369.

Morin I, Ngo HP, Greenall A, Zubko MK, Morrice N, Lydall D (2008) Checkpoint-dependent phosphorylation of Exo1 modulates the DNA damage response. EMBO J *27*, 2400-2410.

Moynahan ME, Jasin M (2010) Mitotic homologous recombination maintains genomic stability and suppresses tumorigenesis. Nat Rev Mol Cell Biol *11*, 196-207.

Mullen JR, Kaliraman V, Brill SJ (2000) Bipartite structure of the Sgs1 DNA helicase in *Saccharomyces cerevisiae*. Genetics *154*, 1101-1114.

Naiki T, Wakayama T, Nakada D, Matsumoto K, Sugimoto K (2004) Association of Rad9 with double-strand breaks through a Mec1-dependent mechanism. Mol Cell Biol *24*, 3277-3285.

Nakada D, Matsumoto K, Sugimoto K (2003) ATM-related Tel1 associates with double-strand breaks through an Xrs2-dependent mechanism. Genes Dev *17*, 1957-1962.

Nassif N, Penney J, Pal S, Engels WR, Gloor GB (1994) Efficient copying of nonhomologous sequences from ectopic sites via P-element-induced gap repair. Mol Cell Biol *14*, 1613-1625.

Navadgi-Patil VM, Burgers PM (2009) The unstructured C-terminal tail of the 9-1-1 clamp subunit Ddc1 activates Mec1/ATR via two distinct mechanisms. Mol Cell *36*, 743-753.

References

Ngo GH, Balakrishnan L, Dubarry M, Campbell JL, Lydall D (2014) The 9-1-1 checkpoint clamp stimulates DNA resection by Dna2-Sgs1 and Exo1. Nucleic Acids Res *42*, 10516-10528.

Ngo GH, Lydall D (2015) The 9-1-1 checkpoint clamp coordinates resection at DNA double strand breaks. Nucleic Acids Res *43*, 5017-5032.

Nimonkar AV, Ozsoy AZ, Genschel J, Modrich P, Kowalczykowski SC (2008) Human exonuclease 1 and BLM helicase interact to resect DNA and initiate DNA repair. Proc Natl Acad Sci USA *105*, 16906-16911.

Nimonkar AV, Genschel J, Kinoshita E, Polaczek P, Campbell JL, Wyman C, Modrich P, Kowalczykowski SC (2011) BLM-DNA2-RPA-MRN and EXO1-BLM-RPA-MRN constitute two DNA end resection machineries for human DNA break repair. Genes Dev *25*, 350-362.

Niu H, Chung WH, Zhu Z, Kwon Y, Zhao W, Chi P, Prakash R, Seong C, Liu D, Lu L, Ira G, Sung P. (2010) Mechanism of the ATP-dependent DNA end-resection machinery from *Saccharomyces cerevisiae*. Nature *467*, 108-111.

Nyberg KA, Michelson RJ, Putnam CW, Weinert TA (2002). Toward maintaining the genome, DNA damage and replication checkpoints. Annu Rev Genet *36*, 617-656.

O'Driscoll M1, Ruiz-Perez VL, Woods CG, Jeggo PA, Goodship JA (2003) A splicing mutation affecting expression of ataxia-telangiectasia and Rad3-related protein (ATR) results in Seckel syndrome. Nat Genet *33*, 497-501.

Ogi H, Goto GH, Ghosh A, Zencir S, Henry E, Sugimoto K (2015) Requirement of the FATC domain of protein kinase Tel1 for localization to DNA ends and target protein recognition. Mol Biol Cell *26*, 3480-3488.

Palmbos PL, Wu D, Daley JM, Wilson TE (2008) Recruitment of *Saccharomyces cerevisiae* Dnl4-Lif1 complex to a double-strand break requires interactions with Yku80 and the Xrs2 FHA domain. Genetics *180*, 1809-1819.

Paull TT, Gellert M (1998) The 3' to 5' exonuclease activity of Mre11 facilitates repair of DNA double-strand breaks. Mol Cell *1*, 969-979.

Pellicioli A, Lee SE, Lucca C, Foiani M, Haber JE (2001) Regulation of *Saccharomyces* Rad53 checkpoint kinase during adaptation from DNA damage-induced G2/M arrest. Mol Cell *7*, 293-300.

Perry J, Kleckner N (2003) The ATRs, ATMs, and TORs are giant HEAT repeat proteins. Cell *112*, 151-155.

Pfander B, Diffley JF (2011) Dpb11 coordinates Mec1 kinase activation with cell cycle-regulated Rad9 recruitment. EMBO J *30*, 4897-4907.

Puddu F, Oelschlaegel T, Guerini I, Geisler NJ, Niu H, Herzog M, Salguero I, Ochoa-Montaño B, Viré E, Sung P, Adams DJ, Keane TM, Jackson SP. (2015) Synthetic viability genomic screening defines Sae2 function in DNA repair. EMBO J *34*, 1509-1522.

Putnam CD, Jaehnig EJ, Kolodner RD (2009) Perspectives on the DNA damage and replication checkpoint responses in *Saccharomyces cerevisiae*. DNA Repair (Amst) *8*, 974-982.

Roy R, Chun J, Powell SN (2012) BRCA1 and BRCA2, different roles in a common pathway of genome protection. Nat Rev Cancer *12*, 68-78.

San Filippo J, P. Sung P, Klein H (2008) Mechanism of eukaryotic homologous recombination. Annu Rev Biochem *77*, 229-257.

Sanchez Y, Bachant J, Wang H, Hu F, Liu D, Tetzlaff M, Elledge SJ. (1999) Control of the DNA damage checkpoint by Chk1 and Rad53 protein kinases through distinct mechanisms. Science *286*, 1166-1171.

Sandell LL, Zakian VA (1993) Loss of a yeast telomere, arrest, recovery, and chromosome loss. Cell *75*, 729-739.

Sarbajna S, Davies D, West SC (2014) Roles of SLX1-SLX4, MUS81-EME1, and GEN1 in avoiding genome instability and mitotic catastrophe. Genes Dev *28*, 1124-1136.

Sartori AA, Lukas C, Coates J, Mistrik M, Fu S, Bartek J, Baer R, Lukas J, Jackson SP (2007) Human CtIP promotes DNA end resection, Nature *450*, 509-514.

Savitsky K, Sfez S, Tagle DA, Ziv Y, Sartiel A, Collins FS, Shiloh Y, Rotman G. (1995) The complete sequence of the coding region of the ATM gene reveals similarity to cell cycle regulators in different species. Hum Mol Genet *4*, 2025-2032.

Schwartz MF, Lee SJ, Duong JK, Eminaga S, Stern DF (2003) FHA domain-mediated DNA checkpoint regulation of Rad53. Cell Cycle *2*, 384-396.

Seeber A, Hauer M, Gasser SM (2013) Nucleosome remodelers in double-strand break repair. Curr Opin Genet Dev *23*, 174-184.

Seong C, Sehorn MG, Plate I, Shi I. Song B, Chi P, Mortensen U, Sung P, Krejci L (2008) Molecular anatomy of the recombination mediator function of *Saccharomyces cerevisiae* Rad52. J Biol Chem *283*, 12166-12174.

Shim EY, Chung WH, Nicolette ML, Zhang Y, Davis M, Zhu Z, Paull TT, Ira G, Lee SE (2010) *Saccharomyces cerevisiae* Mre11/Rad50/Xrs2 and Ku proteins regulate association of Exo1 and Dna2 with DNA breaks. EMBO J *29*, 3370-3380.

Shiotani B, Zou L (2009) Single-stranded DNA orchestrates an ATM-to-ATR switch at DNA breaks. Mol Cell *33*, 547-558.

Shroff R, Arbel-Eden A, Pilch D, Ira G, Bonner WM, Petrini JH, Haber JE, Lichten M (2004) Distribution and dynamics of chromatin modification induced by a defined DNA double-strand break. Curr Biol *14*, 1703-1711.

Sun J, Lee KJ, Davis AJ, Chen DJ (2012) Human Ku70/80 protein blocks exonuclease 1-mediated DNA resection in the presence of human Mre11 or Mre11/Rad50 protein complex. J Biol Chem *287*, 4936-4945.

Sun Z, Hsiao J, Fay DS, Stern DF (1998) Rad53 FHA domain associated with phosphorylated Rad9 in the DNA damage checkpoint. Science *281*, 272-274.

Sung P, Krejci L, Van Komen S, Sehorn MG (2003) Rad51 recombinase and recombination mediators. J Biol Chem *278*, 42729-42732.

Sweeney FD, Yang F, Chi A, Shabanowitz J, Hunt DF, Durocher D (2005) *Saccharomyces cerevisiae* Rad9 acts as a Mec1 adaptor to allow Rad53 activation. Curr Biol *15*, 1364-1375.

Symington LS, Gautier J (2011) Double-strand break end resection and repair pathway choice. Annu Rev Genet *45*, 247-271.

Toczyski DP, Galgoczy DJ, Hartwell LH (1997) CDC5 and CKII control adaptation to the yeast DNA damage checkpoint. Cell *90*, 1097-1106.

Toh GW, O'Shaughnessy AM, Jimeno S, Dobbie IM, Grenon M, Maffini S, O'Rorke A, Lowndes NF. (2006) Histone H2A phosphorylation and H3 methylation are required for a novel Rad9 DSB repair function following checkpoint activation. DNA Repair *5*, 693-703.

Tran PT, Erdeniz N, Dudley S, Liskay RM (2002) Characterization of nuclease-dependent functions of Exo1p in *Saccharomyces cerevisiae*. DNA Repair (Amst) *1*, 895-912.

Trovesi C, Falcettoni M, Lucchini G, Clerici M, Longhese MP (2011) Distinct Cdk1 requirements during single-strand annealing, noncrossover, and crossover recombination. PLoS Genet *7*, e1002263.

Trujillo KM, Yuan SS, Lee EY, Sung P (1998) Nuclease activities in a complex of human recombination and DNA repair factors Rad50, Mre11, and p95. J Biol Chem *273*, 21447-21450.

Trujillo KM, Roh DH, Chen L, Van Komen S, Tomkinson A, Sung P (2003) Yeast Xrs2 binds DNA and helps target Rad50 and Mre11 to DNA ends. J Biol Chem *278*, 48957-48964.

Usui T, Ohta T, Oshiumi H, Tomizawa J, Ogawa H, Ogawa T (1998) Complex formation and functional versatility of Mre11 of budding yeast in recombination. Cell *95*, 705-716.

Usui T, Ogawa H, Petrini JH (2001) A DNA damage response pathway controlled by Tel1 and the Mre11 complex. Mol Cell *7*, 1255-1266.

Usui T, Foster SS, Petrini JH (2009) Maintenance of the DNA-damage checkpoint requires DNA-damage-induced mediator protein oligomerization. Mol Cell *33*, 147-159.

Vaze MB, Pellicioli A, Lee SE, Ira G, Liberi G, Arbel-Eden A, Foiani M, Haber JE (2002) Recovery from checkpoint-mediated arrest after repair of a double-strand break requires Srs2 helicase. Mol Cell *10*, 373-385.

Vialard JE, Gilbert CS, Green CM, Lowndes NF (1998) The budding yeast Rad9 checkpoint protein is subjected to Mec1/Tel1-dependent hyperphosphorylation and interacts with Rad53 after DNA damage. EMBO J *17*, 5679-5688.

Viscardi V, Bonetti D, Cartagena-Lirola H, Lucchini G, Longhese MP (2007) MRX-dependent DNA damage response to short telomeres. Mol Biol Cell *18*, 3047-3058.

Zhao X, Muller EG, Rothstein R (1998) A suppressor of two essential checkpoint genes identifies a novel protein that negatively affects dNTP pools. Mol Cell *2*, 329-340.

Zhou BB, Elledge SJ (2000) The DNA damage response, putting checkpoints in perspective. Nature *408*, 433-439.

Zhu Z, Chung WH, Shim EY, Lee SE, Ira G (2008) Sgs1 helicase and two nucleases Dna2 and Exo1 resect DNA double-strand break ends. Cell *134*, 981-994.

Published online: January 30, 2015

Scientific Report

TRANSPARENT PROCESS

EMBO reports

Escape of Sgs1 from Rad9 inhibition reduces the requirement for Sae2 and functional MRX in DNA end resection

Diego Bonetti[†], Matteo Villa[†], Elisa Gobbini, Corinne Cassani, Giulia Tedeschi & Maria Pia Longhese[*]

Abstract

Homologous recombination requires nucleolytic degradation (resection) of DNA double-strand break (DSB) ends. In *Saccharomyces cerevisiae*, the MRX complex and Sae2 are involved in the onset of DSB resection, whereas extensive resection requires Exo1 and the concerted action of Dna2 and Sgs1. Here, we show that the checkpoint protein Rad9 limits the action of Sgs1/Dna2 in DSB resection by inhibiting Sgs1 binding/persistence at the DSB ends. When inhibition by Rad9 is abolished by the Sgs1-ss mutant variant or by deletion of *RAD9*, the requirement for Sae2 and functional MRX in DSB resection is reduced. These results provide new insights into how early and long-range resection is coordinated.

Keywords double-strand break; Rad9; resection; *Saccharomyces cerevisiae*; Sgs1

Subject Category DNA Replication, Repair & Recombination

DOI 10.15252/embr.201439764 | Received 21 October 2014 | Revised 23 December 2014 | Accepted 5 January 2015

Introduction

DNA double-strand breaks (DSBs) can be repaired by homologous recombination (HR), which uses undamaged homologous DNA sequences as a template for repair in a mostly error-free manner. The first step in HR is the processing of DNA ends by 5′ to 3′ nucleolytic degradation (resection) to generate 3′-ended single-stranded DNA (ssDNA) that can invade a homologous template [1]. This ssDNA generation also induces activation of the DNA damage checkpoint, whose key players are the protein kinases ATM and ATR in mammals as well as their functional orthologs Tel1 and Mec1 in *Saccharomyces cerevisiae* [2].

Initiation of DSB resection requires the conserved MRX/MRN complex (Mre11/Rad50/Xrs2 in yeast; Mre11/Rad50/Nbs1 in mammals) that, together with Sae2, catalyses an endonucleolytic cleavage of the 5′ strands [3–5]. More extensive resection of the 5′ strands depends on two pathways, which require the 5′ to 3′ double-stranded DNA exonuclease Exo1 and the nuclease Dna2 working in concert with the 3′ to 5′ helicase Sgs1 [4,5].

Double-strand break resection is controlled by the activity of cyclin-dependent kinases (Cdk1 in yeast) [6], which promotes DSB resection by phosphorylating Sae2 [7] and Dna2 [8], as well as by ATP-dependent nucleosome remodelling complexes [9]. Recently, the chromatin remodeler Fun30 has been shown to be required for extensive resection [10–12], possibly because it overcomes the resection barrier exerted by the histone-bound checkpoint protein Rad9 [10,13,14].

The MRX/Sae2-mediated initial endonucleolytic cleavage becomes essential to initiate DSB resection when covalent modifications or bulky adducts are present at the DSB ends and prevent the access of the long-range Exo1 and Dna2/Sgs1 resection machinery. For example, Sae2 and the MRX nuclease activity are essential during meiosis to remove Spo11 from the 5′-ended strand of the DSBs [15,16]. Furthermore, both *sae2*Δ and *mre11* nuclease-defective (*mre11-nd*) mutants exhibit a marked sensitivity to methyl methanesulfonate (MMS) and ionizing radiation (IR), which can generate chemically complex DNA termini, and to camptothecin (CPT), which extends the half-life of topoisomerase I (Top1)–DNA cleavable complexes [17]. CPT-induced DNA lesions need to be processed by Sae2 and MRX unless the Ku heterodimer is absent. In fact, elimination of Ku restores partial resistance to CPT in both *sae2*Δ and *mre11-nd* cells [18,19]. This suppression requires Exo1, indicating that Ku increases the requirement for MRX/Sae2 activities in DSB resection by inhibiting Exo1.

To identify other possible mechanisms regulating MRX/Sae2 requirement in DSB resection, we searched for extragenic mutations that suppressed the sensitivity to DNA damaging agents of *sae2*Δ cells. This search allowed the identification of the *SGS1-ss* allele, which suppresses the resection defect of *sae2*Δ cells by escaping Rad9-mediated inhibition of DSB resection. The Sgs1-ss variant is robustly associated with the DSB ends both in the presence and in the absence of Rad9 and resects the DSB more efficiently than wild-type Sgs1. Moreover, we found that Rad9 limits the binding at the DSB of Sgs1, which is in turn responsible for rapid resection in *rad9*Δ cells. We propose that Rad9 limits the activity in DSB resection of Sgs1/Dna2 and the escape from this inhibition can reduce the requirement of Sae2 and functional MRX in DSB resection.

Dipartimento di Biotecnologie e Bioscienze, Università di Milano-Bicocca, Milan, Italy
*Corresponding author. Tel: +39 0264 483543; Fax: +39 0264 483565; E-mail: mariapia.longhese@unimib.it
[†]These two authors have contributed equally to the work

Results and Discussion

Sgs1-ss suppresses the sensitivity to DNA damaging agents of *sae2*Δ and *mre11-nd* mutants

SAE2 deletion causes hypersensitivity to CPT, which creates replication-associated DSBs. The lack of Ku suppresses CPT hypersensitivity of *sae2*Δ mutants, and this rescue requires Exo1 [18,19], indicating that Ku prevents Exo1 from initiating DSB resection. To identify other possible pathways bypassing Sae2 function in DSB resection, we searched for extragenic mutations that suppress the CPT sensitivity of *sae2*Δ cells. CPT-resistant *sae2*Δ candidates were crossed to each other and to the wild-type strain to identify, by tetrad analysis, 15 single-gene suppressor mutants that fell into 11 distinct allelism groups. Genome sequencing of the five non-allelic suppressor clones that stood from the others for the best suppression phenotype identified single-base pair substitutions either in the *TOP1* gene, encoding the CPT target topoisomerase I, or in the *PDR3*, *PDR10* and *SAP185* genes, which encode for proteins involved in multi-drug resistance. The mutation responsible for the suppression in the fifth clone was a single-base pair substitution in the *SGS1* gene (*SGS1-ss*), causing the amino acid change G1298R in the HRDC domain that is conserved in the RecQ helicase family. The identity of the genes that are mutated in the six remaining suppressor clones remained to be determined.

The *SGS1-ss* allele suppressed the sensitivity of the *sae2*Δ mutant not only to CPT, but also to phleomycin (phleo) and MMS, resulting in almost wild-type survival of *sae2*Δ *SGS1-ss* cells treated with these drugs (Fig 1A). The ability of Sgs1-ss to suppress the sensitivity of *sae2*Δ to genotoxic agents was dominant, as *sae2*Δ/*sae2*Δ *SGS1/SGS1-ss* diploid cells were less sensitive to CPT, phleomycin and MMS compared to *sae2*Δ/*sae2*Δ *SGS1/SGS1* diploid cells (Fig 1B).

Besides providing the endonuclease activity to initiate DSB resection, MRX also promotes stable association of Exo1, Sgs1 and Dna2 at the DSB ends [20], thus explaining the severe resection defect of cells lacking the MRX complex compared to cells lacking either Sae2 or the Mre11 nuclease activity. Sgs1-ss suppressed the hypersensitivity to genotoxic agents of *mre11-H125N* cells, which were specifically defective in Mre11 nuclease activity (Fig 1A). By contrast, *mre11*Δ *SGS1-ss* double-mutant cells were as sensitive to genotoxic agents as the *mre11*Δ single mutant (Fig 1A). Altogether, these findings indicate that Sgs1-ss can bypass the requirement of Sae2 or MRX nuclease activity for survival to genotoxic agents, but it still requires the physical integrity of the MRX complex to exert its function.

Sgs1 promotes DSB resection by acting as a helicase [4,5], prompting us to investigate whether Sgs1-ss requires its helicase activity to exert the suppression effect. Both the lack of Sgs1 and its helicase-dead Sgs1-hd variant, carrying the K706A amino acid substitution [21], impaired viability of *sae2*Δ cells [5] (Fig 1C). This synthetic sickness is likely due to poor DSB resection, as it is known to be alleviated by making DNA ends accessible to the Exo1 nuclease [18,19]. The K706A substitution was therefore introduced in Sgs1-ss, thus generating the Sgs1-hd-ss variant, and meiotic tetrads from diploid strains double heterozygous for *sae2*Δ and *sgs1-hd-ss* were analysed for spore viability on YEPD plates. All *sae2*Δ *sgs1-hd-ss* double-mutant spores formed much smaller colonies than each single-mutant spore (Fig 1D), with a colony size similar to that obtained from *sae2*Δ *sgs1-hd* double-mutant spores (Fig 1C). Thus, Sgs1-ss appears to require its helicase activity to suppress the lack of Sae2 function.

Suppression of *sae2*Δ by Sgs1-ss requires Dna2, but not Exo1

The ssDNA formed by Sgs1 unwinding is degraded by the nuclease Dna2, which acts in DSB resection in a parallel pathway with respect to Exo1 [5]. Thus, we asked whether the suppression of *sae2*Δ hypersensitivity to DNA damaging agents by Sgs1-ss requires Exo1 and/or Dna2. Although the lack of Exo1 exacerbated the sensitivity of *sae2*Δ cells to some DNA damaging agents (Fig 1E), the *SGS1-ss* allele was still capable to suppress the sensitivity to CPT, phleomycin and MMS of *sae2*Δ *exo1*Δ double-mutant cells (Fig 1E), indicating the suppression of *sae2*Δ by Sgs1-ss is independent of Exo1.

As *DNA2* is essential for cell viability, *dna2*Δ cells were kept viable by the *pif1-M2* mutation, which impairs the ability of Pif1 to promote formation of long flaps that are substrates for Dna2 [22]. Diploids homozygous for the *pif1-M2* mutation and heterozygous for *sae2*Δ, *dna2*Δ and *SGS1-ss* were generated, followed by sporulation and tetrads dissection. No viable *sae2*Δ *dna2*Δ *pif1-M2* cells could be recovered, and the presence of the *SGS1-ss* allele did not restore viability of *sae2*Δ *dna2*Δ *pif1-M2* triple-mutant spores (Fig 1F). By contrast, tetrads from a diploid homozygous for the *pif1-M2* mutation and heterozygous for *sae2*Δ, *dna2*Δ and *ku70*Δ showed that the lack of Ku70, which relieved Exo1 inhibition [18,19], restored viability of *sae2*Δ *dna2*Δ *pif1-M2* spores (Fig 1G). These findings indicate that Sgs1-ss requires Dna2 to bypass Sae2 requirement.

Sgs1-ss suppresses the adaptation defect of *sae2*Δ cells

A single irreparable DSB triggers a checkpoint-mediated cell cycle arrest. Yeast cells can escape an extended checkpoint arrest and resume cell cycle progression even with an unrepaired DSB (adaptation) [23,24]. Sae2 lacking cells, like other resection deficient mutants, fail to turn off the checkpoint triggered by an unrepaired DSB and remain arrested at G2/M as large budded cells [12,25–27]. To investigate whether Sgs1-ss suppresses the adaptation defect of *sae2*Δ cells, we used JKM139 derivative strains carrying the HO endonuclease gene under the control of a galactose-inducible promoter. Galactose addition leads to generation at the *MAT* locus of a single DSB that cannot be repaired by HR, because the homologous donor loci *HML* or *HMR* are deleted [23]. When G1-arrested cell cultures were spotted on galactose-containing plates, *sae2*Δ *SGS1-ss* cells formed microcolonies with more than two cells more efficiently than *sae2*Δ cells, which were still arrested at the two-cell dumbbell stage after 24 h (Fig 2A). Checkpoint activation was monitored also by following Rad53 phosphorylation, which is required for Rad53 activation and is detectable as a decrease of its electrophoretic mobility. When galactose was added to exponentially growing cell cultures of the same strains, *sae2*Δ and *sae2*Δ *SGS1-ss* mutant cells showed similar amounts of phosphorylated Rad53 after HO induction (Fig 2B), indicating that Sgs1-ss did not affect checkpoint activation. However, Rad53 phosphorylation decreased in *sae2*Δ *SGS1-ss* double-mutant cells within 12–14 h after galactose

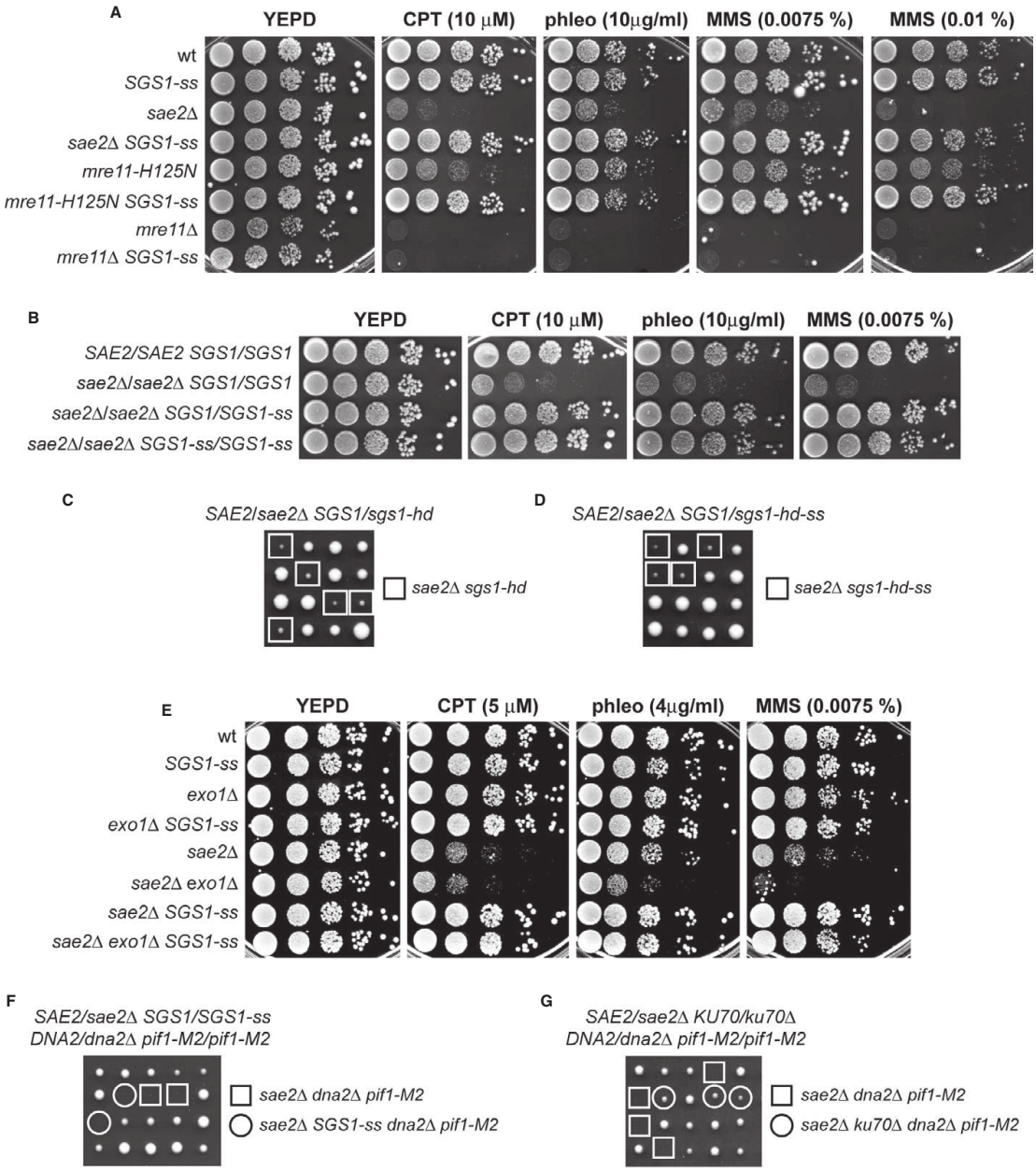

Figure 1. Suppression of the sensitivity to genotoxic agents of *sae2*Δ and *mre11* nuclease-defective mutants by Sgs1-ss.

A, B Exponentially growing cells were serially diluted (1:10), and each dilution was spotted out onto YEPD plates with or without camptothecin (CPT), phleomycin or MMS.

C, D Meiotic tetrads were dissected on YEPD plates that were incubated at 25°C, followed by spore genotyping.

E Exponentially growing cells were serially diluted (1:10), and each dilution was spotted out onto YEPD plates with or without CPT, phleomycin or MMS.

F, G Meiotic tetrads were dissected on YEPD plates that were incubated at 25°C, followed by spore genotyping.

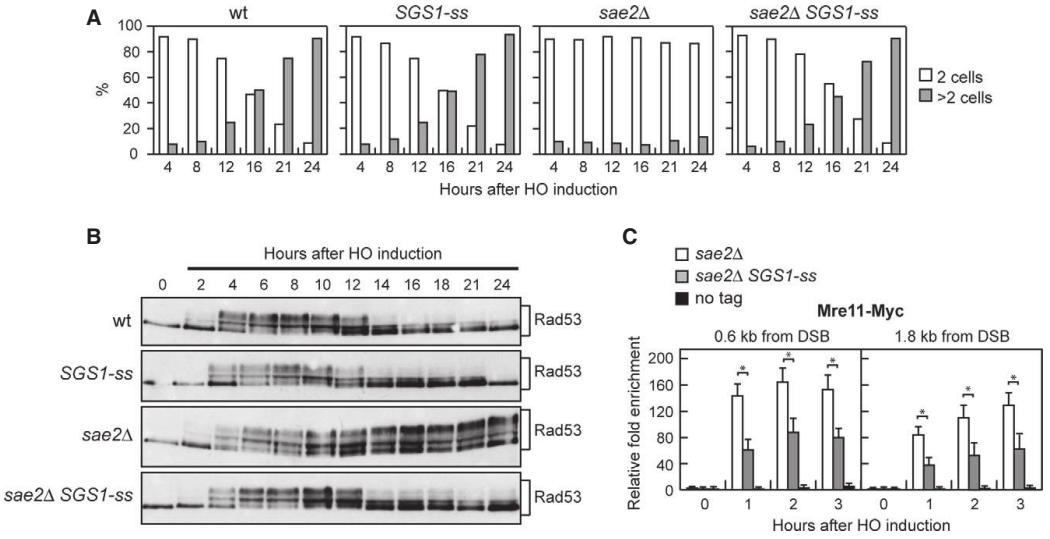

Figure 2. Suppression of the adaptation defect of *sae2*Δ cells by Sgs1-ss.

A YEPR G1-arrested cell cultures of wild-type JKM139 and otherwise isogenic derivative strains were plated on galactose-containing plates (time zero). At the indicated time points, 200 cells for each strain were analysed to determine the frequency of large budded cells and of cells forming microcolonies of more than two cells. The mean values from three independent experiments are represented (n = 3).

B Exponentially growing YEPR cultures of the strains in (A) were transferred to YEPRG (time zero), followed by Western blot analysis with anti-Rad53 antibodies.

C ChIP analysis. Exponentially growing YEPR cell cultures of JKM139 derivative strains were transferred to YEPRG, followed by ChIP analysis of the recruitment of Mre11–Myc at the indicated distance from the HO-cut compared to untagged Mre11 (no tag). In all diagrams, the ChIP signals were normalized for each time point to the corresponding input signal. The mean values are represented with error bars denoting s.d. (n = 3). *$P < 0.01$, t-test.

addition, whereas it persisted longer in *sae2*Δ cells that were defective in re-entering the cell cycle (Fig 2B). Thus, Sgs1-ss suppresses the inability of *sae2*Δ cells to turn off the checkpoint in the presence of an unrepaired DSB.

The adaptation defect of *sae2*Δ cells has been proposed to be due to an increased persistence at DSBs of the MRX complex, which in turn causes unscheduled Tel1 activation [26,27]. We then asked by chromatin immunoprecipitation (ChIP) and quantitative real-time PCR (qPCR) analysis whether Sgs1-ss can reduce the binding of MRX to the DSB ends in *sae2*Δ cells. When HO was induced in exponentially growing cells, the amount of Mre11 bound at the HO-induced DSB end was lower in *sae2*Δ *SGS1-ss* than in *sae2*Δ cells (Fig 2C). As MRX persistence at the DSB in *sae2*Δ cells has been proposed to be due to defective DSB resection, this finding suggests that Sgs1-ss suppresses the resection defect of *sae2*Δ cells.

Sgs1-ss suppresses the resection defect of *sae2*Δ cells

To investigate whether Sgs1-ss suppresses the sensitivity to genotoxic agents and the adaptation defect of *sae2*Δ cells by restoring DSB resection, we used JKM139 derivative strains to monitor directly generation of ssDNA at the DSB ends [23]. Because ssDNA is resistant to cleavage by restriction enzymes, we directly monitored ssDNA formation at the irreparable HO-cut by following the loss of SspI restriction fragments after galactose addition by Southern blot analysis under alkaline conditions, using a single-stranded probe that anneals to the 3′ end at one side of the break (Fig 3A). Resection in *sae2*Δ *SGS1-ss* cells was markedly increased compared to *sae2*Δ cells, indicating that Sgs1-ss suppresses the resection defect caused by the lack of Sae2 (Fig 3B and C).

Repair of a DSB flanked by direct repeats occurs primarily by single-strand annealing (SSA), which requires nucleolytic degradation of the 5′ DSB ends to reach the complementary DNA sequences that can then anneal [28]. To assess whether the Sgs1-ss-mediated suppression of the resection defect caused by the lack of Sae2 was physiologically relevant, we asked whether Sgs1-ss suppresses the SSA defect of *sae2*Δ cells. To this end, we introduced the *SGS1-ss* allele in YMV45 strain, which carries two tandem *leu2* repeats located 4.6 kb apart, with a HO recognition site adjacent to one of the repeats [28]. This strain also harbours a *GAL-HO* construct for galactose-inducible *HO* expression. As expected, accumulation of the repair product was reduced in *sae2*Δ compared to wild-type cells, whereas it occurred with almost wild-type kinetics in *sae2*Δ *SGS1-ss* double-mutant cells (Fig 3D and E), indicating that Sgs1-ss improves SSA-mediated DSB repair in the absence of Sae2.

Altogether, these findings indicate that Sgs1-ss suppresses both the sensitivity to genotoxic agents of *sae2*Δ cells and the MRX persistence at DSBs by restoring DSB resection. Interestingly, the effects of the *SGS1-ss* mutation are opposite to those of the separation-of-function *sgs1-D664*Δ allele, which specifically impairs viability of *sae2*Δ cells and DSB resection without affecting other Sgs1 functions [29].

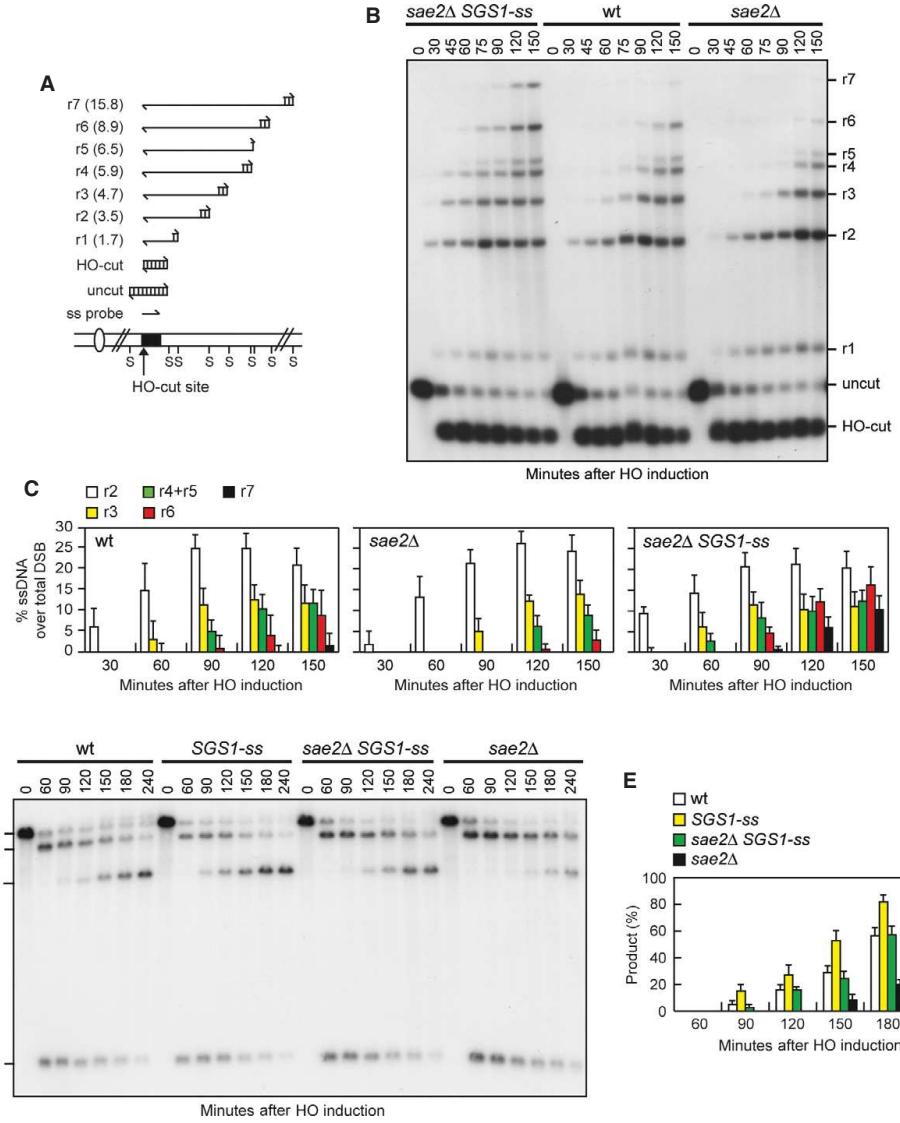

Figure 3. Sgs1-ss suppresses the resection defect of *sae2*Δ cells.

A Method to measure double-strand break (DSB) resection. Gel blots of SspI-digested genomic DNA separated on alkaline agarose gel were hybridized with a single-stranded *MAT* probe (ss probe) that anneals to the unresected strand. 5′–3′ resection progressively eliminates SspI sites (S), producing larger SspI fragments (r1 through r7) detected by the probe.

B DSB resection. YEPR exponentially growing cell cultures of JKM139 derivative strains were transferred to YEPRG at time zero. Genomic DNA was analysed for ssDNA formation at the indicated times after HO induction as described in (A).

C Densitometric analyses. The experiment as in (B) has been independently repeated three times, and the mean values are represented with error bars denoting s.d. (n = 3).

D DSB repair by single-strand annealing (SSA). In YMV45 strain, the HO-cut site is flanked by homologous *leu2* sequences that are 4.6 kb apart. HO-induced DSB formation results in generation of 12- and 2.5-kb DNA fragments (HO-cut) that can be detected by Southern blot analysis with a *LEU2* probe of KpnI-digested genomic DNA. DSB repair by SSA generates an 8-kb fragment (product).

E Densitometric analysis of the product band signals. The intensity of each band was normalized with respect to a loading control (not shown). The mean values are represented with error bars denoting s.d. (n = 3).

Sgs1-ss accelerates DSB resection by escaping Rad9 inhibition

The Sgs1-ss mutant variant can bypass Sae2 requirement in initiation of DSB resection either because it allows Dna2 to substitute for Sae2/MRX endonuclease activity or because it increases the resection efficiency. To distinguish between these two possibilities, we asked whether Sgs1-ss could bypass Sae2 requirement in resecting meiotic DSBs, where the Sae2/MRX-mediated endonucleolytic cleavage is absolutely required to initiate DSB resection by allowing the removal of Spo11 from the DSB ends [15,16]. A *sae2*Δ/*sae2*Δ *SGS1-ss*/*SGS1-ss* diploid strain was constructed and its kinetics of processing/repair of meiotic DSBs generated at the *THR4* hotspot was compared to those of a *sae2*Δ/*sae2*Δ diploid. DSBs disappeared in both wild-type and *SGS1-ss*/*SGS1-ss* cells about 4 h after transfer to sporulation medium, while they persisted until the end of the experiment in both *sae2*Δ/*sae2*Δ and *sae2*Δ/*sae2*Δ *SGS1-ss*/*SGS1-ss* diploid cells (Supplementary Fig S1). Thus, Sgs1-ss cannot substitute the endonucleolytic clipping by Sae2/MRX when this is absolutely required to initiate DSB resection.

Interestingly, the Sgs1-ss mutant variant accelerates both DSB resection and SSA compared to wild-type Sgs1 (Fig 3B–E), suggesting that Sgs1-ss might increase the resection efficiency by escaping the effect of negative regulators of this process. In particular, Rad9 provides a barrier to resection through an unknown mechanism [13,14]. As shown in Fig 4A and B, both *SGS1-ss* and *rad9*Δ mutant cells accumulated the resection products more efficiently than wild-type cells, and the presence of Sgs1-ss did not accelerate further the generation of ssDNA in *rad9*Δ cells. Thus, the lack of Rad9 and the presence of Sgs1-ss appear to increase the efficiency of DSB resection through the same mechanism. Furthermore, cells lacking Rad9 displayed sensitivity to CPT and phleomycin (Fig 4C). Consistent with the finding that the *SGS1-ss* and *rad9*Δ alleles affect the same process, *rad9*Δ was epistatic to *SGS1-ss* with respect to the survival to genotoxic agents, as *sae2*Δ *rad9*Δ *SGS1-ss* cells were as sensitive to CPT and phleomycin as *sae2*Δ *rad9*Δ and *rad9*Δ cells (Fig 4C).

Double-strand break resection in the G1 phase of the cell cycle is specifically inhibited by the Ku complex, whose lack allows nucleolytic processing in G1 cells independently of Cdk1 activity [30]. *RAD9* deletion does not allow DSB resection in G1, but it enhances resection in G1-arrested *ku*Δ cells [31], indicating that Rad9 inhibits DSB resection in G1, but this function becomes apparent only when Ku is absent. To investigate whether Sgs1-ss was capable to counteract the inhibitory function of Rad9 in G1, we monitored DSB resection in *SGS1-ss* and *ku70*Δ *SGS1-ss* cells that were kept arrested in G1 by α-factor during HO induction. Consistent with the requirement of Cdk1 activity for efficient DSB resection, the 3′-ended resection products were barely detectable in wild-type G1 cells, whereas their amount increased in *ku70*Δ G1 cells that, as previously reported [30], accumulated mostly 1.7-, 3.5- and 4.7-kb ssDNA products (r1, r2, r3) (Supplementary Fig S2). By contrast, DSB resection in *SGS1-ss* cells was undistinguishable from that observed in wild-type cells (Supplementary Fig S2), indicating that Sgs1-ss does not allow DSB resection in G1. Furthermore, while *RAD9* deletion enhanced the resection efficiency of *ku70*Δ G1 cells, G1-arrested *ku70*Δ and *ku70*Δ *SGS1-ss* cells accumulated resection products with similar kinetics (Fig 4D and E). Altogether, these findings indicate that Sgs1-ss is not capable to allow DSB resection in G1 either in the presence or in the absence of Ku. As Sgs1-ss function in DSB resection depends on Dna2, whose activity requires Cdk1-mediated phosphorylation [8], the inability of Sgs1-ss to overcome both Ku- and Rad9-mediated inhibition in G1 may be due to the requirement of Cdk1 activity to support Dna2 and therefore Sgs1-ss function in DSB resection.

Rapid DSB resection in *rad9*Δ cells depends mainly on Sgs1

Generation of ssDNA at uncapped telomeres in *rad9*Δ cells has been shown to be more dependent on Dna2/Sgs1 than on Exo1 [32]. This observation, together with the finding that *SGS1-ss* does not accelerate further the generation of ssDNA in *rad9*Δ cells (Fig 4A and B), raises the possibility that Rad9 inhibits DSB resection by limiting Sgs1 activity and that the Sgs1-ss variant can escape this inhibition. We tested this hypothesis by investigating the contribution of Sgs1 and Exo1 to the accelerated DSB resection displayed by *rad9*Δ cells. As shown in Fig 5A and B, *sgs1*Δ was epistatic to *rad9*Δ with respect to DSB resection, as *sgs1*Δ *rad9*Δ double-mutant and *sgs1*Δ single-mutant cells resected the HO-induced DSB with similar kinetics. By contrast, DSB resection in *exo1*Δ *rad9*Δ cells was more efficient than in *exo1*Δ cells, although it was delayed compared to *rad9*Δ cells (Fig 5C and D). Thus, the rapid resection in the absence of Rad9 depends mainly on Sgs1, although also Exo1 contributes to resect the DSB in the absence of Rad9. Consistent with the finding that Sgs1-ss overrides Rad9 inhibition, *SGS1-ss exo1*Δ cells resected the DSB with kinetics similar to that of *rad9*Δ *exo1*Δ cells (Supplementary Fig S3).

Rad9 inhibits DSB resection by limiting Sgs1 association at DNA breaks

If loss of end protection by Rad9 allowed Sgs1 to initiate DSB resection, which normally requires Sae2, then *RAD9* deletion, like Sgs1-ss, should suppress the resection defect of *sae2*Δ cells. Indeed, DSB resection in *sae2*Δ *rad9*Δ cells was as fast as in *rad9*Δ cells, which resected the DSB more efficiently than wild-type and *sae2*Δ cells (Fig 6A and B), indicating that the lack of Rad9 bypasses Sae2 function in DSB resection.

We then asked by ChIP and qPCR analysis whether Rad9 limits Sgs1 activity by regulating Sgs1 binding/persistence to the DSB ends. When HO was induced in exponentially growing cells, the amount of Sgs1 bound at the HO-induced DSB was higher in *rad9*Δ than in wild-type cells (Fig 6C), indicating that Rad9 counteracts Sgs1 recruitment to the DSB. Interestingly, the Sgs1-ss variant was recruited at the DSB with equivalent efficiencies in both exponentially growing wild-type and *rad9*Δ cells (Fig 6C). These differences were not due to different resection kinetics, as we obtained similar results also when the HO-induced DSB was generated in G1-arrested cells (Fig 6D), which resected the DSB very poorly due to the low Cdk1 activity [6]. Interestingly, the amount of Sgs1-ss bound to the DSB was higher than the amount of wild-type Sgs1 in *rad9*Δ cells (Fig 6C and D), suggesting that Sgs1-ss has a higher intrinsic ability to bind/persist at the DSB. Altogether, these results indicate that Rad9 limits the association of Sgs1 to the DSB ends and that the Sgs1-ss variant escapes this inhibition possibly because it binds more tightly the DSB. Interestingly, the robust association of Sgs1-ss to the DSB in G1-arrested cells (low Cdk1 activity) did not result in DSB resection (Supplementary Fig S2) possibly because Sgs1 acts in

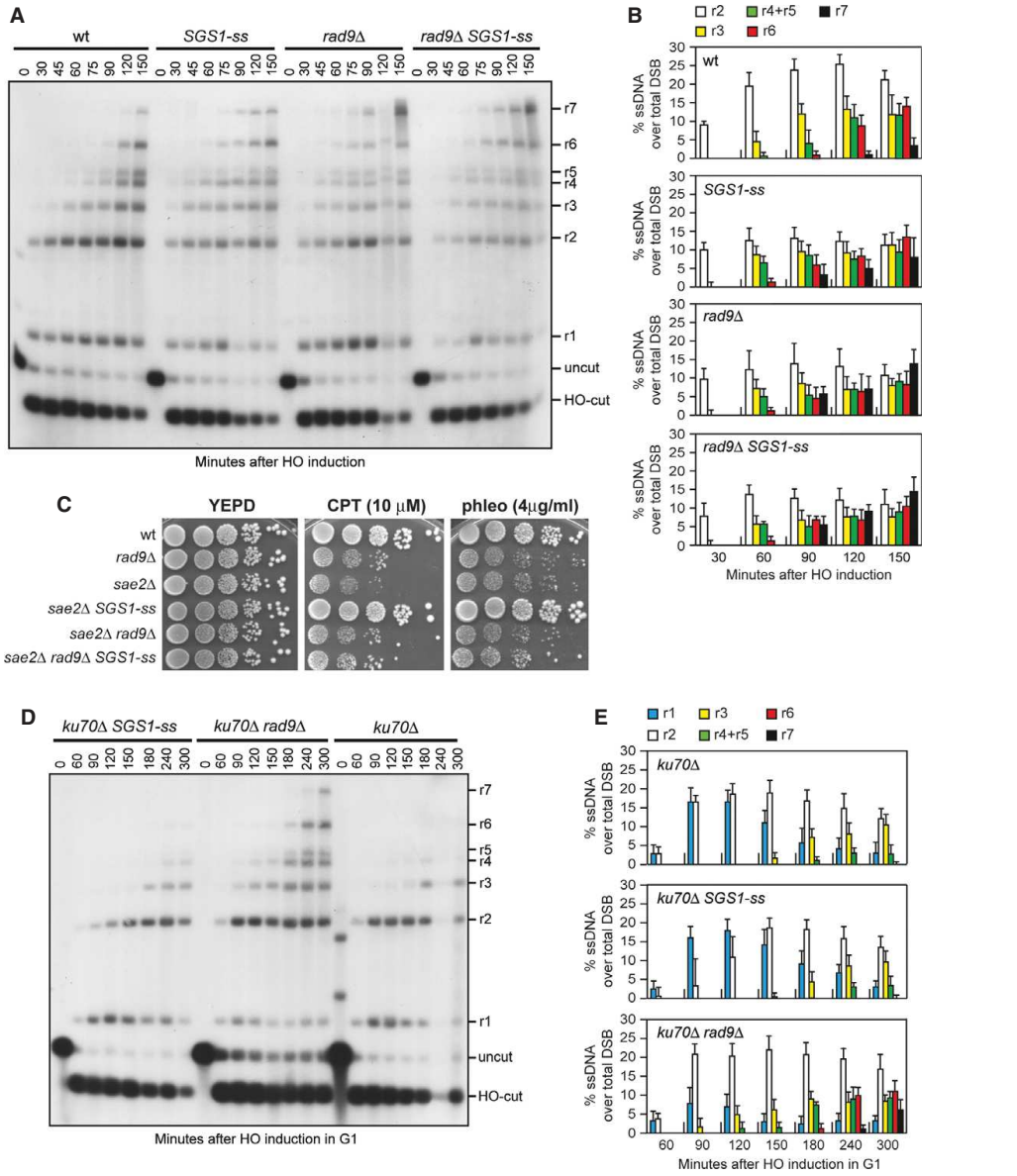

Figure 4. Double-strand break (DSB) resection is accelerated by the same mechanism in *SGS1-ss* and *rad9Δ* cells.

A DSB resection. YEPR exponentially growing cell cultures of JKM139 derivative strains were transferred to YEPRG at time zero. Genomic DNA was analysed for ssDNA formation as described in Fig 3A.

B Densitometric analyses. The experiment as in (A) has been independently repeated three times, and the mean values are represented with error bars denoting s.d. (n = 3).

C Exponentially growing cells were serially diluted (1:10), and each dilution was spotted out onto YEPD plates with or without camptothecin (CPT) or phleomycin.

D DSB resection. HO was induced at time zero in α-factor-arrested JKM139 derivative cells that were kept arrested in G1 with α-factor throughout the experiment. Genomic DNA was analysed for ssDNA formation as described in Fig 3A.

E Densitometric analyses. The experiment as in (D) has been independently repeated three times, and the mean values are represented with error bars denoting s.d. (n = 3).

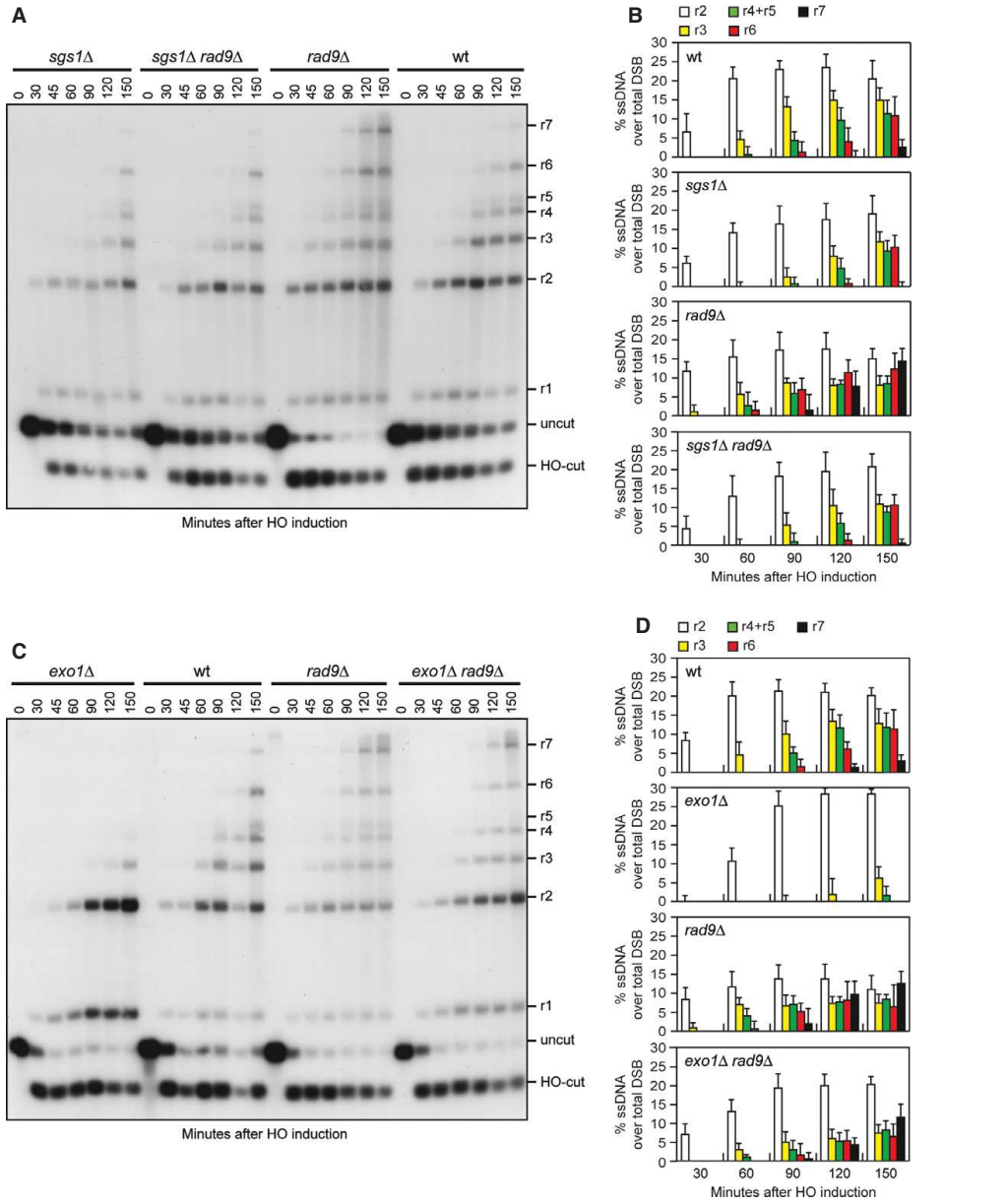

Figure 5. Rapid resection in *rad9*Δ cells depends mainly on Sgs1.

A Double-strand break (DSB) resection. YEPR exponentially growing cell cultures of JKM139 derivative strains were transferred to YEPRG at time zero. Genomic DNA was analysed for ssDNA formation as described in Fig 3A.

B Densitometric analyses. The experiment as in (A) has been independently repeated three times, and the mean values are represented with error bars denoting s.d. (n = 3).

C DSB resection. The experiment was performed as in (A).

D Densitometric analyses. The experiment as in (C) has been independently repeated three times, and the mean values are represented with error bars denoting s.d. (n = 3).

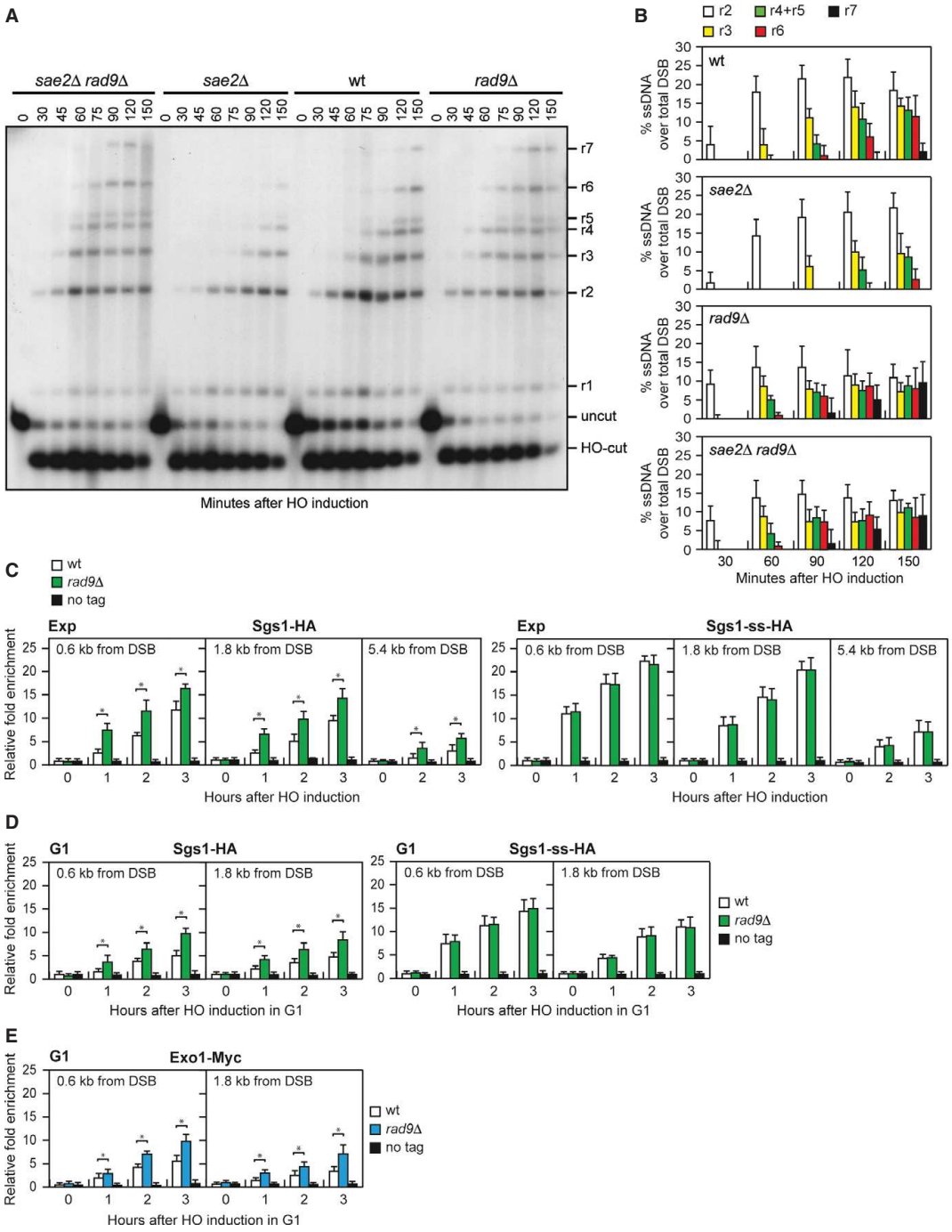
A
sae2Δ rad9Δ
sae2Δ
wt
rad9Δ
0 30 45 60 75 90 120 150
r7
r6
r5
r4
r3
r2
r1
uncut
HO-cut
Minutes after HO induction
B
r2
r4+r5
r7
r3
r6
wt
sae2Δ
rad9Δ
sae2Δ rad9Δ
% ssDNA over total DSB
Minutes after HO induction
C
wt
rad9Δ
no tag
Exp
Sgs1-HA
Sgs1-ss-HA
0.6 kb from DSB
1.8 kb from DSB
5.4 kb from DSB
Relative fold enrichment
Hours after HO induction
D
G1
Hours after HO induction in G1
E
Exo1-Myc

Figure 6.

Figure 6. Rad9 inhibits Sgs1 association at the double-strand breaks (DSBs).

A DSB resection. YEPR exponentially growing cell cultures of JKM139 derivative strains were transferred to YEPRG at time zero. Genomic DNA was analysed for ssDNA formation as described in Fig 3A.

B Densitometric analyses. The experiment as in (A) has been independently repeated three times, and the mean values are represented with error bars denoting s.d. (n = 3).

C ChIP analysis. Exponentially growing YEPR cell cultures of JKM139 derivative strains were transferred to YEPRG, followed by ChIP analysis of the recruitment of Sgs1-HA and Sgs1-ss-HA at the indicated distance from the HO-cut compared to untagged Sgs1 (no tag). In all diagrams, the ChIP signals were normalized for each time point to the corresponding input signal. The mean values are represented with error bars denoting s.d. (n = 3). *P < 0.01, t-test.

D ChIP analysis in G1-arrested cells. As in (C), but showing ChIP analysis of the recruitment of Sgs1-HA and Sgs1-ss-HA in cells that were kept arrested in G1 by α-factor. The mean values are represented with error bars denoting s.d. (n = 3). *P < 0.01, t-test.

E ChIP analysis in G1-arrested cells. As in (C), but showing ChIP analysis of the recruitment of Exo1–Myc in cells that were kept arrested in G1 by α-factor. The mean values are represented with error bars denoting s.d. (n = 3). *P < 0.01, t-test.

DSB resection together with Dna2, whose activity requires Cdk1-mediated phosphorylation [8]. Consistent with a contribution of Exo1 in promoting DSB resection in the absence of Rad9, *rad9*Δ cells showed an increased Exo1 recruitment to the DSB compared to wild-type cells (Fig 6E).

In summary, we show that Rad9 increases the requirement for the MRX/Sae2 activities in DSB resection by inhibiting the action of the Sgs1/Dna2 long-range resection machinery. Extensive resection in Rad9-deficient cells is mainly dependent on Sgs1, whose recruitment at DSBs is inhibited by Rad9. By contrast, Sgs1-ss, which suppresses the resection defect of *sae2*Δ cells, is robustly associated with the DSB ends both in the presence and in the absence of Rad9 and resects the DSB more efficiently than wild-type Sgs1. These findings indicate that Rad9 inhibits the activity of Sgs1/Dna2 by limiting Sgs1 binding/persistence at DSB ends and that the Sgs1-ss mutant variant escapes this inhibition possibly because it is more tightly bound to DNA. Thus, while Ku increases the requirement for the MRX/Sae2 activities in DSB resection by inhibiting preferentially Exo1 [20], Rad9 mainly restricts the action of Sgs1/Dna2. As MRX and Sae2 are especially important for initial processing of DNA ends that contain adducts, the Rad9- and Ku-mediated inhibitions of Sgs1/Dna2 and Exo1 activities in initiating DSB resection ensure that all DSBs are processed in a similar manner independently of their nature.

Materials and Methods

Yeast strains

The yeast strains used in this study are derivatives of W303, JKM139 or SK1 (Supplementary Table S1). Cells were grown in YEP medium (1% yeast extract, 2% peptone) supplemented with 2% glucose (YEPD), 2% raffinose (YEPR) or 2% raffinose and 3% galactose (YEPRG).

Search for suppressors of *sae2*Δ sensitivity to CPT

To search for suppressor mutations of the CPT sensitivity of *sae2*Δ mutant, 5×10^6 *sae2*Δ cells were plated on YEPD in the presence of 30 μM CPT. Survivors were recovered and crossed to wild-type cells to identify by tetrad analysis the suppression events that were due to single-gene mutations. Subsequent genetic analyses allowed grouping the single-gene suppression events in 11 classes. The five classes that showed the most efficient suppression were chosen and the suppressor genes were identified by genome sequencing and genetic analyses. To confirm that the *SGS1-ss* mutation was responsible for the suppression, a *URA3* gene was integrated downstream of the *SGS1-ss* stop codon and the resulting strain was crossed to wild-type cells to verify by tetrad dissection that the suppression of the *sae2*Δ CPT sensitivity co-segregated with the *URA3* allele.

DSB resection

Double-strand break end resection at the *MAT* locus was analysed on alkaline agarose gels as described in Clerici *et al* [30]. Quantitative analysis of DSB resection was performed by calculating the ratio of band intensities for ssDNA and total amount of DSB products.

Synchronous meiotic time course and detection of meiotic DSBs

To obtain synchronous G1/G0 cell population, overnight liquid YEPD cell cultures were diluted to a final concentration of 1×10^7 cells/ml in 200 ml YPA (1% yeast extract, 2% bactopeptone, 1% potassium acetate) and grown for 13 h at 30°C. Cells were then washed and transferred into the same volume of SPM (0.3% potassium acetate, 0.02% raffinose) to induce meiosis. Genomic DNA was digested with EcoRI and separated on native agarose gels. DSBs at the *THR4* hotspot were detected with a 1.6-kb DNA fragment spanning the 5′ region of *THR4*.

Other techniques

ChIP assays were performed as described in Viscardi *et al* [33]. Data are expressed as fold enrichment at the HO-induced DSB over that at the non-cleaved *ARO1* locus, after normalization of each ChIP signals to the corresponding input for each time point. Fold enrichment was then normalized to the efficiency of DSB induction. Rad53 was detected by using anti-Rad53 (ab104232) polyclonal antibodies from Abcam.

Supplementary information for this article is available online: http://embor.embopress.org

Acknowledgements
We thank J. Haber for strains. Michela Clerici and Giovanna Lucchini are acknowledged for critical reading of the manuscript. This work was supported by grants from Associazione Italiana per la Ricerca sul Cancro (AIRC) (Grant No. IG15210) and Cofinanziamento 2010-2011 MIUR/Università di Milano-Bicocca to MPL.

Author contributions

Conceived and designed the experiments: DB, MV, MPL. Performed the experiments: DB, MV, EG, CC, GT. Analysed the data: DB, MV, EG, MPL. Wrote the manuscript: MPL.

Conflict of interest

The authors declare that they have no conflict of interest.

References

1. Symington LS, Gautier J (2011) Double-strand break end resection and repair pathway choice. *Annu Rev Genet* 45: 247 – 271
2. Ciccia A, Elledge SJ (2010) The DNA damage response: making it safe to play with knives. *Mol Cell* 40: 179 – 204
3. Cannavo E, Cejka P (2014) Sae2 promotes dsDNA endonuclease activity within Mre11-Rad50-Xrs2 to resect DNA breaks. *Nature* 514: 122 – 125
4. Mimitou EP, Symington LS (2008) Sae2, Exo1 and Sgs1 collaborate in DNA double-strand break processing. *Nature* 455: 770 – 774
5. Zhu Z, Chung WH, Shim EY, Lee SE, Ira G (2008) Sgs1 helicase and two nucleases Dna2 and Exo1 resect DNA double-strand break ends. *Cell* 134: 981 – 994
6. Ira G, Pellicioli A, Balijja A, Wang X, Fiorani S, Carotenuto W, Liberi G, Bressan D, Wan L, Hollingsworth NM *et al* (2004) DNA end resection, homologous recombination and DNA damage checkpoint activation require CDK1. *Nature* 431: 1011 – 1017
7. Huertas P, Cortés-Ledesma F, Sartori AA, Aguilera A, Jackson SP (2008) CDK targets Sae2 to control DNA-end resection and homologous recombination. *Nature* 455: 689 – 692
8. Chen X, Niu H, Chung WH, Zhu Z, Papusha A, Shim EY, Lee SE, Sung P, Ira G (2011) Cell cycle regulation of DNA double-strand break end resection by Cdk1-dependent Dna2 phosphorylation. *Nat Struct Mol Biol* 18: 1015 – 1019
9. Seeber A, Hauer M, Gasser SM (2013) Nucleosome remodelers in double-strand break repair. *Curr Opin Genet Dev* 23: 174 – 184
10. Chen X, Cui D, Papusha A, Zhang X, Chu CD, Tang J, Chen K, Pan X, Ira G (2012) The Fun30 nucleosome remodeller promotes resection of DNA double-strand break ends. *Nature* 489: 576 – 580
11. Costelloe T, Louge R, Tomimatsu N, Mukherjee B, Martini E, Khadaroo B, Dubois K, Wiegant WW, Thierry A, Burma S *et al* (2012) The yeast Fun30 and human SMARCAD1 chromatin remodellers promote DNA end resection. *Nature* 489: 581 – 584
12. Eapen VV, Sugawara N, Tsabar M, Wu WH, Haber JE (2012) The *Saccharomyces cerevisiae* chromatin remodeler Fun30 regulates DNA end resection and checkpoint deactivation. *Mol Cell Biol* 32: 4727 – 4740
13. Lydall D, Weinert T (1995) Yeast checkpoint genes in DNA damage processing: implications for repair and arrest. *Science* 270: 1488 – 1491
14. Lazzaro F, Sapountzi V, Granata M, Pellicioli A, Vaze M, Haber JE, Plevani P, Lydall D, Muzi-Falconi M (2008) Histone methyltransferase Dot1 and Rad9 inhibit single-stranded DNA accumulation at DSBs and uncapped telomeres. *EMBO J* 27: 1502 – 1512
15. Keeney S, Kleckner N (1995) Covalent protein-DNA complexes at the 5′ strand termini of meiosis-specific double-strand breaks in yeast. *Proc Natl Acad Sci USA* 92: 11274 – 11278
16. Usui T, Ohta T, Oshiumi H, Tomizawa J, Ogawa H, Ogawa T (1998) Complex formation and functional versatility of Mre11 of budding yeast in recombination. *Cell* 95: 705 – 716
17. Deng C, Brown JA, You D, Brown JM (2005) Multiple endonucleases function to repair covalent topoisomerase I complexes in *Saccharomyces cerevisiae*. *Genetics* 170: 591 – 600
18. Mimitou EP, Symington LS (2010) Ku prevents Exo1 and Sgs1-dependent resection of DNA ends in the absence of a functional MRX complex or Sae2. *EMBO J* 29: 3358 – 3369
19. Foster SS, Balestrini A, Petrini JH (2011) Functional interplay of the Mre11 nuclease and Ku in the response to replication-associated DNA damage. *Mol Cell Biol* 31: 4379 – 4389
20. Shim EY, Chung WH, Nicolette ML, Zhang Y, Davis M, Zhu Z, Paull TT, Ira G, Lee SE (2010) *Saccharomyces cerevisiae* Mre11/Rad50/Xrs2 and Ku proteins regulate association of Exo1 and Dna2 with DNA breaks. *EMBO J* 29: 3370 – 3380
21. Mullen JR, Kaliraman V, Brill SJ (2000) Bipartite structure of the Sgs1 DNA helicase in *Saccharomyces cerevisiae*. *Genetics* 154: 1101 – 1114
22. Budd ME, Reis CC, Smith S, Myung K, Campbell JL (2006) Evidence suggesting that Pif1 helicase functions in DNA replication with the Dna2 helicase/nuclease and DNA polymerase delta. *Mol Cell Biol* 26: 2490 – 2500
23. Lee SE, Moore JK, Holmes A, Umezu K, Kolodner RD, Haber JE (1998) *Saccharomyces* Ku70, Mre11/Rad50 and RPA proteins regulate adaptation to G2/M arrest after DNA damage. *Cell* 94: 399 – 409
24. Pellicioli A, Lee SE, Lucca C, Foiani M, Haber JE (2001) Regulation of *Saccharomyces* Rad53 checkpoint kinase during adaptation from DNA damage-induced G2/M arrest. *Mol Cell* 7: 293 – 300
25. Usui T, Ogawa H, Petrini JH (2001) A DNA damage response pathway controlled by Tel1 and the Mre11 complex. *Mol Cell* 7: 1255 – 1266
26. Clerici M, Mantiero D, Lucchini G, Longhese MP (2006) The *Saccharomyces cerevisiae* Sae2 protein negatively regulates DNA damage checkpoint signalling. *EMBO Rep* 7: 212 – 218
27. Clerici M, Trovesi C, Galbiati A, Lucchini G, Longhese MP (2014) Mec1/ATR regulates the generation of single-stranded DNA that attenuates Tel1/ATM signaling at DNA ends. *EMBO J* 33: 198 – 216
28. Vaze MB, Pellicioli A, Lee SE, Ira G, Liberi G, Arbel-Eden A, Foiani M, Haber JE (2002) Recovery from checkpoint-mediated arrest after repair of a double-strand break requires Srs2 helicase. *Mol Cell* 10: 373 – 385
29. Bernstein KA, Mimitou EP, Mihalevic MJ, Chen H, Sunjaveric I, Symington LS, Rothstein R (2013) Resection activity of the Sgs1 helicase alters the affinity of DNA ends for homologous recombination proteins in *Saccharomyces cerevisiae*. *Genetics* 195: 1241 – 1251
30. Clerici M, Mantiero D, Guerini I, Lucchini G, Longhese MP (2008) The Yku70-Yku80 complex contributes to regulate double-strand break processing and checkpoint activation during the cell cycle. *EMBO Rep* 9: 810 – 818
31. Trovesi C, Falcettoni M, Lucchini G, Clerici M, Longhese MP (2011) Distinct Cdk1 requirements during single-strand annealing, noncrossover, and crossover recombination. *PLoS Genet* 7: e1002263
32. Ngo GH, Balakrishnan L, Dubarry M, Campbell JL, Lydall D (2014) The 9-1-1 checkpoint clamp stimulates DNA resection by Dna2-Sgs1 and Exo1. *Nucleic Acids Res* 42: 10516 – 10528
33. Viscardi V, Bonetti D, Cartagena-Lirola H, Lucchini G, Longhese MP (2007) MRX-dependent DNA damage response to short telomeres. *Mol Biol Cell* 18: 3047 – 3058

Published online: January 30, 2015

PLOS | GENETICS

RESEARCH ARTICLE

Sae2 Function at DNA Double-Strand Breaks Is Bypassed by Dampening Tel1 or Rad53 Activity

Elisa Gobbini☯, Matteo Villa☯, Marco Gnugnoli, Luca Menin, Michela Clerici, Maria Pia Longhese*

Dipartimento di Biotecnologie e Bioscienze, Università di Milano-Bicocca, Milano, Italy

☯ These authors contributed equally to this work.
* mariapia.longhese@unimib.it

OPEN ACCESS

Citation: Gobbini E, Villa M, Gnugnoli M, Menin L, Clerici M, Longhese MP (2015) Sae2 Function at DNA Double-Strand Breaks Is Bypassed by Dampening Tel1 or Rad53 Activity. PLoS Genet 11 (11): e1005685. doi:10.1371/journal.pgen.1005685

Editor: Sue Jinks-Robertson, Duke University, UNITED STATES

Received: June 17, 2015

Accepted: October 29, 2015

Published: November 19, 2015

Data Availability Statement: All relevant data are within the paper and its Supporting Information files.

Funding: This work was supported by grants from Associazione Italiana per la Ricerca sul Cancro (AIRC) (grant IG15210) and Cofinanziamento 2010-2011 Ministero dell'Istruzione, dell'Università e della Ricerca (MIUR)/Università di Milano-Bicocca to MPL. The funders had no role in study design, data collection and analysis, decision to publish, or preparation of the manuscript.

Competing Interests: The authors have declared that no competing interests exist.

Abstract

The MRX complex together with Sae2 initiates resection of DNA double-strand breaks (DSBs) to generate single-stranded DNA (ssDNA) that triggers homologous recombination. The absence of Sae2 not only impairs DSB resection, but also causes prolonged MRX binding at the DSBs that leads to persistent Tel1- and Rad53-dependent DNA damage checkpoint activation and cell cycle arrest. Whether this enhanced checkpoint signaling contributes to the DNA damage sensitivity and/or the resection defect of *sae2*Δ cells is not known. By performing a genetic screen, we identify *rad53* and *tel1* mutant alleles that suppress both the DNA damage hypersensitivity and the resection defect of *sae2*Δ cells through an Sgs1-Dna2-dependent mechanism. These suppression events do not involve escaping the checkpoint-mediated cell cycle arrest. Rather, defective Rad53 or Tel1 signaling bypasses Sae2 function at DSBs by decreasing the amount of Rad9 bound at DSBs. As a consequence, reduced Rad9 association to DNA ends relieves inhibition of Sgs1-Dna2 activity, which can then compensate for the lack of Sae2 in DSB resection and DNA damage resistance. We propose that persistent Tel1 and Rad53 checkpoint signaling in cells lacking Sae2 increases the association of Rad9 at DSBs, which in turn inhibits DSB resection by limiting the activity of the Sgs1-Dna2 resection machinery.

Author Summary

Genome instability is one of the most pervasive characteristics of cancer cells and can be due to DNA repair defects and failure to arrest the cell cycle. Among the many types of DNA damage, the DNA double strand break (DSB) is one of the most severe, because it can cause mutations and chromosomal rearrangements. Generation of DSBs triggers a highly conserved mechanism, known as DNA damage checkpoint, which arrests the cell cycle until DSBs are repaired. DSBs can be repaired by homologous recombination, which requires the DSB ends to be nucleolytically processed (resected) to generate single-stranded DNA. In *Saccharomyces cerevisiae*, DSB resection is initiated by the MRX

complex together with Sae2, whereas more extensive resection is catalyzed by both Exo1 and Dna2-Sgs1. The absence of Sae2 not only impairs DSB resection, but also leads to the hyperactivation of the checkpoint proteins Tel1/ATM and Rad53, leading to persistent cell cycle arrest. In this manuscript we show that persistent Tel1 and Rad53 signaling activities in *sae2*Δ cells cause DNA damage hypersensitivity and defective DSB resection by increasing the amount of Rad9 bound at the DSBs, which in turn inhibits the Sgs1-Dna2 resection machinery. As ATM inhibition has been proposed as a strategy for cancer treatment, the finding that defective Tel1 signaling activity restores DNA damage resistance in *sae2*Δ cells might have implications in cancer therapies that use ATM inhibitors for synthetic lethal approaches that are devised to kill tumor cells with defective DSB repair.

Introduction

Programmed DNA double-strand breaks (DSBs) are formed during meiotic recombination and rearrangement of the immunoglobulin genes in lymphocytes. Furthermore, potentially harmful DSBs can arise by exposure to environmental factors, such as ionizing radiations and radiomimetic chemicals, or by failures in DNA replication. DSB generation elicits a checkpoint response that depends on the mammalian protein kinases ATM and ATR, whose functional orthologs in *Saccharomyces cerevisiae* are Tel1 and Mec1, respectively [1]. Tel1/ATM is recruited to DSBs by the MRX (Mre11-Rad50-Xrs2)/MRN (Mre11-Rad50-Nbs1) complex, whereas Mec1/ATR recognizes single-stranded DNA (ssDNA) covered by Replication Protein A (RPA) [2]. Once activated, Tel1/ATM and Mec1/ATR propagate their checkpoint signals by phosphorylating the downstream checkpoint kinases Rad53 (Chk2 in mammals) and Chk1, to couple cell cycle progression with DNA repair [2].

Repair of DSBs can occur by either non-homologous end joining (NHEJ) or homologous recombination (HR). Whereas NHEJ directly joins the DNA ends, HR uses the sister chromatid or the homologous chromosome to repair DSBs. HR requires that the 5' ends of a DSB are nucleolytically processed (resected) to generate 3'-ended ssDNA that can invade an undamaged homologous DNA template [3,4]. In *Saccharomyces cerevisiae*, recent characterization of core resection proteins has revealed that DSB resection is initiated by the MRX complex, which catalyzes an endonucleolytic cleavage near a DSB [4], with the Sae2 protein (CtIP in mammals) promoting MRX endonucleolytic activity [5]. This MRX-Sae2-mediated DNA clipping generates 5' DNA ends that are optimal substrates for the nucleases Exo1 and Dna2, the latter working in concert with the helicase Sgs1 [6–9]. In addition, the MRX complex recruits Exo1, Sgs1 and Dna2 to DSBs independently of the Mre11 nuclease activity [10]. DSB resection is also negatively regulated by Ku and Rad9, which inhibit the access to DSBs of Exo1 and Sgs1-Dna2, respectively [11–14].

The MRX-Sae2-mediated endonucleolytic cleavage is particularly important to initiate resection at DNA ends that are not easily accessible to Exo1 and Dna2-Sgs1. For instance, both *sae2*Δ and *mre11* nuclease defective mutants are completely unable to resect meiotic DSBs, where the Spo11 topoisomerase-like protein remains covalently attached to the 5'-terminated strands [15,16]. Furthermore, the same mutants exhibit a marked sensitivity to camptothecin (CPT), which extends the half-life of DNA-topoisomerase I cleavable complexes [17,18], and to methyl methanesulfonate (MMS), which can generate chemically complex DNA termini. The lack of Rad9 or Ku suppresses both the hypersensitivity to DSB-inducing agents and the resection defect of *sae2*Δ cells [10–14]. These suppression events require Dna2-Sgs1 and Exo1, respectively, indicating that Rad9 increases the requirement for MRX-Sae2 activity in DSB

resection by inhibiting Sgs1-Dna2 [13,14], while Ku mainly limits the action of Exo1 [10–12]. By contrast, elimination of either Rad9 or Ku does not bypass Sae2/MRX function in resecting meiotic DSBs [11,13], likely because Sgs1-Dna2 and Exo1 cannot substitute for the Sae2/MRX-mediated endonucleolytic cleavage when this event is absolutely required to generate accessible 5'-terminated DNA strands.

Sae2 plays an important role also in modulating the checkpoint response. Checkpoint activation in response to DSBs depends primarily on Mec1, with Tel1 playing a minor role [19]. On the other hand, impaired Mre11 endonuclease activity caused by the lack of Sae2 leads to increased MRX persistence at the DSB ends. The enhanced MRX signaling in turn causes unscheduled Tel1-dependent checkpoint activation that is associated to prolonged Rad53 phosphorylation [20–22]. Mutant *mre11* alleles that reduce MRX binding to DSBs restore DNA damage resistance in *sae2*Δ cells and reduce their persistent checkpoint activation without restoring efficient DSB resection [23,24], suggesting that enhanced MRX association to DSBs contributes to the DNA damage hypersensitivity caused by the lack of Sae2. Persistently bound MRX might increase the sensitivity to DNA damaging agents of *sae2*Δ cells by hyperactivating the DNA damage checkpoint. If this were the case, then the DNA damage hypersensitivity of *sae2*Δ cells should be restored by the lack of Tel1 or of its downstream effector Rad53, as they are responsible for the *sae2*Δ enhanced checkpoint signaling [20,22]. However, while Rad53 inactivation has never been tested, *TEL1* deletion not only fails to restore DNA damage resistance in *sae2*Δ cells, but it exacerbates their sensitivity to DNA damaging agents [23,24]. Therefore, other studies are required to understand whether the Tel1- and Rad53-mediated checkpoint signaling has any role in determining the DNA damage sensitivity of *sae2*Δ cells.

By performing a genetic screen, we identified *rad53* and *tel1* mutant alleles that suppress both the hypersensitivity to DNA damaging agents and the resection defect of *sae2*Δ cells by reducing the amount of Rad9 at DSBs. Decreased Rad9 binding at DNA ends bypasses Sae2 function in DNA damage resistance and resection by relieving the inhibition of the Sgs1-Dna2 resection machinery. Altogether our data suggest that the primary cause of the resection defect of *sae2*Δ cells is Rad9 association to DSBs, which is promoted by persistent Tel1 and Rad53 signaling activities in these cells.

Results

The Rad53-H88Y and Tel1-N2021D variants suppress the DNA damage hypersensitivity of *sae2*Δ cells

We have previously described our search for extragenic mutations that suppress the CPT hypersensitivity of *sae2*Δ cells [13]. This genetic screen identified 15 single-gene suppressor mutants belonging to 11 distinct allelism groups. Analysis of genomic DNA by next-generation Illumina sequencing of 5 non allelic suppressor mutants revealed that the DNA damage resistance was due to single base pair substitutions in the genes encoding Sgs1, Top1, or the multidrug resistance proteins Pdr3, Pdr10 and Sap185 [13]. Subsequent genome sequencing and genetic analysis of 2 more non allelic suppressor mutants allowed to link suppression to either the *rad53-H88Y* mutant allele, causing the replacement of Rad53 amino acid residue His88 by Tyr, or the *tel1-N2021D* allele, resulting in the replacement of Tel1 amino acid residue Asn2021 by Asp. Both *rad53-H88Y* and *tel1-N2021D* alleles restored resistance of *sae2*Δ cells not only to CPT, but also to phleomycin (phleo) and MMS (Fig 1A). While both *rad53-H88Y* and *tel1-N2021D* fully rescued the hypersensitivity of *sae2*Δ cells to phleomycin and MMS, the CPT hypersensitivity of *sae2*Δ cells was only partially suppressed by the same alleles (Fig 1A), suggesting that they did not bypass all Sae2 functions.

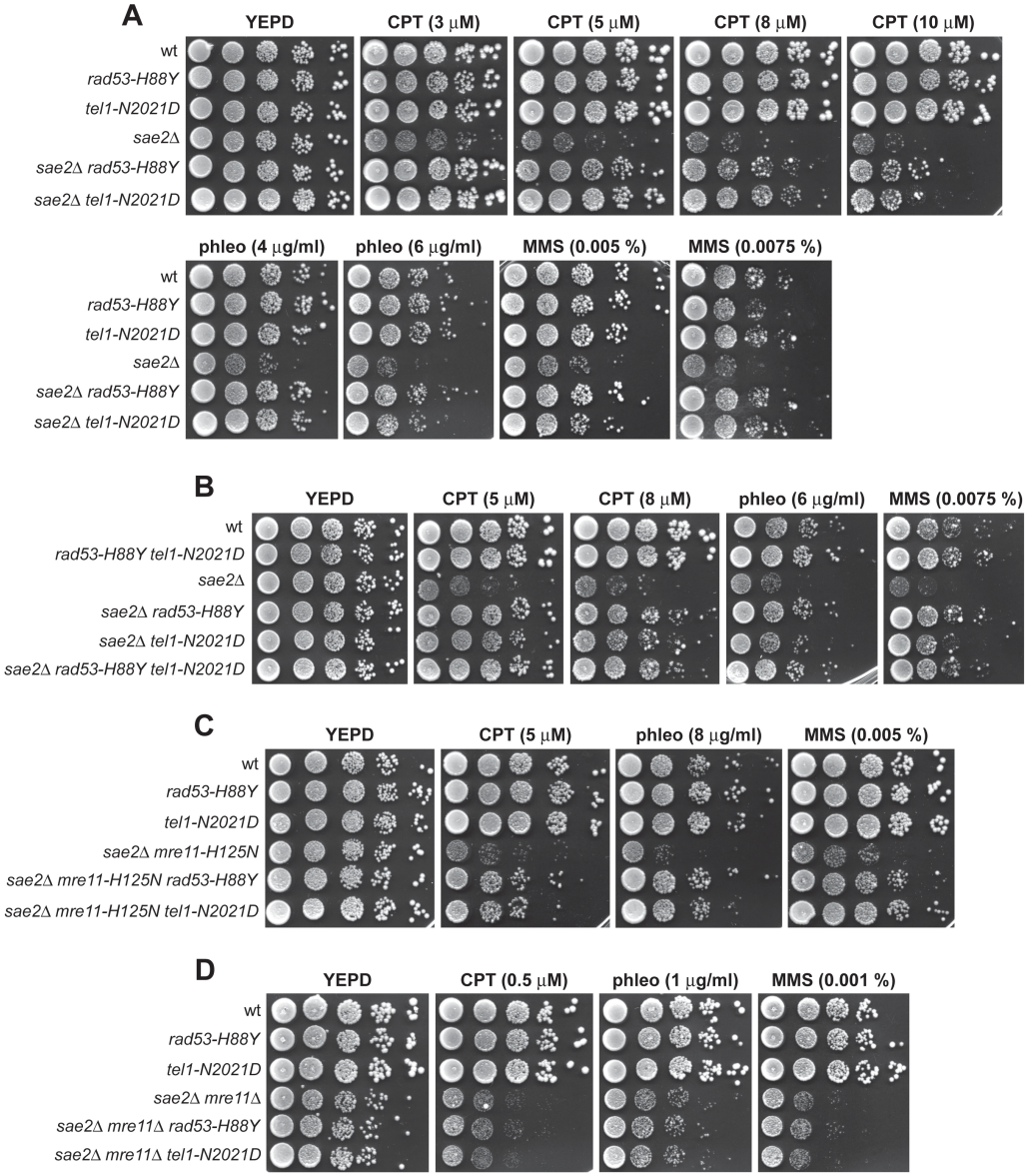

Fig 1. Rad53-H88Y and Tel1-N2021D suppress the hypersensitivity to genotoxic agents of *sae2*Δ cells. (A-D) Exponentially growing cells were serially diluted (1:10) and each dilution was spotted out onto YEPD plates with or without CPT, phleomycin or MMS.

doi:10.1371/journal.pgen.1005685.g001

Both *rad53-H88Y* and *tel1-N2021D* suppressor alleles were recessive, as the sensitivity to genotoxic agents of *sae2*Δ/*sae2*Δ *RAD53*/*rad53-H88Y* and *sae2*Δ/*sae2*Δ *TEL1*/*tel1-N2021D* diploid cells was similar to that of *sae2*Δ/*sae2*Δ *RAD53/RAD53 TEL1/TEL1* diploid cells (S1 Fig), suggesting that *rad53-H88Y* and *tel1-N2021D* alleles encode hypomorphic variants. Furthermore, both variants suppressed the hypersensitivity to DNA damaging agents of *sae2*Δ cells by altering the same mechanism, as *sae2*Δ *rad53-H88Y tel1-N2021D* triple mutant cells survived in the presence of DNA damaging agents to the same extent as *sae2*Δ *rad53-H88Y* and *sae2*Δ *tel1-N2021D* double mutant cells (Fig 1B).

The MRX complex not only provides the nuclease activity for initiation of DSB resection, but also it promotes the binding of Exo1, Sgs1 and Dna2 at the DSB ends [10]. These MRX multiple roles explain the severe DNA damage hypersensitivity and resection defect of cells lacking any of the MRX subunits compared to cells lacking either Sae2 or the Mre11 nuclease activity. As Sae2 has been proposed to activate Mre11 nuclease activity [5], we asked whether the suppression of *sae2*Δ DNA damage hypersensitivity by Rad53-H88Y and Tel1-N2021D requires Mre11 nuclease activity. Both *rad53-H88Y* and *tel1-N2021D* alleles suppressed the hypersensitivity to DNA damaging agents of *sae2*Δ cells carrying the nuclease defective *mre11-H125N* allele (Fig 1C). By contrast, *sae2*Δ *mre11*Δ *rad53-H88Y* and *sae2*Δ *mre11*Δ *tel1-N2021D* triple mutant cells were as sensitive to genotoxic agents as *sae2*Δ *mre11*Δ double mutant cells (Fig 1D), indicating that neither the *rad53-H88Y* nor the *tel1-N2021D* allele can suppress the hypersensitivity to DNA damaging agents of *sae2*Δ *mre11*Δ cells. Altogether, these findings indicate that both Rad53-H88Y and Tel1-N2021D require the physical presence of the MRX complex, but not its nuclease activity, to bypass Sae2 function in cell survival to genotoxic agents.

The Rad53-H88Y variant is defective in the interaction with Rad9 and bypasses the adaptation defect of *sae2*Δ cells by impairing checkpoint activation

A single unrepairable DSB induces a DNA damage checkpoint that depends primarily on Mec1, with Tel1 playing a minor role [19]. This checkpoint response can be eventually turned off, allowing cells to resume cell cycle progression through a process that is called adaptation [25–27]. In the absence of Sae2, cells display heightened checkpoint activation that prevents cells from adapting to an unrepaired DSB [20,22]. This persistent checkpoint activation is due to increased MRX amount/persistence at the DSB that in turn causes enhanced and prolonged Tel1 activation that is associated with persistent Rad53 phosphorylation [20–22,28].

If the *rad53-H88Y* mutation impaired Rad53 activity, then it is expected to suppress the adaptation defect of *sae2*Δ cells by lowering checkpoint activation. We addressed this point by using JKM139 derivative strains, where a single DSB at the *MAT* locus can be generated by expression of the HO endonuclease gene under the control of a galactose-dependent promoter. This DSB cannot be repaired by HR because of the deletion of the homologous donor loci *HML* and *HMR* [27]. We measured checkpoint activation by monitoring the ability of cells to arrest the cell cycle and to phosphorylate Rad53 after HO induction. Both *rad53-H88Y* and *sae2*Δ *rad53-H88Y* cells formed microcolonies of more than 2 cells with higher efficiency than either wild type or *sae2*Δ cells (Fig 2A). Furthermore, the Rad53-H88Y variant was poorly phosphorylated after HO induction both in the presence and in the absence of Sae2 (Fig 2B). Thus, the *rad53-H88Y* mutation suppresses the adaptation defect of *sae2*Δ cells by impairing Rad53 activation.

DNA damage-dependent activation of Rad53 requires its phospho-dependent interaction with Rad9, which acts as a scaffold to allow Rad53 intermolecular authophosphorylation and

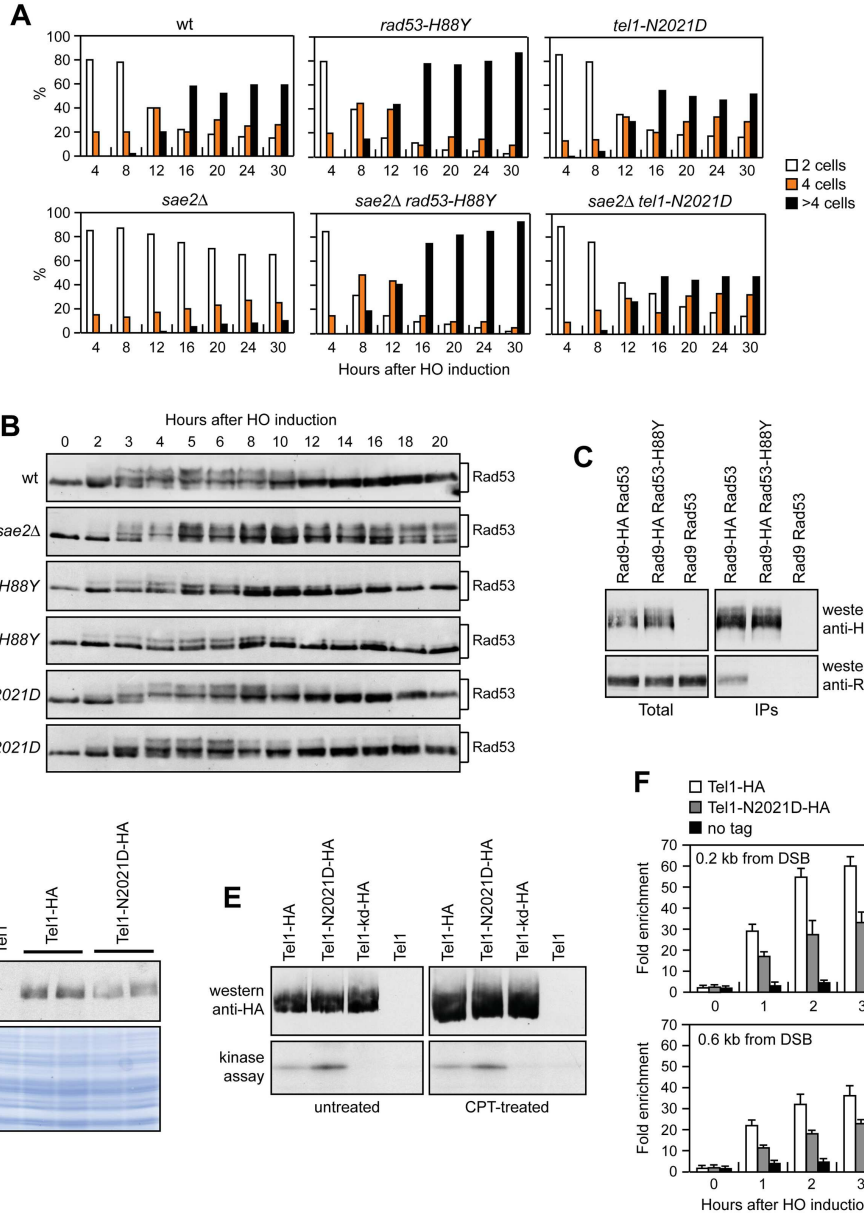

Fig 2. Rad53-H88Y and Tel1-N2021D suppress the checkpoint shut off defect of *sae2*Δ cells. (A) G1-arrested cell cultures of JKM139 derivative strains were plated on galactose-containing plates (time zero). At the indicated time points, 200 cells for each strain were analyzed to determine the frequency of large budded cells (2 cells) and of cells forming microcolonies of 4 or more than 4 cells. (B) Exponentially growing YEPR cultures of the strains in (A) were transferred to YEPRG (time zero), followed by western blot analysis with anti-Rad53 antibodies. (C) Protein extracts were analyzed by western blot with anti-HA or anti-Rad53 antibodies either directly (Total) or after Rad9-HA immunoprecipitation (IPs) with anti-HA antibodies. (D) Protein extracts from

exponentially growing cells were analyzed by western blotting with anti-HA antibodies. The same amounts of protein extracts were separated by SDS-PAGE and stained with Coomassie as loading control. (E) Kinase assay was performed on equal amounts of anti-HA immunoprecipitates of protein extracts from cells either exponentially growing in YEPD or after treatment with 50μM CPT for 1 hour. All the immunoprecipitates were also subjected to western blot analysis using anti-HA antibodies. (F) Relative fold enrichment of Tel1-HA and Tel1-N2021D-HA compared to untagged Tel1 (no tag) at the indicated distance from the HO cleavage site was evaluated after ChIP with anti-HA antibodies and qPCR analysis. In all diagrams, the ChIP signals were normalized for each time point to the amount of the corresponding immunoprecipitated protein and input signal. The mean values are represented with error bars denoting s.d. (n = 3).

doi:10.1371/journal.pgen.1005685.g002

activation [29–31]. Interestingly, the His88 residue, which is replaced by Tyr in the Rad53-H88Y variant, is localized in the forkhead-associated domain 1 of the protein and has been implicated in mediating Rad9-Rad53 interaction [32]. Thus, we asked whether the Rad53-H88Y variant was defective in the interaction with Rad9. When HA-tagged Rad9 was immunoprecipitated with anti-HA antibodies from wild type and *rad53-H88Y* cells grown for 4 hours in the presence of galactose to induce HO, wild type Rad53 could be detected in Rad9-HA immunoprecipitates, whereas Rad53-H88Y did not (Fig 2C). This defective interaction of Rad53-H88Y with Rad9 could explain the impaired checkpoint activation in *sae2*Δ *rad53-H88Y* double mutant cells.

The Tel1-N2021D variant binds poorly to DSBs and bypasses the adaptation defect of *sae2*Δ cells by reducing persistent Rad53 activation

Tel1 signaling activity is responsible for the prolonged Rad53 activation that prevents *sae2*Δ cells to adapt to the checkpoint triggered by an unrepairable DSB [20,22]. Although telomere length in *tel1-N2021D* mutant cells was unaffected both in the presence and in the absence of Sae2 (S2 Fig), the recessivity of *tel1-N2021D* suppressor effect on *sae2*Δ DNA damage hypersensitivity suggests that the N2021D substitution impairs Tel1 function. If this were the case, Tel1-N2021D might suppress the adaptation defect of *sae2*Δ cells by reducing the DSB-induced persistent Rad53 phosphorylation. When G1-arrested cell cultures were spotted on galactose-containing plates to induce HO, wild type, *sae2*Δ, *tel1-N2021D* and *sae2*Δ *tel1-N2021D* cells accumulated large budded cells within 4 hours (Fig 2A). This cell cycle arrest is due to checkpoint activation. In fact, when the same cells exponentially growing in raffinose were transferred to galactose, Rad53 phosphorylation was detectable about 2–3 hours after galactose addition (Fig 2B). However, while *sae2*Δ cells remained arrested as large budded cells for at least 30 hours (Fig 2A) and showed persistent Rad53 phosphorylation (Fig 2B), wild type, *tel1-N2021D* and *sae2*Δ *tel1-N2021D* cells formed microcolonies with more than 2 cells (Fig 2A) and decreased the amounts of phosphorylated Rad53 (Fig 2B) with similar kinetics 10–12 hours after HO induction. Therefore, the Tel1-N2021D variant impairs Tel1 signaling activity, as it rescues the *sae2*Δ adaptation defect by reducing the persistent Rad53 phosphorylation.

The N2021D substitution resides in the Tel1 FAT domain, a helical solenoid that encircles the kinase domain of all the phosphoinositide 3-kinase (PI3K)-related kinases (PIKKs) [33,34], suggesting that this amino acid change might reduce Tel1 kinase activity. Western blot analysis revealed that the amount of Tel1-N2021D was slightly lower than that of wild type Tel1 (Fig 2D). We then immunoprecipitated equivalent amounts of Tel1-HA and Tel1-N2021D-HA variants from both untreated and CPT-treated cells (Fig 2E, top), and we measured their kinase activity in vitro using the known artificial substrate of the PIKKs family PHAS-I (Phosphorylated Heat and Acid Stable protein) [35]. Both Tel1-HA and Tel1-N2021D-HA were capable to phosphorylate PHAS-I, with the amount of phosphorylated substrate being slighly higher in Tel1-N2021D-HA than in Tel1-HA immunoprecipitates (Fig 2E, bottom). This PHAS-I phosphorylation was dependent on Tel1 kinase activity, as it was not detectable when the immunoprecipitates were

prepared from strains expressing either kinase dead Tel1-kd-HA or untagged Tel1 (Fig 2E, bottom). Thus, the *tel1-N2021D* mutation does not affect Tel1 kinase activity.

Interestingly, the FAT domain is in close proximity to the FATC domain, which was shown to be important for Tel1 recruitment to DNA ends [36], suggesting that the Tel1-N2021D variant might be defective in recruitment/association to DSBs. Strikingly, when we analyzed Tel1 and Tel1-N2021D binding at the HO-induced DSB by chromatin immunoprecipitation (ChIP) and quantitative real time PCR (qPCR), the amount of Tel1-N2021D bound at the DSB turned out to be lower than that of wild type Tel1 (Fig 2F). This decreased Tel1-N2021D association was not due to lower Tel1-N2021D levels, as the ChIP signals were normalized for each time point to the amount of immunoprecipitated protein. Thus, the inability of *sae2*Δ *tel1-N2021D* cells to sustain persistent Rad53 phosphorylation after DSB generation can be explained by a decreased association of Tel1-N2021D to DSBs.

Checkpoint-mediated cell cycle arrest is not responsible for the DNA damage hypersensitivity of *sae2*Δ cells

As both Rad53-H88Y and Tel1-N2021D reduce checkpoint signaling in *sae2*Δ cells, we asked whether the increased DNA damage resistance of *sae2*Δ *rad53-H88Y* and *sae2*Δ *tel1-N2021D* cells was due to the elimination of the checkpoint-mediated cell cycle arrest. This hypothesis could not be tested by deleting the *MEC1*, *DDC1*, *RAD24*, *MEC3* or *RAD9* checkpoint genes, because they also regulate DSB resection [37–39]. On the other hand, an HO-induced DSB activates also the Chk1 checkpoint kinase [40], which contributes to arrest the cell cycle in response to DSBs by controlling a pathway that is independent of Rad53 [41]. Importantly, *chk1*Δ cells do not display DNA damage hypersensitivity and are not defective in resection of uncapped telomeres [38,41]. We therefore asked whether *CHK1* deletion restores DNA damage resistance in *sae2*Δ cells. Consistent with the finding that Chk1 contributes to arrest the cell cycle after DNA damage independently of Rad53 [41], Rad53 was phosphorylated with wild type kinetics after HO induction in both *chk1*Δ and *sae2*Δ *chk1*Δ cells (Fig 3A). Furthermore, *CHK1* deletion suppresses the adaptation defect of *sae2*Δ cells. In fact, both *chk1*Δ and *sae2*Δ *chk1*Δ cells spotted on galactose-containing plates formed microcolonies of more than 2 cells with higher efficiency than wild type and *sae2*Δ cells (Fig 3B), although they did it less efficiently than *mec1*Δ cells, where both Rad53 and Chk1 signaling were abrogated [41]. Strikingly, the lack of Chk1 did not suppress the hypersensitivity to DNA damaging agents of *sae2*Δ cells (Fig 3C), although it overrides the checkpoint-mediated cell cycle arrest.

To rule out the possibility that *CHK1* deletion failed to restore DNA damage resistance in *sae2*Δ cells because it impairs DSB resection, we used JKM139 derivative strains to monitor directly generation of ssDNA at the DSB ends in the absence of Chk1. As ssDNA is resistant to cleavage by restriction enzymes, we followed loss of SspI restriction sites as a measure of resection by Southern blot analysis under alkaline conditions, using a single-stranded probe that anneals to the 3' end at one side of the break. Consistent with previous indications that Chk1 is not involved in DNA-end resection [38], *chk1*Δ single mutant cells resected the DSB with wild type kinetics (Fig 3D). Furthermore, *CHK1* deletion did not exacerbate the resection defect of *sae2*Δ cells (Fig 3E). Altogether, these data indicate that the prolonged checkpoint-mediated cell cycle arrest of *sae2*Δ cells is not responsible for their hypersensitivity to DNA damaging agents.

The Rad53-H88Y and Tel1-N2021D variants restore resection and SSA in *sae2*Δ cells

As the checkpoint-mediated cell cycle arrest was not responsible for the DNA damage hypersensitivity of *sae2*Δ cells, we asked whether Rad53-H88Y and/or Tel1-N2021D suppressed the

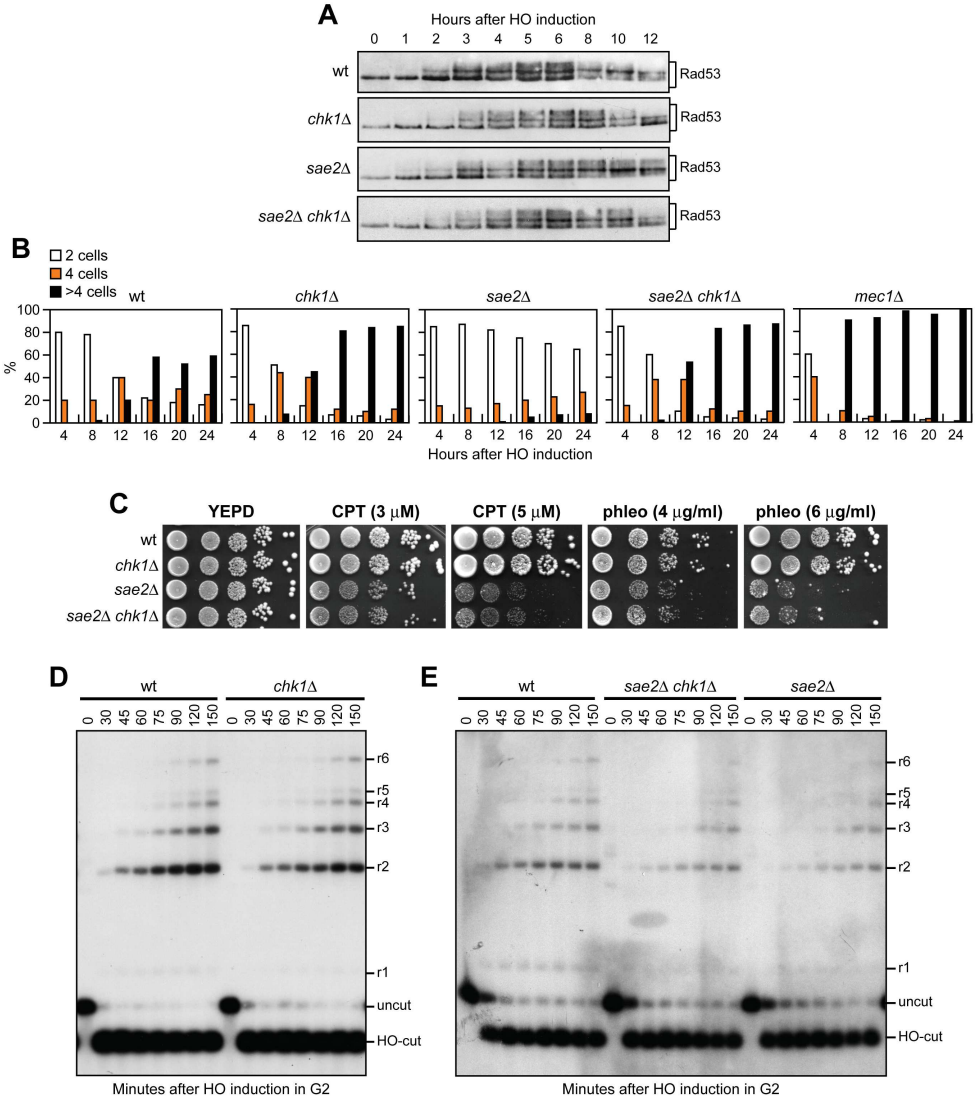

Fig 3. The lack of Chk1 does not suppress the hypersensitivity to DNA damaging agents of *sae2Δ* cells. (A) Exponentially growing YEPR cultures of JKM139 derivative strains were transferred to YEPRG (time zero), followed by western blot analysis with anti-Rad53 antibodies. (B) YEPR G1-arrested cell cultures of JKM139 derivative strains were plated on galactose-containing plates (time zero). At the indicated time points, 200 cells for each strain were analyzed to determine the frequency of large budded cells (2 cells) and of cells forming microcolonies of 4 or more than 4 cells. (C) Exponentially growing cells were serially diluted (1:10) and each dilution was spotted out onto YEPD plates with or without CPT and phleomycin. (D, E) DSB resection. YEPR exponentially growing cultures of JKM139 derivative cells were arrested in G2 with nocodazole and transferred to YEPRG in the presence of nocodazole at time zero. Gel blots of SspI-digested genomic DNA separated on alkaline agarose gel were hybridized with a single-stranded RNA probe that anneals to the unresected strand on one side of the break. 5'-3' resection progressively eliminates SspI sites, producing larger SspI fragments (r1 through r6) detected by the probe.

doi:10.1371/journal.pgen.1005685.g003

*sae2*Δ resection defect. We first measured the efficiency of single-strand annealing (SSA), a mechanism that repairs a DSB flanked by direct DNA repeats when sufficient resection exposes the complementary DNA sequences, which can then anneal to each other [3]. The *rad53-H88Y* and *tel1-N2021D* alleles were introduced in the YMV45 strain, which carries two tandem *leu2* gene repeats located 4.6 kb apart on chromosome III, with a HO recognition site adjacent to one of the repeats [42]. This strain also harbors a *GAL-HO* construct for galactose-inducible *HO* expression. Both Rad53-H88Y and Tel1-N2021D bypass Sae2 function in SSA-mediated DSB repair. In fact, accumulation of the SSA repair product after HO induction occurred more efficiently in both *sae2*Δ *rad53-H88Y* (Fig 4A and 4B) and *sae2*Δ *tel1-N2021D* (Fig 4C and 4D) than in *sae2*Δ cells, where it was delayed compared to wild type.

To confirm that Rad53-H88Y and Tel1-N2021D suppress the SSA defect of *sae2*Δ cells by restoring DSB resection, we used JKM139 derivative strains to monitor directly generation of ssDNA at the DSB ends. Indeed, *sae2*Δ *rad53-H88Y* (Fig 5A) and *sae2*Δ *tel1-N2021D* (Fig 5B) cells resected the HO-induced DSB more efficiently than *sae2*Δ cells, indicating that both Rad53-H88Y and Tel1-N2021D suppress the resection defect of *sae2*Δ cells.

The DSB resection defect of *sae2*Δ cells is thought to be responsible for the increased persistence of MRX at the DSB [43]. Because Rad53-H88Y and Tel1-N2021D restore DSB resection in *sae2*Δ cells, we expected that the same variants also reduce the amount of MRX bound at the DSB. The amount of Mre11 bound at the HO-induced DSB end turned out to be lower in both *sae2*Δ *rad53-H88Y* and *sae2*Δ *tel1-N2021D* than in *sae2*Δ cells (Fig 5C). Therefore, the Rad53-H88Y and Tel1-N2021D variants restore DSB resection in *sae2*Δ cells and reduce MRX association/persistence at the DSB.

Consistent with the finding that Rad53-H88Y and Tel1-N2021D do not fully restore CPT resistance in *sae2*Δ cells (Fig 1A), and therefore do not bypass completely all Sae2 functions, the *rad53-H88Y* and *tel1-N2021D* mutations were unable to suppress the sporulation defects of *sae2*Δ/*sae2*Δ diploid cells (Fig 5D), suggesting that they cannot bypass the requirement for Sae2/MRX endonucleolytic cleavage to remove Spo11 from meiotic DSBs.

Suppression of the DNA damage hypersensitivity of *sae2*Δ cells by Rad53-H88Y and Tel1-N2021D variants requires Sgs1-Dna2

The MRX complex not only provides the nuclease activity for initiation of DSB resection, but also allows extensive resection by promoting the binding at the DSB ends of the resection proteins Exo1 and Sgs1-Dna2 [6,7,10]. Suppression of the DNA damage hypersensitivity of *sae2*Δ cells by Rad53-H88Y and Tel1-N2021D requires the physical presence of the MRX complex but not its nuclease activity (Fig 1C and 1D). As the loading of Exo1, Sgs1-Dna2 at DSBs depends on the MRX complex independently of its nuclease activity [10], we asked whether the investigated suppression events require Exo1, Sgs1 and/or Dna2. This question was particularly interesting, as Rad53 was shown to inhibit resection at uncapped telomeres through phosphorylation and inhibition of Exo1 [38,44]. As shown in Fig 6A, *sae2*Δ suppression by Rad53-H88Y and Tel1-N2021D was Exo1-independent. In fact, although the lack of Exo1 exacerbated the sensitivity to DNA damaging agents of *sae2*Δ cells, both *sae2*Δ *exo1*Δ *rad53-H88Y* and *sae2*Δ *exo1*Δ *tel1-N2021D* triple mutants were more resistant to genotoxic agents than *sae2*Δ *exo1*Δ double mutant cells (Fig 6A).

By contrast, neither Rad53-H88Y nor Tel1-N2021D were able to suppress the sensitivity to DNA damaging agents of *sae2*Δ cells carrying the temperature sensitive *dna2-1* allele (Fig 6B), suggesting that Dna2 activity is required for their suppressor effect. Dna2, in concert with the helicase Sgs1, functions as a nuclease in DSB resection [7]. The *dna2-E675A* allele abolishes Dna2 nuclease activity, which is essential for cell viability and whose requirement is bypassed

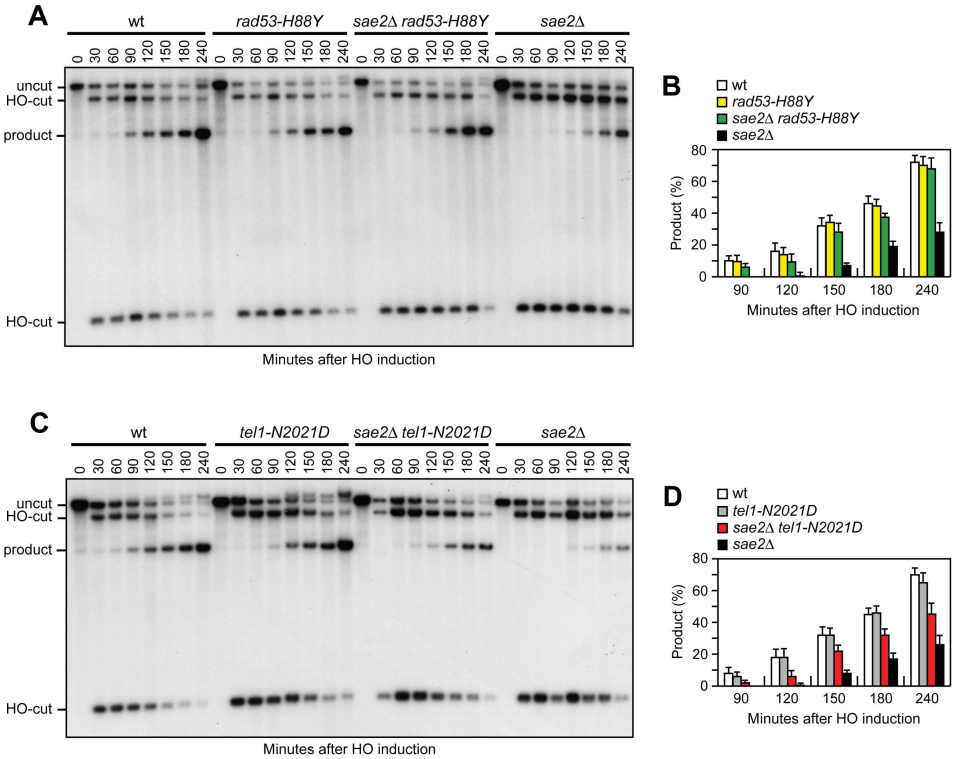

Fig 4. Rad53-H88Y and Tel1-N2021D suppress the SSA defect of *sae2*Δ cells. (A) DSB repair by SSA. YEPR exponentially growing cell cultures of YMV45 derivative strains, carrying the HO-cut site flanked by homologous *leu2* sequences that are 4.6 kb apart, were transferred to YEPRG at time zero. HO-induced DSB formation results in generation of 12 kb and 2.5 kb DNA fragments (HO-cut) that can be detected by Southern blot analysis with a *LEU2* probe of KpnI-digested genomic DNA. DSB repair by SSA generates an 8 kb fragment (product). (B) Densitometric analysis of the product band signals. The experiment as in (A) was independently repeated three times and the mean values are represented with error bars denoting s.d. (n = 3). (C) DSB repair by SSA was analyzed as in (A). (D) Densitometric analysis of the product band signals. The experiment as in (C) was independently repeated three times and the mean values are represented with error bars denoting s.d. (n = 3).

doi:10.1371/journal.pgen.1005685.g004

by the *pif1-M2* mutation that impairs the nuclear activity of the Pif1 helicase [45]. The lack of Sgs1 or expression of the Dna2-E675A variant in the presence of the *pif1-M2* allele impaired viability of *sae2*Δ cells even in the absence of genotoxic agents. The synthetic lethality of *sae2*Δ *sgs1*Δ cells, and possibly of *sae2*Δ *dna2-E675A pif1-M2*, is likely due to defects in DSB resection, as it is known to be suppressed by either *EXO1* overexpression or *KU* deletion [11]. Thus, we asked whether Rad53-H88Y and/or Tel1-N2021D could restore viability of *sae2*Δ *sgs1*Δ and/or *sae2*Δ *dna2-E675A pif1-M2* cells. Tetrad dissection of diploid cells did not allow to find viable spores with the *sae2*Δ *dna2-E675A pif1-M2 rad53-H88Y* (Fig 6C) or *sae2*Δ *dna2-E675A pif1-M2 tel1-N2021D* genotypes (Fig 6D), indicating that neither Rad53-H88Y nor Tel1-N2021D can restore the viability of *sae2*Δ *dna2-E675A pif1-M2* cells. Similarly, no viable *sae2*Δ *sgs1*Δ spores could be recovered, while *sae2*Δ *sgs1*Δ *rad53-H88Y* and *sae2*Δ *sgs1*Δ *tel1-N2021D* triple mutant spores formed very small colonies that could not be further propagated (Fig 6E and 6F). Finally, neither Rad53-H88Y nor Tel1-N2021D, which allowed DNA

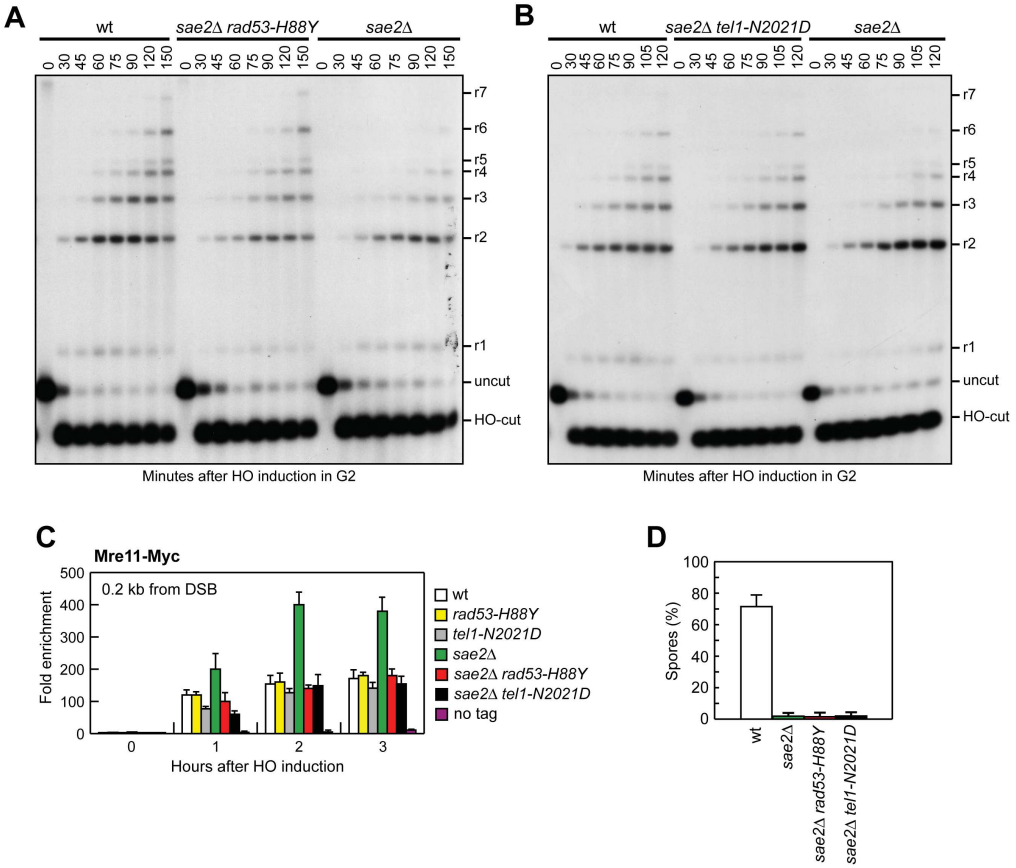

Fig 5. Rad53-H88Y and Tel1-N2021D suppress the resection defect of *sae2*Δ cells. (A, B) DSB resection. YEPR exponentially growing cultures of JKM139 derivative strains were arrested in G2 with nocodazole and transferred to YEPRG in the presence of nocodazole at time zero. Detection of ssDNA was carried out as described in Fig 3D. 5'-3' resection produces SspI fragments indicated as r1 to r7. (C) Exponentially growing YEPR cell cultures of JKM139 derivative strains were transferred to YEPRG. Relative fold enrichment of Mre11-Myc at 0.2 kb from the HO cleavage site was evaluated after ChIP with anti-Myc antibodies and qPCR analysis compared to untagged Mre11 (no tag). In all diagrams, the ChIP signals were normalized for each time point to the amount of the corresponding input signal. The mean values are represented with error bars denoting s.d. (n = 3). (D) Sporulation efficiency. Spores after 24h in sporulation medium of diploid cells homozygous for the indicated mutations.

doi:10.1371/journal.pgen.1005685.g005

damage resistance in *sae2*Δ *exo1*Δ cells (Fig 6A), were able to suppress the growth defect of *sgs1*Δ *exo1*Δ double mutant cells even in the absence of genotoxic agents (Fig 6G). Altogether, these findings indicate that suppression by Rad53-H88Y and Tel1-N2021D of the DNA damage hypersensitivity caused by the absence of Sae2 is dependent on Sgs1-Dna2.

The lack of Rad53 kinase activity suppresses the DNA damage hypersensitivity and the resection defect of *sae2*Δ cells

The Rad53-H88Y protein is defective in interaction with Rad9 (Fig 2C) and therefore fails to undergo autophosphorylation and activation, prompting us to test whether other mutations

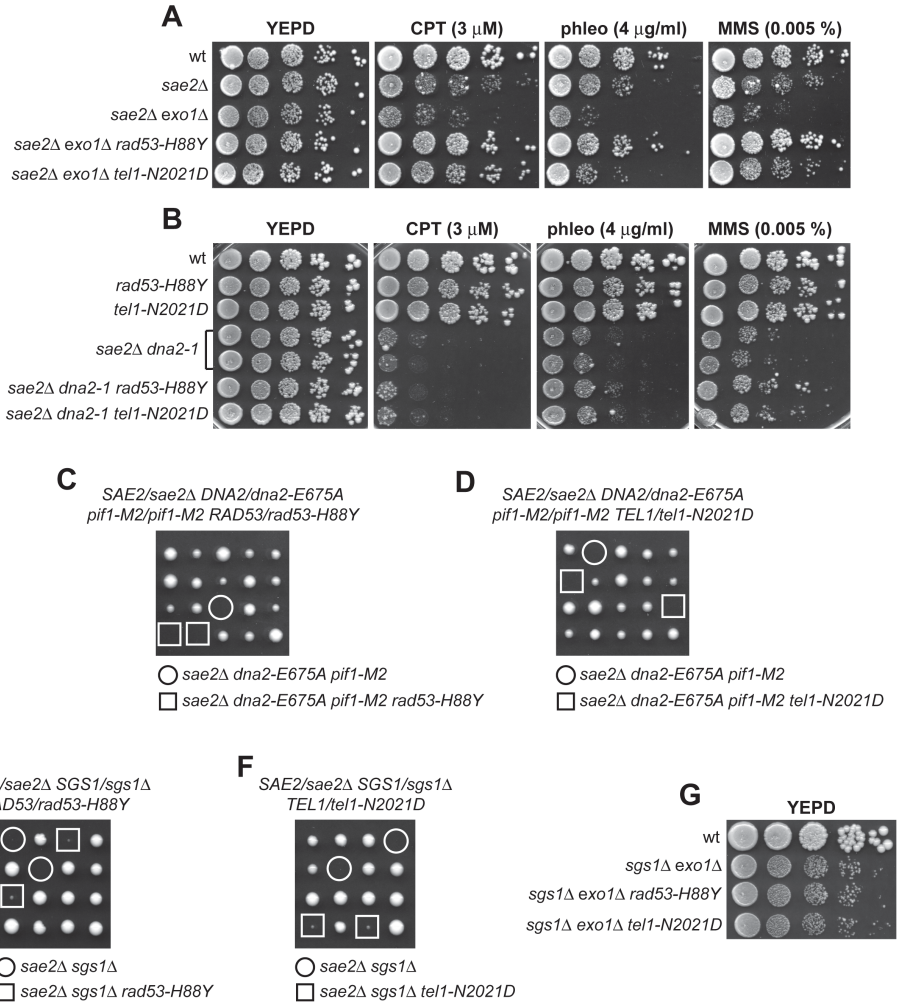

Fig 6. The Rad53-H88Y and Tel1-N2021D bypass of Sae2 function is Sgs1-Dna2-dependent. (A, B) Exponentially growing cells were serially diluted (1:10) and each dilution was spotted out onto YEPD plates with or without CPT, phleomycin or MMS. (C-F) Meiotic tetrads were dissected on YEPD plates that were incubated at 25°C, followed by spore genotyping. (G) Exponentially growing cells were serially diluted (1:10) and each dilution was spotted out onto YEPD plates.

doi:10.1371/journal.pgen.1005685.g006

affecting Rad53 activity can bypass Sae2 functions. To this end, we could not use *rad53*Δ cells because they show growth defects even when the lethal effect of *RAD53* deletion is suppressed by the lack of Sml1 [46]. We then substituted the chromosomal wild type *RAD53* allele with the kinase-defective *rad53-K227A* allele (*rad53-kd*), which does not impair cell viability in the absence of genotoxic agents but affects checkpoint activation [47]. The *rad53-kd* allele rescued the sensitivity of *sae2*Δ cells to CPT and MMS to an extent similar to Rad53-H88Y (Fig 7A).

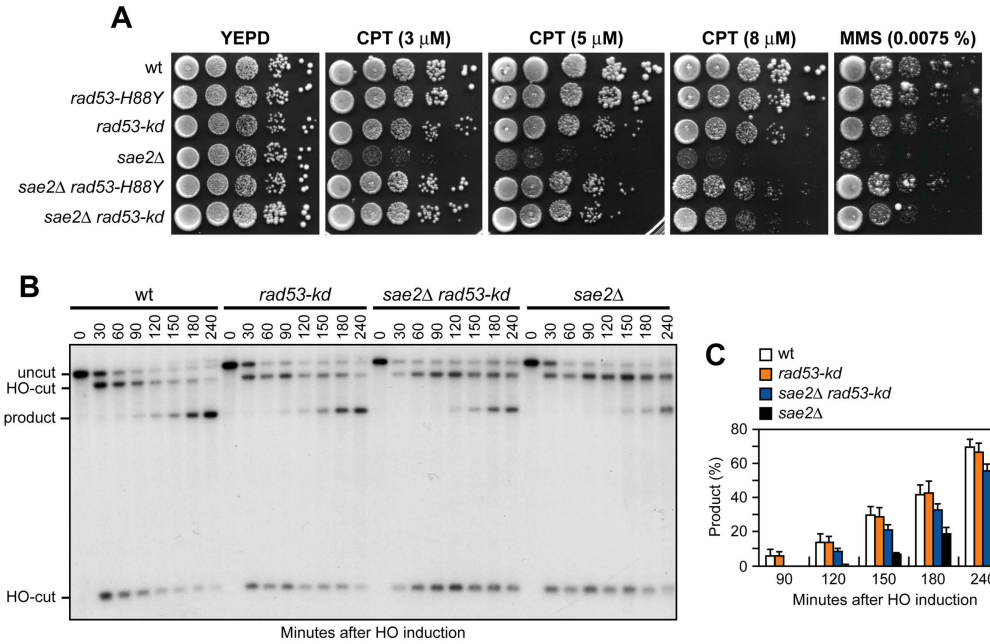

Fig 7. The Rad53-kd variant restores DNA damage resistance and SSA in *sae2*Δ cells. (A) Exponentially growing cells were serially diluted (1:10) and each dilution was spotted out onto YEPD plates with or without CPT or MMS. (B) DSB repair by SSA. The analysis was performed as described in Fig 4A. (C) Densitometric analysis of the product band signals. The experiment as in (B) was independently repeated three times and the mean values are represented with error bars denoting s.d. (n = 3).

doi:10.1371/journal.pgen.1005685.g007

Furthermore, accumulation of the SSA repair products occurred more efficiently in *sae2*Δ *rad53-kd* cells than in *sae2*Δ (Fig 7B and 7C), indicating that the lack of Rad53 kinase activity bypasses Sae2 function in SSA-mediated DSB repair.

The lack of Tel1 kinase activity bypasses Sae2 function at DSBs, whereas Tel1 hyperactivation increases Sae2 requirement

Suppression of *sae2*Δ may be peculiar to Tel1-N2021D, which is poorly recruited to DSBs (Fig 2F), or it might be performed also by *TEL1* deletion (*tel1*Δ) or by expression of a Tel1 kinase defective variant (Tel1-kd). Indeed, the Tel1-kd variant, carrying the G2611D, D2612A, N2616K, and D2631E amino acid substitutions that abolish Tel1 kinase activity in vitro (Fig 2E) [35], rescued the hypersensitivity of *sae2*Δ cells to genotoxic agents to an extent similar to Tel1-N2021D (Fig 8A). The lack of Tel1 kinase activity bypassed also Sae2 function in DSB resection, because *sae2*Δ *tel1-kd* cells repaired a DSB by SSA more efficiently than *sae2*Δ cells (Fig 8B and 8C). By contrast, and consistent with previous studies [23,24], *TEL1* deletion was not capable to suppress the hypersensitivity to DNA damaging agents of *sae2*Δ cells (Fig 8A). Rather, *tel1*Δ *sae2*Δ double mutant cells displayed higher sensitivity to CPT than *sae2*Δ cells (Fig 8A). Altogether, these data indicate that the lack of Tel1 kinase activity can bypass Sae2 function both in DNA damage resistance and DSB resection, but these suppression events require the physical presence of the Tel1 protein.

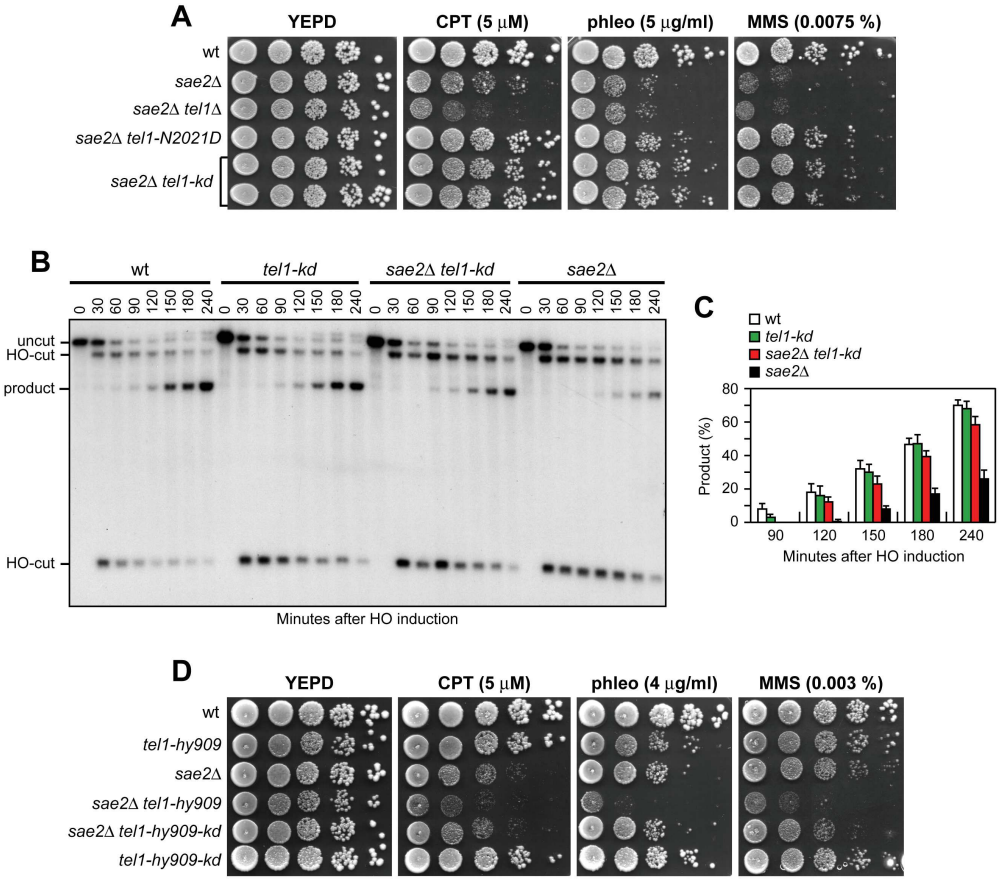

Fig 8. The Tel1-kd variant restores DNA damage resistance and SSA in *sae2Δ* cells. (A) Exponentially growing cells were serially diluted (1:10) and each dilution was spotted out onto YEPD plates with or without CPT, phleomycin or MMS. (B) DSB repair by SSA. The analysis was performed as described in Fig 4A. (C) Densitometric analysis of the product band signals. The experiment as in (B) was independently repeated three times and the mean values are represented with error bars denoting s.d. (n = 3). (D) Exponentially growing cells were serially diluted (1:10) and each dilution was spotted out onto YEPD plates with or without CPT, phleomycin or MMS.

doi:10.1371/journal.pgen.1005685.g008

As impairment of Tel1 function rescued the *sae2*Δ defects, we asked whether Tel1 hyperactivation exacerbates the DNA damage hypersensitivity of *sae2*Δ cells. We previously isolated the *TEL1-hy909* allele, which encodes a Tel1 mutant variant with enhanced kinase activity that causes an impressive telomere overelongation [48]. As shown in Fig 8D, *sae2*Δ *TEL1-hy909* double mutant cells were more sensitive to DNA damaging agents than *sae2*Δ single mutant cells. This enhanced DNA damage sensitivity was likely due to Tel1 kinase activity, as *sae2*Δ cells expressing a kinase defective Tel1-hy909-kd variant were as sensitive to DNA damaging agents as *sae2*Δ cells (Fig 8D). Thus, impairment of Tel1 activity bypasses Sae2 function at DSBs, whereas Tel1 hyperactivation increases the requirement for Sae2 in survival to genotoxic stress.

The absence of Tel1 failed not only to restore DNA damage resistance in *sae2*Δ cells (Fig 8A), but also to suppress their SSA defect (Fig 9A and 9B). The difference in the effects of *tel1*Δ and *tel1-kd* was not due to checkpoint signaling, as Rad53 phosphorylation decreased with similar kinetics in both *sae2*Δ *tel1-kd* and *sae2*Δ *tel1*Δ double mutant cells 10–12 hours after HO induction (Fig 9C). Interestingly, SSA-mediated DSB repair occurred with wild type kinetics in *tel1-kd* mutant cells (Fig 8B and 8C), while *tel1*Δ cells repaired a DSB by SSA less efficiently than wild type cells (Fig 9A and 9B), suggesting that Tel1 might have a function at DSBs that does not require its kinase activity. Indeed, *TEL1* deletion was shown to slight impair DSB resection [19]. Furthermore, it did not exacerbate the resection defect [19] and the hypersensitivity to DNA damaging agents of *mre11*Δ cells (Fig 9D), suggesting that the absence of Tel1 can impair MRX function. Tel1 was also shown to promote MRX association at DNA ends flanked by telomeric DNA repeats independently of its kinase activity [49], and we are showing that suppression of *sae2*Δ by Tel1-N2021D requires the physical presence of the MRX complex (Fig 1D). Thus, it is possible that the lack of Tel1 fails to bypass Sae2 function at DSBs because it reduces MRX association at DSBs to a level that is not sufficient to restore DNA damage resistance and DSB resection in *sae2*Δ cells. Indeed, the amount of Mre11 bound at the HO-induced DSB was decreased in *tel1*Δ, but not in *tel1-kd* cells, compared to wild type (Fig 9E). In agreement with a partial loss of Tel1 function, the Tel1-N2021D variant, whose association to DSBs is diminished compared to wild type Tel1 but not abolished (Fig 2F), only slightly decreased Mre11 association to the DSB (Fig 9E). As the rescue of *sae2*Δ by Tel1-N2021D requires the physical presence of the MRX complex, this Tel1 function in promoting MRX association to DSBs can explain the inability of *tel1*Δ to bypass Sae2 function in DNA damage resistance and resection.

Tel1 and Rad53 kinase activities promote Rad9 binding to the DSB ends

The suppression of the DNA damage hypersensitivity of *sae2*Δ cells by Rad53-H88Y and Tel1-N2021D requires Dna2-Sgs1 (Fig 6B–6G). Because Sgs1-Dna2 activity is counteracted by Rad9, whose lack restores DSB resection in *sae2*Δ cells [13,14], we asked whether suppression of the DSB resection defect of *sae2*Δ cells by Rad53 or Tel1 dysfunction might be due to decreased Rad9 association to the DSB ends. We have previously shown that wild type and *sae2*Δ cells have similar amounts of Rad9 bound at 1.8 kb from the DSB (Fig 10A) [43]. However, a robust increase in the amount of Rad9 bound at 0.2 kb and 0.6 kb from the DSB was detected in *sae2*Δ cells compared to wild type (Fig 10A) [14]. Strikingly, this enhanced Rad9 accumulation in *sae2*Δ cells was reduced in the presence of the Rad53-kd or Tel1-kd variant, which both decreased the amount of Rad9 bound at the DSB also in otherwise wild type cells (Fig 10A). Thus, Rad9 association close to the DSB depends on Rad53 and Tel1 kinase activity.

Rad9 inhibits DSB resection by counteracting Sgs1 recruitment to DSBs [13] and, as expected, Sgs1 binding to DSBs was lower in *sae2*Δ cells than in wild type (Fig 10B). By contrast, the presence of Rad53-kd or Tel1-kd variants increased the amount of Sgs1 at the DSB in both wild type and *sae2*Δ cells (Fig 10B). Together with the observation that the suppression of *sae2*Δ hypersensitivity to genotoxic agents by Rad53 and Tel1 dysfunctions requires Sgs1-Dna2, these findings indicate that the lack of Rad53 or Tel1 kinase activity restores DSB resection in *sae2*Δ cells by decreasing Rad9 association close to the DSB and therefore by relieving Sgs1-Dna2 inhibition. Although both *rad53-kd* and *tel1-kd* cells showed some lowering of Rad9 binding at DSBs compared to wild type cells (Fig 10A), they did not appear to accelerate SSA, suggesting that this extent of Rad9 binding is anyhow sufficient to limit resection in a wild type context.

Rad9 is known to be enriched at the sites of damage by interaction with histone H2A that has been phosphorylated on serine 129 (γH2A) by Mec1 and Tel1 [50–53]. As the lack of γH2A suppresses the SSA defect of *sae2*Δ cells [14], Tel1 activity might increase the amount of Rad9

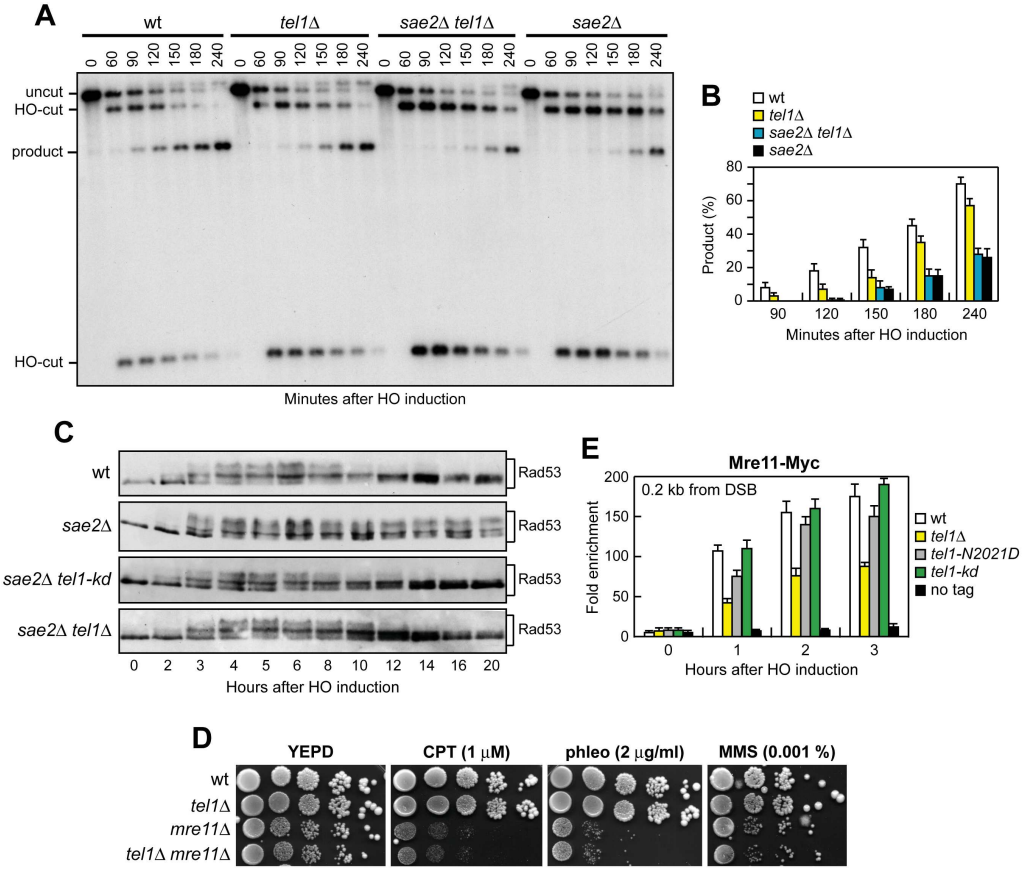

Fig 9. The lack of Tel1 does not restore DNA damage resistance and SSA in *sae2*Δ cells. (A) DSB repair by SSA. The analysis was performed as described in Fig 4A. (B) Densitometric analysis of the product band signals. The experiment as in (A) was independently repeated three times and the mean values are represented with error bars denoting s.d. (n = 3). (C) Exponentially growing YEPR cell cultures of JKM139 derivative strains were transferred to YEPRG (time zero), followed by western blot analysis with anti-Rad53 antibodies of protein extracts prepared at the indicated time points. (D) Exponentially growing cells were serially diluted (1:10) and each dilution was spotted out onto YEPD plates with or without CPT, phleomycin or MMS. (E) ChIP analysis. Exponentially growing YEPR cell cultures of JKM139 derivative strains were transferred to YEPRG. Recruitment of Mre11-Myc compared to untagged Mre11 (no tag) at 0.2 kb from the HO-cut was determined by ChIP analysis and qPCR. In all diagrams, the ChIP signals were normalized for each time point to the amount of the corresponding input signal. The mean values are represented with error bars denoting s.d. (n = 3).

doi:10.1371/journal.pgen.1005685.g009

bound at the DSB in *sae2*Δ cells by promoting generation of γH2A. Indeed, the *hta1-S129A* allele, which encodes a H2A variant where Ser129 is replaced by a non-phosphorylatable alanine residue, thus causing the lack of γH2A, suppressed the resection defect of *sae2*Δ cells (S3 Fig). Furthermore, γH2A formation turned out to be responsible for the enhanced Rad9 binding close to the break site, as *sae2*Δ *hta1-S129A* cells showed wild type levels of Rad9 bound at the DSB (Fig 10C). Finally, γH2A formation close to the DSB depends on Tel1 kinase activity, as γH2A at the DSB was not detectable in *sae2*Δ *tel1-kd* cells (Fig 10D). Altogether, these data indicate that Tel1 promotes Rad9 association to DSB in *sae2*Δ cells through γH2A generation.

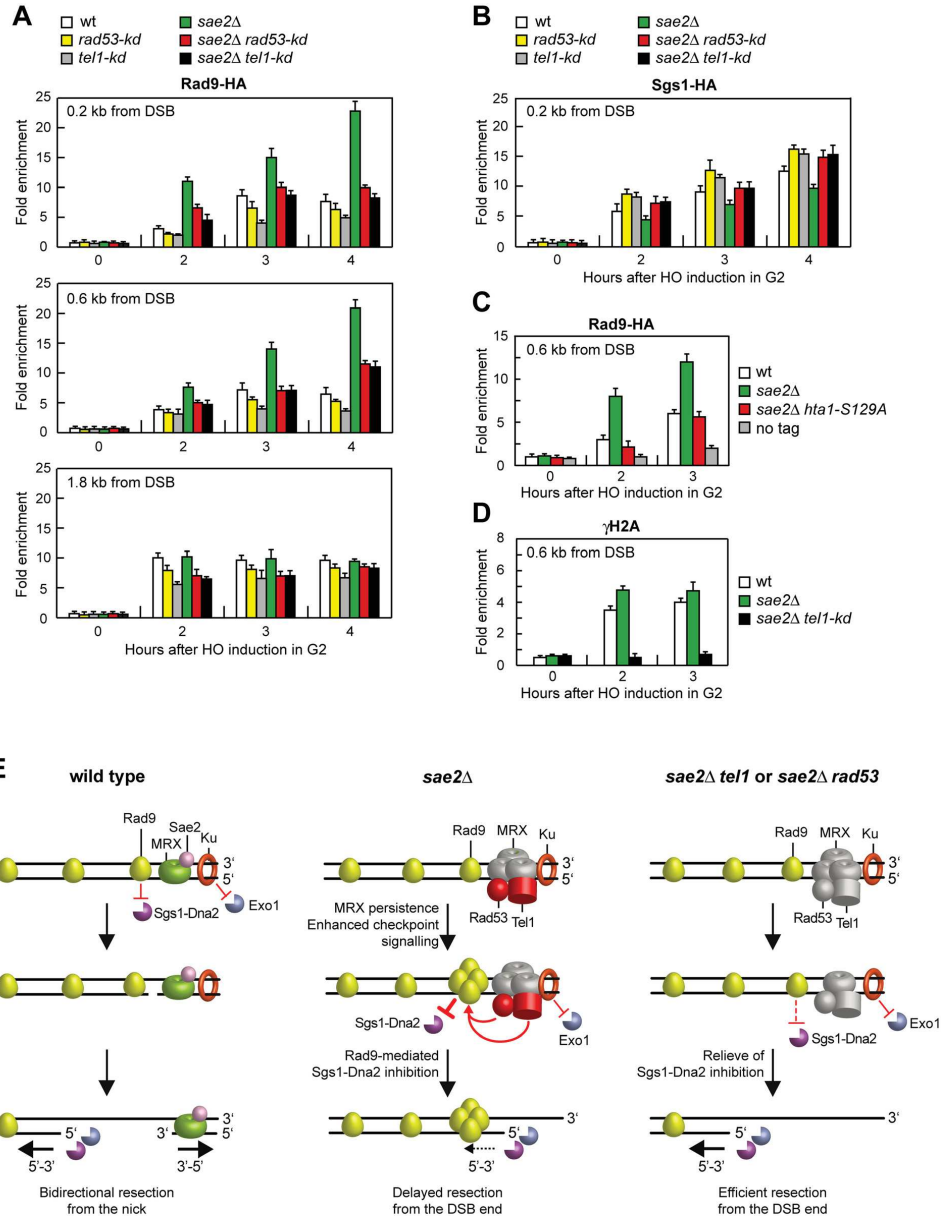

Fig 10. Rad53-kd and Tel1-kd prevent Rad9 association at DSBs. (A) Exponentially growing YEPR cell cultures of JKM139 derivative strains were arrested in G2 with nocodazole and transferred to YEPRG in the presence of nocodazole. Recruitment of Rad9-HA at the indicated distance from the HO-cut was determined by ChIP and qPCR. In all diagrams, the ChIP signals were normalized for each time point to the amount of the corresponding input signal. The mean values are represented with error bars denoting s.d. (n = 3). (B) As in (A), but showing Sgs1-HA binding. (C) As in (A). All strains carried also the deletion of *HTA2* gene. (D) As in (A), but showing γH2A binding. (E) Model for the role of Sae2 at DSBs. (Left) Sae2 activates the Mre11 endonuclease

activity to incise the 5' strand. Generation of the nick allows bidirectional processing by Exo1/Sgs1-Dna2 in the 5'-3' direction from the nick and MRX in the 3' to 5' direction toward the DSB ends. Ku and Rad9 inhibit DSB resection by limiting Exo1 and Sgs1-Dna2, respectively. (Middle) The absence of Sae2 impairs the MRX nuclease activity (non functional MRX nuclease is in grey). As a consequence, the endonucleolytic cleavage of the 5' strand does not occur and resection is carried out by Exo1 and Dna2-Sgs1 that degrade the 5' strands from the DSB ends. Impairment of Mre11 nuclease activity also causes increased MRX association at the DSB, which leads to enhanced Tel1-dependent Rad53 activation. Tel1 and Rad53 activities limit DSB resection from the DSB end (dashed arrow) by increasing the amount of DSB-bound Rad9, which inhibits Sgs1-Dna2 recruitment at DSBs. (Right) Impairments of Tel1 or Rad53 activity (non functional Tel1 and Rad53 are in grey) restore efficient resection in *sae2*Δ cells by relieving Rad9-mediated inhibition of Sgs1-Dna2. Restored DSB resection by Sgs1-Dna2 also reduces MRX persistence at the DSB.

doi:10.1371/journal.pgen.1005685.g010

Discussion

Cells lacking Sae2 not only are defective in DSB resection, but also show persistent DSB-induced checkpoint activation that causes a prolonged cell cycle arrest. This enhanced checkpoint signaling is due to persistent MRX binding at the DSBs, which activates a Tel1-dependent checkpoint that is accompanied by Rad53 phosphorylation [20,22]. While failure to remove MRX from the DSBs has been shown to sensitize *sae2*Δ cells to genotoxic agents [23,24], the possible contribution of the DNA damage checkpoint in determining the DNA damage hypersensitivity and the resection defect of *sae2*Δ cells has never been studied in detail.

We show that impairment of Rad53 activity either by affecting its interaction with Rad9 (Rad53-H88Y) or by abolishing its kinase activity (Rad53-kd) suppresses the sensitivity to DNA damaging agents of *sae2*Δ cells. A similar effect can be detected also when Tel1 function is compromised either by reducing its recruitment to DSBs (Tel1-N2021D) or by abrogating its kinase activity (Tel1-kd). These suppression effects are not due to the escape of the checkpoint-mediated cell cycle arrest, as *CHK1* deletion, which overrides the persistent cell cycle arrest of *sae2*Δ cells, does not suppress the hypersensitivity of the same cells to DNA damaging agents. Rather, we found that impairment of Rad53 or Tel1 signaling suppresses the resection defect of *sae2*Δ by decreasing the amount of Rad9 bound very close to the break site. As it is known that Rad9 inhibits Sgs1-Dna2 [13,14], this reduced Rad9 association at DSBs relieves inhibition of Sgs1-Dna2 activity that can then compensate for the lack of Sae2 function in DSB resection. In this view, active Rad53 and Tel1 increase the requirement for Sae2 in DSB resection by promoting Rad9 binding to DSBs and therefore by inhibiting Sgs1-Dna2. Consistent with a role of Sgs1 in removing MRX from the DSBs [54], the relieve of Sgs1-Dna2 inhibition by Rad53 or Tel1 dysfunction leads to a reduction of MRX association to DSBs in *sae2*Δ cells.

Our finding that Tel1 or Rad53 inactivation can restore both DNA damage resistance and DSB resection in *sae2*Δ cells is apparently at odds with previous findings that attenuation of the Rad53-dependent checkpoint signaling by decreasing MRX association to DSBs suppresses the DNA damage hypersensitivity of *sae2*Δ cells but not their resection defect [23,24]. Noteworthy, the bypass of Sae2 function by Rad53 or Tel1 dysfunction requires the physical presence of MRX bound at DSBs, which is known to promote stable association of Exo1, Sgs1 and Dna2 to DSBs [10]. Thus, we speculate that a reduced MRX association at DSBs allows *sae2*Δ cells to initiate DSB resection by relieving Rad9-mediated inhibition of Sgs1-Dna2 activity. As DSB repair by HR has been shown to require limited amount of ssDNA at DSB ends [55,56], the ssDNA generated by this initial DSB processing might be sufficient to restore DNA damage resistance in *sae2*Δ cells even when wild type levels of resection are not restored because DSB-bound MRX is not enough to ensure stable Sgs1 and Dna2 association.

Surprisingly, *TEL1* deletion, which relieves the persistent Tel1-dependent checkpoint activation caused by the lack of Sae2, did not restore DNA damage resistance and DSB resection in *sae2*Δ cells. We found that the lack of Tel1 protein affects the association of MRX to the DSB ends independently of its kinase activity. As the rescue of *sae2*Δ by Tel1-N2021D requires the physical presence of the MRX complex, this reduced MRX-DNA association can explain the

inability of *TEL1* deletion to restore DNA damage resistance and resection in *sae2*Δ cells. Therefore, while an enhanced Tel1 signaling activity in the absence of Sae2 leads to DNA damage hypersensitivity and resection defects, a sufficient amount of Tel1 needs to be present at DSBs to support MRX function at DSBs.

How do Rad53 and Tel1 control Rad9 association to DSB? Rad53-mediated phosphorylation of Rad9 does not appear to promote Rad9 binding to the DSB [57,58]. Because Rad53 and RPA compete for binding to Sgs1 [59], it is tempting to propose that impaired Rad53 signaling activity might shift Sgs1 binding preference from Rad53 to RPA, leading to increased Sgs1 association to RPA-coated DNA that can counteract Rad9 binding and inhibition of resection. In turn, Tel1 and Mec1 can phosphorylate Rad9 [60,61], and abrogation of these phosphorylation events rescues the sensitivity to DNA damaging agents of *sae2*Δ cells [14], suggesting that Tel1 might control Rad9 association to DSBs directly through phosphorylation. On the other hand, Tel1 promotes generation of γH2A [50–53], which counteracts DSB resection by favoring Rad9 association at the DSB [43]. We show that expression of a non-phosphorylatable H2A variant in *sae2*Δ cells suppresses their resection defect and prevents the accumulation of Rad9 at the DSB. Furthermore, γH2A generation close to the break site depends on Tel1 kinase activity. Thus, although we cannot exclude a direct control of Tel1 on Rad9 association to DNA ends, our findings indicate that Tel1 acts in this process mostly through γH2A generation.

Altogether, our results support a model whereby Tel1 and Rad53, once activated, limit DSB resection by promoting Rad9 binding to DSBs and therefore by inhibiting Sgs1-Dna2. Sae2 activates Mre11 endonucleolytic activity that clips the 5'-terminated DNA strand, thus generating 5' and 3' tailed substrates that can be processed by Exo1/Sgs1-Dna2 and Mre11 activity, respectively (Fig 10E, left). When Sae2 function fails, defective Mre11 nuclease activity causes increased MRX persistence at the DSB that leads to enhanced and prolonged Tel1-dependent Rad53 activation. As a consequence, Tel1- and Rad53-mediated phosphorylation events increase the amount of Rad9 bound at the DSB, which inhibits DSB resection by counteracting Sgs1-Dna2 activity (Fig 10E, middle). Dysfunction of Rad53 or Tel1 reduces Rad9 recruitment at the DSB ends and therefore relieves inhibition of Sgs1-Dna2, which can compensate for the lack of Sae2 in DNA damage resistance and resection (Fig 10E, right). Altogether, these findings indicate that the primary cause of the resection defect of *sae2*Δ cells is an enhanced Rad9 binding to DSBs that is promoted by the persistent MRX-dependent Tel1 and Rad53 signaling activities.

ATM inhibition has been proposed as a strategy for cancer treatment [62]. Therefore, the observation that dampening Tel1/ATM signaling activity restores DNA damage resistance in *sae2*Δ cells might have implications in cancer therapies that use ATM inhibitors for synthetic lethal approaches to threat tumors with deficiencies in the DNA damage response.

Materials and Methods

Yeast strains

The yeast strains used in this study are derivatives of W303, JKM139 and YMV45 strains and are listed in S1 Table. Cells were grown in YEP medium (1% yeast extract, 2% peptone) supplemented with 2% glucose (YEPD), 2% raffinose (YEPR) or 2% raffinose and 3% galactose (YEPRG).

Search for suppressors of *sae2*Δ sensitivity to CPT

To search for suppressor mutations of the CPT-sensitivity of *sae2*Δ mutant, $5x10^6$ *sae2*Δ cells were plated on YEPD in the presence of 30μM CPT. Survivors were crossed to wild type cells

to identify by tetrad analysis the suppression events that were due to single-gene mutations. Genomic DNA from two single-gene suppressors was analyzed by next-generation Illumina sequencing (IGA technology services) to identify mutations altering open reading frames within the reference *S. cerevisiae* genome. To confirm that *rad53-H88Y* and *tel1-N2021D* mutations were responsible for the suppression, either *URA3* or *HIS3* gene was integrated downstream of the *rad53-H88Y* and *tel1-N2021D* stop codon, respectively, and the resulting strain was crossed to wild type cells to verify by tetrad dissection that the suppression of the *sae2*Δ CPT sensitivity co-segregated with the *URA3* or *HIS3* allele.

DSB resection and repair by SSA

DSB end resection at the *MAT* locus in JKM139 derivative strains was analyzed on alkaline agarose gels as previously described [63]. DSB formation and repair in YMV45 strain were detected by Southern blot analysis using an *Asp*718-*Sal*I fragment containing part of the *LEU2* gene as a probe as previously described [63]. Quantitative analysis of the repair product was performed by calculating the ratio of band intensities for SSA product with respect to a loading control.

Other techniques

Protein extracts for western blot analysis were prepared by TCA precipitation. ChIP assays were performed as previously described [64]. Data are expressed as fold enrichment at the HO-induced DSB over that at the non-cleaved *ARO1* locus, after normalization of each ChIP signals to the corresponding amount of immunoprecipitated protein and input for each time point. Fold enrichment was then normalized to the efficiency of DSB induction. The kinase assay and coimmunoprecipitation were performed as previously described [48]. Rad53 was detected by using anti-Rad53 polyclonal antibodies (ab104232) from Abcam. γH2A was immunoprecipitated by using anti-γH2A antibodies (ab15083) from Abcam.

Supporting Information

S1 Fig. *rad53-H88Y* and *tel1-N2021D* suppressor alleles are recessive. Exponentially growing cells were serially diluted (1:10) and each dilution was spotted out onto YEPD plates with or without the indicated genotoxic agents.
(TIF)

S2 Fig. The Tel1-N2021D variant does not affect telomere length. Genomic DNA prepared from exponentially growing cells was digested with *Xho*I and hybridized with a poly(GT) telomere-specific probe.
(TIF)

S3 Fig. The lack of γH2A suppresses the resection defect of *sae2*Δ cells. DSB resection. YEPR exponentially growing cultures of JKM139 derivative cells with the indicated genotypes were arrested in G2 with nocodazole and transferred to YEPRG in the presence of nocodazole at time zero. All strains carried also the deletion of *HTA2* gene. Gel blots of SspI-digested genomic DNA separated on alkaline agarose gel were hybridized with a single-stranded RNA probe that anneals to the unresected strand on one side of the break. 5'-3' resection progressively eliminates SspI sites, producing larger SspI fragments (r1 through r7) detected by the probe.
(TIF)

S1 Table. List of yeast strains described in this work.
(DOC)

Acknowledgments

We thank J. Haber, T. Petes and L. Symington for strains. We are grateful to Marina Martina for preliminary results and to Giovanna Lucchini for critical reading of the manuscript.

Author Contributions

Conceived and designed the experiments: EG MV MC MPL. Performed the experiments: EG MV MG LM MC. Analyzed the data: EG MV MC MPL. Wrote the paper: MPL.

References

1. Gobbini E, Cesena D, Galbiati A, Lockhart A, Longhese MP (2013) Interplays between ATM/Tel1 and ATR/Mec1 in sensing and signaling DNA double-strand breaks. DNA Repair 12: 791–799. doi: 10.1016/j.dnarep.2013.07.009 PMID: 23953933
2. Ciccia A, Elledge SJ (2010) The DNA damage response: making it safe to play with knives. Mol Cell 40: 179–204. doi: 10.1016/j.molcel.2010.09.019 PMID: 20965415
3. Mehta A, Haber JE (2014) Sources of DNA double-strand breaks and models of recombinational DNA repair. Cold Spring Harb Perspect Biol 6: a016428. doi: 10.1101/cshperspect.a016428 PMID: 25104768
4. Symington LS, Gautier J (2011) Double-strand break end resection and repair pathway choice. Annu Rev Genet 45: 247–271. doi: 10.1146/annurev-genet-110410-132435 PMID: 21910633
5. Cannavo E, Cejka P (2014) Sae2 promotes dsDNA endonuclease activity within Mre11-Rad50-Xrs2 to resect DNA breaks. Nature 514: 122–125. doi: 10.1038/nature13771 PMID: 25231868
6. Mimitou EP, Symington LS (2008) Sae2, Exo1 and Sgs1 collaborate in DNA double-strand break processing. Nature 455: 770–774. doi: 10.1038/nature07312 PMID: 18806779
7. Zhu Z, Chung WH, Shim EY, Lee SE, Ira G (2008) Sgs1 helicase and two nucleases Dna2 and Exo1 resect DNA double-strand break ends. Cell 134: 981–994. doi: 10.1016/j.cell.2008.08.037 PMID: 18805091
8. Cejka P, Cannavo E, Polaczek P, Masuda-Sasa T, Pokharel S, Campbell JL, et al. (2010) DNA end resection by Dna2-Sgs1-RPA and its stimulation by Top3-Rmi1 and Mre11-Rad50-Xrs2. Nature 467: 112–116. doi: 10.1038/nature09355 PMID: 20811461
9. Niu H, Chung WH, Zhu Z, Kwon Y, Zhao W, Chi P, et al. (2010) Mechanism of the ATP-dependent DNA end-resection machinery from *Saccharomyces cerevisiae*. Nature 467: 108–111. doi: 10.1038/nature09318 PMID: 20811460
10. Shim EY, Chung WH, Nicolette ML, Zhang Y, Davis M, Zhu Z, et al. (2010) *Saccharomyces cerevisiae* Mre11/Rad50/Xrs2 and Ku proteins regulate association of Exo1 and Dna2 with DNA breaks. EMBO J 29: 3370–3380. doi: 10.1038/emboj.2010.219 PMID: 20834227
11. Mimitou EP, Symington LS (2010) Ku prevents Exo1 and Sgs1-dependent resection of DNA ends in the absence of a functional MRX complex or Sae2. EMBO J 29: 3358–3369. doi: 10.1038/emboj.2010.193 PMID: 20729809
12. Foster SS, Balestrini A, Petrini JH (2011) Functional interplay of the Mre11 nuclease and Ku in the response to replication-associated DNA damage. Mol Cell Biol 31: 4379–4389. doi: 10.1128/MCB.05854-11 PMID: 21876003
13. Bonetti D, Villa M, Gobbini E, Cassani C, Tedeschi G, Longhese MP (2015) Escape of Sgs1 from Rad9 inhibition reduces the requirement for Sae2 and functional MRX in DNA end resection. EMBO Rep 16: 351–361. doi: 10.15252/embr.201439764 PMID: 25637499
14. Ferrari M, Dibitetto D, De Gregorio G, Eapen VV, Rawal CC, Lazzaro F, et al. (2015) Functional interplay between the 53BP1-ortholog Rad9 and the Mre11 complex regulates resection, end-tethering and repair of a double-strand break. PLoS Genet 11: e1004928. doi: 10.1371/journal.pgen.1004928 PMID: 25569305
15. Keeney S, Kleckner N (1995) Covalent protein-DNA complexes at the 5' strand termini of meiosis-specific double-strand breaks in yeast. Proc Natl Acad Sci USA 92: 11274–11278. PMID: 7479978
16. Usui T, Ohta T, Oshiumi H, Tomizawa J, Ogawa H, Ogawa T (1998) Complex formation and functional versatility of Mre11 of budding yeast in recombination. Cell 95: 705–716. PMID: 9845372
17. Liu C, Pouliot JJ, Nash HA (2002) Repair of topoisomerase I covalent complexes in the absence of the tyrosyl-DNA phosphodiesterase Tdp1. Proc Natl Acad Sci USA 99: 14970–14975. PMID: 12397185
18. Deng C, Brown JA, You D, Brown JM (2005) Multiple endonucleases function to repair covalent topoisomerase I complexes in *Saccharomyces cerevisiae*. Genetics 170: 591–600. PMID: 15834151

19. Mantiero D, Clerici M, Lucchini G, Longhese MP (2007) Dual role for *Saccharomyces cerevisiae* Tel1 in the checkpoint response to double-strand breaks. EMBO Rep 8: 380–387. PMID: 17347674

20. Usui T, Ogawa H, Petrini JH (2001) A DNA damage response pathway controlled by Tel1 and the Mre11 complex. Mol Cell 7: 1255–1266. PMID: 11430828

21. Lisby M, Barlow JH, Burgess RC, Rothstein R (2004) Choreography of the DNA damage response: spatiotemporal relationships among checkpoint and repair proteins. Cell 118: 699–713. PMID: 15369670

22. Clerici M, Mantiero D, Lucchini G, Longhese MP (2006) The *Saccharomyces cerevisiae* Sae2 protein negatively regulates DNA damage checkpoint signalling. EMBO Rep 7: 212–218. PMID: 16374511

23. Chen H, Donnianni RA, Handa N, Deng SK, Oh J, Timashev LA, et al. (2015) Sae2 promotes DNA damage resistance by removing the Mre11-Rad50-Xrs2 complex from DNA and attenuating Rad53 signaling. Proc Natl Acad Sci USA 112: 1880–1887.

24. Puddu F, Oelschlaegel T, Guerini I, Geisler NJ, Niu H, Herzog M, et al. (2015) Synthetic viability genomic screening defines Sae2 function in DNA repair. EMBO J 34: 1509–1522. doi: 10.15252/embj.201590973 PMID: 25899817

25. Sandell LL, Zakian VA (1993) Loss of a yeast telomere: arrest, recovery, and chromosome loss. Cell 75: 729–739. PMID: 8242745

26. Toczyski DP, Galgoczy DJ, Hartwell LH (1997) CDC5 and CKII control adaptation to the yeast DNA damage checkpoint. Cell 90: 1097–1106. PMID: 9323137

27. Lee SE, Moore JK, Holmes A, Umezu K, Kolodner RD, Haber JE (1998) *Saccharomyces* Ku70, Mre11/Rad50 and RPA proteins regulate adaptation to G2/M arrest after DNA damage. Cell 94: 399–409. PMID: 9708741

28. Fukunaga K, Kwon Y, Sung P, Sugimoto K (2011) Activation of protein kinase Tel1 through recognition of protein-bound DNA ends. Mol Cell Biol 31: 1959–1971. doi: 10.1128/MCB.05157-11 PMID: 21402778

29. Sun Z, Hsiao J, Fay DS, Stern DF (1998) Rad53 FHA domain associated with phosphorylated Rad9 in the DNA damage checkpoint. Science 281: 272–274. PMID: 9657725

30. Gilbert CS, Green CM, Lowndes NF (2001) Budding yeast Rad9 is an ATP-dependent Rad53 activating machine. Mol Cell 8: 129–136. PMID: 11511366

31. Sweeney FD, Yang F, Chi A, Shabanowitz J, Hunt DF, Durocher D (2005) *Saccharomyces cerevisiae* Rad9 acts as a Mec1 adaptor to allow Rad53 activation. Curr Biol 15: 1364–1375. PMID: 16085488

32. Durocher D, Henckel J, Fersht AR, Jackson SP (1999) The FHA domain is a modular phosphopeptide recognition motif. Mol Cell 4: 387–394. PMID: 10518219

33. Bosotti R, Isacchi A, Sonnhammer EL (2000) FAT: a novel domain in PIK-related kinases. Trends Biochem Sci 25: 225–227. PMID: 10782091

34. Baretić D, Williams RL (2014) PIKKs—the solenoid nest where partners and kinases meet. Curr Opin Struct Biol 29: 134–142. doi: 10.1016/j.sbi.2014.11.003 PMID: 25460276

35. Mallory JC, Petes TD (2000) Protein kinase activity of Tel1p and Mec1p, two *Saccharomyces cerevisiae* proteins related to the human ATM protein kinase. Proc Natl Acad Sci USA 97: 13749–13754. PMID: 11095737

36. Ogi H, Goto GH, Ghosh A, Zencir S, Henry E, Sugimoto K (2015) Requirement of the FATC domain of protein kinase Tel1 for localization to DNA ends and target protein recognition. Mol Biol Cell 26: 3480–3488. doi: 10.1091/mbc.E15-05-0259 PMID: 26246601

37. Lydall D, Weinert T (1995) Yeast checkpoint genes in DNA damage processing: implications for repair and arrest. Science 270: 1488–1491. PMID: 7491494

38. Jia X, Weinert T, Lydall D (2004) Mec1 and Rad53 inhibit formation of single-stranded DNA at telomeres of *Saccharomyces cerevisiae cdc13-1* mutants. Genetics 166: 753–764. PMID: 15020465

39. Ngo GH, Lydall D (2015) The 9-1-1 checkpoint clamp coordinates resection at DNA double strand breaks. Nucleic Acids Res 43: 5017–5032. doi: 10.1093/nar/gkv409 PMID: 25925573

40. Pellicioli A, Lee SE, Lucca C, Foiani M, Haber JE (2001) Regulation of *Saccharomyces* Rad53 checkpoint kinase during adaptation from DNA damage-induced G2/M arrest. Mol Cell 7: 293–300. PMID: 11239458

41. Sanchez Y, Bachant J, Wang H, Hu F, Liu D, Tetzlaff M, et al. (1999) Control of the DNA damage checkpoint by Chk1 and Rad53 protein kinases through distinct mechanisms. Science 286: 1166–1171. PMID: 10550056

42. Vaze MB, Pellicioli A, Lee SE, Ira G, Liberi G, Arbel-Eden A, et al. (2002) Recovery from checkpoint-mediated arrest after repair of a double-strand break requires Srs2 helicase. Mol Cell 10: 373–385. PMID: 12191482

43. Clerici M, Trovesi C, Galbiati A, Lucchini G, Longhese MP (2014) Mec1/ATR regulates the generation of single-stranded DNA that attenuates Tel1/ATM signaling at DNA ends. EMBO J 33: 198–216. doi: 10.1002/embj.201386041 PMID: 24357557

44. Morin I, Ngo HP, Greenall A, Zubko MK, Morrice N, Lydall D (2008) Checkpoint-dependent phosphorylation of Exo1 modulates the DNA damage response. EMBO J 27: 2400–2410. doi: 10.1038/emboj.2008.171 PMID: 18756267

45. Budd ME, Choe Wc, Campbell JL (2000) The nuclease activity of the yeast *DNA2* protein, which is related to the RecB-like nucleases, is essential in vivo. J Biol Chem 275: 16518–16529. PMID: 10748138

46. Zhao X, Muller EG, Rothstein R (1998) A suppressor of two essential checkpoint genes identifies a novel protein that negatively affects dNTP pools. Mol Cell 2: 329–340. PMID: 9774971

47. Fay DS, Sun Z, Stern DF (1997) Mutations in *SPK1/RAD53* that specifically abolish checkpoint but not growth-related functions. Curr Genet 31: 97–105. PMID: 9021124

48. Baldo V, Testoni V, Lucchini G, Longhese MP (2008) Dominant *TEL1-hy* mutations compensate for Mec1 lack of functions in the DNA damage response. Mol Cell Biol 28: 358–375. PMID: 17954565

49. Hirano Y, Fukunaga K, Sugimoto K (2009) Rif1 and Rif2 inhibit localization of Tel1 to DNA ends. Mol Cell 33: 312–322. doi: 10.1016/j.molcel.2008.12.027 PMID: 19217405

50. Shroff R, Arbel-Eden A, Pilch D, Ira G, Bonner WM, Petrini JH, et al. (2004) Distribution and dynamics of chromatin modification induced by a defined DNA double-strand break. Curr Biol 14: 1703–1711. PMID: 15458641

51. Javaheri A, Wysocki R, Jobin-Robitaille O, Altaf M, Côté J, Kron SJ (2006) Yeast G1 DNA damage checkpoint regulation by H2A phosphorylation is independent of chromatin remodeling. Proc Natl Acad Sci USA 103: 13771–13776. PMID: 16940359

52. Toh GW, O'Shaughnessy AM, Jimeno S, Dobbie IM, Grenon M, Maffini S, et al. (2006) Histone H2A phosphorylation and H3 methylation are required for a novel Rad9 DSB repair function following checkpoint activation. DNA Repair 5: 693–703. PMID: 16650810

53. Hammet A, Magill C, Heierhorst J, Jackson SP (2007) Rad9 BRCT domain interaction with phosphorylated H2AX regulates the G1 checkpoint in budding yeast. EMBO Rep 8: 851–857. PMID: 17721446

54. Bernstein KA, Mimitou EP, Mihalevic MJ, Chen H, Sunjaveric I, Symington LS et al. (2013) Resection activity of the Sgs1 helicase alters the affinity of DNA ends for homologous recombination proteins in *Saccharomyces cerevisiae*. Genetics 195: 1241–1251. doi: 10.1534/genetics.113.157370 PMID: 24097410

55. Ira G, Haber JE (2002) Characterization of RAD51-independent break-induced replication that acts preferentially with short homologous sequences. Mol Cell Biol 22: 6384–6392. PMID: 12192038

56. Jinks-Robertson S, Michelitch M, Ramcharan S (1993) Substrate length requirements for efficient mitotic recombination in *Saccharomyces cerevisiae*. Mol Cell Biol 13: 3937–3950. PMID: 8321201

57. Naiki T, Wakayama T, Nakada D, Matsumoto K, Sugimoto K (2004) Association of Rad9 with double-strand breaks through a Mec1-dependent mechanism. Mol Cell Biol 24: 3277–3285. PMID: 15060150

58. Usui T, Foster SS, Petrini JH (2009) Maintenance of the DNA-damage checkpoint requires DNA-damage-induced mediator protein oligomerization. Mol Cell 33: 147–159. doi: 10.1016/j.molcel.2008.12.022 PMID: 19187758

59. Hegnauer AM, Hustedt N, Shimada K, Pike BL, Vogel M, Amsler P, et al. (2012) An N-terminal acidic region of Sgs1 interacts with Rpa70 and recruits Rad53 kinase to stalled forks. EMBO J 31: 3768–3783. doi: 10.1038/emboj.2012.195 PMID: 22820947

60. Emili A (1998) *MEC1*-dependent phosphorylation of Rad9p in response to DNA damage. Mol Cell 2: 183–189. PMID: 9734355

61. Vialard JE, Gilbert CS, Green CM, Lowndes NF (1998) The budding yeast Rad9 checkpoint protein is subjected to Mec1/Tel1-dependent hyperphosphorylation and interacts with Rad53 after DNA damage. EMBO J 17: 5679–5688. PMID: 9755168

62. Cremona CA, Behrens A (2014) ATM signalling and cancer. Oncogene 33: 3351–3360. doi: 10.1038/onc.2013.275 PMID: 23851492

63. Trovesi C, Falcettoni M, Lucchini G, Clerici M, Longhese MP (2011) Distinct Cdk1 requirements during single-strand annealing, noncrossover, and crossover recombination. PLoS Genet 7: e1002263. doi: 10.1371/journal.pgen.1002263 PMID: 21901114

64. Viscardi V, Bonetti D, Cartagena-Lirola H, Lucchini G, Longhese MP (2007) MRX-dependent DNA damage response to short telomeres. Mol Biol Cell 18: 3047–3058. PMID: 17538011